HYBRID ZONOTOPES: A MIXED-INTEGER SET REPRESENTATION FOR THE ANALYSIS OF HYBRID SYSTEMS

by

Trevor J. Bird

A Dissertation

Submitted to the Faculty of Purdue University

In Partial Fulfillment of the Requirements for the degree of

Doctor of Philosophy

School of Mechanical Engineering

West Lafayette, Indiana

December 2022

THE PURDUE UNIVERSITY GRADUATE SCHOOL
STATEMENT OF COMMITTEE APPROVAL

Dr. Neera Jain, Chair

School of Mechanical Engineering

Dr. George Chiu

School of Mechanical Engineering

Dr. Dionysios Aliprantis

School of Electrical and Computer Engineering

Dr. Jianghai Hu

School of Electrical and Computer Engineering

Approved by:

Dr. Nicole Key

To my parents

for their guidance and unwavering support at every step of this amazing journey

ACKNOWLEDGMENTS

There are so many people who have helped me throughout this amazing experience, and these pages are not nearly enough to give them all the thanks they deserve. First, I would like to thank my advisor Professor Neera Jain for her guidance, support, and patience over the past five years. Dr. Jain exemplifies what it means to be an academic, her passion for science and excitement towards exploring the unknown in no small part inspired me to push the boundaries of what I thought I was capable of achieving. I am grateful for the lessons she has taught me, and I am forever indebted to her for the numerous opportunities she has provided, and continues to provide, to me.

I am also incredibly grateful to Professors Justin Koeln and Herschel Pangborn. My graduate research experience, and this dissertation, would not have been as fulfilling without their contributions to them. Our meetings have been a highlight of each week, and I will genuinely miss the unscheduled hours spent brainstorming. I look forward to following the work that continues to come from the collaboration between the Jain Research Lab, the Energy Systems Control Laboratory, and the Pangborn Advanced Controls Lab. A special thank you goes to Jacob Siefert, to work with someone as bright as Jacob who approaches these problems from a different angle than my own has taught me a lot, and his contributions to the work presented in this dissertation have been invaluable. I would also like to thank Kasidit Muenprasitivej for his help with deriving models of benchmark problems. I would also like to thank the members of my advisory committee, Professors George Chiu, Dionysios Aliprantis, and Jianghai Hu, for their valuable insights, constructive comments, and encouragement.

I would like to thank the members of the Jain Research Lab—Austin, Rian, Ana, Akash, Aaron, Yeshaswi, Karan, Katie, Marcin, Madi, Michael, Jianqi, Reynolds, Matt, Uduak, Michael, Ara, Ethan, and Sibi—for the stimulating discussions, Thursday lunches, game nights, and countless hours spent helping me refine papers and presentations. I would also like to thank the Ray W. Herrick Laboratories and all the people who call this lab home, for providing such an inclusive and collaborative environment. Having such an amazing group

of colleagues, and friends, has been a boon to both my academic achievements and personal growth. I am proud to call myself a Herrick graduate.

To my family, I would not be where I am without you. I want to thank my parents—Alan and Elizabeth—for their guidance, unwavering support, and unconditional love. The work presented in this dissertation would not have been possible without the role you play in my life. I hope to be the role model you both have been in my life to those around me, and I hope to make you proud in my future accomplishments. To my siblings Tyler and Cass, thank you for your friendship, love, and support throughout my life.

Finally, and most importantly, I would like to thank my partner Pradnya. I came to Purdue to earn my doctorate degree, but my greatest achievement from these years is finding someone as loving, brave, intelligent, and caring as you. Thank you for supporting me through these final years and always helping me decompress when I needed it most. I am excited to begin the next chapter of my life with you, and can't wait to see what the coming years hold.

This material is based upon work supported by the National Science Foundation under Award No. DGE-1333468. Any opinions, findings, and conclusions or recommendations expressed in this material are those of the author(s) and do not necessarily reflect the views of the National Science Foundation.

TABLE OF CONTENTS

LIST OF TABLES

LIST OF FIGURES

ABSTRACT

Set-based methods have been leveraged in many engineering applications from robust control and global optimization, to probabilistic planning and estimation. While useful, these methods have most widely been applied to analysis over sets that are convex, due to their ease in both representation and calculation. The representation and analysis of nonconvex sets is inherently complex. When nonconvexity arises in design and control applications, the nonconvex set is often over-approximated by a convex set to provide conservative results. However, the level of conservatism may be large and difficult to quantify, often leading to trivial results and requiring repetitive analysis by the engineer. Nonconvexity is inherent and unavoidable in many applications, such as the analysis of hybrid systems and robust safety constraints.

In this dissertation, I present a new nonconvex set representation named the *hybrid zonotope*. The hybrid zonotope builds upon a combination of recent advances in the compact representation of convex sets in the controls literature with methods leveraged in solving mixed-integer programming problems. It is shown that the hybrid zonotope is equivalent to the union of an exponential number of convex sets while using a linear number of continuous and binary variables in the set's representation. I provide identities for, and derivations of, the set operations of hybrid zonotopes for linear mappings, Minkowski sums, generalized intersections, halfspace intersections, Cartesian products, unions, complements, point containment, set containment, support functions, and convex enclosures. I also provide methods for redundancy removal and order reduction to improve the compactness and computational efficiency of the represented sets. Therefore proving the hybrid zonotopes expressive power and applicability to many nonconvex set-theoretic methods. Beyond basic set operations, I specifically show how the exact forward and backward reachable sets of linear hybrid systems may be found using identities that are calculated algebraically and scale linearly. Numerical examples show the scalability of the proposed methods and how they may be used to verify the safety and performance of complex systems. These exact methods may also be used to evaluate the level of conservatism of the existing approximate methods provided in the literature.

1. INTRODUCTION

The use of sets is ubiquitous in modern control theory. While present in the majority of robust and optimal control formulations, set based methods have found further use for evaluation of reachable sets, safety verification, parameter estimation, global optimization, and fault detection [1]. Deployment of set-based approaches is necessary when certain properties, such as safety or performance, of a system must be guaranteed. Multiple set representations have been developed to perform these tasks; those with the most mature theory and widespread use in controls are ellipsoids, halfspace and vertex representation polytopes, and zonotopes [1]. While suitable for many applications, these set representations share a common disadvantage in their convexity. Nonconvexity is inherent in many applications, such as reachability of nonlinear [2] and hybrid systems [3], active fault diagnostics [4], and safety constraints in optimal and robust control [5].

1.1 Representing Nonconvex Sets

When admissible, nonconvex sets are often represented as the implicit union of a collection of convex sets [6]. Thus, the number of sets required to accurately represent the true nonconvex set is proportional to the number of nonconvex features. When set operations are performed on the nonconvex set, the number of features grow, as does the number of convex sets used in the implicit representation. A worst-case exponential growth in complexity, in both the representation and computation, may incur as set operations are iteratively performed. This sharp increase in complexity often leads to the analysis becoming computationally intractable. To stifle this growth, many algorithms employ merging and approximation techniques to reduce computational burden at the cost of accuracy [7]–[12]. These methods are often used in safety verification (reachability analysis) when satisfaction of an outer (inner) approximation guarantees that the performance criteria is met by the true set [10], albeit only in a conservative sense. However, in the case of safety constraints, e.g. obstacle avoidance and multi-agent control, nonconvexity is inherent and unavoidable, and requires the explicit representation of the nonconvex set [13].

Convex polytopes given by their half-space and vertex representation, denoted by H- and V-rep respectively, have been a primary tool for many set theoretic methods. Their construction is intuitive, and the ability to convert between H- and V-rep leads to closure under all set operations that maintain convexity. When convexity is not maintained, such as with complement and union operations, the resulting nonconvex set may be defined as a collection of convex polytopes [6]. These collections of convex polytopes may then be used in optimization algorithms by enforcing their explicit union as hyperplane arrangements through introducing binary variables and mixed-integer constraints [13]. This flexibility has led to algorithms for solving many set-theoretic controls problems [12], [14].

While useful, the computational burden and complexity of H- and V-rep polytopes has a worst-case exponential growth for basic set operations [15]. Furthermore, the necessity to convert between H- and V-rep is cumbersome and involves computationally expensive vertex and facet enumeration [16], thus limiting their use to problems with small dimension (generally no greater than five) and few features. Given this, zonotopes have found increased popularity due to their ability to compactly represent high dimensional sets with many features, albeit with the limitation that the sets be centrally symmetric [17]. The introduction of constrained zonotopes has overcome the zonotopes' inherent symmetry to establish a set capable of representing arbitrary convex polytopes with closure under linear mappings, Minkowski sums, and generalized intersections [18]. A major benefit of constrained zonotopes is that their set operations are determined by identities that are computed algebraically and scale linearly, thus remaining numerically stable for large problems. Similar to zonotopes [19], the constrained zonotope representation lends itself to efficient order reduction techniques for over-approximations [18] while inner-approximations may be performed through methods at the cost of a higher computational effort [20]. Constrained zonotopes may be used in place of H- and V-rep polytopes in many applications involving convex sets and boast improvements in computation time and complexity [18], [21]–[24]; however, the ability to represent nonconvex polytopes has been limited to the implicit union of a collection of constrained zonotopes.

1.2 Reachable Sets of Hybrid Systems

Hybrid system theory has found increased use for modeling and control synthesis due to its ability to capture the mixed continuous and discrete dynamics exhibited by many engineered systems [25]. While providing a powerful tool, the analysis and control of hybrid systems is inherently complex. Even in the case of linear hybrid systems, basic properties such as stability and controllability may not be easily determined from the system model [26]–[28]. Thus, hybrid systems under closed-loop control may not not exhibit the intended behavior under certain operating conditions. Set-based methods for reachability analysis and safety verification are often deployed when certain properties of a system, such as safety or performance, must be guaranteed. These methods are well established for linear time-invariant systems using convex sets [1], [12]. However, the application of set-based methods to nonlinear and hybrid systems often result in nonconvex sets [29]. The reader is directed to the review papers [10] on set propagation techniques, [2] on Taylor approximations, and [30] on Hamilton Jacobi techniques, and the references therein for detailed discussion on the state of the art.

In the case of linear hybrid systems, nonconvexity arises in reachable sets due to discrete inputs, switching of dynamic subsystems, and reset maps. The exact reachable set may be determined by partitioning the state space into a set of closed convex sets, often referred to as guard sets. The reachable set of hybrid systems may then be found using techniques developed for linear systems using a finite number of convex sets and iteratively propagating the appropriate dynamics within each partition [11]. However, when an intersection with a guard set occurs or an uncertain discrete input is applied, the reach set branches, resulting in a worst-case exponential growth in the number of convex sets required to represent the reachable space as their implicit union [31]. This analysis may be performed in either the forward or backward sense [14], [32], [33]. However, this growth in complexity is often compounded when considering backwards reachable sets with disturbances, as analysis relies on computing or approximating Minkowski differences [34], [35]. This approach becomes computationally intractable for large time horizons.

To avoid this exponential growth in set representation complexity, researchers often approximate the true reachable set, given by the implicit union of a finite number of convex sets, by a reduced number of convex sets. One such method propagates the dynamics of the system by branching along each guard set, then uses clustering methods to over-approximate groups of convex sets by fewer convex sets [8], [9]. This approach provides computational efficiency at the cost of conservatism in the reachable set itself, although the specific trade-off is application-dependent. Another approach is to search each region of the partitioned state space individually and then over-approximate transitions along the guard sets [11], [31]. This approach is computationally efficient as it only deals with one convex set at a time and avoids unnecessary error by only over-approximating nonconvex sets along guard set intersections. However, it is not guaranteed to converge when the reach set intersects a guard partially, without fully transitioning into another partition. [34]

Several nonconvex set representations have been developed that leverage higher order mappings to provide a tighter enclosure of the reachable sets of nonlinear systems. The most notable of these nonconvex set representations are polynomial models with set remainders, e.g. Taylor models [36] and polynomial zonotopes [37]. Although offering a closer approximation of the true set, these polynomial approaches have a case-specific trade-off between convergence, accuracy, and computational cost. Such sets may provide tighter enclosures of the nonconvex reachable sets of hybrid systems, thus requiring fewer branches in the analysis [37]. However, these sets are generally not closed under intersection operations and require ad hoc routines to detect guard set intersections [31], [36]. The recent work of Kochdumper and Althoff introduces the constrained polynomial zonotope [38], a hybrid of polynomial zonotopes [37] and constrained zonotopes [18]. By adding equality constraints to the set definition of the polynomial zonotope, this class of polynomial models are closed under intersection set operations, thus increasing their usefulness in the analysis of hybrid systems. However, handling the worst-case exponential growth in set representation complexity still requires over-approximations that are difficult to compute.

Alternatively, implicit methods for performing reach set analysis of hybrid systems leverage optimal control theory. The level set method poses the reach set problem as the level sets of the solution to the Hamilton Jacobi equations [39]. Although well suited for the

analysis of general nonlinear and hybrid systems, the level set method scales exponentially with respect to the state dimension and becomes intractable for higher dimensional systems (generally no more than four) [30]. For systems with a specific structure, techniques have been proposed that reduce this exponential growth by decomposing the system into subsystems [40]. Another implicit method is to find counter examples posed as optimization problems. This approach seeks to verify the existence of any trajectory from an initial set to a specified target set by solving a series of optimization programs [26], [41], [42]. However these methods only provide safety certificates when a counter example is found and are not well suited to complexity reduction.

Table 1.1. Summary table of existing methods for reachability analysis of hybrid systems.

Author(s)	Efficient	High Dimension	Exact	Outer-Approximation	Forward/ Backward
Mitchel et al. [39] (2005)			×	×	F/B
Herceg et al. [12] (2013)			×	×	F/B
Guernic et al. [43] (2009)	×			×	F
Fan et al. [44] (2016)	×			×	F
Frehse et al. [8] (2011)	×	×		×	F
Chen et al. [45] (2013)	×	×		×	F
Althoff [46] (2015)	×	×		×	F
Schupp et al. [47] (2017)	×	×		×	F
Bogomolov et al. [48] (2019)	×	×		×	F

A summary of the discussed methods is provided in Table 1.1. While useful, existing approaches either become computationally intractable or rely on over-approximations with case-specific trade-offs in accuracy and computational effort. Over-approximations are only valid for safety verification and avoiding unsafe regions in robust control. Furthermore, the error associated with such over-approximations may be large and difficult to quantify, thus resulting in conservative results at best, and trivial solutions at worst [49]. In all of these set-based approaches, detecting guard set intersections and avoiding exponential growth in the set representation complexity remains the primary challenge [10].

1.3 Dissertation Objective

Motivated by the above discussion, the contribution of this dissertation is two fold.

- **Hybrid zonotopes:** to deliver a mixed-integer set representation applicable to a broad class of nonconvex set-theoretic methods.
- **Exact reachability:** to develop a framework for the propagation of reachable sets of linear hybrid systems that exhibit linear growth in set representation complexity.

In this dissertation, I derive a new mixed-integer set representation named the *hybrid zonotope* that is able to compactly represent nonconvex sets with an exponential number of features using a linear number of continuous and discrete variables. I show that the hybrid zonotope is equivalent to the union of 2^N constrained zonotopes—convex polytopes—through the addition of N binary zonotope factors. I show how the hybrid zonotope may be converted into this collection of constrained zonotopes for visualization and analysis. I prove the hybrid zonotope's closure under linear mappings, Minkowski sums, generalized intersections, halfspace intersections, Cartesian products, unions, and complements. Finally, to improve computational efficiency, I provide methods for reducing the complexity of the set representation through redundancy removal and order reduction. Thus providing a nonconvex set representation applicable to a broad class of set-theoretic methods.

Beyond the derivations of basic set operations, I show how the forward, and backward, reachable sets of linear hybrid systems may be represented exactly, and propagated, as hybrid zonotopes. I derive identities for reachable sets of linear hybrid systems modeled as both mixed logical dynamical systems as well as linear systems closed-loop under model predictive control, in both the forward and backward sense. I show through multiple examples how these methods may be used to verify the safety and performance of the considered classes of systems, with reduced conservatism and better scalability when compared to previous methods in the literature. I also show how the hybrid zonotope may be used to solve general multiparametric quadratic programs and compactly represent the set of optimal solutions. Numerical experiments show the scalability of the proposed approach and compare it to existing methods.

1.4 Dissertation Outline

The remainder of this dissertation is organized as follows. In Chapter 2 I provide the necessary background on basic set operations, several existing set representations, and reachability analysis. In Chapter 3 I formally define the hybrid zonotope set representation, prove several of its properties, and derive identities for basic set operations. In Chapter 4 I present closed-form solutions for the exact forward reachable sets of linear hybrid systems and closed-loop MPC. In Chapter 5 I develop closed-form solutions for the exact backward reachable sets of linear hybrid systems and closed-loop MPC. In Chapter 6 I present methods for reducing the complexity of hybrid zonotopes to generate over-approximations. Finally, some concluding remarks and suggestions for future areas of research are made in Chapter 7.

2. BACKGROUND

In this chapter I provide the necessary background on existing work that will be leveraged in the remainder of the dissertation. First, notation is provided in Section 2.1 followed by the definitions of basic set operations in Section 2.2. I then discuss the existing set representations related to the presented work in Section 2.3. Finally, I finish the chapter by discussing the reachability analysis of discrete-time systems in Section 2.4.

2.1 Notation

Sets are denoted by uppercase calligraphic letters, e.g., $\mathcal{Z} \subset \mathbb{R}^n$. The topological boundary of a set is denoted by $\partial\mathcal{Z}$ and its interior by $\mathcal{Z}^\circ$. The closure of a set is denoted by $\overline{\mathcal{Z}}$ such that $\overline{\mathcal{Z}}$ includes both the interior and boundary of $\mathcal{Z}$. Commas in subscripts are used to distinguish between properties that are defined for multiple sets; e.g., $n_{g,z}$ describes the complexity of the representation of $\mathcal{Z}$ while $n_{g,w}$ describes the complexity of the representation of $\mathcal{W}$. The n-dimensional unit hypercube is denoted by

$$\mathcal{B}_\infty^n = \{x \in \mathbb{R}^n \mid \|x\|_\infty \leq 1\} \ ,$$

and the n-dimensional constrained unit hypercube is denoted by

$$\mathcal{B}_\infty^n(A, b) = \{x \in \mathbb{R}^n \mid \|x\|_\infty \leq 1 \ , \ Ax = b\} \ .$$

The set of all n-dimensional binary vectors is denoted by $\{-1, 1\}^n$, e.g.,

$$\{-1, 1\}^2 = \left\{ \begin{bmatrix} 1 \\ 1 \end{bmatrix}, \begin{bmatrix} 1 \\ -1 \end{bmatrix}, \begin{bmatrix} -1 \\ 1 \end{bmatrix}, \begin{bmatrix} -1 \\ -1 \end{bmatrix} \right\} .$$

The cardinality of the discrete set $\mathcal{T}$ is denoted by $|\mathcal{T}|$; e.g., $|\mathcal{T}| = 8$ for $\mathcal{T} = \{-1, 1\}^3$. The concatenation of two column vectors to a single column vector is denoted by $(\xi_1 \ \xi_2) = [\xi_1^T \ \xi_2^T]^T$. The bold $\mathbf{1}$ and $\mathbf{0}$ denote matrices of all 1 and 0 elements, respectively, and $\mathbf{I}$ denotes

the identity matrix with dimensions indicated by subscripts when not easily deduced from context.

2.2 Set Operations

Given the sets $\mathcal{Z}$, $\mathcal{W}$, $\mathcal{X} \subset \mathbb{R}^n$, $\mathcal{Y} \subset \mathbb{R}^m$, and matrix $R \in \mathbb{R}^{m \times n}$, the linear mapping of $\mathcal{Z}$ by R is given by (2.1a), the Minkowski sum of $\mathcal{Z}$ and $\mathcal{W}$ is given by (2.1b), the Minkowski difference, also referred to as the Pontryagin difference, of $\mathcal{W}$ from $\mathcal{Z}$ is given by (2.1c), the generalized intersection of $\mathcal{Z}$ and $\mathcal{Y}$ under R is given by (2.1d), the standard intersection for $R = \mathbf{I}$ is denoted by $\cap$, the union of $\mathcal{Z}$ and $\mathcal{W}$ is given by (2.1e), the closure of the complement of $\mathcal{Z}$ is given by (2.1f), the closure of the complement of $\mathcal{Z}$ defined over the set $\mathcal{X}$ is given by (2.1g), the support function of $\mathcal{Z}$ in a direction $l \in \mathbb{R}^n$ is given by (2.1h), the supporting halfspace in a direction $l \in \mathbb{R}^n$ is given by (2.1i) such that $\mathcal{Z} \subseteq \mathcal{H}_l^-$, the convex hull of $\mathcal{Z}$ is given by (2.1j), and the Cartesian product of $\mathcal{Z}$ and $\mathcal{Y}$ is given by (2.1k). The reader is directed to [50] and [51] for detailed discussions on these basic set operations.

$$R\mathcal{Z} = \{Rz \mid z \in \mathcal{Z}\} \tag{2.1a}$$

$$\mathcal{Z} \oplus \mathcal{W} = \{z + w \mid z \in \mathcal{Z},\ w \in \mathcal{W}\} \tag{2.1b}$$

$$\mathcal{Z} \ominus \mathcal{W} = \{x \in \mathbb{R}^n \mid x + w \in \mathcal{Z}\ \forall\, w \in \mathcal{W}\} \tag{2.1c}$$

$$\mathcal{Z} \cap_R \mathcal{Y} = \{z \in \mathcal{Z} \mid Rz \in \mathcal{Y}\} \tag{2.1d}$$

$$\mathcal{Z} \cup \mathcal{W} = \{x \in \mathbb{R}^n \mid x \in \mathcal{Z} \vee x \in \mathcal{W}\} \tag{2.1e}$$

$$\overline{\mathcal{Z}^c} = \{x \in \mathbb{R}^n \mid x \notin \mathcal{Z}^\circ\} \tag{2.1f}$$

$$\mathcal{C}_{\mathcal{X}}(\mathcal{Z}) = \{x \in \mathcal{X} \mid x \notin \mathcal{Z}^\circ\} \tag{2.1g}$$

$$\rho_{\mathcal{Z}}(l) = \sup_{z \in \mathcal{Z}} l^T z \tag{2.1h}$$

$$\mathcal{H}_l^- = \left\{z \in \mathbb{R}^n \;\middle|\; l^T z \leq \rho_{\mathcal{Z}}(l)\right\} \tag{2.1i}$$

$$\mathrm{CH}(\mathcal{Z}) = \left\{\sum_{\mathrm{i}=1}^{n} \lambda_{\mathrm{i}} z_{\mathrm{i}} \;\middle|\; \sum_{\mathrm{i}=1}^{n} \lambda_{\mathrm{i}} = 1, \lambda_{\mathrm{i}} \geq 0, z_{\mathrm{i}} \in \mathcal{Z},\ \forall\, \mathrm{i} \in \{1, \ldots, n\}, n \in \mathbb{N}\right\} \tag{2.1j}$$

$$\mathcal{Z} \times \mathcal{Y} = \{(z\ y) \mid z \in \mathcal{Z},\ y \in \mathcal{Y}\} \tag{2.1k}$$

2.3 Set Representations

In this section I provide a review of the existing set representations related to the presented work. I begin with a discussion on convex polytopes in their vertex and halfspace representations in Section 2.3.1 and the nonconvex representation of collections of convex polytopes as hyperplane arrangements in Section 2.3.2. I then discuss the representation of symmetric convex polytopes as zonotopes in Section 2.3.3 and their extension to the representation of arbitrary convex polytopes as constrained zonotopes in Section 2.3.4.

2.3.1 Convex Polytopes

A polytopic set is one with a topological boundary consisting of faces that may be defined by hyperplanes. Convex polytopes are compact sets that may be defined by the intersection of a collection of halfspaces, each one describing a face of the set.

Definition 2.3.1 (H-rep Polytope)**.** *The set $\mathcal{P} \subset \mathbb{R}^n$ is a convex polytope if there exists $H \in \mathbb{R}^{n \times n_h}$ and $f \in \mathbb{R}^{n_h}$ such that*

$$\mathcal{P} = \{x \in \mathbb{R}^n \mid Hx \leq f\} \ . \tag{2.2}$$

The convex polytope is given in its halfspace representation (H-rep) in Definition 2.3.1 and is equivalent to the intersection of a finite number of halfspaces as $\mathcal{P} = \bigcap_{\mathrm{i}=1}^{n_h} \mathcal{H}_\mathrm{i}^-$, where $\mathcal{H}_\mathrm{i}^- = \{x \in \mathbb{R}^n \mid h_\mathrm{i}^T x \leq f_\mathrm{i}\}$ is the i^{th} half space defined by the i^{th} row of the matrix H and vector f. Convex polytopes may also be represented by the collection of vertices at the intersections of the n_h halfspaces.

Definition 2.3.2 (V-rep Polytope)**.** *The set $\mathcal{P} \subset \mathbb{R}^n$ is a convex polytope if there exists $v_\mathrm{i} \in \mathbb{R}^n$ for $\mathrm{i} = 1, \ldots, n_v$ such that*

$$\mathcal{P} = \left\{ x = \sum_{\mathrm{i}=1}^{n_v} \alpha_\mathrm{i} v_\mathrm{i} \;\middle|\; \alpha_\mathrm{i} \geq 0,\ \sum_{\mathrm{i}=1}^{n_v} \alpha_\mathrm{i} = 1 \right\} \ . \tag{2.3}$$

The convex polytope is given in its vertex representation (V-rep) in Definition 2.3.2 and is equivalent to the convex hull of the discrete set of vertices $v_\mathrm{i} \in \mathbb{R}^n$ for $\mathrm{i} = 1, \ldots, n_v$. The

representation of a 2-dimensional polytope in both H- and V-rep is depicted in Figure 2.1. Convex polytopes given by their H- and V-representations are closed under linear mappings, Minkowski sums, and generalized intersections. In H-rep, the computation of generalized intersections and linear mappings is efficient if R is square and invertible [15] with time complexity scaling as $\mathcal{O}(n^3)$, and standard intersections scaling as $\mathcal{O}(1)$ [52]. However, the computational and representation complexity growth of Minkowski sums is exponential [15] with time complexity scaling as $\mathcal{O}(2^n)$ [52]. In V-rep, the computation of linear mappings and Minkowski sums is exponential with time complexity scaling as $\mathcal{O}(mn2^n)$ and $\mathcal{O}(n2^{2n})$ respectively [52]. The computation of generalized intersections in V-rep is NP-hard [16]. The use of convex polytopes over these basic set operations requires converting between H- and V-rep. Such conversions are cumbersome and involve computationally expensive vertex and facet enumeration [16], further limiting their use to problems with relatively small dimension (generally no greater than 5) and over short time horizons.

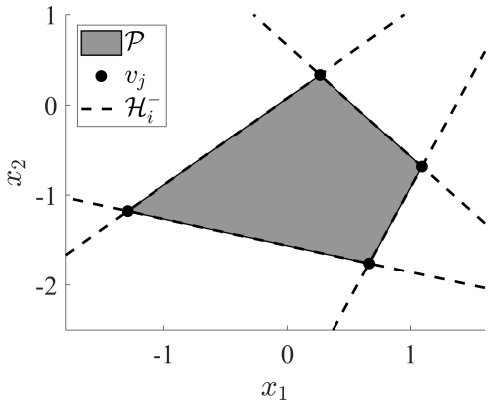

Figure 2.1. Example of representing a convex polytope in H- and V-rep.

2.3.2 Hyperplane Arrangements

The unions and complements of a collection of H-rep polytopes may be defined by introducing binary variables and linear mixed-integer inequality constraints. The general form of such nonconvex mixed-integer polyhedral sets is given by a hyperplane arrangement.

Definition 2.3.3 (Hyperplane Arrangement)**.** [13] *The set $\mathcal{A} \subseteq \mathbb{R}^n$ is a hyperplane arrangement if there exists a collection of sign tuples $\Sigma \subseteq \{-,+\}^{n_h}$ such that*

$$\mathcal{A} = \bigcup_{\sigma \in \Sigma} \mathcal{P}(\sigma) \,, \tag{2.4}$$

where $\mathcal{P}(\sigma) = \bigcap_{\mathrm{i}=1}^{n_h} \mathcal{H}_{\mathrm{i}}^{\sigma(\mathrm{i})}$, $\mathcal{H}_{\mathrm{i}}^{-} = \{x \in \mathbb{R}^n \mid h_{\mathrm{i}}^T x \leq f_{\mathrm{i}}\}$, and $\mathcal{H}_{\mathrm{i}}^{+} = \{x \in \mathbb{R}^n \mid h_{\mathrm{i}}^T x \geq f_{\mathrm{i}}\}$. If $\Sigma = \{\sigma \in \{-,+\}^{n_h} \mid \mathcal{P}(\sigma) \neq \emptyset\}$, then $\mathcal{A} = \mathbb{R}^n$ and $\mathcal{P}(\sigma)$ is a collection of convex, disjoint polytopes partitioning the space.

By considering the two halfspaces that are divided by the i^{th} hyperplane, $\mathcal{H}_{\mathrm{i}}^{-}$ and $\mathcal{H}_{\mathrm{i}}^{+}$, the hyperplane arrangement partitions the state space into a finite collection of disjoint cells [13]. Choosing sign tuples $\Sigma \subseteq \{-,+\}^{n_h}$ then allows the hyperplane arrangement to represent the union of a collection of H-rep polytopes by only enforcing specific combinations of the halfspace constraints to be active for each entry σ of the discrete set [13]. This approach may be used to define the closure of the complement of an H-rep polytope defined over a region of interest $\mathcal{X}$ as

$$\mathcal{C}_{\mathcal{X}}(\mathcal{P}) = \left\{ x \in \mathbb{R}^n \;\middle|\; Hx \geq f - M\alpha \,,\; \alpha \in \{0,1\}^{n_h},\; \sum_{\mathrm{i}=1}^{n_h} \alpha_{\mathrm{i}} \leq n_h - 1 \right\} , \tag{2.5}$$

where M is the so called Big-M constant [53] chosen sufficiently large such that

$$M \geq \max_{x \in \mathcal{X}} f - Hx \,. \tag{2.6}$$

The mixed-integer formulation given by (2.5) enforces that only one of the halfspace constraints is active at a time and leads to a unique set of sign tuples Σ, thus there exists a hyperplane arrangement such that $\mathcal{C}_{\mathcal{X}}(\mathcal{P}) = \mathcal{A}$ [13]. This approach may be extended to collections of polytopes as described in [54]. An example of the hyperplane arrangement representing the complement (2.5) of an H-rep polytope is depicted in Figure 2.2.

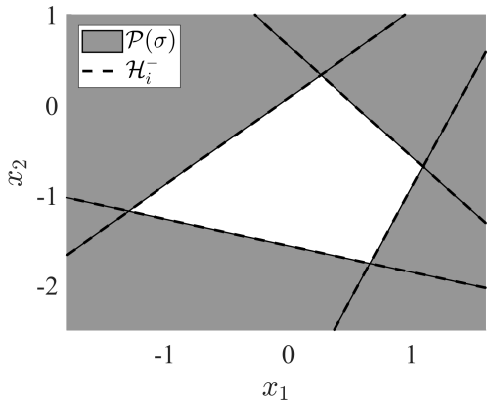

Figure 2.2. Example of the hyperplane arrangement representing the complement of a convex polytope given by (2.5).

2.3.3 Zonotopes

A zonotope is a centrally symmetric, convex polytope that may be represented as the affine image of a unit hypercube.

Definition 2.3.4 (G-rep Zonotope)**.** [17] *The set* $\mathcal{Z} \subset \mathbb{R}^n$ *is a zonotope if there exists* $G \in \mathbb{R}^{n \times n_g}$ *and* $c \in \mathbb{R}^n$ *such that*

$$\mathcal{Z} = \{G\xi + c \mid \xi \in \mathcal{B}_\infty^{n_g}\} \ . \tag{2.7}$$

The zonotope is given in Generator-representation (G-rep), and the shorthand notation of $\mathcal{Z} = \langle G, c \rangle \subset \mathbb{R}^n$ is used to denote the set given by (2.7). A zonotope is the set of points given by all linear combinations of the center c with the weighted generators—the columns of $G = \begin{bmatrix} g^{(1)} & \cdots & g^{(n_g)} \end{bmatrix}$—such that their weights $\xi = (\xi_1 \ \cdots \ \xi_{n_g})$, called factors, lie within the unit hypercube $\mathcal{B}_\infty^{n_g} = \{\xi \in \mathbb{R}^{n_g} \mid \|\xi\|_\infty \leq 1\}$. A zonotope is therefore equivalent to the Minkowski sum of a collection of closed line segments, the $g^{(\mathrm{i})}$ generators in G, shifted by the center, c. An example of a two-dimensional zonotope represented by three generators is depicted in Figure 2.3. The zonotope $\mathcal{Z} \subset \mathbb{R}^n$ is n dimensional for any $n_g \geq n$ number of generators such that the rank of G is equal to n; in other words, the column space of G spans $\mathbb{R}^n$. The complexity of the set is reflected by the number of generators, n_g, and the order of the zonotope is defined as $o = n_g/n$. When the dimension of G is unrestricted, the

center and generator matrix can be constructed to represent any compact polytope that is both convex and centrally symmetric.

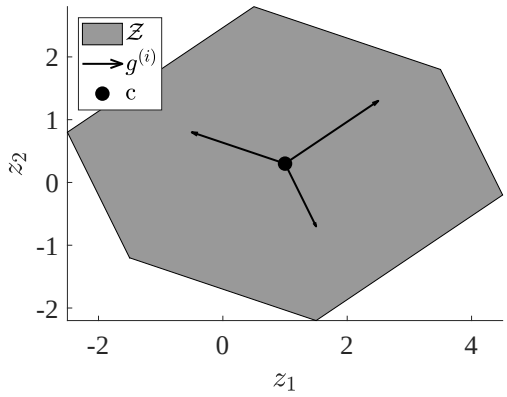

Figure 2.3. Example of representing a symmetric, convex polytope as a zonotope in G-rep.

Zonotopes are able to compactly represent convex polytopes because of their combinatorial nature resulting in the representation of sets with up to $2\binom{n_g}{n}$ features [55]. The conversion from a zonotope in G-rep to an H-rep polytope is therefore a computationally expensive enumeration problem [11]. Another beneficial attribute is that the linear mappings and Minkowski sums of the zonotopes $\mathcal{Z} = \langle G_z, c_z \rangle \subset \mathbb{R}^n$ and $\mathcal{W} = \langle G_w, c_w \rangle \subset \mathbb{R}^n$ may be computed efficiently through the identities:

$$R\mathcal{Z} = \langle RG_z, Rc_z \rangle \,, \tag{2.8a}$$

$$\mathcal{Z} \oplus \mathcal{W} = \langle [G_z \; G_w], c_z + c_x \rangle \,. \tag{2.8b}$$

The time complexity of linear mappings given by (2.8a) scales as $\mathcal{O}(mn^2)$ for matrix $R \in \mathbb{R}^{m \times n}$, and that of Minkowski sums given by (2.8b) scales as $\mathcal{O}(n)$ [10]. These computationally efficient set operations allow zonotopes to be used for high dimensional problems; however, the complexity of the set grows as $n_g = n_{g,z} + n_{g,w}$ for Minkowski sums.

2.3.4 Constrained Zonotopes

The utility of the zonotope may be extended by adding a set of linear equality constraints to the mapped unit hypercube.

Definition 2.3.5 (CG-rep Constrained Zonotope)**.** [18] *The set $\mathcal{Z}_c \subset \mathbb{R}^n$ is a constrained zonotope if there exists $G \in \mathbb{R}^{n \times n_g}$, $c \in \mathbb{R}^n$, $A \in \mathbb{R}^{n_c \times n_g}$, and $b \in \mathbb{R}^{n_c}$ such that*

$$\mathcal{Z}_c = \{G\xi + c \mid \xi \in \mathcal{B}_\infty^{n_g},\ A\xi = b\}\ . \tag{2.9}$$

The constrained zonotope is given in Constrained Generator-representation (CG-rep), and the shorthand notation of $\mathcal{Z}_c = \langle G, c, A, b\rangle \subset \mathbb{R}^n$ is used to denote the set given by (2.9). Through the addition of the linear equality constraints $A\xi = b$, the affine image of the constrained constrained unit hypercube $\mathcal{B}_\infty^{n_g}(A, b) = \{\xi \in \mathbb{R}^{n_g} \mid \|\xi\|_\infty \leq 1,\ A\xi = b\}$ is no longer restricted to be symmetric. Indeed when the number of generators n_g and constraints n_c are unrestricted, a constrained zonotope may be constructed to represent any convex polytope [18]. Consider the example constrained zonotope $\mathcal{Z}_c = \langle G_z, c_z, A_z, b_z\rangle \subset \mathbb{R}^2$ given by [18]

$$\mathcal{Z}_c = \left\langle \begin{bmatrix} 1.5 & -1.5 & 0.5 \\ 1 & 0.5 & -1 \end{bmatrix}, \begin{bmatrix} 0 \\ 0 \end{bmatrix}, \begin{bmatrix} 1 & 1 & 1 \end{bmatrix}, 1 \right\rangle\ . \tag{2.10}$$

From the definition of the constrained zonotope, the zonotope defined by $\mathcal{Z} = \langle G_z, c_z\rangle$ will satisfy $\mathcal{Z}_c \subseteq \mathcal{Z}$ as $\mathcal{Z}_c$ and $\mathcal{Z}$ share the same generators; however, $\mathcal{Z}_c$ has fewer degrees of freedom due to the additional equality constraints. This relationship between zonotopes and constrained zonotopes is depicted in Fig 2.4. The degree of freedom order of a constrained zonotope is defined as $o_d = (n_g - n_c)/n$. When the G and A matrices are full rank, a necessary condition that a constrained zonotope will form an n dimensional subset of $\mathbb{R}^n$ is given by $o_d \geq 1$.

Constrained zonotopes are closed under linear mappings, Minkowski sums, and intersections, so that performing these operations on constrained zonotopes results in yet another constrained zonotope. Linear mappings and Minkowski sums follow directly from the identities for zonotopes (2.8), while generalized intersections add an additional k constraints.

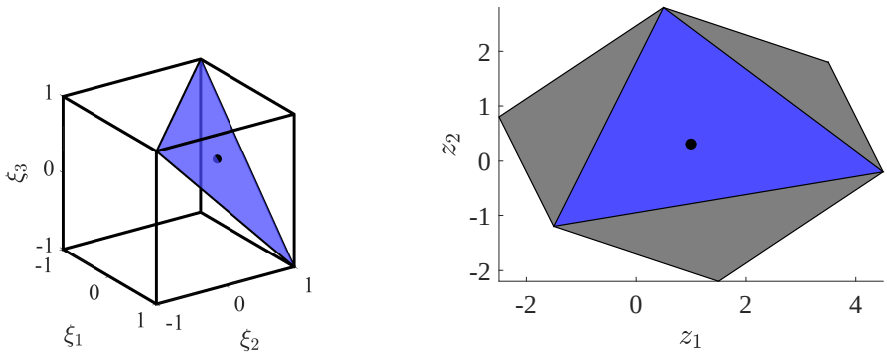

(a) (b)

Figure 2.4. Example of a constrained zonotope given by (2.10). (2.4a) Constrained unit hypercube $\mathcal{B}_\infty^3(A, b)$. (2.4b) Constrained zonotope $\mathcal{Z}_c = \langle G_z, c_z, A_z, b_z \rangle$ generated as the affine image of the constrained unit hypercube plotted over $\mathcal{Z} = \langle G_z, c_z \rangle$ taken as the affine image of the entire unit hypercube.

For $\mathcal{Z} = \langle G_z, c_z, A_z, b_z \rangle$, $\mathcal{W} = \langle G_w, c_w, A_w, b_w \rangle \subset \mathbb{R}^n$, $\mathcal{Y} = \langle G_y, c_y, A_y, b_y \rangle \subset \mathbb{R}^m$, and $R \in \mathbb{R}^{m \times n}$, these basic set operations are determined through the following identities [18]:

$$R\mathcal{Z} = \langle RG_z, Rc_z, A_z, b_z \rangle, \tag{2.11a}$$

$$\mathcal{Z} \oplus \mathcal{W} = \left\langle \begin{bmatrix} G_z & G_w \end{bmatrix}, c_z + c_w, \begin{bmatrix} A_z & \mathbf{0} \\ \mathbf{0} & A_w \end{bmatrix}, \begin{bmatrix} b_z \\ b_w \end{bmatrix} \right\rangle, \tag{2.11b}$$

$$\mathcal{Z} \cap_R \mathcal{Y} = \left\langle \begin{bmatrix} G_z & \mathbf{0} \end{bmatrix}, c_z, \begin{bmatrix} A_z & \mathbf{0} \\ \mathbf{0} & A_y \\ RG_z & -G_y \end{bmatrix}, \begin{bmatrix} b_z \\ b_y \\ c_y - Rc_z \end{bmatrix} \right\rangle. \tag{2.11c}$$

The time complexity of linear mappings given by (2.11a) scales as $\mathcal{O}(mn^2)$, that of Minkowski sums given by (2.11b) scales as $\mathcal{O}(n)$, that of generalized intersections given by (2.11c) scales as $\mathcal{O}(mn^2)$ and reduces to $\mathcal{O}(n)$ for standard intersections when $R = \mathbf{I}$ [10]. Similar to zonotopes, these basic set operations of constrained zonotopes are efficient and scale well to high dimensional problems; however, the representation complexity includes growth in both the number of generators and constraints. The representation complexity of Minkowski sums

grows as $n_g = n_{g,z} + n_{g,w}$ and $n_c = n_{c,z} + n_{c,w}$. The representation complexity of generalized intersections grows as $n_g = n_{g,z} + n_{g,y}$ and $n_c = n_{c,z} + n_{c,y} + m$.

2.4 Reachability Analysis

Reachability analysis consists of computing the set of states reachable by a dynamic system from a specified set for all admissible inputs and disturbances to the system [1]. The reachability problem may be formulated in either the forward or backward sense, that is:

- Forward reachability answers the question "Given a set of states $\mathcal{R}_k$ at time k, find the set of all states that may be reached from $\mathcal{R}_k$ at time $k+T$."
- Backward reachability answers the question "Given a set of states $\mathcal{R}_{T+k}$ at time $T+k$, find the set of all states at time k that the set is reachable by."

Forward reachability is most often deployed for safety verification and may be used to provide *a posteriori* certificates of a system's robustness [56], while backward reachability is often used in dynamic games [39], synchronizing layers of hierarchical controllers [21], and generating controlled invariant sets [14]. Both the forward and backward propagation of sets may be considered in the open or closed-loop case and is well established in the literature for linear time-invariant systems using convex sets.

Consider the discrete-time dynamic system modeled by the difference equation

$$x_+ = f(x, u, v)\,, \tag{2.12}$$

where $x \in \mathbb{R}^{n_x}$ is the state of the system, $u \in \mathbb{R}^{n_u}$ is the controllable input to the system belonging to the compact set of all admissible inputs $\mathcal{U} \subset \mathbb{R}^{n_u}$, and $v \in \mathbb{R}^{n_v}$ is a disturbance belonging to the compact set $\mathcal{V} \subset \mathbb{R}^{n_v}$. Beginning from a set of initial states $\mathcal{X}_0$, the set of states reachable by the dynamic system (2.12) in one discrete time step is then given by the forward reachable set

$$\mathcal{R}_+ = \{x_+ \in \mathbb{R}^{n_x} \mid \exists\, x \in \mathcal{X}_0,\ u \in \mathcal{U},\ v \in \mathcal{V},\ \text{s.t. } x_+ = f(x, u, v)\}\ . \tag{2.13}$$

The set $\mathcal{R}_+$ given by (2.13) is the set of all states such that there exists a trajectory given by the solution of (2.12) from an initial state $x \in \mathcal{X}_0$ under an admissible control input $u \in \mathcal{U}$ and possible disturbance $v \in \mathcal{V}$ [1], [10], [14]. Given a set of states $\mathcal{X}$, the set of states that $\mathcal{X}$ is reachable from for all possible disturbances through the dynamic system (2.12) in one discrete time step is then given by the backward reachable set

$$\mathcal{R}_- = \{x_- \in \mathbb{R}^{n_x} \mid \exists u \in \mathcal{U}, \text{ s.t. } f(x_-, u, v) \subseteq \mathcal{X} \, \forall \, v \in \mathcal{V}\} \ . \tag{2.14}$$

The set $\mathcal{R}_-$ given by (2.14) is the set of all states that can be driven to $\mathcal{X}$ by some admissible control input $u \in \mathcal{U}$ despite any possible disturbance $v \in \mathcal{V}$ [1], [14].

When (2.12) is given by the discrete-time linear time-invariant system $x_+ = Ax+Bu+Wv$ with $\mathcal{X}_0, \mathcal{U}$, and $\mathcal{V}$ given by convex polytopes, the forward reachable set (2.13) may be found using basic set operations as [14]

$$\mathcal{R}_+ = A\mathcal{X}_0 \oplus B\mathcal{U} \oplus W\mathcal{V} \, . \tag{2.15}$$

Similarly, when the state transition matrix A is invertible and the target set $\mathcal{X}$ is given by a convex polytope, the backward reachable set (2.14) may be found using basic set operations as [14]

$$\mathcal{R}_- = A^{-1}((\mathcal{X} \ominus W\mathcal{V}) \oplus (-B\mathcal{U})) \, . \tag{2.16}$$

The methods given by (2.15) and (2.16) are classified as set propagation techniques for reachability analysis and may be applied iteratively to find the set of states reachable in k time steps, denoted by $\mathcal{R}_k$ [10].

3. HYBRID ZONOTOPES

This chapter introduces the *hybrid zonotope* set definition, as presented in the two manuscripts by Trevor J. Bird, Herschel C. Pangborn, Neera Jain, and Justin P. Koeln in [57], provisionally accepted by *Automatica*, and Trevor J. Bird and Neera Jain in the *IEEE Control Systems Letters* [58], and is included here with minor modifications. In Section 3.1 I formally define the hybrid zonotope, discuss its relation to constrained zonotopes, and provide two illustrative examples. In Section 3.2 I prove the hybrid zonotopes' closure under linear mappings, Minkowski sums, generalized intersections, halfspace intersections, Cartesian products, unions, and complements. Beyond set operations, Section 3.2 demonstrates how the point and set containment of hybrid zonotopes may be determined by evaluating the feasibility of a mixed-integer linear program, as well as how to determine bounds and convex enclosures. In Section 3.3 I describe how the hybrid zonotope forms a binary tree that may be leveraged to reduce the complexity of converting the hybrid zonotope into a collection of convex subsets. Finally, in Section 3.4 I provide a numerical example demonstrating how the complements of hybrid zonotopes may be used as safety constraints in an obstacle avoidance problem. All technical contributions of this chapter were made by Trevor J. Bird while being advised by Professor Neera Jain at Purdue University, as well as Professor Justin P. Koeln (University of Texas Dallas) and Professor Herschel Pangborn (The Pennsylvania State University).

3.1 Set Definition

This section introduces the definition of hybrid zonotopes as an extension of the constrained zonotope through the addition of a vector of binary factors.

Definition 3.1.1 (HCG-rep Hybrid Zonotope)**.** *The set $\mathcal{Z}_h \subset \mathbb{R}^n$ is a hybrid zonotope if there exists $G^c \in \mathbb{R}^{n\times n_g}$, $G^b \in \mathbb{R}^{n\times n_b}$, $c \in \mathbb{R}^n$, $A^c \in \mathbb{R}^{n_c\times n_g}$, $A^b \in \mathbb{R}^{n_c\times n_b}$, and $b \in \mathbb{R}^{n_c}$ such that*

$$\mathcal{Z}_h = \left\{ \begin{bmatrix} G^c & G^b \end{bmatrix} \begin{bmatrix} \xi^c \\ \xi^b \end{bmatrix} + c \;\middle|\; \begin{bmatrix} \xi^c \\ \xi^b \end{bmatrix} \in \mathcal{B}_\infty^{n_g} \times \{-1,1\}^{n_b}, \; \begin{bmatrix} A^c & A^b \end{bmatrix} \begin{bmatrix} \xi^c \\ \xi^b \end{bmatrix} = b \right\}. \tag{3.1}$$

The hybrid zonotope is given in *Hybrid Constrained Generator-representation* (HCG-rep), and the shorthand notation of $\mathcal{Z}_h = \langle G^c, G^b, c, A^c, A^b, b\rangle \subset \mathbb{R}^n$ is used to denote the set given by (3.1). When $n_b = 0$, the hybrid zonotope set representation is equivalent to the constrained zonotope given by Def. 2.3.5. When $n_b \neq 0$, the vector of binary factors may take on values from the discrete set $\{-1, 1\}^{n_b}$ containing 2^{n_b} elements. The hybrid zonotope therefore consists of a mapping of a continuous space shifted by contributions from a discrete, finite set. This shifting in equality constraints and centers is depicted in Fig. 3.1 where a single binary factor having $G^b = \mathbf{1}$ and $A^b = 1$ is added to the example constrained zonotope (2.10) resulting in

$$\mathcal{Z}_h = \left\langle \begin{bmatrix} 1.5 & -1.5 & 0.5 \\ 1 & 0.5 & -1 \end{bmatrix}, \begin{bmatrix} 1 \\ 1 \end{bmatrix}, \begin{bmatrix} 0 \\ 0 \end{bmatrix}, \begin{bmatrix} 1 & 1 & 1 \end{bmatrix}, 1, 1 \right\rangle . \tag{3.2}$$

Given that $\|\xi^b\|_\infty = 1$ for all $\xi^b \in \{-1, 1\}^{n_b}$, the hybrid zonotope is a more general class than the zonotope and constrained zonotope set representations. That is, the hybrid zonotope definition includes one additional constraint on the space of factors being projected – namely, that some of them must be binary.

Lemma 3.1.1. *Given any hybrid zonotope* $\mathcal{Z}_h = \langle G^c, G^b, c, A^c, A^b, b\rangle \subset \mathbb{R}^n$*, the zonotope* $\mathcal{Z} = \langle [G^c\ G^b], c\rangle \subset \mathbb{R}^n$ *and constrained zonotope* $\mathcal{Z}_c = \langle [G^c\ G^b], c, [A^c\ A^b], b\rangle \subset \mathbb{R}^n$ *satisfy* $\mathcal{Z}_h \subseteq \mathcal{Z}_c \subseteq \mathcal{Z}$*.*

Proof. For any $z \in \mathcal{Z}_h$ there exists some $\|\xi^c\|_\infty \leq 1$ and $\xi^b \in \{-1, 1\}^{n_b}$ such that $A^c\xi^c + A^b\xi^b = b$ and $z = G^c\xi^c + G^b\xi^b + c$. Letting $\xi = (\xi^c\ \xi^b)$ implies that $\|\xi\|_\infty \leq 1$, $z = [G^c G^b]\xi + c$, and $[A^c\ A^b]\xi = b$, thus $z \in \mathcal{Z}_c$ and $\mathcal{Z}_h \subseteq \mathcal{Z}_c$. Furthermore, for any $z \in \mathcal{Z}_c$ there exists some ξ such that $\|\xi\|_\infty \leq 1$, $[A^c\ A^b]\xi = b$, and $z = [G^c\ G^b]\xi + c$, thus $z \in \mathcal{Z}$, $\mathcal{Z}_c \subseteq \mathcal{Z}$, and therefore $\mathcal{Z}_h \subseteq \mathcal{Z}_c \subseteq \mathcal{Z}$. □

The equivalence of the hybrid zonotope with a finite collection of constrained zonotopes is established through the following theorem relying on the closure of hybrid zonotopes under union operations as proven in Section 3.2.2.

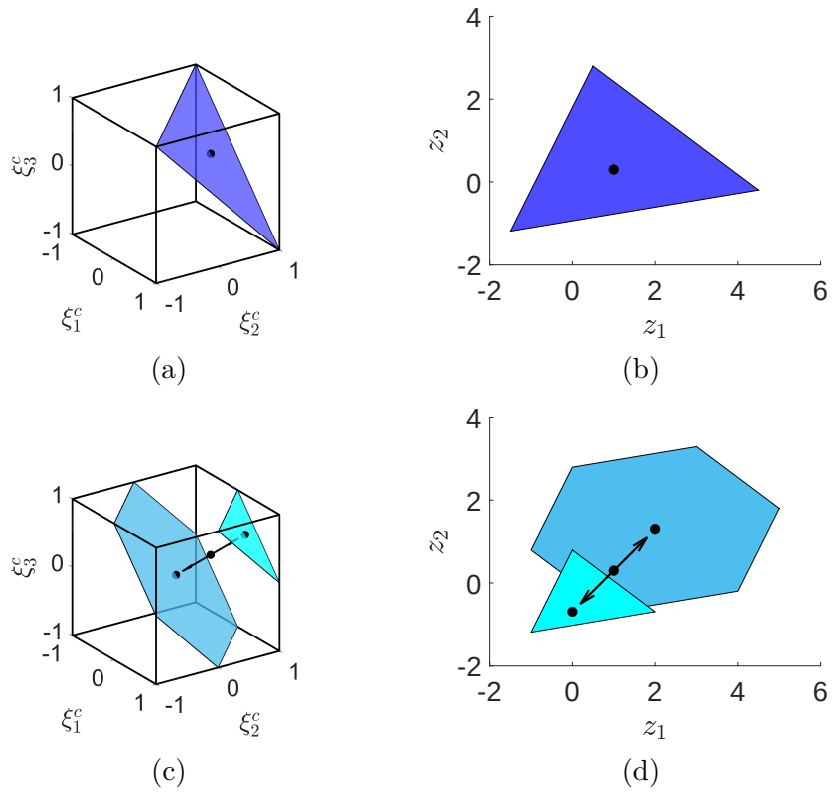

Figure 3.1. Example hybrid zonotope (3.2) generated by adding one binary factor to the constrained zonotope (2.10). (3.1a) Constrained unit hypercube $\mathcal{B}^3_\infty(A^c, b)$. (3.1b) Constrained zonotope taken as the affine image of (3.1a), $\mathcal{Z}_c = G^c\mathcal{B}^3_\infty(A^c, b) \oplus c$. (3.1c) Adding one binary factor to the constrained unit hypercube results in two possible shifts in the hyperplane, $A^c\xi^c = b - A^b\xi^b_1$ and $A^c\xi^c = b - A^b\xi^b_2$, one for each entry of the discrete set $\xi^b_{\rm i} \in \{-1, 1\}$. (3.1d) Hybrid zonotope taken as the affine image of (3.1c) with shifted centers, $\mathcal{Z}_h = G^c\mathcal{B}^3_\infty(A^c, b - A^b\xi^b_1) \oplus (c + G^b\xi^b_1) \cup G^c\mathcal{B}^3_\infty(A^c, b - A^b\xi^b_2) \oplus (c + G^b\xi^b_2)$.

Theorem 3.1.1. *The set $\mathcal{Z}_h \subset \mathbb{R}^n$ is a hybrid zonotope if and only if it is the union of a finite number of constrained zonotopes.*

Proof. Let $\xi^b_{\rm i}$ be an entry of the discrete set $\{-1, 1\}^{n_b}$ containing 2^{n_b} elements. Define the constrained zonotope

$$\mathcal{Z}_{c,{\rm i}} = \left\langle G^c, c + G^b\xi^b_{\rm i}, A^c, b - A^b\xi^b_{\rm i} \right\rangle . \tag{3.3}$$

For any $z \in \mathcal{Z}_{c,\mathrm{i}}$ there exists some $\xi^c \in \mathcal{B}_\infty^{n_g}$ such that $z = G^c\xi^c + G^b\xi^b_\mathrm{i} + c$ and $A^c\xi^c + A^b\xi^b_\mathrm{i} = b$. Thus $z \in \mathcal{Z}_h$. Given that the choice of z is arbitrary and the set $\{-1,1\}^{n_b}$ is finite,

$$\bigcup_{\mathrm{i}=1}^{2^{n_b}} \mathcal{Z}_{c,\mathrm{i}} \subseteq \mathcal{Z}_h \,.$$

For any $z \in \mathcal{Z}_h$, there exists some $\xi^c \in \mathcal{B}_\infty^{n_g}$ and $\xi^b \in \{-1,1\}^{n_b}$ such that $z = G^c\xi^c + G^b\xi^b + c$ and $A^c\xi^c + A^b\xi^b = b$. Also, for $\xi^b = \xi^b_\mathrm{i} \Rightarrow z \in \mathcal{Z}_{c,\mathrm{i}}$, thus

$$\mathcal{Z}_h \subseteq \bigcup_{\mathrm{i}=1}^{2^{n_b}} \mathcal{Z}_{c,\mathrm{i}} \,,$$

and $\mathcal{Z}_h = \bigcup_{\mathrm{i}=1}^{2^{n_b}} \mathcal{Z}_{c,\mathrm{i}}$.

Conversely, given any finite collection of constrained zonotopes $\mathcal{Z}_{c,\mathrm{i}} \subset \mathbb{R}^n$ for $\mathrm{i} = 1,\dots,N$, the hybrid zonotope generated by successive union operations as $\mathcal{Z}_h = \mathcal{Z}_{c,1} \cup (\mathcal{Z}_{c,2} \cup (\cdots \cup \mathcal{Z}_{c,N}))$ is an exact representation of the union of the N constrained zonotopes by Proposition 3.2.6, therefore $\bigcup_{\mathrm{i}=1}^{N} \mathcal{Z}_{c,\mathrm{i}} = \mathcal{Z}_h$. □

The hybrid zonotope exhibits the same combinatorial properties as zonotopes, where a symmetric polytope with up to $2\binom{n_g}{n}$ features may be represented with n_g continuous factors [55]. Introducing n_b binary factors, the hybrid zonotope may represent 2^{n_b} zonotopes each having potentially $2\binom{n_g}{n}$ features. This concept is further explored through the following example.

Example 3.1.1. *Let the set $\mathcal{Z}_c = \langle G_z, c_z, A_z, b_z\rangle \subset \mathbb{R}^2$ be the example constrained zonotope given in [18], where*

$$\mathcal{Z}_c = \left\langle \begin{bmatrix} 1.5 & -1.5 & 0.5 \\ 1 & 0.5 & -1 \end{bmatrix}, \begin{bmatrix} 0 \\ 0 \end{bmatrix}, \begin{bmatrix} 1 & 1 & 1 \end{bmatrix}, 1 \right\rangle ,$$

and define a hybrid zonotope with continuous generators $G^c = G_z$, binary generators $G^b = 2G_z$, and center c_z giving

$$\mathcal{Z}_{h,1} = \langle G_z, 2G_z, c_z, \emptyset, \emptyset, \emptyset\rangle \,. \tag{3.4}$$

By adding $n_b = 3$ binary factors, $\mathcal{Z}_{h,1}$ is equivalent to $2^{n_b} = 8$ copies of the zonotope $\mathcal{Z} = \langle G_z, c_z \rangle$ with centers shifted by $2G_z\xi^b \ \forall \ \xi^b \in \{-1, 1\}^3$, as depicted in Fig. 3.2a. Defining another hybrid zonotope that includes linear equality constraints on the continuous factors as $A^c = A_z$, $A^b = \mathbf{0}$, and $b = b_z$ giving

$$\mathcal{Z}_{h,2} = \langle G_z, 2G_z, c_z, A_z, \mathbf{0}, b_z \rangle \ , \tag{3.5}$$

results in a hybrid zonotope equivalent to eight copies of the constrained zonotope $\mathcal{Z}_c$, again with centers shifted by the contribution of the binary generators as shown in Fig. 3.2b. Including the binary factors in the equality constraints by defining another hybrid zonotope with $A^b = A_z$ gives

$$\mathcal{Z}_{h,3} = \langle G_z, 2G_z, c_z, A_z, A_z, b_z \rangle \ , \tag{3.6}$$

as shown in Fig. 3.2c. In contrast to the previous hybrid zonotopes, $\mathcal{Z}_{h,3}$ does not represent identical copies. Instead, the linear equality constraints on the continuous factors are also shifted by each of the eight discrete values of the binary factors. When doing so, it is possible that these shifted equality constraints may be infeasible and thus map to empty constrained zonotopes, which happens exactly once in the given example.

The result of Theorem 3.1.1 provides a method of converting from a hybrid zonotope to a collection of constrained zonotopes, and vice versa, allowing methods developed for the analysis and visualization of other set representations to be applied to hybrid zonotopes. However, the conversion from HCG-rep to a collection of CG-reps, $\mathcal{Z}_{c,\mathrm{i}} \forall \mathrm{i} \in \{1, \ldots, 2^{n_b}\}$ given by (3.3), is an enumeration problem that grows exponentially with respect to the number of binary factors. Use of the hybrid zonotope is therefore most advantageous when these conversions are not necessary and the set may be used directly for the analysis and control of complex dynamical systems, as discussed in the remainder of this dissertation.

3.2 Set Operations

This section proves the hybrid zonotopes closure under linear mappings, Minkowski sums, generalized intersections, halfspace intersections, Cartesian products, unions, and comple-

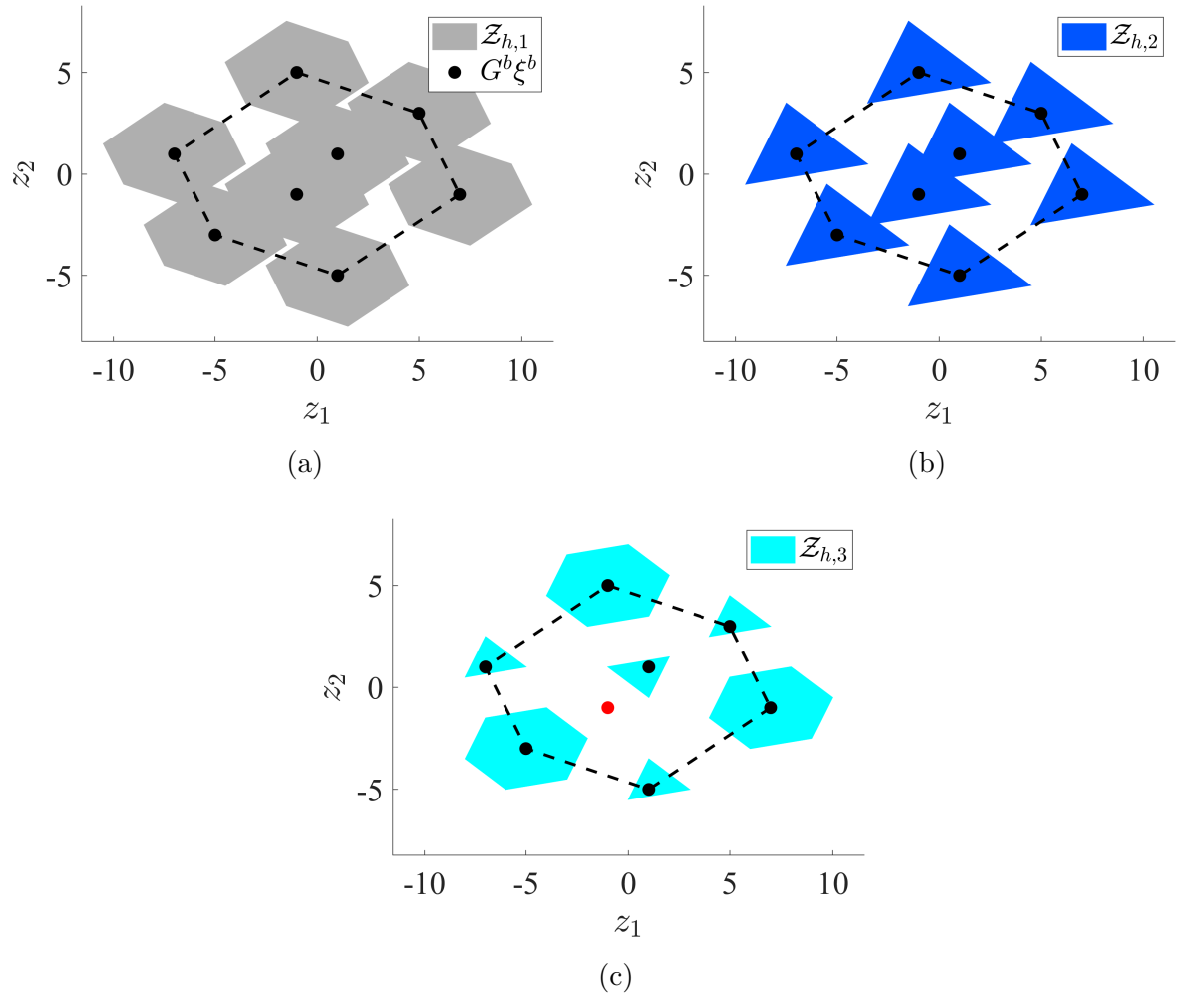

Figure 3.2. Hybrid zonotopes given in Ex. 3.1.1. Note that the convex hull of the eight discrete points given by $G^b\xi^b$ is equivalent to the zonotope $\mathcal{Z} = \langle G^b, \mathbf{0} \rangle$ as depicted by the dashed lines. (3.2a) Without linear equality constraints, the hybrid zonotope $\mathcal{Z}_{h,1}$, given by (3.4), represents eight copies of a continuous zonotope with centers shifted by the contribution of the binary factors and generators. (3.2b) Including constraints on only the continuous factors results in $\mathcal{Z}_{h,2}$, given by (3.5), and is equivalent to eight copies of the constrained zonotope $\mathcal{Z}_c$. (3.2c) When the equality constraints include terms for the binary factors in $\mathcal{Z}_{h,3}$, given by (3.6), the shifted constrained zonotopes are no longer identical. Also note that in this final case, the discrete value of the binary factors depicted by the red • results in an infeasible set of continuous constraints and thus maps to an empty constrained zonotope.

ments. The derivation of the identities for linear mappings, Minkowski sums, generalized intersections, halfspace intersections, and Cartesian Products are provided in Section 3.2.1

and follow closely from those derived for constrained zonotopes. The union and complement operations require the embedding of mixed-integer constraints, as discussed in Section 3.2.2 and 3.2.3. The time complexity and specific growth in set representation complexity for each set operation is discussed at the end of the respective section. In Section 3.2.4 it is shown how the point and set containment of hybrid zonotopes may be verified by evaluating the feasibility of a mixed-integer linear program. In Section 3.2.5 it is shown how the bounds of a hybrid zonotope in a given direction may be determined by evaluating the set's support function, and that these bounds can be used to define tight convex enclosures.

3.2.1 Linear Mappings, Minkowski Sums, Generalized Intersections, Halfspace Intersections, and Cartesian Products

The identities for linear mappings, Minkowski sums, generalized intersections [18, Prop. 1], and halfspace intersections [20, Thm. 1] of constrained zonotopes may be extended to hybrid zonotopes by including the additional binary constraint as follows. The Cartesian product is also defined similar to those of zonotopes and constrained zonotopes.

Proposition 3.2.1 (Linear Mapping)**.** *For any hybrid zonotope*

$$\mathcal{Z}_h = \left\langle G_z^c, G_z^b, c_z, A_z^c, A_z^b, b_z \right\rangle \subset \mathbb{R}^n \,,$$

and matrix $R \in \mathbb{R}^{m \times n}$*, the linear mapping of* $\mathcal{Z}_h$ *by* R *is given by*

$$R\mathcal{Z}_h = \left\langle RG_z^c, RG_z^b, Rc_z, A_z^c, A_z^b, b_z \right\rangle \,. \tag{3.7}$$

Proof. For ease of readability, let $\xi_z = (\xi_z^c \ \xi_z^b)$, $G_z = [G_z^c \ G_z^b]$, and $A_z = [A_z^c \ A_z^b]$. Let $\mathcal{Z}_R$ denote the hybrid zonotope given by the right-hand side of (3.7). For any point $z \in \mathcal{Z}_h$ there exists some $\xi_z \in \mathcal{B}_\infty^{n_{g,z}} \times \{-1, 1\}^{n_{b,z}}$ such that $A_z\xi_z = b_z$ and $z = G_z\xi_z + c_z$. Multiplying both sides of z by R gives $Rz = RG_z\xi_z + Rc_z$ and $Rz \in \mathcal{Z}_R$, thus $R\mathcal{Z}_h \subseteq \mathcal{Z}_R$.

Conversely, for any point $r \in \mathcal{Z}_R$ there exists some $\xi_r \in \mathcal{B}_\infty^{n_{g,z}} \times \{-1, 1\}^{n_{b,z}}$ such that $A_z\xi_r = b_z$ and $r = RG_z\xi_r + Rc_z$. Thus there exists some $z \in \mathcal{Z}_h$ such that $Rz = r$. Therefore $\mathcal{Z}_R \subseteq R\mathcal{Z}_h$ and $R\mathcal{Z}_h = \mathcal{Z}_R$. □

Proposition 3.2.2 (Minkowski Sum)**.** *For any hybrid zonotopes*

$$\mathcal{Z}_h = \left\langle G_z^c, G_z^b, c_z, A_z^c, A_z^b, b_z \right\rangle \subset \mathbb{R}^n \,,$$
$$\mathcal{W}_h = \left\langle G_w^c, G_w^b, c_w, A_w^c, A_w^b, b_w \right\rangle \subset \mathbb{R}^n \,,$$

the Minkowski sum of $\mathcal{Z}_h$ *and* $\mathcal{W}_h$ *is given by*

$$\mathcal{Z}_h \oplus \mathcal{W}_h = \left\langle \begin{bmatrix} G_z^c & G_w^c \end{bmatrix}, \begin{bmatrix} G_z^b & G_w^b \end{bmatrix}, c_z + c_w, \begin{bmatrix} A_z^c & \mathbf{0} \\ \mathbf{0} & A_w^c \end{bmatrix}, \begin{bmatrix} A_z^b & \mathbf{0} \\ \mathbf{0} & A_w^b \end{bmatrix}, \begin{bmatrix} b_z \\ b_w \end{bmatrix} \right\rangle . \tag{3.8}$$

Proof. For ease of readability, let $\xi_{\mathrm{i}} = (\xi_{\mathrm{i}}^c \ \xi_{\mathrm{i}}^b)$, $G_{\mathrm{i}} = [G_{\mathrm{i}}^c \ G_{\mathrm{i}}^b]$, and $A_{\mathrm{i}} = [A_{\mathrm{i}}^c \ A_{\mathrm{i}}^b]$ for $\mathrm{i} = z,\ w$. Let $\mathcal{X}$ denote the hybrid zonotope given by the right-hand side of (3.8). For any $z \in \mathcal{Z}_h$ there exists some $\xi_z \in \mathcal{B}_\infty^{n_{g,z}} \times \{-1,1\}^{n_{b,z}}$ such that $A_z\xi_z = b_z$ and $z = G_z\xi_z + c_z$. Similarly for any $w \in \mathcal{W}_h$ there exists some $\xi_w \in \mathcal{B}_\infty^{n_{g,w}} \times \{-1,1\}^{n_{b,w}}$ such that $A_w\xi_w = b_w$ and $w = G_w\xi_w + c_w$. Let $\xi_x^c = (\xi_z^c \ \xi_w^c)$ and $\xi_x^b = (\xi_z^b \ \xi_w^b)$. Then $\xi_x \in \mathcal{B}_\infty^{n_{g,z}+n_{g,w}} \times \{-1,1\}^{n_{b,z}+n_{b,w}}$ and

$$\begin{bmatrix} A_z^c & \mathbf{0} \\ \mathbf{0} & A_w^c \end{bmatrix} \xi_x^c + \begin{bmatrix} A_z^b & \mathbf{0} \\ \mathbf{0} & A_w^b \end{bmatrix} \xi_x^b = \begin{bmatrix} b_z^b \\ b_w^b \end{bmatrix} . \tag{3.9}$$

Adding z and w together gives

$$z + w = [G_z^c \ G_w^c]\xi_x^c + [G_z^b \ G_w^b]\xi_x^b + (c_z + c_w) \,, \tag{3.10}$$

thus $z + w \in \mathcal{X}$ and $\mathcal{Z}_h \oplus \mathcal{W}_h \subseteq \mathcal{X}$.

Conversely, for any $x \in \mathcal{X}$ there exists some $\xi_x \in \mathcal{B}_\infty^{n_{g,z}+n_{g,w}} \times \{-1,1\}^{n_{b,z}+n_{b,w}}$ such that (3.9) holds and $x = z + w$ as defined by (3.10). Letting $\xi_x^c = (\xi_z^c \ \xi_w^c)$ and $\xi_x^b = (\xi_z^b \ \xi_w^b)$ gives $x \in \mathcal{Z}_h \oplus \mathcal{W}_h$ and $\mathcal{X} \subseteq \mathcal{Z}_h \oplus \mathcal{W}_h$, therefore $\mathcal{Z}_h \oplus \mathcal{W}_h = \mathcal{X}$. □

Proposition 3.2.3 (Generalized Intersection)**.** *For any hybrid zonotopes*

$$\mathcal{Z}_h = \left\langle G_z^c, G_z^b, c_z, A_z^c, A_z^b, b_z \right\rangle \subset \mathbb{R}^n \,,$$
$$\mathcal{Y}_h = \left\langle G_y^c, G_y^b, c_y, A_y^c, A_y^b, b_y \right\rangle \subset \mathbb{R}^m \,,$$

and matrix $R \in \mathbb{R}^{m \times n}$*, the generalized intersection of* $\mathcal{Z}_h$ *and* $\mathcal{Y}_h$ *under* R *is given by*

$$\mathcal{Z}_h \cap_R \mathcal{Y}_h = \left\langle \begin{bmatrix} G_z^c & \mathbf{0} \end{bmatrix}, \begin{bmatrix} G_z^b & \mathbf{0} \end{bmatrix}, c_z, \begin{bmatrix} A_z^c & \mathbf{0} \\ \mathbf{0} & A_y^c \\ RG_z^c & -G_y^c \end{bmatrix}, \begin{bmatrix} A_z^b & \mathbf{0} \\ \mathbf{0} & A_y^b \\ RG_z^b & -G_y^b \end{bmatrix}, \begin{bmatrix} b_z \\ b_y \\ c_y - Rc_z \end{bmatrix} \right\rangle . \tag{3.11}$$

Proof. For ease of readability, let $\xi_{\mathrm{i}} = (\xi_{\mathrm{i}}^c \ \xi_{\mathrm{i}}^b)$, $G_{\mathrm{i}} = [G_{\mathrm{i}}^c \ G_{\mathrm{i}}^b]$, and $A_{\mathrm{i}} = [A_{\mathrm{i}}^c \ A_{\mathrm{i}}^b]$ for $\mathrm{i} = z, \ y$. Let $\mathcal{S}$ denote the hybrid zonotope given by the right-hand side of (3.11). For any $s \in \mathcal{S}$ there exists some $\xi_s \in \mathcal{B}_\infty^{n_{g,z}+n_{g,y}} \times \{-1, 1\}^{n_{b,z}+n_{b,y}}$ such that

$$\begin{bmatrix} A_z^c & \mathbf{0} \\ \mathbf{0} & A_y^c \\ RG_z^c & -G_y^c \end{bmatrix} \xi_s^c + \begin{bmatrix} A_z^b & \mathbf{0} \\ \mathbf{0} & A_y^b \\ RG_z^b & -G_y^b \end{bmatrix} \xi_s^b = \begin{bmatrix} b_z \\ b_y \\ c_y - Rc_z \end{bmatrix}, \tag{3.12}$$

and $s = [G_z^c \ \mathbf{0}]\xi_s^c + [G_z^b \ \mathbf{0}]\xi_s^b + c_z$. Letting $\xi_s^c = (\xi_z^c \ \xi_y^c)$ and $\xi_s^b = (\xi_z^b \ \xi_y^b)$ gives $s = G_z\xi_z + c_z$ and $A_z\xi_z = b_z$, thus $s \in \mathcal{Z}_h$. From the final two rows of the equality constraints, $A_y\xi_y = b_y$ and $Rx = G_y\xi_y + c_y$ giving $Rx \in \mathcal{Y}_h$. Therefore $s \in \mathcal{Z}_h \cap_R \mathcal{Y}_h$ and $\mathcal{S} \subseteq \mathcal{Z}_h \cap_R \mathcal{Y}_h$.

Conversely, for any $z \in \mathcal{Z}_h \cap_R \mathcal{Y}_h$ there exists some $\xi_z \in \mathcal{B}_\infty^{n_{g,z}} \times \{-1, 1\}^{n_{b,z}}$ such that $A_z\xi_z = b_z$ and $z = G_z\xi_z + c_z$. Furthermore, there exists some $y \in \mathcal{Y}_h$ such that $y = G_y\xi_y + c_y = Rz$, where $\xi_y \in \mathcal{B}_\infty^{n_{g,y}} \times \{-1, 1\}^{n_{b,y}}$ and $A_y\xi_y = b_y$. Letting $\xi_s^c = (\xi_z^c \ \xi_y^c)$ and $\xi_s^b = (\xi_z^b \ \xi_y^b)$ implies that $\xi_s \in \mathcal{B}_\infty^{n_{g,z}+n_{g,y}} \times \{-1, 1\}^{n_{b,z}+n_{b,y}}$ satisfies (3.12), and $z = [G_z^c \ \mathbf{0}]\xi_s^c + [G_z^b \ \mathbf{0}]\xi_s^b + c_z$. Therefore, $z \in \mathcal{S}$, $\mathcal{Z}_h \cap_R \mathcal{Y}_h \subseteq \mathcal{S}$, and $\mathcal{Z}_h \cap_R \mathcal{Y}_h = \mathcal{S}$. □

Proposition 3.2.4 (Generalized Halfspace Intersection)**.** *For any hybrid zonotope* $\mathcal{Z}_h = \left\langle G_z^c, G_z^b, c_z, A_z^c, A_z^b, b_z \right\rangle \subset \mathbb{R}^n$ *and halfspace* $\mathcal{H}^- = \{x \in \mathbb{R}^n \mid h^T x \leq f\} \subset \mathbb{R}^m$*, and matrix* $R \in \mathbb{R}^{m \times n}$*, the generalized intersection of* $\mathcal{Z}_h$ *and* $\mathcal{H}^-$ *under* R *is given by*

$$\mathcal{Z}_h \cap_R \mathcal{H}^- = \left\langle \begin{bmatrix} G_z^c & \mathbf{0} \end{bmatrix}, G_z^b, c_z, \begin{bmatrix} A_z^c & \mathbf{0} \\ h^T RG_z^c & \frac{d_m}{2} \end{bmatrix}, \begin{bmatrix} A_z^b \\ h^T RG_z^b \end{bmatrix}, \begin{bmatrix} b_z \\ f - h^T Rc_z - \frac{d_m}{2} \end{bmatrix} \right\rangle , \tag{3.13}$$

$$d_m = f - h^T Rc_z + \sum_{\mathrm{i}=1}^{n_{g,z}} |h^T Rg_z^{(c,\mathrm{i})}| + \sum_{\mathrm{i}=1}^{n_{b,z}} |h^T Rg_z^{(b,\mathrm{i})}| .$$

Proof. For ease of readability, let $\xi_z = (\xi_z^c \ \xi_z^b)$, $G_z = [G_z^c \ G_z^b]$, and $A_z = [A_z^c \ A_z^b]$. Let $\mathcal{Q}$ denote the hybrid zonotope given by the right-hand side of (3.13). For any $q \in \mathcal{Q}$ there exists some $\xi_q \in \mathcal{B}_\infty^{n_{g,z}+1} \times \{-1,1\}^{n_{b,z}}$ such that

$$\begin{bmatrix} A_z^c & \mathbf{0} \\ h^T R G_z^c & \frac{d_m}{2} \end{bmatrix} \xi_q^c + \begin{bmatrix} A_z^b \\ h^T R G_z^b \end{bmatrix} \xi_q^b = \begin{bmatrix} b_z \\ f - h^T R c_z - \frac{d_m}{2} \end{bmatrix}, \tag{3.14}$$

and $q = [G_z^c \ \mathbf{0}]\xi_q^c + G_z^b \xi_q^b + c_z$. Let $\xi_q^c = (\xi_z^c \ \xi_h)$ and $\xi_q^b = \xi_z^b$ for $\xi_z^c \in \mathbb{R}^{n_{g,z}}$, $\xi_h \in \mathbb{R}$, and $\xi_z^b \in \{-1,1\}^{n_{b,z}}$. Then $q = G_z \xi_z + c_z$ giving $q \in \mathcal{Z}_h$. Expanding the second row of (3.14) gives $h^T R(G_z \xi_z + c_z) = f - (\frac{d_m}{2}\xi_h + \frac{d_m}{2})$. From the definition of d_m and that $\|\xi_h\|_\infty \leq 1$ it follows that

$$h^T R q \in \left[h^T R c_z - \sum_{\mathrm{i}=1}^{n_{g,z}} |h^T R g_z^{(c,\mathrm{i})}| - \sum_{\mathrm{i}=1}^{n_{b,z}} |h^T R g_z^{(b,\mathrm{i})}|, f \right], \tag{3.15}$$

therefore $Rq \in \mathcal{H}^-$ and $\mathcal{Q} \subseteq \mathcal{Z}_h \cap_R \mathcal{H}^-$.

Conversely, for any point $z \in \mathcal{Z}_h \cap_R \mathcal{H}^-$ there exists some $\xi_z \in \mathcal{B}_\infty^{n_{g,z}} \times \{-1,1\}^{n_{b,z}}$ such that $A_z \xi_z = b_z$, $z = G_z \xi_z + c_z$, and $h^T R z \leq f$. Thus $h^T R z \in [\alpha, f]$ for some $\alpha \leq h^T R z$ for all $z \in \mathcal{Z}_h \cap_R \mathcal{H}^-$. Choose $\alpha = h^T R c_z - \sum_{\mathrm{i}=1}^{n_{g,z}} |h^T R g_z^{(c,\mathrm{i})}| - \sum_{\mathrm{i}=1}^{n_{b,z}} |h^T R g_z^{(b,\mathrm{i})}|$ and let $\beta = h^T R c_z + \sum_{\mathrm{i}=1}^{n_{g,z}} |h^T R g_z^{(c,\mathrm{i})}| + \sum_{\mathrm{i}=1}^{n_{b,z}} |h^T R g_z^{(b,\mathrm{i})}|$, then by Lemma 3.1.1 $h^T R \mathcal{Z}_h \subseteq [\alpha, \beta]$ [59]. Let $\xi_q^c = (\xi_z^c \ \xi_h)$ and $\xi_q^b = \xi_z^b$. The above then implies that $\xi_q \in \mathcal{B}_\infty^{n_{g,z}+1} \times \{-1,1\}^{n_{b,z}}$ satisfies (3.14), and $z = [G_z^c \ \mathbf{0}]\xi_q^c + G_z^b \xi_q^b + c_z \in \mathcal{Q}$. Therefore $\mathcal{Z}_h \cap_R \mathcal{H}^- \subseteq \mathcal{Q}$ and $\mathcal{Z}_h \cap_R \mathcal{H}^- = \mathcal{Q}$. □

Proposition 3.2.5 (Cartesian Product)**.** *For any hybrid zonotopes*

$$\mathcal{Z}_h = \left\langle G_z^c, G_z^b, c_z, A_z^c, A_z^b, b_z \right\rangle \subset \mathbb{R}^n,$$
$$\mathcal{Y}_h = \left\langle G_y^c, G_y^b, c_y, A_y^c, A_y^b, b_y \right\rangle \subset \mathbb{R}^m,$$

their Cartesian product is given by

$$\mathcal{Z}_h \times \mathcal{Y}_h = \left\langle \begin{bmatrix} G_z^c & \mathbf{0} \\ \mathbf{0} & G_y^c \end{bmatrix}, \begin{bmatrix} G_z^b & \mathbf{0} \\ \mathbf{0} & G_y^b \end{bmatrix}, \begin{bmatrix} c_z \\ c_y \end{bmatrix}, \begin{bmatrix} A_z^c & \mathbf{0} \\ \mathbf{0} & A_y^c \end{bmatrix}, \begin{bmatrix} A_z^b & \mathbf{0} \\ \mathbf{0} & A_y^b \end{bmatrix}, \begin{bmatrix} b_z \\ b_y \end{bmatrix} \right\rangle \subset \mathbb{R}^{n+m}. \tag{3.16}$$

Proof. For ease of readability, let $\xi_{\mathrm{i}} = (\xi_{\mathrm{i}}^c \ \xi_{\mathrm{i}}^b)$, $G_{\mathrm{i}} = [G_{\mathrm{i}}^c \, G_{\mathrm{i}}^b]$, and $A_{\mathrm{i}} = [A_{\mathrm{i}}^c \ A_{\mathrm{i}}^b]$ for $\mathrm{i} = z,\ y,\ d$. Let $\mathcal{D} \subset \mathbb{R}^{n+m}$ be the hybrid zonotope given by the right-hand side of (3.16). For any $d \in \mathcal{D}$ there exists some $\xi_d \in \mathcal{B}_\infty^{n_{g,z}+n_{g,y}} \times \{-1,1\}^{n_{b,z}+n_{b,y}}$ such that

$$d = \begin{bmatrix} G_z & \mathbf{0} \\ \mathbf{0} & G_y \end{bmatrix} \xi_d + \begin{bmatrix} c_z \\ c_y \end{bmatrix}, \tag{3.17}$$

and

$$\begin{bmatrix} A_z & \mathbf{0} \\ \mathbf{0} & A_y \end{bmatrix} \xi_d = \begin{bmatrix} b_z \\ b_y \end{bmatrix}. \tag{3.18}$$

Therefore $[\mathbf{I}_n \ \mathbf{0}_m]d \in \mathcal{Z}_h$ and $[\mathbf{0}_n \ \mathbf{I}_m]d \in \mathcal{Y}_h$ and $\mathcal{D} \subseteq \mathcal{Z}_h \times \mathcal{Y}_h$.

Conversely, for any $\delta \in \mathcal{Z}_h \times \mathcal{Y}_h$ there exists some $\xi_z \in \mathcal{B}_\infty^{n_{g,z}} \times \{-1,1\}^{n_{b,z}}$ and $\xi_y \in \mathcal{B}_\infty^{n_{g,y}} \times \{-1,1\}^{n_{b,y}}$ such that

$$\delta = \begin{bmatrix} G_z \\ \mathbf{0} \end{bmatrix} \xi_z + \begin{bmatrix} \mathbf{0} \\ G_y \end{bmatrix} \xi_y + \begin{bmatrix} c_z \\ c_y \end{bmatrix}, \tag{3.19}$$

and

$$\begin{bmatrix} A_z \\ \mathbf{0} \end{bmatrix} \xi_z^c + \begin{bmatrix} \mathbf{0} \\ A_y \end{bmatrix} \xi_y^c = \begin{bmatrix} b_z \\ b_y \end{bmatrix}. \tag{3.20}$$

Therefore $\delta \in \mathcal{D}$, $\mathcal{Z}_h \times \mathcal{Y}_h \subseteq \mathcal{D}$ and $\mathcal{D} = \mathcal{Z}_h \times \mathcal{Y}_h$. □

The set representation complexity of hybrid zonotopes grow linearly for each of the identities defined for the above set operations. The specific growth for Minkowski sums, generalized intersections, halfspace intersections, and Cartesian products are given in Table 3.1, while no growth in complexity is exhibited by linear mappings. The time complexity for each of the basic set operations of hybrid zonotopes is also given in Table 3.1. Note that the time complexities of the generalized intersections are dominated by the linear mapping by R and reduce to $\mathcal{O}(n_1)$ for regular intersections and $\mathcal{O}(n_1(n_{g,1} + n_{b,1}))$ for regular halfspace intersections, i.e. when $R = \mathbf{I}$.

Table 3.1. Set representation complexity growth for Minkowski sums, generalized intersections, halfspace intersections, and Cartesian products given by hybrid zonotopes $\mathcal{Z}_h = \mathcal{Z}_{h,1} \odot \mathcal{Z}_{h,2}$ of appropriate dimension and matrix $R \in \mathbb{R}^{n_2 \times n_1}$.

Set Operation	$\mathcal{Z}_h$ Representation Complexity			Time Complexity
	n_g	n_b	n_c	$\mathcal{O}(\cdot)$
$R\mathcal{Z}_{h,1}$	$n_{g,1}$	$n_{b,1}$	$n_{c,1}$	$\mathcal{O}(n_1 n_2(n_{g,1} + n_{b,1}))$
$\mathcal{Z}_{h,1} \oplus \mathcal{Z}_{h,2}$	$n_{g,1} + n_{g,2}$	$n_{b,1} + n_{b,2}$	$n_{c,1} + n_{c,2}$	$\mathcal{O}(n_1)$
$\mathcal{Z}_{h,1} \cap_R \mathcal{Z}_{h,2}$	$n_{g,1} + n_{g,2}$	$n_{b,1} + n_{b,2}$	$n_{c,1} + n_{c,2} + n_2$	$\mathcal{O}(n_1 n_2(n_{g,1} + n_{b,1}))$
$\mathcal{Z}_{h,1} \cap_R \mathcal{H}^-$	$n_{g,1} + 1$	$n_{b,1}$	$n_{c,1} + 1$	$\mathcal{O}(n_1 n_2(n_{g,1} + n_{b,1}))$
$\mathcal{Z}_{h,1} \times \mathcal{Z}_{h,2}$	$n_{g,1} + n_{g,2}$	$n_{b,1} + n_{b,2}$	$n_{c,1} + n_{c,2}$	$\mathcal{O}(1)$

3.2.2 Unions

In this section, the closure of hybrid zonotopes under union operations is proven. This is achieved by including the generators and constraints of both operating sets within the resulting hybrid zonotope. By introducing one additional binary factor, the union switches between which of two sets are active by constraining the factors of the inactive set to a fixed value. The proposition and technical proof will be followed by a discussion of its underlying principles and how the growth of set representation complexity may be reduced.

Proposition 3.2.6 (Union)**.** *For any two hybrid zonotopes* $\mathcal{Z}_h = \langle G_z^c, G_z^b, c_z, A_z^c, A_z^b, b_z \rangle \subset \mathbb{R}^n$ *and* $\mathcal{W}_h = \langle G_w^c, G_w^b, c_w, A_w^c, A_w^b, b_w \rangle \subset \mathbb{R}^n$*, define the vectors* $\hat{G}^b \in \mathbb{R}^n$*,* $\hat{c} \in \mathbb{R}^n$*,* $\hat{A}_z^b \in \mathbb{R}^{n_{c,z}}$*,* $\hat{b}_z \in \mathbb{R}^{n_{c,z}}$*,* $\hat{A}_w^b \in \mathbb{R}^{n_{c,w}}$*, and* $\hat{b}_w \in \mathbb{R}^{n_{c,w}}$*, such that*

$$\begin{bmatrix} \mathbf{I} & \mathbf{I} \\ -\mathbf{I} & \mathbf{I} \end{bmatrix} \begin{bmatrix} \hat{G}^b \\ \hat{c} \end{bmatrix} = \begin{bmatrix} G_w^b \mathbf{1} + c_z \\ G_z^b \mathbf{1} + c_w \end{bmatrix}, \begin{bmatrix} -\mathbf{I} & \mathbf{I} \\ \mathbf{I} & \mathbf{I} \end{bmatrix} \begin{bmatrix} \hat{A}_z^b \\ \hat{b}_z \end{bmatrix} = \begin{bmatrix} b_z \\ -A_z^b \mathbf{1} \end{bmatrix}, \begin{bmatrix} -\mathbf{I} & \mathbf{I} \\ \mathbf{I} & \mathbf{I} \end{bmatrix} \begin{bmatrix} \hat{A}_w^b \\ \hat{b}_w \end{bmatrix} = \begin{bmatrix} -A_w^b \mathbf{1} \\ b_w \end{bmatrix}.$$

Then the union of $\mathcal{Z}_h$ and $\mathcal{W}_h$ is the hybrid zonotope $\mathcal{Z}_h \cup \mathcal{W}_h = \langle G_u^c, G_u^b, c_u, A_u^c, A_u^b, b_u \rangle \subset \mathbb{R}^n$ where

$$
\begin{aligned}
G_u^c &= \begin{bmatrix} G_z^c & G_w^c & \mathbf{0} \end{bmatrix}, G_u^b = \begin{bmatrix} G_z^b & G_w^b & \hat{G}^b \end{bmatrix}, c_u = \hat{c}, \\
A_u^c &= \begin{bmatrix} A_z^c & \mathbf{0} & \mathbf{0} \\ \mathbf{0} & A_w^c & \mathbf{0} \\ & A_3^c & I \end{bmatrix}, A_u^b = \begin{bmatrix} A_z^b & \mathbf{0} & \hat{A}_z^b \\ \mathbf{0} & A_w^b & \hat{A}_w^b \\ & A_3^b & \end{bmatrix}, b_u = \begin{bmatrix} \hat{b}_z \\ \hat{b}_w \\ b_3 \end{bmatrix}, \\
A_3^c &= \begin{bmatrix} \mathbf{I} & \mathbf{0} \\ -\mathbf{I} & \mathbf{0} \\ \mathbf{0} & \mathbf{I} \\ \mathbf{0} & -\mathbf{I} \\ \mathbf{0} & \mathbf{0} \\ \mathbf{0} & \mathbf{0} \\ \mathbf{0} & \mathbf{0} \\ \mathbf{0} & \mathbf{0} \end{bmatrix}, A_3^b = \begin{bmatrix} \mathbf{0} & \mathbf{0} & \frac{1}{2}\mathbf{1} \\ \mathbf{0} & \mathbf{0} & \frac{1}{2}\mathbf{1} \\ \mathbf{0} & \mathbf{0} & -\frac{1}{2}\mathbf{1} \\ \mathbf{0} & \mathbf{0} & -\frac{1}{2}\mathbf{1} \\ \frac{1}{2}\mathbf{I} & \mathbf{0} & \frac{1}{2}\mathbf{1} \\ -\frac{1}{2}\mathbf{I} & \mathbf{0} & \frac{1}{2}\mathbf{1} \\ \mathbf{0} & \frac{1}{2}\mathbf{I} & -\frac{1}{2}\mathbf{1} \\ \mathbf{0} & -\frac{1}{2}\mathbf{I} & -\frac{1}{2}\mathbf{1} \end{bmatrix}, b_3 = \begin{bmatrix} \frac{1}{2}\mathbf{1} \\ \frac{1}{2}\mathbf{1} \\ \frac{1}{2}\mathbf{1} \\ \frac{1}{2}\mathbf{1} \\ \mathbf{0} \\ \mathbf{1} \\ \mathbf{0} \\ \mathbf{1} \end{bmatrix}.
\end{aligned}
\tag{3.21}
$$

Proof. Let $\mathcal{X} = \langle G_u^c, G_u^b, c_u, A_u^c, A_u^b, b_u \rangle$ denote the hybrid zonotope given by (3.21). For any $x \in \mathcal{X}$ there exists some $\xi_x^c \in \mathcal{B}_\infty^{n_{g,x}}$ and $\xi_x^b \in \{-1, 1\}^{n_{b,x}}$ such that $A_u^c \xi_x^c + A_u^b \xi_x^b = b_u$ and $x = G_u^c \xi_x^c + G_u^b \xi_x^b + c_u$. Let $\xi_x^c = (\xi_z^c \ \xi_w^c \ \xi_u^c)$, where $\xi_z^c \in \mathbb{R}^{n_{g,z}}$, $\xi_w^c \in \mathbb{R}^{n_{g,w}}$, and $\xi_u^c \in \mathbb{R}^{2(n_{g,z}+n_{g,w}+n_{b,z}+n_{b,w})}$, and $\xi_x^b = (\xi_z^b \ \xi_w^b \ \xi_u^b)$, where $\xi_z^b \in \{-1, 1\}^{n_{b,z}}$, $\xi_w^b \in \{-1, 1\}^{n_{b,w}}$, and $\xi_u^b \in \{-1, 1\}$. To prove that $\mathcal{X} \subseteq \mathcal{Z}_h \cup \mathcal{W}_h$, it is first shown that when $\xi_u^b = 1$ the factors ξ_w^c and ξ_w^b are constrained to $\mathbf{0}$ and $-\mathbf{1}$, respectively. Then by construction the remaining generators and constraints give the exact definition of the set $\mathcal{Z}_h$. It is then shown that the set $\mathcal{W}_h$ is similarly recovered when $\xi_u^b = -1$.

Expanding the third row of the equality constraints $A_u^c \xi_x^c + A_u^b \xi_x^b = b_u$ gives

$$\xi_z^c = \frac{1}{2}\mathbf{1} - \frac{1}{2}\xi_u^b - \xi_{u,1}^c = -\frac{1}{2}\mathbf{1} + \frac{1}{2}\xi_u^b + \xi_{u,2}^c \,, \tag{3.22a}$$

$$\xi_w^c = \frac{1}{2}\mathbf{1} + \frac{1}{2}\xi_u^b - \xi_{u,3}^c = -\frac{1}{2}\mathbf{1} - \frac{1}{2}\xi_u^b + \xi_{u,4}^c \,, \tag{3.22b}$$

$$\frac{1}{2}\xi_z^b = -\frac{1}{2}\xi_u^b - \xi_{u,5}^c = -\mathbf{1} + \frac{1}{2}\xi_u^b + \xi_{u,6}^c \,, \tag{3.22c}$$

$$\frac{1}{2}\xi_w^b = \frac{1}{2}\xi_u^b - \xi_{u,7}^c = -\mathbf{1} - \frac{1}{2}\xi_u^b + \xi_{u,8}^c \,, \tag{3.22d}$$

where $\xi_u^c = (\xi_{u,1}^c \ \cdots \ \xi_{u,8}^c)$. Letting $\xi_u^b = 1$, (3.22) reduces to

$$\xi_z^c = -\xi_{u,1}^c = \xi_{u,2}^c \,, \tag{3.23a}$$

$$\xi_w^c = \mathbf{1} - \xi_{u,3}^c = -\mathbf{1} + \xi_{u,4}^c \,, \tag{3.23b}$$

$$\xi_z^b = -\mathbf{1} - 2\xi_{u,5}^c = -\mathbf{1} + 2\xi_{u,6}^c \,, \tag{3.23c}$$

$$\xi_w^b = \mathbf{1} - 2\xi_{u,7}^c = -3\mathbf{1} + 2\xi_{u,8}^c \,. \tag{3.23d}$$

Given that $\|\xi_u^c\|_\infty \leq 1$, (3.23b) and (3.23d) are only satisfied for $\xi_w^c = \mathbf{0}$ and $\xi_w^b = -\mathbf{1}$ respectively, while (3.23a) and (3.23c) are satisfied for any $\|\xi_z^c\|_\infty \leq 1$ and $\xi_z^b \in \{-1, 1\}^{n_{b,z}}$. Let $\xi_x^c = (\xi_z^c \ \mathbf{0} \ \xi_u^c)$ and $\xi_x^b = (\xi_z^b \ -\mathbf{1} \ 1)$. Expanding $x = G_u^c \xi_x^c + G_u^b \xi_x^b + c_u$ gives

$$x = G_z^c \xi_z^c + G_w^c \mathbf{0} + \mathbf{0}\xi_u^c + G_z^b \xi_z^b - G_w^b \mathbf{1} + \hat{G}^b + \hat{c} \,, \tag{3.24}$$

and, after substituting $-G_w^b \mathbf{1} + \hat{G}^b + \hat{c} = c_z$, reduces to $x = G_z^c \xi_z^c + G_z^b \xi_z^b + c_z$. Expanding the first two rows of the equality constraints $A_u^c \xi_x^c + A_u^b \xi_x^b = b_u$ results in

$$\begin{aligned} A_z^c \xi_z^c + A_z^b \xi_z^b + \hat{A}_z^b &= \hat{b}_z \,, \\ A_w^c \mathbf{0} - A_w^b \mathbf{1} + \hat{A}_w^b &= \hat{b}_w \,, \end{aligned} \tag{3.25}$$

which, after substituting $\hat{b}_z - \hat{A}_z^b = b_z$ and $\hat{b}_w - \hat{A}_w^b = -A_w^b \mathbf{1}$, gives $A_z^c \xi_z^c + A_z^b \xi_z^b = b_z$ and $-A_w^b \mathbf{1} = -A_w^b \mathbf{1}$. Combining (3.23)-(3.25) results in $x \in \mathcal{Z}_h$ for $\xi_u^b = 1$.

Now let $\xi_u^b = -1$ and (3.22) reduce to

$$\xi_z^c = \mathbf{1} - \xi_{u,1}^c = -\mathbf{1} + \xi_{u,2}^c \,, \tag{3.26a}$$

$$\xi_w^c = -\xi_{u,3}^c = \xi_{u,4}^c \,, \tag{3.26b}$$

$$\xi_z^b = \mathbf{1} - 2\xi_{u,5}^c = -3\mathbf{1} + 2\xi_{u,6}^c \,, \tag{3.26c}$$

$$\xi_w^b = -\mathbf{1} - 2\xi_{u,7}^c = -\mathbf{1} + 2\xi_{u,8}^c \,. \tag{3.26d}$$

Given that $\|\xi_u^c\|_\infty \leq 1$, (3.26a) and (3.26c) are only satisfied for $\xi_z^c = \mathbf{0}$ and $\xi_z^b = -\mathbf{1}$ respectively, while (3.26b) and (3.26d) are satisfied for any $\|\xi_w^c\|_\infty \leq 1$ and $\xi_w^b \in \{-1, 1\}^{n_{b,w}}$. Let $\xi_x^c = (\mathbf{0}\ \xi_w^c\ \xi_u^c)$ and $\xi_x^b = (-\mathbf{1}\ \xi_w^b\ -1)$. Expanding $x = G_u^c \xi_x^c + G_u^b \xi_x^b + c_u$ gives

$$x = G_z^c \mathbf{0} + G_w^c \xi_w^c + \mathbf{0}\xi_u^c - G_z^b \mathbf{1} + G_w^b \xi_w^b - \hat{G}^b + \hat{c} \tag{3.27}$$

and, after substituting $-G_z^b \mathbf{1} - \hat{G}^b + \hat{c} = c_w$, reduces to $x = G_w^c \xi_w^c + G_w^b \xi_w^b + c_w$. Expanding the first two rows of the equality constraints $A_u^c \xi_x^c + A_u^b \xi_x^b = b_u$ results in

$$\begin{aligned} A_z^c \mathbf{0} - A_z^b \mathbf{1} - \hat{A}_z^b &= \hat{b}_z \\ A_w^c \xi_z^c + A_w^b \xi_w^b - \hat{A}_w^b &= \hat{b}_w \end{aligned} \tag{3.28}$$

which, after substituting $\hat{b}_z + \hat{A}_z^b = -A_z^b \mathbf{1}$ and $\hat{b}_w + \hat{A}_w^b = b_w$, gives $-A_z^b \mathbf{1} = -A_z^b \mathbf{1}$ and $A_w^c \xi_w^c + A_w^b \xi_w^b = b_w$. Combining (3.26)-(3.28) results in $x \in \mathcal{W}_h$ for $\xi_u^b = -1$. Given that $\xi_u^b \in \{-1, 1\}$ and that the choice of $x \in \mathcal{X}$ is arbitrary, $\mathcal{X} \subseteq \mathcal{Z}_h \cup \mathcal{W}_h$.

Conversely, for any $z \in \mathcal{Z}_h$ there exists some $\xi_z^c \in \mathcal{B}_\infty^{n_{g,z}}$ and $\xi_z^b \in \{-1, 1\}^{n_{b,z}}$ such that $A_z^c \xi_z^c + A_z^b \xi_z^b = b_z$ and $z = G_z^c \xi_z^c + G_z^b \xi_z^b + c_z$. Letting $\xi_x^c = (\xi_z^c\ \mathbf{0}\ \xi_u^c)$ and $\xi_x^b = (\xi_z^b\ -\mathbf{1}\ 1)$, (3.25) is satisfied and (3.23) implies that $\|\xi_u^c\|_\infty \leq 1$. Applying (3.24) then gives $z \in \mathcal{X}$. For any $w \in \mathcal{W}_h$ there exists some $\xi_w^c \in \mathcal{B}_\infty^{n_{g,w}}$ and $\xi_w^b \in \{-1, 1\}^{n_{b,w}}$ such that $A_w^c \xi_w^c + A_w^b \xi_w^b = b_w$ and $w = G_w^c \xi_w^c + G_w^b \xi_w^b + c_w$. Letting $\xi_x^c = (\mathbf{0}\ \xi_w^c\ \xi_u^c)$ and $\xi_x^b = (-\mathbf{1}\ \xi_w^b\ -1)$, (3.28) is satisfied and (3.26) implies that $\|\xi_u^c\|_\infty \leq 1$. Applying (3.27) then gives $w \in \mathcal{X}$. Given that the choice of $z \in \mathcal{Z}_h$ and $w \in \mathcal{W}_h$ is arbitrary, $\mathcal{Z}_h \cup \mathcal{W}_h \subseteq \mathcal{X}$ and therefore $\mathcal{Z}_h \cup \mathcal{W}_h = \mathcal{X}$. □

The union set operation given by Proposition 3.2.6 introduces $2(n_{g,z}+n_{g,w}+n_{b,z}+n_{b,w})$ "slack" continuous factors, ξ_u^c, and one switching binary factor, ξ_u^b. The additional $2(n_{g,z}+n_{g,w}+n_{b,z}+n_{b,w})$ linear equality constraints, $A_3^c(\xi_z^c\ \xi_w^c)+I\xi_u^c+A_3^b(\xi_z^b\ \xi_w^b\ \xi_u^b)=b_3$, implement the switch between which of the two sets are active as

$$\begin{aligned} \xi_u^b = 1 \implies & \begin{matrix} (\xi_z^c\ \xi_z^b) \in \mathcal{B}_\infty^{n_{g,z}} \times \{-1,1\}^{n_{b,z}} \\ (\xi_w^c\ \xi_w^b) = (\mathbf{0}\ -\mathbf{1}) \end{matrix} \\ \xi_u^b = -1 \implies & \begin{matrix} (\xi_z^c\ \xi_z^b) = (\mathbf{0}\ -\mathbf{1}) \\ (\xi_w^c\ \xi_w^b) \in \mathcal{B}_\infty^{n_{g,w}} \times \{-1,1\}^{n_{b,w}} \end{matrix} \end{aligned} , \tag{3.29}$$

The hatted constants, $\hat{G}^b$, $\hat{c}$, $\hat{A}_z^b$, $\hat{b}_z$, $\hat{A}_w^b$, and $\hat{b}_w$, multiplied by the binary switch, ξ_u^b, then account for the binary factors being constrained to $-\mathbf{1}$ instead of $\mathbf{0}$, the change of centers, and the feasibility of the constraints of the inactive set to represent the exact union of two hybrid zonotopes by a single hybrid zonotope.

For ease of understanding, Proposition 3.2.6 applies these constraints to all continuous and binary factors; however, in practice it is only necessary, and beneficial, to apply these constraints to factors that map through non-zero generators. This fact stems from the observation that the factors and generator matrices may be parsed, for the example of $x \in \mathcal{Z}$ in the proof of Proposition 3.2.6, such that $\xi_w = (\xi_{w,\neq 0}\ \xi_{w,=0})$ and $G_w = [G_{w,\neq 0}\ \mathbf{0}]$. Using this partition, the equation for x then reduces to

$$x = G_z\xi_z + G_{w,\neq 0}\xi_{w,\neq 0} + \hat{G}^b + \hat{c}\,, \tag{3.30}$$

and only the factors $\xi_{w,\neq 0}$ must be constrained to cancel their contribution to x. Feasibility is maintained in the remaining equality constraints since the feasible values of $\xi_{w,=0}^c = \mathbf{0}$ and $\xi_{w,=0}^b = -\mathbf{1}$ still exist, although not strictly enforced. This modification is accomplished by replacing the identity matrices in A_3^c and A_3^b with staircase matrices having a single one in

each row located in the ith column corresponding to the index of each non-zero generator. For example, the union of hybrid zonotopes $\mathcal{Z}$ and $\mathcal{W}$ with generator matrices given by

$$G_z^c = \begin{bmatrix} g_z^{c(1)} & \mathbf{0} & \mathbf{0} & g_z^{c(4)} \end{bmatrix}, \quad G_z^b = \begin{bmatrix} g_z^{b(1)} & \mathbf{0} & \mathbf{0} \end{bmatrix},$$
$$G_w^c = \begin{bmatrix} g_w^{c(1)} & g_w^{c(2)} \end{bmatrix}, \qquad G_w^b = \begin{bmatrix} g_w^{b(1)} & \mathbf{0} & g_w^{b(3)} & \mathbf{0} \end{bmatrix},$$

may be represented using the staircase matrices

$$S_z^c = \begin{bmatrix} 1 & 0 & 0 & 0 \\ 0 & 0 & 0 & 1 \end{bmatrix}, \quad S_z^b = \begin{bmatrix} 1 & 0 & 0 \end{bmatrix},$$
$$S_w^c = \begin{bmatrix} 1 & 0 \\ 0 & 1 \end{bmatrix}, \qquad S_w^b = \begin{bmatrix} 1 & 0 & 0 & 0 \\ 0 & 0 & 1 & 0 \end{bmatrix}.$$

The matrices in the third row of the equality constraints of (3.21) then become

$$A_3^c = \begin{bmatrix} S_z^c & \mathbf{0} \\ -S_z^c & \mathbf{0} \\ \mathbf{0} & S_w^c \\ \mathbf{0} & -S_w^c \\ \mathbf{0} & \mathbf{0} \\ \mathbf{0} & \mathbf{0} \\ \mathbf{0} & \mathbf{0} \\ \mathbf{0} & \mathbf{0} \end{bmatrix}, A_3^b = \begin{bmatrix} \mathbf{0} & \mathbf{0} & \frac{1}{2}\mathbf{1} \\ \mathbf{0} & \mathbf{0} & \frac{1}{2}\mathbf{1} \\ \mathbf{0} & \mathbf{0} & -\frac{1}{2}\mathbf{1} \\ \mathbf{0} & \mathbf{0} & -\frac{1}{2}\mathbf{1} \\ \frac{1}{2}S_z^b & \mathbf{0} & \frac{1}{2}\mathbf{1} \\ -\frac{1}{2}S_z^b & \mathbf{0} & \frac{1}{2}\mathbf{1} \\ \mathbf{0} & \frac{1}{2}S_w^b & -\frac{1}{2}\mathbf{1} \\ \mathbf{0} & -\frac{1}{2}S_w^b & -\frac{1}{2}\mathbf{1} \end{bmatrix}. \tag{3.31}$$

Making this substitution reduces the growth in the set representation complexity by introducing fewer "slack" factors and equality constraints. This is especially useful when factors appear in the constraints and not the generator matrices, for example, when applying Proposition 3.2.6 multiple times. Let $n_{g,z}^r$ and $n_{b,z}^r$ denote the number of nonzero continuous and

binary generators in the representation of $\mathcal{Z}_h$ and $n^r_{g,w}$ and $n^r_{b,w}$ for $\mathcal{W}_h$, then the set representation complexity growth of the union operation is given by

$$n_g = n_{g,z} + n_{g,w} + 2(n^r_{g,z} + n^r_{b,z} + n^r_{g,w} + n^r_{b,w}) \,, \tag{3.32a}$$

$$n_b = n_{b,z} + n_{b,w} + 1 \,, \tag{3.32b}$$

$$n_c = n_{c,z} + n_{c,w} + 2(n^r_{c,z} + n^r_{c,z} + n^r_{c,w} + n^r_{c,w}) \,. \tag{3.32c}$$

3.2.3 Complements

This section provides an identity for the representation of the complements of constrained zonotopes as hybrid zonotopes over a bounded region of interest. It is then shown how this identity implies the closure of hybrid zonotopes under complement set operations.

The point containment problem for the constrained zonotope $\mathcal{Z}_c = \langle G, c, A, b\rangle \subset \mathbb{R}^n$ may be determined by solving the Linear Program (LP) [18, Proposition 2]

$$z \in \mathcal{Z}_c \iff \min \left\{ \|\xi\|_\infty \;\middle|\; \begin{bmatrix} G \\ A \end{bmatrix} \xi = \begin{bmatrix} z - c \\ b \end{bmatrix} \right\} \leq 1 \,. \tag{3.33}$$

The complement of a constrained zonotope may then be defined by modifying the result in [4] using the constrained zonotope's lifted zonotope representation [18].

Lemma 3.2.1. *[4, Lemma 2] Given a constrained zonotope $\mathcal{Z}_c = \langle G, c, A, b\rangle \subset \mathbb{R}^n$ with $o_d \geq 1$ and $x \in \mathbb{R}^n$, let*

$$\begin{aligned} \delta^*(x) = \min_{\delta,\xi}\ & \delta \\ s.t.\ & \begin{bmatrix} x \\ \mathbf{0} \end{bmatrix} = \begin{bmatrix} G \\ A \end{bmatrix} \xi + \begin{bmatrix} c \\ -b \end{bmatrix} \,, \\ & \|\xi\|_\infty \leq 1 + \delta \,. \end{aligned} \tag{3.34}$$

Then $x \notin \mathcal{Z}_c \iff \delta^*(x) > 0$.

The condition given in Lemma 3.2.1 may be relaxed to give the closure of the complement by using non-strict inequalities, i.e. $x \in \overline{\mathcal{Z}_c^c} \iff \delta^*(x) \geq 0$, noting that $\delta^*(x) = 0$ occurs

when $x \in \partial\mathcal{Z}_c$ [60]. When an upper bound on the minimum infinity norm is defined such that $\mathcal{X} \subseteq \{G\xi + c \mid \|\xi\|_\infty \leq 1 + \delta_m,\ A\xi = b\}$, then $x \in \mathcal{C}_\mathcal{X}(\mathcal{Z}_c) \implies \delta^*(x) \in [0, \delta_m]$. Inspired by the use of complements of zonotopes in [61], the closure of the complement of a constrained zonotope is now defined as a hybrid zonotope.

Proposition 3.2.7 (Complement)**.** *Given any full dimensional, nonempty constrained zonotope $\mathcal{Z}_c = \langle G, c, A, b\rangle \subset \mathbb{R}^n$ and a convex, bounded region of interest $\mathcal{X} \supseteq \mathcal{Z}_c$, define positive scalars δ_m and λ_m such that $\mathcal{X} \subseteq \{G\xi + c \mid \|\xi\|_\infty \leq 1 + \delta_m,\ A\xi = b\}$ and $\lambda_m \geq \max\left\{\|\lambda\|_\infty \mid |[G^T\ A^T]\lambda| \leq 1\right\}$, and let $m = \delta_m + 1$. Define the interval sets*

$$\{G_{f,1}\xi_{f,1} + c_{f,1} \mid \|\xi_{f,1}\|_\infty \leq 1\} = \left[-\left(m + \tfrac{\delta_m}{2}\right)\mathbf{1}_{2n_{g,z}} \quad , \quad \left(1 + \tfrac{\delta_m}{2}\right)\mathbf{1}_{2n_{g,z}}\right],$$
$$\{G_{f,2}\xi_{f,2} + c_{f,2} \mid \|\xi_{f,2}\|_\infty \leq 1\} = \begin{bmatrix} -\left(m + \frac{3\delta_m}{2} + 1\right)\mathbf{1}_{2n_{g,z}} & , & \frac{\delta_m}{2}\mathbf{1}_{2n_{g,z}} \\ -2\mathbf{1}_{2n_{g,z}} & , & \mathbf{0}_{2n_{g,z}} \end{bmatrix}.$$

Then the closure of the complement of $\mathcal{Z}_c$ within the region of interest $\mathcal{X}$ is given by the hybrid zonotope $\mathcal{C}_\mathcal{X}(\mathcal{Z}_c) = \langle G_c^c, G_c^b, c_c, A_c^c, A_c^b, b_c\rangle \subset \mathbb{R}^n$ where,

$$\begin{aligned}
&G_c^c = \begin{bmatrix} mG & \mathbf{0} \end{bmatrix},\ G_c^b = \mathbf{0},\ c_c = c,\\
&A_c^c = \begin{bmatrix} mA & \mathbf{0} & \mathbf{0} & \mathbf{0} \\ A_{PF}^c & G_{f,1} & \mathbf{0} & \\ A_{DF}^c & \mathbf{0} & \mathbf{0} & \\ A_{CS}^c & \mathbf{0} & G_{f,2} & \end{bmatrix}, A_c^b = \begin{bmatrix} \mathbf{0} \\ \mathbf{0} \\ \mathbf{0} \\ A_{CS}^b \end{bmatrix}, b_c = \begin{bmatrix} b \\ c_{f,1} \\ b_{DF} \\ c_{f,2} \end{bmatrix},\\
&A_{PF}^c = \begin{bmatrix} m\mathbf{I} & -\frac{\delta_m}{2} & \mathbf{0} & \mathbf{0} & \mathbf{0} \\ -m\mathbf{I} & -\frac{\delta_m}{2} & \mathbf{0} & \mathbf{0} & \mathbf{0} \end{bmatrix},\\
&A_{DF}^c = \begin{bmatrix} \mathbf{0} & \mathbf{0} & \lambda_m\begin{bmatrix} G^T & A^T \end{bmatrix} & \frac{1}{2}\mathbf{I} & -\frac{1}{2}\mathbf{I} \\ \mathbf{0} & \mathbf{0} & \mathbf{0} & \frac{1}{2}\mathbf{1} & \frac{1}{2}\mathbf{1} \end{bmatrix}, b_{DF} = \begin{bmatrix} \mathbf{0} \\ 1 - n_g \end{bmatrix},\\
&A_{CS}^c = \begin{bmatrix} -m\mathbf{I} & \frac{\delta_m}{2} & \mathbf{0} & \mathbf{0} & \mathbf{0} \\ m\mathbf{I} & \frac{\delta_m}{2} & \mathbf{0} & \mathbf{0} & \mathbf{0} \\ \mathbf{0} & \mathbf{0} & \mathbf{0} & \mathbf{I} & \mathbf{0} \\ \mathbf{0} & \mathbf{0} & \mathbf{0} & \mathbf{0} & \mathbf{I} \end{bmatrix}, A_{CS}^b = \begin{bmatrix} m\mathbf{I} & \mathbf{0} \\ \mathbf{0} & m\mathbf{I} \\ -\mathbf{I} & \mathbf{0} \\ \mathbf{0} & -\mathbf{I} \end{bmatrix}.
\end{aligned} \tag{3.35}$$

Proof. Let $\mathcal{W}_h = \langle G_c^c, G_c^b, c_c, A_c^c, A_c^b, b_c \rangle \subset \mathbb{R}^n$ denote the hybrid zonotope given by (3.35). For any $w \in \mathcal{W}_h$ there exists some $\xi_w^c \in \mathcal{B}_\infty^{n_{g,w}}$ and $\xi_w^b \in \{-1,1\}^{n_{b,w}}$ such that $A_c^c\xi_w^c + A_c^b\xi_w^b = b_c$ and $w = G_c^c\xi_w^c + G_c^b\xi_w^b + c_c$. Let $\xi_w^c = (\xi_c^c\ \xi_\delta^c\ \xi_\lambda^c\ \xi_{\mu,1}^c\ \xi_{\mu,2}^c\ \xi_{f,1}^c\ \xi_{f,2}^c)$, where $\xi_c^c \in \mathbb{R}^{n_{g,z}}$, $\xi_\delta^c \in \mathbb{R}$, $\xi_\lambda^c \in \mathbb{R}^{n+n_{c,z}}$, $\xi_{\mu,1,2}^c \in \mathbb{R}^{n_{g,z}}$, $\xi_{f,1}^c \in \mathbb{R}^{2n_{g,z}}$, and $\xi_{f,2}^c \in \mathbb{R}^{4n_{g,z}}$, and $\xi_w^b = (\xi_1^b\ \xi_2^b)$, where $\xi_{1,2}^b \in \{-1,1\}^{n_{g,z}}$. Then $w = mG\xi_c^c + c$ and the first row of $A_c^c\xi^c + A_c^b\xi^b = b_c$ gives $mA\xi_c^c = b$. Expanding the second row of $A_c^c\xi_w^c + A_c^b\xi_w^b = b_c$ gives

$$\begin{bmatrix} m\xi_c^c \\ -m\xi_c^c \end{bmatrix} + \begin{bmatrix} -\frac{\delta_m}{2}\xi_\delta^c \\ -\frac{\delta_m}{2}\xi_\delta^c \end{bmatrix} = -G_{f,1}\xi_{f,1}^c + c_{f,1}\,, \tag{3.36}$$

which implies that $m\xi_c^c - \frac{\delta_m}{2}\xi_\delta^c \le (1+\frac{\delta_m}{2})\mathbf{1}$ and $-m\xi_c^c - \frac{\delta_m}{2}\xi_\delta^c \le (1+\frac{\delta_m}{2})\mathbf{1}$. Expanding the third row of $A_c^c\xi_w^c + A_c^b\xi_w^b = b_c$ gives

$$\begin{aligned} &\lambda_m \begin{bmatrix} G^T & A^T \end{bmatrix} \xi_\lambda^c + \frac{1}{2}\xi_{\mu,1}^c - \frac{1}{2}\xi_{\mu,2}^c = \mathbf{0}\,, \\ &\frac{1}{2}\left(\xi_{\mu,1}^c + \xi_{\mu,2}^c\right)^T \mathbf{1} = 1 - n_{g,z}\,. \end{aligned} \tag{3.37}$$

Expanding the fourth row of $A_c^c\xi_w^c + A_c^b\xi_w^b = b_c$ gives

$$\begin{bmatrix} -m\xi_c^c + \frac{\delta_m}{2}\xi_\delta^c + (1+\delta_m)\xi_1^b \\ m\xi_c^c + \frac{\delta_m}{2}\xi_\delta^c + (1+\delta_m)\xi_2^b \\ \xi_{\mu,1}^c - \xi_1^b \\ \xi_{\mu,2}^c - \xi_2^b \end{bmatrix} = -G_{f,2}\xi_{f,2}^c + c_{f,2}\,, \tag{3.38}$$

which implies that $-m\xi_c^c + \frac{\delta_m}{2}\xi_\delta^c + (1+\delta_m)\xi_1^b \le \frac{\delta_m}{2}\mathbf{1}$, $m\xi_c^c + \frac{\delta_m}{2}\xi_\delta^c + (1+\delta_m)\xi_1^b \le \frac{\delta_m}{2}\mathbf{1}$, $\xi_{\mu,1}^c \le \xi_1^b$, and $\xi_{\mu,2}^c \le \xi_2^b$. Define the change of variables

$$\begin{aligned} &\xi = m\xi_c^c\,,\ \delta = \frac{\delta_m}{2}\xi_\delta^c + \frac{\delta_m}{2}\,,\ \lambda = \lambda_m\xi_\lambda^c \\ &\mu_{1,2} = \frac{1}{2}\xi_{\mu,1,2}^c + \frac{1}{2}\,,\ p_{1,2} = \frac{1}{2}\xi_{1,2}^b + \frac{1}{2}\,. \end{aligned} \tag{3.39}$$

Carrying these change of variables through the above constraints results in

$$w = G\xi + c,\ A\xi = b,\ \|\xi\|_\infty \leq 1 + \delta, \tag{3.40a}$$

$$\begin{bmatrix} G^T & A^T \end{bmatrix} \lambda + \mu_1 - \mu_2 = \mathbf{0},\ (\mu_1 + \mu_2)^T \mathbf{1} = 1, \tag{3.40b}$$

$$\begin{aligned} -2(1+\delta_m)(1-p_1) &\leq \xi - \delta - \mathbf{1},\ \mu_1 \leq p_1, \\ -2(1+\delta_m)(1-p_2) &\leq -\xi - \delta - \mathbf{1},\ \mu_1 \leq p_1, \end{aligned} \tag{3.40c}$$

$$\delta \in [0, \delta_m],\ \mu_{1,2} \in [0,1]^{n_{g,z}},\ p_{1,2} \in \{0,1\}^{n_{g,z}}, \tag{3.40d}$$

where (3.40a) is the primal feasibility, resulting from (3.36), (3.40b) is the dual feasibility, resulting from (3.37), and (3.40c) is the complementary slackness, resulting from (3.38), KKT conditions of the LP (3.34) [61]. Given that the LP is convex, the KKT conditions are necessary and sufficient; thus $\delta = \delta^*(w)$. Recalling Lemma 3.2.1, the constraint $\delta \in [0, \delta_m]$ in (3.40d) results in $w \in \overline{\mathcal{Z}_c^c}$. Given that the choice of $w \in \mathcal{W}_h$ is arbitrary $\mathcal{W}_h \subseteq \overline{\mathcal{Z}_c^c}$.

Conversely, for any $z \in \mathcal{C}_\mathcal{X}(\mathcal{Z}_c)$, there exists some ξ such that $z = G\xi + c$, $A\xi = b$, and $\delta^*(z) \in [0, \delta_m]$. Since $\delta^*(z)$ is the minimum of the convex LP (3.34), there exists some λ, $\mu_{1,2} \geq \mathbf{0}$, and $p_{1,2} \in \{-1,1\}^{n_{g,z}}$ such that (3.40) holds. Letting $\xi_w^c = (\xi_c^c\ \xi_\delta^c\ \xi_\lambda^c\ \xi_{\mu,1}^c\ \xi_{\mu,2}^c\ \xi_{f,1}^c\ \xi_{f,2}^c)$, $\xi_w^b = (\xi_1^b\ \xi_2^b)$, and applying the change of variables (3.39), the above implies that $\xi_w^c \in \mathcal{B}_\infty^{n_{g,w}}$, $\xi_w^b \in \{-1,1\}^{n_{b,w}}$, $A_c^c \xi_w^c + A_c^b \xi_w^b = b_c$, and $z = G_c^c \xi_w^c + G_c^b \xi_w^b + c_c$; thus $z \in \mathcal{W}_h$. Given that the choice of $z \in \mathcal{C}_\mathcal{X}(\mathcal{Z}_c)$ is arbitrary, $\mathcal{C}_\mathcal{X}(\mathcal{Z}_c) \subseteq \mathcal{W}_h$ and $\mathcal{W}_h \cap \mathcal{X} = \mathcal{C}_\mathcal{X}(\mathcal{Z}_c)$. □

The complement set operation given by Proposition 3.2.7 embeds the mixed integer formulation of the KKT conditions of the LP (3.34) directly within the equality constraints of the hybrid zonotope set definition. The limitation that the proposed identity is only valid over the bounded region $\mathcal{X}$ is due to the so called "big-M" constant, δ_m, that appears in the complementary slackness condition (3.40c) [53]. The representation complexity of the hybrid zonotope $\mathcal{C}_\mathcal{X}(\mathcal{Z}_c) \subset \mathbb{R}^n$ defined by Proposition 3.2.7 is given by

$$n_{g,c} = 9n_{g,z} + n_{c,z} + n + 1\,, \tag{3.41a}$$

$$n_{b,c} = 2n_{g,z}\,, \tag{3.41b}$$

$$n_{c,c} = 7n_{g,z} + n_{c,z} + 1\,, \tag{3.41c}$$

where n is the dimension, $n_{g,z}$ is the number of generators, and $n_{c,z}$ is the number of constraints of $\mathcal{Z}_c = \langle G, c, A, b \rangle \subset \mathbb{R}^n$.

Theorem 3.2.1. *Hybrid zonotopes are closed under complement set operations.*

Proof. As proven in Theorem 3.1.1, a set is a hybrid zonotope if and only if it is the union of the finite collection of constrained zonotopes $\mathcal{Z}_{c,\mathrm{i}}$ given by (3.3). Thus given any hybrid zonotope $\mathcal{Z}_h$, by De Morgan's law, the closure of the complement of $\mathcal{Z}_h$ is given by

$$\overline{\mathcal{Z}_h^c} = \overline{\left(\bigcup_{\xi_{\mathrm{i}}^b \in \mathcal{T}} \mathcal{Z}_{c,\mathrm{i}} \right)^c} = \bigcap_{\xi_{\mathrm{i}}^b \in \mathcal{T}} \overline{\mathcal{Z}_{c,\mathrm{i}}^c} \,. \tag{3.42}$$

Furthermore, given the representation of $\overline{\mathcal{Z}_{c,\mathrm{i}}^c}$ by Proposition 3.2.7 as a hybrid zonotope and the closure of hybrid zonotopes under intersections, it follows that $\overline{\mathcal{Z}_h^c}$ is a hybrid zonotope. □

Remark 3.2.1. *The KKT conditions are necessary but no longer sufficient for the nonconvex point containment problem of the hybrid zonotope (see Proposition 3.2.8). To avoid this issue, the result of Theorem 3.2.1 ensures that all $|\mathcal{T}|$ local minima satisfying (3.34) are enforced over the region of interest $\mathcal{X}$. Although the growth in the set representation given by (3.41) is increased proportional to the number of nonempty constrained zonotopes $|\mathcal{T}|$, this trend is similar to that encountered when representing the complements of nonconvex sets as hyperplane arrangements [13].*

Remark 3.2.2. *Note that the representations of constrained and hybrid zonotopes are not unique. For example, given the hybrid zonotope $\mathcal{Z}_h = \mathcal{C}_{\mathcal{X}}(\mathcal{Z}_c)$, it holds that $\mathcal{C}_{\mathcal{X}}(\mathcal{Z}_h) = \mathcal{Z}_c$ for any $\mathcal{X} \supseteq \mathcal{Z}_c$. While the points represented by these two sets are equivalent, their representations are not.*

3.2.4 Point and Set Containment

Following the evaluation of point containment of constrained zonotopes by solving linear programs [18, Prop. 2], the point containment of a hybrid zonotope requires the evaluation of the feasibility of an Mixed-Integer Linear Program (MILP).

Proposition 3.2.8 (Point Containment)**.** *For any* $\mathcal{Z}_h = \left\langle G^c, G^b, c, A^c, A^b, b \right\rangle \subset \mathbb{R}^n$,

$$\mathcal{Z}_h \neq \emptyset \iff \left\{ \|\xi^c\|_\infty \leq 1 \,,\, \xi^b \in \{-1,1\}^{n_b} \;\middle|\; A^c\xi^c + A^b\xi^b = b \right\} \neq \emptyset \,, \tag{3.43}$$

$$z \in \mathcal{Z}_h \iff \left\{ \|\xi^c\|_\infty \leq 1 \,,\, \xi^b \in \{-1,1\}^{n_b} \;\middle|\; \begin{bmatrix} G^c & G^b \\ A^c & A^b \end{bmatrix} \begin{bmatrix} \xi^c \\ \xi^b \end{bmatrix} = \begin{bmatrix} z - c \\ b \end{bmatrix} \right\} \neq \emptyset \,. \tag{3.44}$$

Proof. Following the proof of [18, Prop. 2]. By Def. 3.1.1, $z \in \mathcal{Z}_h$ if and only if there exists some ξ^c and ξ^b such that $\|\xi^c\|_\infty \leq 1$, $\xi^b \in \{-1,1\}^{n_b}$, $A^c\xi^c + A^b\xi^b = b$, and $z = G^c\xi^c + G^b\xi^b + c$. Choosing $(\xi^c\ \xi^b)$ to be any factors such that the right-hand side of (3.44) is feasible, $z \in \mathcal{Z}_h$ if and only if (3.44) holds. When (3.43) is satisfied, the point $z = G^c\xi^c + G^b\xi^b + c$, where $(\xi^c\ \xi^b)$ are any factors such that the right-hand side of (3.43) is feasible, belongs to $\mathcal{Z}_h$ by Def. 3.1.1 and therefore $\mathcal{Z}_h \neq \emptyset$. If no such point exists, (3.43) will not be satisfied. □

Note that the right-hand sides of (3.43) and (3.44) are the feasible space of a MILP with the constraints

$$\xi^c \in \mathcal{B}_\infty^{n_g} \,,\, \xi^b \in \{-1,1\}^{n_b} \,,\, A^c\xi^c + A^b\xi^b = b \,, \tag{3.45a}$$

$$z = G^c\xi^c + G^b\xi^b + c \,. \tag{3.45b}$$

Given a point $z \in \mathbb{R}^n$, by Proposition 3.2.8, $z \in \mathcal{Z}_h$ if the mixed-integer constraints (3.45a)-(3.45b) are feasible. If the constraints (3.45a) are infeasible then $\mathcal{Z}_h = \emptyset$.

The set containment of two hybrid zonotopes may be determined by evaluating if the intersection of the closure of the complement of one of the sets with the other is empty leveraging Theorem 3.2.1 and Proposition 3.2.8.

Proposition 3.2.9 (Set Containment)**.** *For any two hybrid zonotopes* $\mathcal{Z}_h \subset \mathbb{R}^n$ *and* $\mathcal{W}_h \subset \mathbb{R}^n$*, define* $\mathcal{C}_\mathcal{X}(\mathcal{Z}_h)$ *by Proposition 3.2.7 for a region of interest* $\mathcal{X}$ *such that* $\mathcal{X} \supseteq \mathcal{W}_h$*, then*

$$\mathcal{W}_h \subset \mathcal{Z}_h \iff \mathcal{W}_h \cap \mathcal{C}_\mathcal{X}(\mathcal{Z}_h) = \emptyset \,. \tag{3.46}$$

Proof. Let $\mathcal{W}_h \subset \mathcal{Z}_h$. Then for any $w \in \mathcal{W}_h$ it holds that $w \in \mathcal{Z}_h^\circ$ and thus $w \notin \overline{\mathcal{Z}^c}$. Given that the choice of w is arbitrary and $\mathcal{X}$ is chosen such that $\mathcal{X} \supseteq \mathcal{W}_h$ implies that $w \in \mathcal{X}$

and therefore $\mathcal{W}_h \cap \mathcal{C}_{\mathcal{X}}(\mathcal{Z}_h) = \emptyset$. Conversely, let $\mathcal{W}_h \cap \mathcal{C}_{\mathcal{X}}(\mathcal{Z}_h) = \emptyset$. Then for any $w \in \mathcal{W}_h$ it holds that $w \in \mathcal{Z}_h^\circ \cap \mathcal{X}$. Given that the choice of w is arbitrary and $\mathcal{X}$ is chosen such that $\mathcal{X} \supseteq \mathcal{W}_h$ implies that $w \in \mathcal{X}$ and therefore $\mathcal{W}_h \subset \mathcal{Z}_h$. □

Remark 3.2.3. *A tight region of interest $\mathcal{X}$ satisfying $\mathcal{X} \supseteq \mathcal{W}_h$ may always be found as the interval hull of $\mathcal{W}_h$ by solving $2n$ MILPs, as discussed in Section 3.2.5. Alternatively, a sufficient enclosure $\mathcal{X}$ may be found algebraically (see [59] for interval hulls of zonotopes) as the interval hull of the zonotope $\mathcal{Z} = \langle [G^c \; G^b], c \rangle$ satisfying $\mathcal{Z}_h \subseteq \mathcal{Z} \subseteq \mathcal{X}$ by Lemma 3.1.1.*

The set containment of two zonotopes is a difficult problem. Indeed necessary and sufficient conditions have yet to be obtained [62]. In [60] it is proven that numerically verifying the set containment of two zonotopes is co-NP-complete and propose solving the problem either by enumerating the vertices of the subset $\mathcal{W}_h$ or through solving a nonconvex optimization problem. The method proposed here extends this type of verification to nonconvex sets and amounts to a search of the hybrid zonotopes integer feasible space to find if any solution exists, which is NP-complete. Although set containment may be verified leveraging Propositions 3.2.8 and 3.2.9, the problem remains numerically challenging. Nonetheless, Proposition 3.2.9 offers a promising mixed-integer approach, especially when the superset $\mathcal{Z}_h$ is a constrained zonotope in CG-rep and Proposition 3.2.7 may be directly applied to represent its complement.

3.2.5 Support Functions and Convex Enclosures

While solving MILPs to obtain a global optimum is NP-hard, determining their feasibility is NP-complete and may often be decided quickly compared to performing optimization [63]. The intersection of a hybrid zonotope and a given halfspace may be detected by determining if $\mathcal{Z}_h \cap \mathcal{H}^- = \emptyset$ through Propositions 3.2.4 and 3.2.8 through such a feasibility check. However, it is often desirable to determine the bounds of a hybrid zonotope in a given direction $l \in \mathbb{R}^n$, e.g. to discover the maximum possible constraint violation of a system when its reachable set is given in HCG-rep. To find these tight bounds, the notion of support functions are now extended to hybrid zonotopes.

Definition 3.2.1 (Support Function)**.** *The support function of a hybrid zonotope* $\mathcal{Z}_h \subset \mathbb{R}^n$ *is*

$$\rho_{\mathcal{Z}_h}(l) = \max \left\{ l^T z \,\middle|\, z \in \mathcal{Z}_h \right\} , \tag{3.47}$$

and it holds that $\mathcal{Z}_h \subset \mathcal{H}_l^-$ *for the supporting halfspace*

$$\mathcal{H}_l^- = \left\{ z \in \mathbb{R}^n \,\middle|\, l^T z \leq \rho_{\mathcal{Z}_h}(l) \right\} . \tag{3.48}$$

When (3.47) is solved to obtain a global optimum, the supporting halfspace (3.48) is tight in the sense that the corresponding hyperplane intersects the set $\mathcal{Z}_h$ and $\mathcal{Z}_h \subset \mathcal{H}_l^-$ [43]. The containment constraint that $z \in \mathcal{Z}_h$ in (3.47) follows from Proposition 3.2.9, and $\rho_{\mathcal{Z}_h}(l)$ can be found by solving the single MILP

$$\rho_{\mathcal{Z}_h}(l) = \max \left\{ l^T (G^c \xi^c + G^b \xi^b + c) \,\middle|\, \begin{array}{c} A^c \xi^c + A^b \xi^b = b \,, \\ \|\xi^c\|_\infty \leq 1 \,,\ \xi^b \in \{-1, 1\}^{n_b} \end{array} \right\} . \tag{3.49}$$

In the analysis of convex sets, support functions are often used to provide tight polytopic enclosures of the set in H-rep as the intersection of multiple supporting halfspaces [8], [15], [43], [59], [64], [65]. Sampling the support function of a convex set over the collection of directions $\mathcal{L} \subseteq \mathbb{R}^n$ generates the over-approximating template polyhedron in H-rep

$$\lceil \mathcal{X} \rceil_{\mathcal{L}} = \bigcap_{l \in \mathcal{L}} \left\{ x \in \mathbb{R}^n \,\middle|\, l^T x \leq \rho_{\mathcal{X}}(l) \right\} , \tag{3.50}$$

such that $\lceil \mathcal{X} \rceil_{\mathcal{L}} \supseteq \mathcal{X}$. The accuracy of the over-approximating H-rep polytope increases with the number of directions sampled and indeed for convex sets it holds that $\lceil \mathcal{X} \rceil_{\mathcal{L}} = \mathcal{X}$ for $\mathcal{L} = \mathbb{R}^n$ [59], [64].

Proposition 3.2.10 (Convex Enclosure)**.** *Given any hybrid zonotope* $\mathcal{Z}_h \subset \mathbb{R}^n$*, its convex hull* $CH(\mathcal{Z}_h)$*, and collection of directions* $\mathcal{L} \subseteq \mathbb{R}^n$*, it holds that the template polyhedron* $\lceil \mathcal{Z}_h \rceil_{\mathcal{L}}$ *defined by* (3.50) *satisfies*

$$\mathcal{Z}_h \subseteq CH(\mathcal{Z}_h) \subseteq \lceil \mathcal{Z}_h \rceil_{\mathcal{L}} , \tag{3.51}$$

and $CH(\mathcal{Z}_h) = \lceil \mathcal{Z}_h \rceil_{\mathcal{L}}$ *for* $\mathcal{L} = \mathbb{R}^n$.

Proof. Let $l \in \mathcal{L} \subseteq \mathbb{R}^n$. By Theorem 3.1.1, every hybrid zonotope is equivalent to the union of a finite number of constrained zonotopes $\mathcal{Z}_h = \bigcup_{\mathrm{i}=1}^{2^{n_b}} \mathcal{Z}_{c,\mathrm{i}}$, where $\mathcal{Z}_{c,\mathrm{i}}$ is given by (3.3). Based on the definition of convex hulls, $\mathcal{Z}_h \subseteq \mathrm{CH}(\mathcal{Z}_h)$ and therefore $\mathcal{Z}_h \subseteq \mathrm{CH}(\bigcup_{\mathrm{i}=1}^{2^{n_b}} \mathcal{Z}_{c,\mathrm{i}})$. Sampling the support function of $\mathcal{Z}_h$ for l then gives $\rho_{\mathcal{Z}_h}(l) \geq \rho_{\mathcal{Z}_{c,\mathrm{i}}}(l)\ \forall\, \mathrm{i} \in \{1, \dots, 2^{n_b}\}$. Furthermore the support function of a convex hull is given by $\rho_{\mathrm{CH}(\bigcup \mathcal{Z}_{c,\mathrm{i}})}(l) = \max\{\rho_{\mathcal{Z}_{c,1}}(l), \dots, \rho_{\mathcal{Z}_{c,2^{n_b}}}(l)\}$ [59]. Thus $\rho_{\mathcal{Z}_h}(l) = \rho_{\mathrm{CH}(\bigcup \mathcal{Z}_{c,\mathrm{i}})}(l)$. Applying Definition 3.2.1 gives $\mathcal{Z}_h \subseteq \mathrm{CH}(\mathcal{Z}_h) \subset \mathcal{H}_l^-$ and iterating over all $l \in \mathcal{L}$ concludes the proof. □

Proposition 3.2.10 provides a method of generating tight convex enclosures of hybrid zonotopes by solving a series of MILPs. The simplest compact enclosure is given by sampling the support function in the n cardinal directions, i.e. $\mathcal{L} = \{\mathrm{e}_1, \dots, \mathrm{e}_n, -\mathrm{e}_1, \dots, -\mathrm{e}_n\} \subset \mathbb{R}^n$ where e_i is the standard i^{th} unit vector, and is referred to as the hybrid zonotope's interval hull. The interval hull is the tightest axis oriented box containing the set and is given by the n-dimensional interval

$$\mathcal{B}(\mathcal{Z}_h) = \begin{bmatrix} \rho_{\mathcal{Z}_h}(-\mathrm{e}_1) & , & \rho_{\mathcal{Z}_h}(\mathrm{e}_1) \\ \vdots & , & \vdots \\ \rho_{\mathcal{Z}_h}(-\mathrm{e}_n) & , & \rho_{\mathcal{Z}_h}(\mathrm{e}_n) \end{bmatrix}. \tag{3.52}$$

Convex enclosures generated by Proposition 3.2.10 of the hybrid zonotope (3.6) from Example 3.1.1 with varying number of directions sampled evenly from the unit circle are depicted in Figure 3.3.

3.3 Binary Trees

As proven in Theorem 3.1.1, a hybrid zonotope with n_b binary factors is equivalent to the union of the 2^{n_b} constrained zonotopes $\mathcal{Z}_{c,\mathrm{i}}$ given by (3.3). When it is necessary to decompose a hybrid zonotope into a collection of constrained zonotopes, enumeration of the set $\{-1, 1\}^{n_b}$ may become intractable for large n_b. However, it is possible that some of the elements $\xi_\mathrm{i}^b \in \{-1, 1\}^{n_b}$ map to empty constrained zonotopes and therefore do not contribute

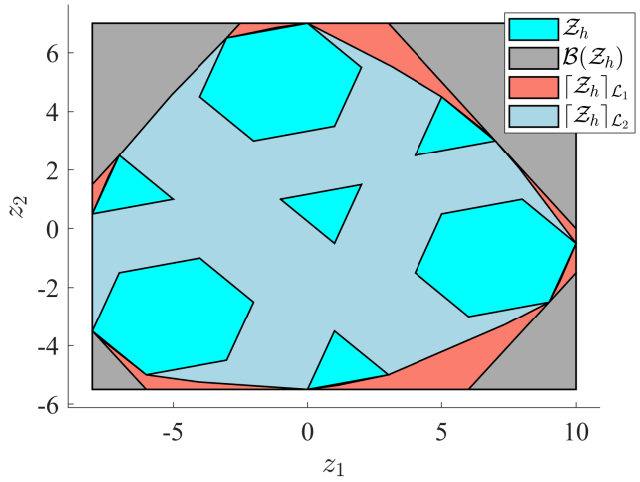

Figure 3.3. Example of generating tight convex enclosures of a hybrid zonotope by sampling the set's support function. The collection of directions $\mathcal{L}_1$ and $\mathcal{L}_2$ are evenly spaced around the unit circle in 8 and 100 directions, respectively.

points to the hybrid zonotope. In this section it is shown how the enumeration problem of decomposing hybrid zonotopes may be reduced by iteratively growing binary trees in parallel with set operations.

For a hybrid zonotope $\mathcal{Z}_h$, let $\mathcal{T} \subseteq \{-1, 1\}^{n_b}$ be the set of discrete elements that map to nonempty constrained zonotopes, that is $\mathcal{T} = \{\xi_{\mathrm{i}}^b \in \{-1, 1\}^{n_b} \mid \mathcal{Z}_{c,\mathrm{i}} \neq \emptyset\}$. Leveraging Theorem 3.1.1 and $\mathcal{Z}_h \cup \emptyset = \mathcal{Z}_h$, it follows that

$$\mathcal{Z}_h = \bigcup_{\xi_{\mathrm{i}}^b \in \mathcal{T}} \mathcal{Z}_{c,\mathrm{i}} \,. \tag{3.53}$$

The enumeration problem in decomposing hybrid zonotopes may therefore be reduced by only considering the values of the binary factors belonging to $\mathcal{T}$. The discrete set $\mathcal{T}$ also gives a measure of how efficient the set is—ideally a hybrid zonotope representing 2^N constrained zonotopes would only have N binary factors.

The hybrid zonotope is a mixed integer set representation [66] and may be described by a rooted binary tree [67]. The root of the binary tree is the hybrid zonotope $\mathcal{Z}_h$ and the nonempty leaves are the constrained zonotopes $\mathcal{Z}_{c,\mathrm{i}} \,\forall\, \xi_{\mathrm{i}}^b \in \mathcal{T}$. The binary tree consists of n_b

layers, where the jth layer branches on the value of the jth binary factor. Each layer of the tree between the root and leaves consists of branch nodes given by hybrid zonotopes

$$\mathcal{Z}^{\mathrm{j}}_{h,\mathrm{i}} = \left\langle G^c, G^b_d, c + G^b_a \xi^b_{\mathrm{i}}, A^c, A^b_d, b - A^b_a \xi^b_{\mathrm{i}} \right\rangle , \tag{3.54}$$

where the binary generator and constraint matrices are partitioned such that $G^b = [G^b_a \; G^b_d]$, where G^b_a are the j columns for the ancestor nodes multiplied by $\xi^b_{\mathrm{i}} \in \{-1, 1\}^{\mathrm{j}}$ for the ith branch node of the layer, and G^b_d the remaining columns for the binary factors that are branched on by the descendants. The binary tree and relation between each node for a hybrid zonotope with $n_b / \log_2(|\mathcal{T}|) = 1.5$ is depicted in Fig. 3.4.

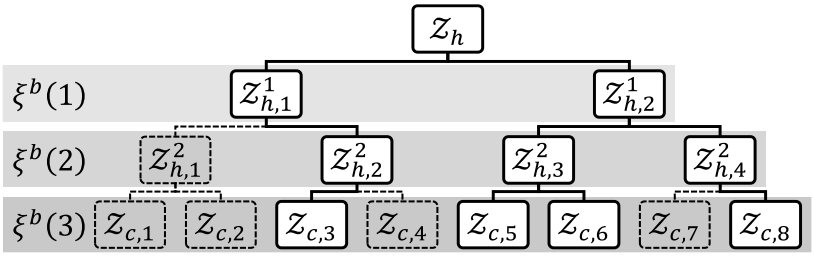

Figure 3.4. Example of the binary tree for a hybrid zonotope $\mathcal{Z}_h$ with three binary factors. The set $\mathcal{T}$ is depicted by the bold black lines and empty nodes are grey with dashed borders. In this example, the relations between layers of the binary tree are given by $\mathcal{Z}_h = \mathcal{Z}^1_{h,1} \cup \mathcal{Z}^1_{h,2}$, $\mathcal{Z}^1_{h,1} = \mathcal{Z}^2_{h,2} = \mathcal{Z}_{c,3}$, $\mathcal{Z}^1_{h,2} = \mathcal{Z}^2_{h,3} \cup \mathcal{Z}^2_{h,4}$, $\mathcal{Z}^2_{h,3} = \mathcal{Z}_{c,5} \cup \mathcal{Z}_{c,6}$, and $\mathcal{Z}^2_{h,4} = \mathcal{Z}_{c,8}$.

The set $\mathcal{T}$ may be found with any MILP algorithm that explores the constrained space of factors given by (3.45a), e.g., branch and cut [53], and is referred to as the integer feasible set of the MILP. Although many algorithms exist that may be used to find $\mathcal{T}$, the computational burden grows as the number of variables increases. Through all set operations of hybrid zonotopes, the constraints on the factors of the operating sets are imposed directly in the resulting hybrid zonotope. Thus the hybrid zonotope generated through set operations with additional binary factors may only branch from the nonempty leaves of the operating sets.

Given a hybrid zonotope $\mathcal{Z}_{h,1}$ with integer feasible set $\mathcal{T}_1 \subseteq \{-1, 1\}^{n_{b,1}}$, let $\mathcal{Z}_{h,2}$ be a hybrid zonotope found through set operations applied to $\mathcal{Z}_{h,1}$ introducing k additional binary factors. Rather than finding $\mathcal{T}_2 \subseteq \{-1, 1\}^{n_{b,1}+k}$ by solving the MILP (3.45a) for $\mathcal{Z}_{h,2}$

directly, it is possible to leverage the fact that the leaves of $\mathcal{Z}_{h,2}$ are the descendants of $\mathcal{Z}_{h,1}$, where $\mathcal{T}_1$ is already known. Thus an alternative approach is to solve the MILP (3.45a) for the $|\mathcal{T}_1|$ branch nodes given by (3.54) at layer $n_{b,1}$, each having only k binary factors. The new integer feasible set $\mathcal{T}_2$ is then given by the union of the results from these $|\mathcal{T}_1|$ MILPs appended to the values of $\mathcal{T}_1$. This approach is described in Algorithm 1.

Algorithm 1 Branching the binary tree of $\mathcal{Z}_{h,2}$ on the descendants of $\mathcal{Z}_{h,1}$.

Input: $\mathcal{Z}_{h,2} = \langle G^c, G^b, c, A^c, A^b, b \rangle$, $\mathcal{T}_1 \subseteq \{-1, 1\}^{n_{b,1}}$
Output: $\mathcal{T}_2 \subseteq \{-1, 1\}^{n_{b,2}}$

1: **for** $\xi_{\mathrm{i}}^b \in \mathcal{T}_1$ **do**
2: $\quad \mathcal{Z}_{h,\mathrm{i}}^{n_{b,1}} \leftarrow$ (3.54) for ξ_{i}^b
3: $\quad$ Solve MILP to find integer feasible set $\mathcal{T}$ of $\mathcal{Z}_{h,\mathrm{i}}^{n_{b,1}}$
4: $\quad$ Append entries of $\mathcal{T}$ to ξ_{i}^b and store in $\mathcal{T}_2$
5: **end for**

Since finding $\mathcal{T}$ amounts to an exhaustive search of the integer feasible space of the MILP (3.45a), Algorithm 1 aims to reduce the number of branches that must be searched at each iteration by solving more, smaller MILPs. Each of these smaller MILPs search the subtrees branching on the binary factors added since the last search has been performed. Thus leveraging information stored in the set $\mathcal{T}_1$ prevents searching nodes that have already been determined as infeasible during previous iterations. Note that Algorithm 1 is NP-hard with worst-case exponential run time. Nevertheless, this approach may allow the decomposition of complex hybrid zonotopes into a collection of constrained zonotopes when many set operations are applied iteratively.

3.4 Numerical Example: Obstacle Avoidance

This example considers the problem of formulating a model predictive controller (MPC) for an agent moving from an initial condition to a target point while avoiding collision with multiple obstacles. In [5] it is shown that over-approximating polytopic obstacles using zonotopes sharing a common structure leads to considerable improvements in the computation time of the MPC. However, once the over-approximation is found, the zonotope must be converted back to an H-rep polytope [5] to represent its complement as hyperplane arrange-

ments [13]. Here it is shown how the same safety constraint may be formulated directly as a hybrid zonotope representing the complements of the obstacles.

This example considers a single agent in $2D$ space with continuous dynamics given by

$$\dot{x} = \begin{bmatrix} \mathbf{0} & I_2 \\ \mathbf{0} & -\frac{\mu}{M} I_2 \end{bmatrix} x + \begin{bmatrix} \mathbf{0} \\ \frac{1}{M} I_2 \end{bmatrix} u \,, \tag{3.55}$$

where $x_{1,2}$ is the position and $x_{3,4}$ the velocity of the agent, the control actions are the acceleration in the $1, 2$ coordinates, and the model parameters are $\mu = 3$ and $M = 60$ [5]. The obstacles are over-approximated by a zonotope denoted by $\mathcal{Z}_{\text{i}}$, and their union is given by the hybrid zonotope $\mathcal{Z}_{h,O} = \bigcup \mathcal{Z}_{\text{i}}$. The optimal action of the agent at each time step under the proposed MPC is given by the solution to the mixed-integer quadratic program

$$\begin{aligned} \min_{u} \; & x_N^T P x_N + \sum_{k=0}^{N-1} x_k^T Q x_k + u_k^T R u_k \\ & \text{s.t. } \forall\, k \in [0, N-1] \,,\; x_{k+1} = A x_k + B u_k \,, \\ & u_k \in \mathcal{U} \,,\; x_{k+1} \in \mathcal{C}_{\mathcal{X}}(\mathcal{Z}_{h,O}) \times \mathbb{R}^2 \,, \end{aligned} \tag{3.56}$$

where x_0 is fixed to the sampled state of the system, $\mathcal{U} = \{u \in \mathbb{R}^2 \mid \|u\|_\infty \leq 1\}$ is the set of all admissible control inputs, and the states are constrained to the nonconvex safe set $\mathcal{C}_{\mathcal{X}}(\mathcal{Z}_{h,O}) \times \mathbb{R}^2$ for $\mathcal{X} = \{x \in \mathbb{R}^2 \mid \|x\|_\infty \leq 2\}$. The A and B matrices used in the MPC formulation are given by the zero-order hold transform of (3.55) with a discrete time step of $T_s = 0.5$. The MPC parameters are set to $Q = I_4$, $P = 10 I_4$, $R = I_2$, and $N = 10$ [5]. The safe set, $\mathcal{C}_{\mathcal{X}}(\mathcal{Z}_{h,O}) \times \mathbb{R}^2$ generated through Theorem 3.2.1 and Proposition 3.2.7 with two example trajectories of the simulated closed-loop plant are shown in Fig. 3.5.

The MPC problem (3.56) is formulated using YALMIP [68] and solved using Gurobi [69] with MATLAB on a desktop computer using one core of a 3.0 GHz Intel i7 processor with 32 GB of RAM. The computation time to formulate and solve the MPC (3.56), analyzed over 100 trials with randomly sampled initial conditions, is given in Table 3.2. The computation time is compared to the equivalent problem formulated using hyperplane arrangements to define the safety constraint $\mathcal{C}_{\mathcal{X}}(\mathcal{Z}_{h,O})$ (see Section 2.3.2 and [13, Sec. 2.1]). It is noted

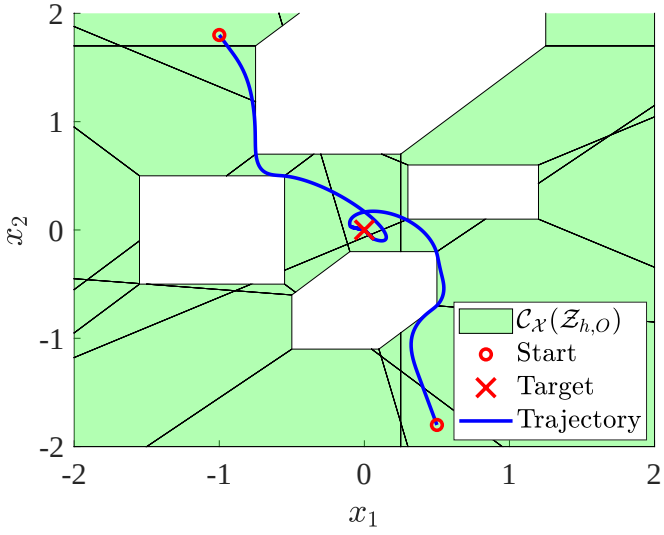

Figure 3.5. Hybrid zonotope defined as the complement of the union of the obstacles, $\mathcal{C}_{\mathcal{X}}(\mathcal{Z}_{h,O})$, and trajectories of the simulated closed-loop system. Black lines depict the decomposition of the hybrid zonotope $\mathcal{C}_{\mathcal{X}}(\mathcal{Z}_{h,O})$ into constrained zonotopes by Theorem 3.1.1.

that additional methods exist to further reduce the complexity of hyperplane arrangements, such as logarithmic formulations and merging adjacent cells [70], each introducing additional overhead in the formulation of the problem. It is also noted that hyperplane arrangements have a mature theory in obstacle avoidance, including methods to guarantee the constraint satisfaction of the plant's continuous dynamics [71]. Nevertheless, the use of hybrid zonotopes shows a considerable improvement in the average solution time in this case, namely a reduction by $\sim 47\%$.

Table 3.2. Computation times to formulate and solve the MPC problem (3.56) analyzed over 100 trials.

$\mathcal{C}_{\mathcal{X}}(\mathcal{Z}_{h,O})$	Average (s)	Maximum (s)
Hybrid Zonotope	0.10	0.24
Hyperplane Arrangement	0.19	0.25

3.5 Chapter Summary

This chapter has presented a new mixed-integer set representation named the *hybrid zonotope*. Hybrid zonotopes extend zonotopes and constrained zonotopes to represent the nonconvex union of an exponential number of convex sets using a linear number of continuous and discrete variables. I have shown how hybrid zonotopes may be decomposed into a collection of constrained zonotopes for visualization and analysis. I have derived set operations for linear mappings, Minkowski sums, generalized intersections, halfspace intersections, Cartesian productions, unions, and complements, thereby providing a nonconvex set representation with applicability to a broad range of set-theoretic methods. I have shown how the bounds of a hybrid zonotope may be found by solving a mixed-integer linear program, and that doing so provides a method for generating tight convex enclosures. I have shown how every hybrid zonotope has an underlying binary tree that may be leveraged to reduce the complexity of converting them into a collection of a convex sets. Furthermore, I have developed an algorithm that leverages the propagation of this binary tree through set operations to avoid repetitive calculations. A numerical example has shown the use of hybrid zonotopes as safety constraints in an obstacle avoidance problem and showed improved computation time over the conventional method using hyperplane arrangements.

4. FORWARD REACHABLE SETS OF HYBRID SYSTEMS

In this chapter I present a closed-form solution to the exact reachable sets of linear hybrid systems as hybrid zonotopes. Identities are derived for both hybrid systems modeled as Mixed Logical Dynamical (MLD) systems, as presented by Trevor J. Bird, Herschel C. Pangborn, Neera Jain, and Justin P. Koeln in [57], provisionally accepted by *Automatica*, and closed-loop systems under Model Predictive Control (MPC), as presented by Trevor J. Bird, Neera Jain, Herschel C. Pangborn, and Justin P. Koeln, in the *Proceedings of the 2022 American Controls Conference* [72], both are included here with minor modifications. The presented methods are given by identities that don't require solving any optimization programs or taking set approximations. The proposed approach captures the worst-case exponential growth in the number of convex sets required to represent the nonconvex reachable set of a hybrid system while exhibiting only linear growth in the complexity of the hybrid zonotope set representation. All technical contributions of this chapter were made by Trevor J. Bird while being advised by Professor Neera Jain at Purdue University, as well as Professor Justin P. Koeln (University of Texas Dallas) and Professor Herschel Pangborn (The Pennsylvania State University).

The remainder of this chapter is organized as follows. In Sec. 4.1 I derive an identity for the forward propagation of hybrid system dynamics as hybrid zonotopes and provide two numerical examples. In Sec. 4.2 I show how the optimality conditions of linear MPC may be embedded within the hybrid zonotope set definition, resulting in the representation of the explicit multiparametric solution. Using the set of explicit MPC solutions, I show how the closed-loop dynamics of a linear time-invariant system under MPC may be propagated using hybrid zonotopes.

4.1 Reachable Sets of MLD Systems

In this section I derive an identity for representing exact reachable sets of discrete-time hybrid automata modeled as Mixed Logical Dynamical (MLD) systems [73] using hybrid zonotopes. This identity contains all guard set intersections implicitly as properties of the MLD model and avoids solving any optimization programs or using approximation techniques

to determine guard crossings, changes in dynamics, or reset maps. This approach is desirable as it is both computationally efficient and exact. Numerical examples show the hybrid zonotope's ability to compactly represent nonconvex reachable sets with an exponential number of features. This section is organized as follows. First I describe the modeling of hybrid systems as mixed logical dynamical systems in Sec. 4.1.1. In Section 4.1.2, I present a closed-form solution to the forward reachable sets of MLD systems and a redundancy removal technique is described in Section 4.1.3. Finally, in Section 4.1.4 I provide two numerical examples, one of which compares the proposed approach to two previous exact methods.

4.1.1 Mixed Logical Dynamical (MLD) Systems

As first introduced in [73], the Mixed Logical Dynamical (MLD) system modeling framework combines continuous and binary variables with logical relations in mixed-integer inequalities to express complex dynamic systems. It has been shown in [73], [74] that such a framework can be used to model systems that have mixed continuous and discrete states and inputs, piece-wise affine and bilinear dynamics, finite state machines, qualitative outputs, and those with any combination of the former. An MLD system with linear discrete-time dynamics may be expressed as

$$x_+ = Ax + B_u u + B_w w + B_{aff} \,, \tag{4.1a}$$

$$\text{s.t.} \;\; E_x x + E_u u + E_w w \leq E_{aff} \,, \tag{4.1b}$$

where $x \in \mathbb{R}^{n_{xc}} \times \{0,1\}^{n_{xl}}$ are the system states, $u \in \mathbb{R}^{n_{uc}} \times \{0,1\}^{n_{ul}}$ are the control inputs, and $w \in \mathbb{R}^{n_{rc}} \times \{0,1\}^{n_{rl}}$ are auxiliary variables. The number of inequality constraints is denoted by n_e such that $E_{aff} \in \mathbb{R}^{n_\text{e}}$. Given any fixed state x and input u, the trajectory of the MLD system in a single time step is given by the difference equation (4.1a) for any auxiliary variable w that satisfy the inequality constraints (4.1b).

When formulating an MLD model (4.1), the so-called "big-M" constants used in the mixed-integer inequalities to relate continuous values to logical statements are chosen for a

user-defined subset of the state space, $\mathcal{X} \subset \mathbb{R}^{n_{xc}} \times \{0,1\}^{n_{xl}}$, and set of admissible control inputs, $\mathcal{U} \subset \mathbb{R}^{n_{uc}} \times \{0,1\}^{n_{ul}}$ [73]. It follows that for the bounded state-input domain over which the MLD model is defined, the auxiliary variables will belong to a compact set $\mathcal{W} \subset \mathbb{R}^{n_{rc}} \times \{0,1\}^{n_{rl}}$. The MLD representation and set of possible auxiliary variables $\mathcal{W}$ of linear discrete-time hybrid systems may be generated automatically using the modeling tool Hybrid System DEscription Language (HYSDEL) [75].

4.1.2 Forward Reachable Sets of MLD Systems

A closed-form solution to the forward reachable sets of MLD systems as hybrid zonotopes is now presented.

Theorem 4.1.1. *Consider the MLD system described by (4.1) with $x \in \mathcal{R}_k \subseteq \mathcal{X} \subset \mathbb{R}^{n_{xc}} \times \{0,1\}^{n_{xl}}$, $u \in \mathcal{U} \subset \mathbb{R}^{n_{uc}} \times \{0,1\}^{n_{ul}}$, and $w \in \mathcal{W} \subset \mathbb{R}^{n_{rc}} \times \{0,1\}^{n_{rl}}$ given in HCG-rep. Let*

$$\mathcal{V} = \begin{bmatrix} B_u \\ E_u \end{bmatrix} \mathcal{U} \oplus \begin{bmatrix} B_w \\ E_w \end{bmatrix} \mathcal{W} \oplus \begin{bmatrix} B_{aff} \\ \mathbf{0} \end{bmatrix},$$

and define the polyhedron $\mathcal{H} = \{s \in \mathbb{R}^{n_e} \mid s \leq E_{aff}\} \subset \mathbb{R}^{n_e}$. Then the set of states reachable in one time step is given by the hybrid zonotope

$$\mathcal{R}_{k+1} = [\mathbf{I}_n \ \mathbf{0}] \left[\left(\begin{bmatrix} A \\ E_x \end{bmatrix} \mathcal{R}_k \oplus \mathcal{V} \right) \cap_{[\mathbf{0} \ \mathbf{I}_{n_e}]} \mathcal{H} \right]. \tag{4.2}$$

Proof. Let $\tilde{\mathcal{R}}$ denote the hybrid zonotope given by the right-hand side of (4.2) and $\mathcal{R}_{k+1}$ denote the set of states reachable by the MLD system (4.1) in one time step. For any $r \in \mathcal{R}_{k+1}$ there exists some $x \in \mathcal{R}_k$, $u \in \mathcal{U}$, and $w \in \mathcal{W}$ such that $E_x x + E_u u + E_w w \leq E_{aff}$ and $r = Ax + B_u u + B_w w + B_{aff}$. Let $\Gamma = [A^T \ E_x^T]^T$ and

$$v = \begin{bmatrix} B_u \\ E_u \end{bmatrix} u + \begin{bmatrix} B_w \\ E_w \end{bmatrix} w + \begin{bmatrix} B_{aff} \\ \mathbf{0} \end{bmatrix}. \tag{4.3}$$

Then $v \in \mathcal{V}$ and $(\Gamma x+v) \in \Gamma\mathcal{R}_k \oplus \mathcal{V}$. Furthermore, $r = [\mathbf{I}_n\ \mathbf{0}]\,(\Gamma x+v)$ and $[\mathbf{0}\ \mathbf{I}_{n_e}]\,(\Gamma x+v) \in \mathcal{H}$. Thus $r \in \tilde{\mathcal{R}}$ and $\mathcal{R}_{k+1} \subseteq \tilde{\mathcal{R}}$.

Conversely, for any $\tilde{r} \in \tilde{\mathcal{R}}$ there exists some $x \in \mathcal{R}_k$ and $v \in \mathcal{V}$ such that $\tilde{r} = [\mathbf{I}_n\ \mathbf{0}]\,(\Gamma x + v)$ and $[\mathbf{0}\ \mathbf{I}_{n_e}]\,(\Gamma x + v) \in \mathcal{H}$. For any $v \in \mathcal{V}$, there exists some $u \in \mathcal{U}$ and $w \in \mathcal{W}$ such that v is given by (4.3). Then $\tilde{r} = Ax + B_u u + B_w w + B_{aff}$ such that $E_x x + E_u u + E_w w \in \mathcal{H} \Leftrightarrow E_x x + E_u u + E_w w \leq E_{aff}$. Therefore $\tilde{r} \in \mathcal{R}_{k+1}$, $\tilde{\mathcal{R}} \subseteq \mathcal{R}_{k+1}$, and $\tilde{\mathcal{R}} = \mathcal{R}_{k+1}$. □

Remark 4.1.1. *Given that the MLD system (4.1) is only defined over the bounded subset of the state space $\mathcal{X}$ chosen when formulating the MLD model, the set of states reachable from $\mathcal{R}_k$ in one time step is given by Theorem 4.1.1 only when $\mathcal{R}_k \subseteq \mathcal{X}$. When applying Theorem 4.1.1 iteratively to find the set of states reachable for $k = 0, \ldots, N$ time steps, $\mathcal{R}_N$ may be a subset of the true reachable set if $\mathcal{R}_{\mathrm{j}} \not\subseteq \mathcal{X}$ for some $\mathrm{j} \in \{0, \ldots, N\}$. This is due to the implicit reduction of the feasible space of the MLD system's mixed-integer inequality constraints caused by introducing big-M constants [53]. The condition that $\mathcal{R}_{\mathrm{j}} \subseteq \mathcal{X}$ may be verified by Proposition 3.2.9.*

By enforcing the MLD system's mixed-integer inequality constraints as halfspace intersections with hybrid zonotopes, Theorem 4.1.1 provides a method of determining the exact set of states reachable by MLD systems defined by (4.1). This approach is desirable as the propagation of the system dynamics is given by an identity and is computed algebraically. In contrast with existing approaches [9]–[11], the intersections with guard sets are handled implicitly as properties of the MLD system and require no iterative approximations or optimization programs. Furthermore, the growth in complexity of the set is a linear function of the number of iterative applications of Theorem 4.1.1. Specifically, given an initial set of states $\mathcal{R}_0 \subset \mathbb{R}^{n_{xc}} \times \{0,1\}^{n_{xl}}$ and set of admissible control inputs $\mathcal{U} \subset \mathbb{R}^{n_{uc}} \times \{0,1\}^{n_{ul}}$ in

HCG-rep, the set of states reachable by the MLD system (4.1) in k time steps is a hybrid zonotope $\mathcal{R}_k$ with representation complexity given by

$$n_{g,r}(k) = (n_{g,u} + n_{rc} + n_{\mathrm{e}})k + n_{g,0} \,, \tag{4.4a}$$

$$n_{b,r}(k) = (n_{b,u} + n_{rl})k + n_{b,0} \,, \tag{4.4b}$$

$$n_{c,r}(k) = (n_{c,u} + n_{\mathrm{e}})k + n_{c,0} \,. \tag{4.4c}$$

The time complexity of (4.2) is dominated by the linear mapping of $\mathcal{R}_0$ and scales as $\mathcal{O}(n(n+n_{\mathrm{e}})(n_{g,0}+n_{b,0}))$, where $n = n_{xc}+n_{xl}$. Given that $a_1 n_{g,0} = a_2 n_{b,0} = a_3 n_{\mathrm{e}} = n$ for some $a_{\mathrm{i}} \in \mathbb{R}$, the time complexity of k iterations of (4.2) scales as $\mathcal{O}(n^3 k)$.

4.1.3 Redundant Inequality Constraints

It is possible that some of the inequality constraints of the MLD system (4.1b) are always satisfied by the elements of $\mathcal{R}_k$ and $\mathcal{U}$ and therefore do not need to be enforced within the hybrid zonotope $\mathcal{R}_{k+1}$. That is, $\mathrm{e}^{\mathrm{i}}_x x + \mathrm{e}^{\mathrm{i}}_u u + \mathrm{e}^{\mathrm{i}}_w w < \mathrm{e}^{\mathrm{i}}_{aff}\ \forall\, x \in \mathcal{R}_k,\ u \in \mathcal{U}$, and $w \in \mathcal{W}$, where e^{i} is the i^{th} row of the matrix E. In this case, including the i^{th} inequality constraint in $\mathcal{R}_{k+1}$ is unnecessary and its removal reduces both $n_{c,r}$ and $n_{g,r}$ because the slack factor enforcing the inequality constraint is also unnecessary. This redundancy may be detected by evaluating the feasibility of an MILP with constraints

$$\begin{aligned} \begin{bmatrix} A^c_r & A^b_r \end{bmatrix} \begin{bmatrix} \xi^c_r \\ \xi^b_r \end{bmatrix} = b \,,\ \xi^b_r \in \{-1, 1\}^{n_{b,r}} \\ \left\| (\xi^c_x\ \xi^c_u\ \xi^c_w\ \xi_{h,\mathrm{j}\neq\mathrm{i}}) \right\|_\infty \leq 1 \,,\ 1 \leq \xi_{h,\mathrm{i}} \,, \end{aligned} \tag{4.5}$$

where $\xi^c_r = (\xi^c_x\ \xi^c_u\ \xi^c_w\ \xi_h)$, and the i^{th} slack factor, $\xi_{h,\mathrm{i}}$, is removed from the infinity norm constraint and instead constrained to be greater than or equal to 1. If the MILP is infeasible, then the i^{th} inequality constraint may be removed.

4.1.4 Numerical Examples

This section presents the forward reachable sets of two linear MLD systems in the form of (4.1). In both examples, the reachable set is found through iterative application of Theorem 4.1.1 and redundant inequality constraints and binary factors are removed using the methods described in Sections 4.1.3 and 6.1.3, respectively. MLD representations of the presented hybrid systems are obtained using HYSDEL 3.0 [75]. Optimization problems are solved using Gurobi [69]. Figures are generated by decomposing the hybrid zonotope into a collection of constrained zonotopes by Theorem 3.1.1 and converting them to H-rep polytopes. If the order of the constrained zonotopes are below 50, they are converted to an H-rep polytope using the Multi-Parametric Toolbox (MPT) [12], otherwise tight over-approximations are found by sampling the support function (3.47) in 250 uniformly-distributed directions. Numerical results are generated with MATLAB on a desktop computer using four cores of a 3.0 GHz Intel i7 processor with 32 GB of RAM.

Piece-Wise Affine System with Two Equilibrium Points

Consider the discrete-time Piece-Wise Affine (PWA) system given by

$$x[k+1] = \begin{cases} \begin{bmatrix} 0.75 & 0.25 \\ -0.25 & 0.75 \end{bmatrix} x[k] + \begin{bmatrix} -0.25 \\ -0.25 \end{bmatrix}, & \text{if } x_1 \leq 0\,, \\ \begin{bmatrix} 0.75 & -0.25 \\ 0.25 & 0.75 \end{bmatrix} x[k] + \begin{bmatrix} 0.25 \\ -0.25 \end{bmatrix}, & \text{otherwise}\,. \end{cases} \tag{4.6}$$

This hybrid system consists of two stable, autonomous subsystems, each having an equilibrium point at $x = \pm[1\ 0]^T$. The PWA system can be represented as an MLD system by introducing two continuous auxiliary variables, $n_{rc} = 2$, one binary auxiliary variable, $n_{rl} = 1$, and ten inequality constraints, $n_{\mathrm{e}} = 10$. The states reachable by (4.6) in $N = 15$ time steps are shown in Fig. 4.1. The set representation dimensions and computation times are given in Table 4.1 for the reachable sets with and without redundancy removal.

Table 4.1. Results of reachability analysis for (4.6) with redundancy removal, $\mathcal{R}_{15}^r$, and without, $\mathcal{R}_{15}$. Reported computation times include all steps from initializing $\mathcal{R}_0$ to generating the set with shown dimensions.

Set	$n_{g,r}$	$n_{c,r}$	$n_{b,r}$	$\lvert\mathcal{T}\rvert$	Time (sec)
$\mathcal{R}_{15}$	182	150	15	2	0.02
$\mathcal{R}_{15}^r$	142	110	1	2	0.36

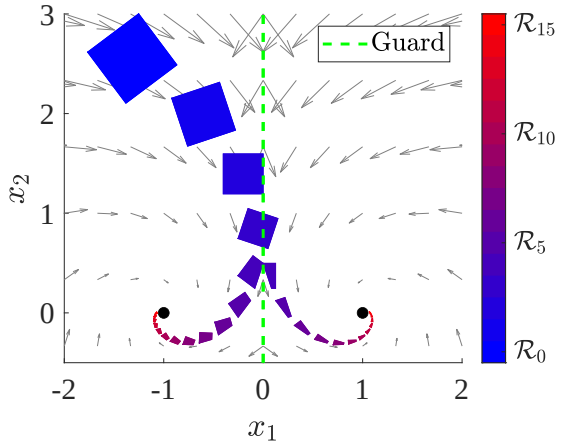

Figure 4.1. Reachable set of PWA system (4.6) with two subsystems, each having an equilibrium point depicted by $\bullet$ and autonomous dynamics with vector fields depicted by $\rightarrow$.

The auxiliary binary variable in the MLD representation of this PWA system indicates which side of the guard a state is located. If the reachable set is fully contained on one side of the guard, then only one value of the binary auxiliary variable is feasible. When a guard crossing occurs at $k = 3$, the introduced binary variable has a feasible value of $-1 \vee 1$ and branches the reachable set. No additional guard crossings occur in all following time steps. Thus the feasible value of the subsequent binary variables are dependent on that of the one introduced at $k = 3$—i.e. a state can only be on the right-hand side of the guard if it is a trajectory from a state crossing the guard at $k = 3$. The redundancy removal techniques given in Section 6.1.3 capture these dependencies to reduce the reachable set having fifteen binary factors and a full binary tree with $2^{15} = 32,768$ leaves to one with *two leaves from a single binary factor*. In this example, 40 of the inequality constraints are identified as redundant and removed using the method described in Section 4.1.3.

Thermostat-Controlled Heated Rooms

This example extends the heated room scenario given in [11], where the thermostatic control and heat exchange among adjacent rooms is modeled as a hybrid system. The continuous temperature dynamic of the i^{th} room is modeled as

$$\dot{x}_{\mathrm{i}} = c \cdot h_{\mathrm{i}} + b_{\mathrm{i}}(u - x_{\mathrm{i}}) + \sum_{\mathrm{i}\neq\mathrm{j}} a_{\mathrm{ij}}(x_{\mathrm{j}} - x_{\mathrm{i}}) \,, \tag{4.7}$$

where the heat transfer coefficient a_{ij} is 1 between adjacent rooms and 0 otherwise, the heat transfer coefficient between the room and the outside environment is $b_{\mathrm{i}} = 0.08q$ where q is the number of exposed walls, the heating power is $c = 15$ with $h_{\mathrm{i}} \in \{0, 1\}$ for rooms with heaters and $h_{\mathrm{i}} = 0$ otherwise, and the outside temperature may take on any value within the interval $u \in [0, 0.1]$ [11]. Heaters located in select rooms are controlled by discrete-time thermostats that turn on when the sampled temperature in the room decreases below 22°C and turn off when it increases above 24°C. The closed-loop temperature dynamics of the building may be modeled as an MLD system by introducing one binary state, three auxiliary binary variables, and nine inequality constraints for each heater.

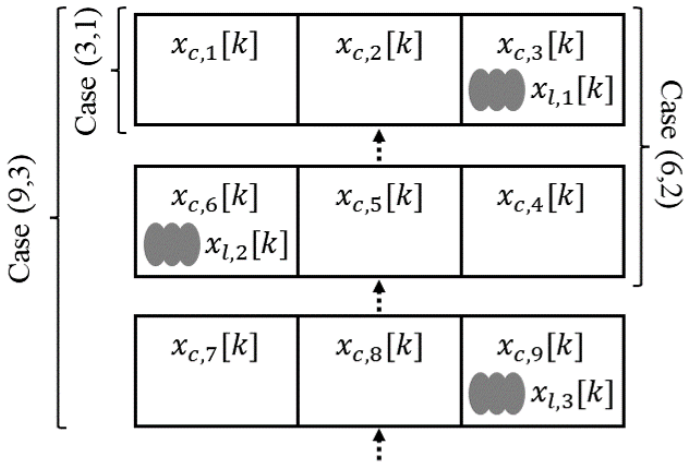

Figure 4.2. Room layout and heater locations for a varying number of rooms. The pattern shown is repeated for Case$(12, 4)$.

Four cases are considered with $n_{xc} = 3p$ continuous and $n_{xl} = 1p$ discrete states for $p = 1, \ldots, 4$. Each case is coded as Case(n_{xc}, n_{xl}) to denote the varying building layout

shown in Fig. 4.2. Heaters are located in every third room such that $h_j \in \{0, 1\}$ for $j = 3p$ as depicted in Fig. 4.2. Using a discrete time step of $T_s = 0.01$ and a zero-order-hold discrete transform of the continuous dynamics (4.7), the reachable set of the four MLD systems for a time interval of $t = [0, 1]$ is generated as hybrid zonotopes with dimensions reported in Table 4.2. The set of initial temperatures are given by $x_c[0] = (x_0 \ x_0) \pm 0.1$ where $x_0 = [23 \ 23.5 \ 23.5 \ 22.5 \ 23 \ 22.5]^T$. All heaters begin on such that $x_l[0] = \mathbf{1}$. The computation time of each step of the proposed method is provided in Table 4.3. Four 2D projections of the reachable set for Case$(6, 2)$ are plotted in Fig. 4.3.

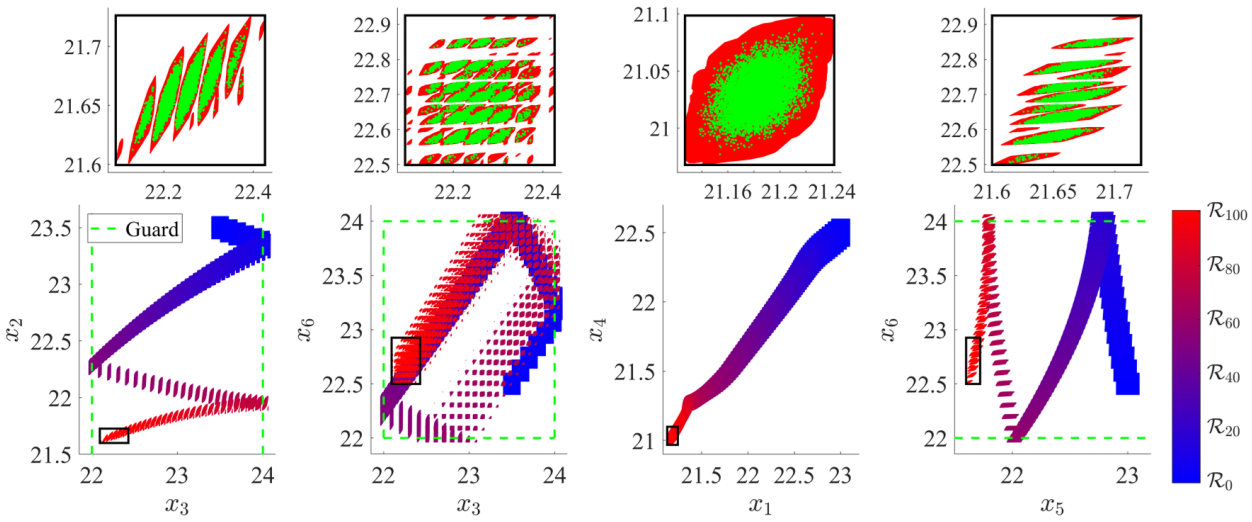

Figure 4.3. Projections of the reachable set of the heated room MLD system Case$(6, 2)$. Supporting halfspaces in each state dimension at the final time step shown by black boxes. Zoomed in plots of the final reachable set shown with 10^4 randomly sampled, simulated trajectories given by green dots.

In Table 4.2 it is shown how hybrid zonotopes are able to capture possible exponential growth in the complexity of the nonconvex reachable set through linear growth in set representation complexity. In Case$(3, 1)$, the hybrid zonotope $\mathcal{R}_{100}$ is equivalent to the union of 39 convex subsets using 1003 continuous and 300 binary factors. As the complexity of the system is increased through the other three cases, more guard crossings occur over the 100 step horizon and the resulting reachable set is increasingly nonconvex. In Case$(12, 4)$, the hybrid zonotope $\mathcal{R}_{100}$ is equivalent to the union of over 410×10^3 convex subsets using 3712 continuous and 1200 binary factors. After applying the proposed redundancy removal

techniques, the reduced hybrid zonotope $\mathcal{R}_{100}^r$ represents the nonconvex reachable set using only 484 continuous factors, 58 binary factors, and 372 constraints.

Table 4.2. Set dimensions of reachability analysis for the heated rooms with redundancy removal, $\mathcal{R}_{100}^r$, and without, $\mathcal{R}_{100}$.

	$\mathcal{R}_{100}$			$\mathcal{R}_{100}^r$			
Case	$n_{g,r}$	$n_{b,r}$	$n_{c,r}$	$n_{g,r}$	$n_{b,r}$	$n_{c,r}$	$\lvert\mathcal{T}\rvert$
$(3,1)$	1003	300	900	261	19	113	39
$(6,2)$	1906	600	1800	283	29	177	657
$(9,3)$	2809	900	2700	445	64	336	66523
$(12,4)$	3712	1200	3600	484	58	372	410605

The scalability of the proposed approach can be seen in Table 4.3. The computational complexity of Theorem 4.1.1 to find the unreduced set $\mathcal{R}_{100}$ scales as $\mathcal{O}(n^3)$ and is reflected in the reported computation times. On the other hand, the use of Algorithm 1 to explore the hybrid zonotope's binary tree is NP-hard. However, the complexity of the binary tree is a direct consequence of the number of discrete changes in the hybrid dynamics of the system. In Case$(3,1)$ the number of nonempty leaves of the binary tree is relatively small, and Algorithm 1 contributes only 4% of the total computation time. In Case$(12,4)$, the time spent on Algorithm 1 jumps to nearly 92% of the total computation time. However when comparing this value to $\lvert\mathcal{T}\rvert$, the average time spent per nonempty leaf explored only ranges from $2.2-7.3$ms across all cases. The computational burden of detecting redundant inequality constraints grows with the representation complexity of the hybrid zonotope; however, the number of evaluations of the NP-complete problem is finitely given by the number of constraints.

Table's 4.4 and 4.5 compare the use of hybrid zonotopes to represent the reachable set of the thermostat-controlled heated rooms to two existing exact methods:

M1 represent the reachable set as a collection of constrained zonotopes generated using the algorithm described in [43, Algorithm 1],

Table 4.3. Computation times in seconds for all operations within the readability analysis. The total time to find the reduced set $\mathcal{R}^r_{100}$ is given by the sum of the individual operations.

Case	Theorem 4.1.1	Alg. 1	Redundancy	Total
$(3, 1)$	0.20	0.11	2.17	2.49
$(6, 2)$	0.84	1.43	8.15	10.41
$(9, 3)$	2.24	168.91	51.33	222.49
$(12, 4)$	3.87	3001.54	264.30	3269.71

M2 implicitly represent the reachable set by iterating over the mixed-integer constraints of the MLD system given by (4.1) as described in [76] and implemented using YALMIP [68].

While both of these methods provide the same reachable set as the proposed method using hybrid zonotopes, there are distinctions. Computing reachable sets using M1 results in a worst-case exponential growth in representation complexity, as shown in Table 4.4. This growth in complexity resulted in the final Case$(12, 4)$ being terminated on the 86^{th} time step after 20 hours of computation time. Furthermore, the resulting set consists of multiple convex sets, thus requiring each set to be analyzed to verify properties of the nonconvex reachable set. The reachable set given by M2, on the other hand, is compact and fast to generate, as shown in Table 4.5. Similar to the results of Theorem 4.1.1, the use of the MLD system model results in only linear growth in representation complexity. However, this set is given implicitly as mixed continuous and binary variables with inequality constraints. While defining the same reachable set, this representation does not have closure under set operations and is therefore only suitable for verifying the existence of trajectories by solving optimization programs.

The time to detect halfspace intersections and evaluate support functions (3.47) using hybrid zonotopes with and without redundancy removal, denoted by HCG-r and HCG respectively, is compared to the same operations using methods M1 and M2 in Fig. 4.4. In these results, the direction vector $l_\mathrm{i} \in \mathbb{R}^{n_{xc}}$ is randomly sampled 100 times and the support function $\rho_{\mathcal{R}_{100}}(l_\mathrm{i})$ solved to find a global optimum. To provide a realistic comparison of halfspace detection, the 100 halfspaces are split into 50 true—$\mathcal{H}^-_\mathrm{i} = \left\{x \in \mathbb{R}^{n_{xc}} \,\middle|\, l_\mathrm{i}^T x \leq \rho_{\mathcal{R}_{100}}(l_\mathrm{i})\right\}$—

Table 4.4. Computation time and representation complexity for method M1. The total number of generators and constraints summed over the collection of constrained zonotopes is reported by n_g and n_c respectively.

Case	n_g	n_c	Sets	Time (s)
$(3,1)$	1833	82	17	7.99
$(6,2)$	32807	2597	285	118.95
$(9,3)$	1710990	229680	13590	10015.69
$(12,4)$	DNF	DNF	DNF	$> 72 \times 10^3$

Table 4.5. Computation time and representation complexity for method M2. The number of continuous variables is given by n_g, the number of binary variable is given by n_b, and the number of *inequality* constraints is given by n_c.

Case	n_g	n_b	n_c	Time (s)
$(3,1)$	403	401	2315	0.71
$(6,2)$	706	802	4430	0.72
$(9,3)$	1009	1203	6545	0.71
$(12,4)$	1312	1604	8660	0.74

and 50 false—$\mathcal{H}_\mathrm{i}^+ = \left\{ x \in \mathbb{R}^{n_{xc}} \;\middle|\; l_\mathrm{i}^T x \geq 1.1\rho_{\mathcal{R}_{100}}(l_\mathrm{i}) \right\}$—results such that $\mathcal{R}_{100} \cap \mathcal{H}_\mathrm{i}^- \neq \emptyset$ and $\mathcal{R}_{100} \cap \mathcal{H}_\mathrm{i}^+ = \emptyset$.

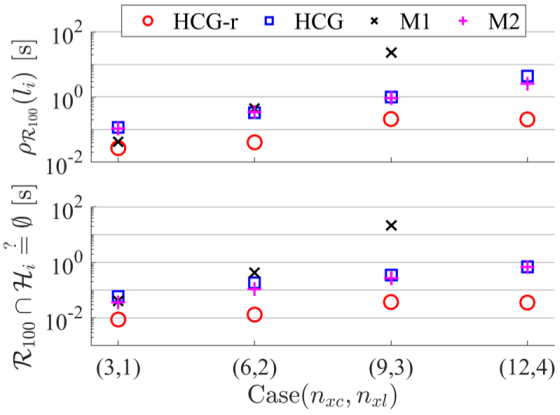

Figure 4.4. Average time to compute support functions and to detect halfspace intersections with the reachable sets.

In Fig. 4.4, the average computation times are similar between HCG and M2. The computation time of M1 grows sharply in Case$(9,3)$, where the number of convex sets, and

linear programs to be solved, jumps by two orders of magnitude. The reachable set given by the reduced hybrid zonotope, HCG-r, has the lowest computation times. However, this increased efficiency is at the cost of additional overhead in the generation of the set as shown in Table 4.3.

4.2 Reachable Sets of Closed-Loop MPC

In this section I present a closed-form solution to the exact reachable sets of closed-loop systems under linear model predictive control (MPC) using hybrid zonotopes. This is accomplished by directly embedding the Karush Kuhn Tucker conditions of a parametric quadratic program within the hybrid zonotope set definition as mixed-integer constraints, and thus representing the set of all optimizers over a set of parameters. Using the set of explicit MPC solutions, I show how the plant's closed-loop dynamics may be propagated through an identity that is calculated algebraically. Beyond reachability analysis, I show that the set of optimizers represented by a hybrid zonotope may be decomposed to give the explicit solution of general multi-parametric quadratic programs as a collection of constrained zonotopes.

The remainder of this section is organized as follows. In Section 4.2.1 I provide some background on the lack of existing work in the reachability analysis of closed-loop systems under MPC to motivate the approach. Then in Section 4.2.2 I discuss multiparametric quadratic programming. In Section 4.2.3 I show how the set of all optimizers of a parametric quadratic program may be defined as a hybrid zonotope. In Section 4.2.4 I show that the hybrid zonotope containing all optimizers of an MPC formulated as a multiparametric quadratic program may be used to propagate the reachable set of the closed-loop system. Finally, an illustrative example is provided in Section 4.2.5.

4.2.1 Motivation

Model Predictive Control (MPC) has found considerable success in both academia and industry due to its performance, robustness, and versatility [77]. The most common MPC implementation recursively solves for the sequence of control inputs that minimizes a quadratic

cost based on future operation of the open-loop plant as predicted by a linear, discrete-time model. Robustness and stability may be guaranteed *a priori* through strategic use of convex constraint sets and terminal objectives determined offline [14], [78]. While guaranteeing robustness, these methods are rarely exact and introduce an application-dependent level of conservatism to the controller design. Such conservatism may lead to performance degradation or unnecessarily limit the operating regime of the closed-loop system [79]. Furthermore, the resulting controllers are often complex, hindering their real-time implementation for systems with fast update rates [80]. An alternative approach is to verify that robustness and performance specifications are met by a nominal controller *a posteriori* through reachability analysis and safety verification of the closed-loop plant [10].

Despite the plethora of research on MPC, reachability analysis of the closed-loop system is widely absent from the literature. It has been shown that a closed-loop system under linear MPC may be modeled as a hybrid system by embedding the Karush Kuhn Tucker (KKT) conditions of the quadratic program within the governing equations [81]. Reachability may then be verified via optimization to determine if any trajectory from an initial set, to a specified target set, exists by solving a series of mixed-integer linear programs [41].

Alternatively, set-based reachability may be performed by determining the explicit MPC law and modeling the closed-loop plant as a piecewise affine system [42], [81]. However, finding the explicit control law is in itself a computationally intensive operation and results in a worst-case exponential number of critical regions with respect to the prediction horizon, state dimension, and number of constraints [14]. When the explicit control law may be determined, the resulting hybrid system, having guard sets determined by the critical regions of the explicit MPC, is often overly complex. Set-based reachability of such hybrid systems results in a worst-case exponential growth in the number of convex sets required to represent the nonconvex reachable set [10]. To stifle this growth, current algorithms for reachability of hybrid systems employ over approximation techniques [8], [10]. While useful for verifying safety, solutions leveraging over-approximations are not capable of guaranteeing performance criteria [10]. Scalable set-based methods for the reachability analysis of closed-loop MPC are still needed to fill this gap.

4.2.2 Multiparametric Quadratic Programming

Consider the bounded, strictly convex multiparametric Quadratic Program (mp-QP) given by

$$\begin{aligned} \min_{z} \ & \frac{1}{2} z^T Q z + q^T z \\ \text{s.t. } & Hz + Sx \leq f \ , \ x \in \mathcal{X} \ , \end{aligned} \tag{4.8}$$

where the parameters belong to a compact set $\mathcal{X} \subset \mathbb{R}^{n_x}$, $Q \in \mathbb{R}^{n_z \times n_z}$, $Q \succ 0$, $q \in \mathbb{R}^{n_z}$, $H \in \mathbb{R}^{n_h \times n_z}$, $S \in \mathbb{R}^{n_h \times n_x}$, and $f \in \mathbb{R}^{n_h}$. Note that objective functions with an additional term $x^T P z$ may be brought to the standard form (4.8) through the change of variables $z = \tilde{z} + Q^{-1} P^T x$ [82]. The set of feasible parameters $\mathcal{X}_{feas} \subseteq \mathcal{X}$ satisfying the constraints of (4.8) may be partitioned into a collection of non-overlapping critical regions such that $\mathcal{X}_{feas} = \bigcup \mathcal{CR}_{\mathrm{i}}$. Each critical region is a convex polytope where a unique combination of the inequality constraints are active at the solution of the QP. Within each of these critical regions, the optimizer of (4.8) is an affine function of the parameter given by $z^*(x) = F_{\mathrm{i}} x + g_{\mathrm{i}}$ for all $x \in \mathcal{CR}_{\mathrm{i}}$. The set of all optimizers within the i^{th} critical region may be expressed as

$$\mathcal{Z}_{\mathrm{i}}^* = \{F_{\mathrm{i}} x + g_{\mathrm{i}} \mid x \in \mathcal{CR}_{\mathrm{i}}\} \subset \mathbb{R}^{n_z}. \tag{4.9}$$

The set of all optimizers over the entire parameter set $\mathcal{X}_{feas} \subseteq \mathcal{X}$ is then given by $\mathcal{Z}^*(x) = \bigcup \mathcal{Z}_{\mathrm{i}}^*$. This result is a direct consequence of the KKT conditions of optimality; the reader is directed to [14], [82] and the references therein for derivations and detailed discussion.

4.2.3 Zonotopic Representation and Explicit Solution of mp-QPs

It is now proven that if the mp-QP (4.8) is bounded, then the set of all optimizers may be represented as a hybrid zonotope. It is then shown how the decomposition of the hybrid zonotope by Theorem 3.1.1 gives the explicit solution of the mp-QP as a collection of constrained zonotopes.

Assumption 4.2.1. *The set of feasible optimizers of the mp-QP (4.8) is given by the compact set $\mathcal{Z} \subset \mathbb{R}^{n_z}$.*

When the mp-QP (4.8) satisfies Assumption 4.2.1, there exists a zonotope $\overline{\mathcal{Z}} = \{G_z\xi_z + c_z \mid \|\xi_z\|_\infty \leq 1\} \subset \mathbb{R}^{n_z}$ such that $G_z \in \mathbb{R}^{n_z \times n_z}$ is full rank and $\mathcal{Z} \subseteq \overline{\mathcal{Z}}$. Let the parameter set be given by the hybrid zonotope $\mathcal{X} = \langle G_x^c, G_x^b, c_x, A_x^c, A_x^b, b_x\rangle \subset \mathbb{R}^{n_x}$. Then $x \in \mathcal{X}$ if there exists some $\xi_x^c \in \mathcal{B}_\infty^{n_{g,x}}$ and $\xi_x^b \in \{-1,1\}^{n_{b,x}}$ satisfying $A_x^c\xi_x^c + A_x^b\xi_x^b = b_x$ such that $x = G_x^c\xi_x^c + G_x^b\xi_x^b + c_x$. Substituting $z = G_z\xi_z + c_z$ and $x = G_x^c\xi_x^c + G_x^b\xi_x^b + c_x$ into (4.8), the optimizer is given as a function of $\xi_x = (\xi_x^c\ \xi_x^b)$ to obtain

$$z^*(\xi_x) = G_z\xi_z^*(\xi_x) + c_z\,, \tag{4.10a}$$

$$\begin{aligned}\xi_z^*(\xi_x) = \arg\min_{\xi_z}\ & \frac{1}{2}\xi_z^T\overline{Q}\xi_z + \overline{q}^T\xi_z \\ \text{s.t. }\ & \overline{H}\xi_z + \overline{S}^c\xi_x^c + \overline{S}^b\xi_x^b \leq \overline{f}\,,\end{aligned} \tag{4.10b}$$

where $\overline{Q} = G_z^TQG_z$, $\overline{q}^T = c_z^TQG_z + q^TG_z$, $\overline{H} = HG_z$, $\overline{S}^c = SG_x^c$, $\overline{S}^b = SG_x^b$, and $\overline{f} = f - (Hc_z + Sc_x)$. Given that the columns of G_z are chosen such that they are linearly independent, $\overline{Q} \succ 0$ and the QP (4.10b) is strictly convex. Thus for any fixed ξ_x, the KKT conditions of optimality are both necessary and sufficient such that

$$\overline{H}\xi_z + \overline{S}^c\xi_x^c + \overline{S}^b\xi_x^b \leq \overline{f}\,, \tag{4.11a}$$

$$\overline{Q}\xi_z + \overline{H}^T\mu = -\overline{q}\,, \tag{4.11b}$$

$$\mu^T\left(\overline{H}\xi_z + \overline{S}^c\xi_x^c + \overline{S}^b\xi_x^b - \overline{f}\right) = 0\,,\ \mu \geq \mathbf{0}\,, \tag{4.11c}$$

holds for some $\mu \in \mathbb{R}^{n_h}$ if and only if $\xi_z = \arg\min$ (4.10b).

Now define positive scalars m and m_μ such that

$$\begin{aligned} m \geq \max\ & \left\|\overline{H}\xi_z + \overline{S}^c\xi_x^c + \overline{S}^b\xi_x^b - \overline{f}\right\|_\infty \\ \text{s.t }\ & (4.11a)\,,\ \|(\xi_z\ \xi_x^c\ \xi_x^b)\|_\infty \leq 1\,,\end{aligned} \tag{4.12a}$$

$$m_\mu\mathbf{1} \geq \mu \text{ s.t. } (4.11)\ \forall\ \|(\xi_z\ \xi_x^c\ \xi_x^b)\|_\infty \leq 1\,. \tag{4.12b}$$

Although the variables μ are not necessarily unique, an upper bound (4.12b) may be found using the method described in [81, Lemma 1] such that there exists some $\mu \in [0, m_\mu]^{n_h}$ satisfying the KKT conditions (4.11) for all $\|(\xi_z\ \xi_x^c\ \xi_x^b)\|_\infty \leq 1$. These constants may be found for a specific parameter set $\mathcal{X}$ or, when the analysis is to be performed for N parameter sets $\mathcal{X}_\mathrm{i}$, for a single over-approximative set $\mathcal{X}_p$ such that $\mathcal{X}_\mathrm{i} \subseteq \mathcal{X}_p$ for all $\mathrm{i} = 1, \ldots, N$. The KKT conditions may then be enforced as linear mixed-integer constraints by introducing n_h binary auxiliary variables $p \in \{0,1\}^{n_h}$. Applying this approach to the considered optimization problem, $\xi_z = \arg\min$ (4.10b) if and only if the following Mixed-Integer Linear Program (MILP) is feasible:

$$\overline{H}\xi_z + \overline{S}^c\xi_x^c + \overline{S}^b\xi_x^b \leq \overline{f}\,, \tag{4.13a}$$

$$\overline{Q}\xi_z + \overline{H}^T\mu = -\overline{q}\,, \tag{4.13b}$$

$$\begin{aligned} -m(1-p) \leq \overline{H}\xi_z + \overline{S}^c\xi_x^c + \overline{S}^b\xi_x^b - \overline{f}\,, \\ \mathbf{0} \leq \mu \leq m_\mu p\,,\ p \in \{0,1\}^{n_h}\,, \end{aligned} \tag{4.13c}$$

where (4.13a) is the primal feasibility, (4.13b) is the dual feasibility, and (4.13c) is the complementary slackness KKT conditions of (4.10b) [83]. While any constants satisfying (4.12) will suffice, tight upper bounds provide computational benefits [53].

Theorem 4.2.1. *Let positive scalars m and m_μ be given by (4.12) and define the interval set*

$$\{G_s\xi_s + c_s \mid \|\xi_s\|_\infty \leq 1\} = \begin{bmatrix} \alpha & , & \overline{f} \\ \overline{f} - \frac{m}{2}\mathbf{1} & , & \beta \\ -2\mathbf{1}_{n_h} & , & \mathbf{0} \end{bmatrix},$$

where $\alpha \leq \overline{H}\xi_z + \overline{S}^c\xi_x^c + \overline{S}^b\xi_x^b$ and $\overline{H}\xi_z + \overline{S}^c\xi_x^c + \overline{S}^b\xi_x^b + \frac{m}{2}\mathbf{1} \leq \beta$ for all $\xi_z \in \mathcal{B}_\infty^{n_z}$, $\xi_x^c \in \mathcal{B}_\infty^{n_{g,x}}$, and $\xi_x^b \in \{-1,1\}^{n_{b,x}}$. Then the set of all optimizers of the QP (4.10) defined over the parameter set $\mathcal{X} = \langle G_x^c, G_x^b, c_x, A_x^c, A_x^b, b_x\rangle \subset \mathbb{R}^{n_x}$ is the hybrid zonotope $\mathcal{Z}^*(x) = \langle G_*^c, G_*^b, c_*, A_*^c, A_*^b, b_*\rangle \subset \mathbb{R}^{n_z}$ where

$$
\begin{aligned}
G_*^c &= \begin{bmatrix} \mathbf{0}_{n_z \times n_{g,x}} & G_z & \mathbf{0} \end{bmatrix}, \; G_*^b = \mathbf{0}, \; c_* = c_z, \\
A_*^c &= \begin{bmatrix} A_x^c & \mathbf{0} & \mathbf{0} & \mathbf{0} \\ \mathbf{0} & \overline{Q} & \frac{m_\mu}{2}\overline{H}^T & \mathbf{0} \\ \overline{S}^c & \overline{H} & \mathbf{0} & \\ \overline{S}^c & \overline{H} & \mathbf{0} & G_s \\ \mathbf{0} & \mathbf{0} & \mathbf{I} & \end{bmatrix}, \; A_*^b = \begin{bmatrix} A_x^b & \mathbf{0} \\ \mathbf{0} & \mathbf{0} \\ \overline{S}^b & \mathbf{0} \\ \overline{S}^b & -\frac{m}{2}\mathbf{I} \\ \mathbf{0} & -\mathbf{I} \end{bmatrix}, \\
b_* &= \begin{bmatrix} b_x \\ -\overline{q} - \frac{m_\mu}{2}\overline{H}^T\mathbf{1} \\ c_s \end{bmatrix}.
\end{aligned} \tag{4.14}
$$

Proof. Let $\mathcal{Z}_h = \langle G_*^c, G_*^b, c_*, A_*^c, A_*^b, b_* \rangle \subset \mathbb{R}^{n_z}$ denote the hybrid zonotope given by (4.14). For any $z \in \mathcal{Z}_h$ there exists some $\xi^c \in \mathcal{B}_\infty^{n_{g,*}}$ and $\xi^b \in \{-1,1\}^{n_{b,*}}$ such that $A_*^c\xi^c + A_*^b\xi^b = b_*$ and $z = G_*^c\xi^c + G_*^b\xi^b + c_*$. Let $\xi^c = (\xi_x^c \; \xi_z^c \; \xi_\mu^c \; \xi_s^c)$ and $\xi^b = (\xi_x^b \; \xi_p^b)$, where $\xi_x^c \in \mathbb{R}^{n_{g,x}}$, $\xi_z^c \in \mathbb{R}^{n_z}$, $\xi_\mu^c \in \mathbb{R}^{n_h}$, $\xi_s^c \in \mathbb{R}^{3n_h}$, $\xi_x^b \in \{-1,1\}^{n_{b,x}}$, and $\xi_p^b \in \{-1,1\}^{n_h}$. Then $z = G_z\xi_z^c + c_z$. Expanding the first row of the constraints gives $A_x^c\xi_x^c + A_x^b\xi_x^b = b_x$, so that $x = G_x^c\xi_x^c + G_x^b\xi_x^b + c_x \in \mathcal{X}$. Expanding the second row of constraints gives

$$
\overline{Q}\xi_z^c + \overline{H}^T\left(\frac{m_\mu}{2}\xi_\mu^c + \frac{m_\mu}{2}\right) = -\overline{q}\,. \tag{4.15}
$$

Expanding the final three rows of constraints results in

$$
\begin{bmatrix} \overline{S}^c\xi_x^c + \overline{S}^b\xi_x^b + \overline{H}\xi_z^c \\ \overline{S}^c\xi_x^c + \overline{S}^b\xi_x^b + \overline{H}\xi_z^c - \frac{m}{2}\xi_p^b \\ \xi_\mu^c - \xi_p^b \end{bmatrix} = -G_s\xi_s^c + c_s\,. \tag{4.16}
$$

Given that $\|\xi_s^c\|_\infty \leq 1$, (4.16) implies that $\overline{H}\xi_z^c + \overline{S}^c\xi_x^c + \overline{S}^b\xi_x^b \leq \overline{f}$, $-m(\frac{1}{2} - \frac{1}{2}\xi_p^b) \leq \overline{H}\xi_z^c + \overline{S}^c\xi_x^c + \overline{S}^b\xi_x^b - \overline{f}$, and $\xi_\mu^c \leq \xi_p^b$. Define the change of variables

$$
\mu = \frac{m_\mu}{2}\xi_\mu^c + \frac{m_\mu}{2}\mathbf{1}\,, \; p = \frac{1}{2}\xi_p^b + \frac{1}{2}\mathbf{1}\,, \tag{4.17}
$$

giving $\mu \in [0, m_\mu]^{n_h}$ and $p \in \{0,1\}^{n_h}$. Carrying these change of variables through the above constraints results in (4.15) being equivalent to the dual feasibility condition (4.13b), and (4.16) being equivalent to the primal feasibility (4.13a) and complementary slackness (4.13c) KKT conditions. Thus $\xi_z^c = \arg\min$ (4.10b), $z \in \mathcal{Z}^*(x)$, and $\mathcal{Z}_h \subseteq \mathcal{Z}^*(x)$.

Conversely, for any $z^* \in \mathcal{Z}^*(x)$ there exists some $\xi_z^c \in \mathcal{B}_\infty^{n_z}$, $\xi_x^c \in \mathcal{B}_\infty^{n_{g,x}}$, $\xi_x^b \in \{-1,1\}^{n_{b,x}}$, $\mu \in [0, m_\mu]^{n_h}$, and $p \in \{0,1\}^{n_h}$ such that $z^* = G_z \xi_z^c + c_z$, $A_x^c \xi_x^c + A_x^b \xi_x^b = b_x$, and (4.13) holds. Again let $\xi^c = (\xi_z^c \ \xi_x^c \ \xi_\mu^c \ \xi_s^c)$ and $\xi^b = (\xi_x^b \ \xi_p^b)$. Applying the change of variables (4.17) implies that $\|\xi_\mu^c\|_\infty \leq 1$ and $\xi_p^b \in \{-1,1\}^{n_h}$. Then (4.15) is satisfied, and (4.16) implies that $\|\xi_s\|_\infty \leq 1$. Thus $\xi^c \in \mathcal{B}_\infty^{n_{g,*}}$, $\xi^b \in \{-1,1\}^{n_{b,*}}$, $A_*^c \xi^c + A_*^b \xi^b = b_*$, $z^* = G_*^c \xi^c + c_*$, and $z^* \in \mathcal{Z}_h$. Therefore $\mathcal{Z}^*(x) \subseteq \mathcal{Z}_h$ and $\mathcal{Z}_h = \mathcal{Z}^*(x)$. □

Corollary 4.2.1. *The decomposition of $\mathcal{Z}^*(x) \subset \mathbb{R}^{n_z}$ as defined by Theorem 4.2.1 into its equivalent collection of constrained zonotopes is the explicit multiparametric solution of the QP (4.10).*

Proof. Let $\mathcal{Z}^*(x) = \langle G_*^c, G_*^b, c_*, A_*^c, A_*^b, b_* \rangle \subset \mathbb{R}^{n_z}$ denote the hybrid zonotope given by (4.14). The set $\mathcal{Z}^*(x)$ is equivalent to the collection of $|\mathcal{T}|$ constrained zonotopes

$$\begin{aligned} \mathcal{Z}^*(x) &= \bigcup_{\xi_{\mathrm{i}}^b \in \mathcal{T}} \mathcal{Z}_{c,\mathrm{i}}^* \,, \\ \mathcal{Z}_{c,\mathrm{i}}^* &= \left\langle G_*^c, c_*, A_*^c, b_* - A_*^b \xi_{\mathrm{i}}^b \right\rangle \,, \end{aligned} \tag{4.18}$$

for $\mathcal{T} = \left\{ \xi_{\mathrm{i}}^b \in \{-1,1\}^{n_b} \;\middle|\; \mathcal{Z}_{c,\mathrm{i}}^* \neq \emptyset \right\}$ by Theorem 3.1.1. The hybrid zonotope

$$\mathcal{X}_{feas} = \left\langle \begin{bmatrix} G_x^c & \mathbf{0} \end{bmatrix}, \begin{bmatrix} G_x^b & \mathbf{0} \end{bmatrix}, c_x, A_*^c, A_*^b, b_* \right\rangle \subseteq \mathcal{X} \,, \tag{4.19}$$

is then the set of all feasible parameters and is equivalent to the collection of constrained zonotopes

$$\begin{aligned} \mathcal{X}_{feas} &= \bigcup_{\xi_{\mathrm{i}}^b \in \mathcal{T}} \mathcal{CR}_{\mathrm{i}} \,, \\ \mathcal{CR}_{\mathrm{i}} &= \left\langle [G_x^c \ \mathbf{0}], c_x + [G_x^b \ \mathbf{0}] \xi_{\mathrm{i}}^b, A_*^c, b_* - A_*^b \xi_{\mathrm{i}}^b \right\rangle \,. \end{aligned} \tag{4.20}$$

For any $x \in \mathcal{CR}_\mathrm{i}$ there exists some $\xi^c \in \mathcal{B}_\infty^{n_g,*}$ such that $A_*^c\xi^c + A_*^b\xi_\mathrm{i}^b = b_*$ and $x = [G_x\ \mathbf{0}]\,\xi^c + \left[G_x^b\ \mathbf{0}\right]\xi_\mathrm{i}^b + c_x$. Letting $z^* = G_*^c\xi^c + c_*$ then gives $z^* \in \mathcal{Z}_{c,\mathrm{i}}^*$. Given that the QP (4.10) is strictly convex, for any fixed $x \in \mathcal{CR}_\mathrm{i}$ there exists a unique $z^* \in \mathcal{Z}_{c,\mathrm{i}}^*$ such that the KKT conditions hold. The fact that constrained zonotopes are convex polytopes [18] concludes the proof. □

By embedding the KKT conditions as mixed-integer constraints within the space of factors, the optimality of the QP is enforced over the parameter set $\mathcal{X}$. Without loss of generality, consider the case when the parameter set $\mathcal{X}$ has no binary factors and thus represents a convex polytope. In doing so, the set of optimizers $\mathcal{Z}^*(x)$ only contains binary factors corresponding to the mixed-integer form of the KKT conditions, where a value of 1 in the i^{th} entry of ξ^b indicates that the i^{th} inequality constraint is active. The discrete set of feasible combinations of binary factors $\mathcal{T}$ then contains the collection of active sets such that $\xi_z = \arg\min$ (4.10b) over the set of feasible parameters $\mathcal{X}_{feas}$. This result follows closely from mp-QP critical region exploration methods where the binary tree of enumerated combinations of active constraints is explored by evaluating the feasibility of a series of linear programs [84]. In Corollary 4.2.1, this same binary tree is explored when finding the set $\mathcal{T}$ through a search of the integer feasible space of the hybrid zonotope, which may be performed efficiently using existing MILP solvers as discussed in Section 3.3. Once $\mathcal{T}$ is known, the decomposition of $\mathcal{X}_{feas}$ into critical regions and $\mathcal{Z}^*(x)$ into the corresponding sets of optimizers with n_x degrees of freedom is easily accomplished.

Remark 4.2.1. *In Theorem 4.2.1 it is only required that the parameter set $\mathcal{X}$ is compact. In the case that the hybrid zonotope $\mathcal{X}$ over which the mp-QP is defined is disjoint, the resulting collection of constrained zonotopes (4.18) giving the explicit multiparametric solution of the QP are no longer required to be continuous. However, when the parameter set is chosen as the constrained zonotope (convex polytope) $\mathcal{X} = \langle G_x^c, \emptyset, c_x, A_x^c, \emptyset, b_x\rangle$, Corollary 4.2.1 generalizes to previous mp-QP results [14], [82].*

Remark 4.2.2. *The discrete set of feasible binary factors $\mathcal{T} = \left\{\xi_\mathrm{i}^b \in \{-1,1\}^{n_b} \middle| \mathcal{Z}_{c,\mathrm{i}}^* \neq \emptyset\right\}$ is determined based on which of the convex subsets of $\mathcal{Z}^*(x)$ are nonempty by Theorem 3.1.1. When the quadratic program is degenerate for some combination of active constraints*

corresponding to $\xi_{\mathrm{i}}^b \in \mathcal{T}$*, the resulting critical region* $\mathcal{CR}_{\mathrm{i}} \subset \mathbb{R}^{n_x}$ *by* (4.20) *may not be full dimensional [14]. This can be detected by maximizing a scalar* $\rho \in \mathbb{R}$ *such that there exists some* $c_b \in \mathbb{R}^{n_x}$ *and* $\rho\mathcal{B}_\infty^{n_x} \oplus c_b \subseteq \mathcal{CR}_{\mathrm{i}}$ *by solving a linear program [20, Sec. 5.2]. When* $\rho = 0$*, the* i^{th} *critical region* $\mathcal{CR}_{\mathrm{i}}$ *is not full dimensional and therefore* $\mathcal{Z}_{c,\mathrm{i}}^*$ *is redundant [14]. The decomposition of the set* $\mathcal{Z}^*(x)$ *by* (4.18) *is then equivalently given over the discrete set* $\mathcal{T}_r = \mathcal{T} \setminus \{\xi_{\mathrm{i}}^b\}$.

Remark 4.2.3. *Certain "dual" factors* ξ_μ^c *may be constant when a constraint is never activated by the complementary slackness condition* (4.13c)*. Such redundant factors may be detected and removed when their corresponding values of* ξ_p^b *in* $\mathcal{T}$ *are constant. Additionally, the "slack" factors* ξ_s^c *introduced in Theorem 4.2.1 to enforce inequality constraints may be redundant for certain parameter sets* $\mathcal{X}$*. These redundant factors and constraints may be detected and removed using the method described in Section 4.1.3. Redundant binary factors may be detected and removed based on the discrete set* $\mathcal{T}$ *using the method described in Section 6.1.3.*

4.2.4 Forward Reachable Sets of Linear MPC

Consider the discrete-time Linear Time-Invariant (LTI) system

$$x_{k+1} = Ax_k + Bu_k\,, \tag{4.21}$$

where $x_k \in \mathbb{R}^{n_x}$ is the vector of states and $u_k \in \mathbb{R}^{n_u}$ is the vector of inputs at time k, and the linear dynamics (4.21) with matrices $A \in \mathbb{R}^{n_x \times n_x}$ and $B \in \mathbb{R}^{n_x \times n_u}$ are referred to in short by the tuple (A, B). The control input of the nominal LTI system (4.21) under MPC is determined by solving the optimization program

$$\begin{aligned} \min_{u,x}\ & x_N^T Q_N x_N + \sum_{k=0}^{N-1} x_k^T Q x_k + u_k^T R u_k \\ \text{s.t. }\ & x_{k+1} = Ax_k + Bu_k\,,\ u_k \in \mathcal{U}\ \forall\, k \in [0, N-1]\,, \\ & x_k \in \mathcal{X}\ \forall\, k \in [1, N-1]\,,\ x_N \in \mathcal{X}_N\,, \end{aligned} \tag{4.22}$$

where x_0 is fixed to the sampled state of the system, $\mathcal{U} \subset \mathbb{R}^{n_u}$ is the set of all admissible control inputs, the predicted trajectories of the system are constrained to belong to the set $\mathcal{X} \subseteq \mathbb{R}^{n_x}$, the final state is constrained to belong to the terminal set $\mathcal{X}_N \subseteq \mathcal{X}$, and the states and inputs have weights $Q, Q_N \succeq 0$ and $R \succ 0$, respectively [14]. For ease of readability, the MPC formulation is provided as a regulator problem; however, the following results may be modified to handle reference tracking, soft constraints, and disturbance preview information as described in [82].

The trajectory of the LTI system (4.21) over the prediction horizon $\hat{X} = (x_1 \ \cdots \ x_N)$ as a function of the control inputs $\hat{U} = (u_0 \ \cdots \ u_{N-1})$ and initial state x_0 is given by $\hat{X} = \hat{A}x_0 + \hat{B}\hat{U}$ where

$$\hat{A} = \begin{bmatrix} A \\ A^2 \\ \vdots \\ A^N \end{bmatrix}, \ \hat{B} = \begin{bmatrix} B & \mathbf{0} & \cdots & \mathbf{0} & \mathbf{0} \\ AB & B & \mathbf{0} & \ddots & \mathbf{0} \\ \vdots & \vdots & \ddots & \vdots & \vdots \\ A^{N-1}B & A^{N-2}B & \cdots & AB & B \end{bmatrix}. \tag{4.23}$$

The optimal sequence of control inputs $\hat{U}^*(x_0)$ under the MPC (4.22) is then given by

$$\begin{aligned} \hat{U}^*(x_0) = \arg\min_{\hat{U}} \ & \frac{1}{2}\hat{U}^T(\hat{B}^T\hat{Q}\hat{B} + \hat{R})\hat{U} + x_0^T\hat{A}^T\hat{Q}\hat{B}\hat{U} \\ \text{s.t. } & \hat{U} \in \mathcal{U} \times \cdots \times \mathcal{U}\,, \\ & \hat{A}x_0 + \hat{B}\hat{U} \in \mathcal{X} \times \cdots \times \mathcal{X} \times \mathcal{X}_N\,, \end{aligned} \tag{4.24}$$

where $\hat{Q} = \text{diag}(Q, \cdots, Q, Q_N)$, and $\hat{R} = \text{diag}(R, \cdots, R)$. Once the optimization program (4.24) has been solved, the control input $u_0^*(x_0) = [\mathbf{I}_{n_u} \ \mathbf{0}]\,\hat{U}^*(x_0)$ is applied to the plant, a new state is sampled, and the process is repeated.

Assumption 4.2.2. *The constraint sets of the MPC are compact, full dimensional H-rep polytopes given by*

$$\mathcal{U} = \{u \in \mathbb{R}^{n_u} \mid H_u u \leq f_u\} \subset \mathbb{R}^{n_u} , \tag{4.25a}$$

$$\mathcal{X} = \{x \in \mathbb{R}^{n_x} \mid H_x x \leq f_x\} \subset \mathbb{R}^{n_x} , \tag{4.25b}$$

$$\mathcal{X}_N = \{x \in \mathbb{R}^{n_x} \mid H_N x \leq f_N\} \subset \mathbb{R}^{n_x} , \tag{4.25c}$$

where $H_u \in \mathbb{R}^{n_{hu} \times n_u}$, $H_x \in \mathbb{R}^{n_{hx} \times n_x}$, *and* $H_N \in \mathbb{R}^{n_{hn} \times n_x}$.

Define the change of variables

$$\begin{aligned} z^*(x_0) &= \hat{U}^*(x_0) + \overline{P} x_0 , \\ \overline{P} &= (\hat{B}^T \hat{Q} \hat{B} + \hat{R})^{-1} \hat{B}^T \hat{Q}^T \hat{A} . \end{aligned} \tag{4.26}$$

The optimization problem (4.24) may then be expressed in terms of z as

$$\begin{aligned} z^*(x_0) = \arg\min_z \; & \frac{1}{2} z^T (\hat{B}^T \hat{Q} \hat{B} + \hat{R}) z \\ \text{s.t.} \; & \begin{bmatrix} \hat{H}_u \\ \hat{H}_x \hat{B} \end{bmatrix} z + \begin{bmatrix} -\hat{H}_u \overline{P} \\ \hat{H}_x (\hat{A} - \hat{B} \overline{P}) \end{bmatrix} x_0 \leq \begin{bmatrix} \hat{f}_u \\ \hat{f}_x \end{bmatrix} , \end{aligned} \tag{4.27}$$

where $\hat{H}_u = \text{diag}(H_u, \cdots, H_u)$, $\hat{f}_u = (f_u \; \cdots \; f_u)$, $\hat{H}_x = \text{diag}(H_x, \cdots, H_x, H_N)$, and $\hat{f}_x = (f_x \; \cdots \; f_x \; f_N)$. Assumption 4.2.2 assures that the mp-QP (4.27) is bounded and therefore satisfies Assumption 4.2.1. Following the same procedures in Section 4.2.3, let $\mathcal{Z}$ denote the compact set of optimizers of the mp-QP (4.27). Then there exists some zonotope $\overline{\mathcal{Z}} = \{G_z \xi_z + c_z \mid \|\xi_z\|_\infty \leq 1\}$ such that $\mathcal{Z} \subseteq \overline{\mathcal{Z}}$ and $G_z \in \mathbb{R}^{N n_u \times N n_u}$ is full rank. Let the set of initial conditions be given in HCG-rep as $\mathcal{X}_0 = \langle G_x^c, G_x^b, c_x, A_x^c, A_x^b, b_x \rangle \subset \mathbb{R}^{n_x}$. Substituting

$z = G_z\xi_z + c_z \in \overline{\mathcal{Z}}$ and $x_0 = G_x^c\xi_x^c + G_x^b\xi_x^b + c_x \in \mathcal{X}_0$, (4.27) is a strictly convex mp-QP over the parameter set $\mathcal{X}_0$ in the standard form of (4.10) defined by the matrices

$$\begin{aligned}
&\overline{Q} \equiv G_z^T(\hat{B}^T\hat{Q}\hat{B} + \hat{R})G_z,\ \overline{q}^T \equiv c_z^T(\hat{B}^T\hat{Q}\hat{B} + \hat{R})G_z,\\
&\overline{H} \equiv \begin{bmatrix} \hat{H}_u G_z \\ \hat{H}_x\hat{B}G_z \end{bmatrix},\ \overline{f} \equiv \begin{bmatrix} \hat{f}_u - \hat{H}_u c_z + \hat{H}_u\overline{P}c_x \\ \hat{f}_x - \hat{H}_x\hat{B}c_z - \hat{H}_x(\hat{A} - \hat{B}\overline{P})c_x \end{bmatrix},\\
&\overline{S}^c \equiv \begin{bmatrix} -\hat{H}_u\overline{P}G_x^c \\ \hat{H}_x(\hat{A} - \hat{B}\overline{P})G_x^c \end{bmatrix},\ \overline{S}^b \equiv \begin{bmatrix} -\hat{H}_u\overline{P}G_x^b \\ \hat{H}_x(\hat{A} - \hat{B}\overline{P})G_x^b \end{bmatrix}.
\end{aligned} \tag{4.28}$$

Theorem 4.2.2. *Define the set of all optimizers of the mp-QP (4.28) as $\mathcal{Z}^*(x_0) = \langle G_*^c, G_*^b, c_*, A_*^c, A_*^b, b_*\rangle \subset \mathbb{R}^{Nn_u}$ over the set of initial states $\mathcal{X}_0 = \langle G_x^c, G_x^b, c_x, A_x^c, A_x^b, b_x\rangle \subseteq \mathcal{X}_{feas}$ by Theorem 4.2.1. Then the set of states reachable by the plant (A_p, B_p) under MPC (4.22) in one time step is given by the hybrid zonotope $\mathcal{R}_+ = \langle G_r^c, G_r^b, c_r, A_r^c, A_r^b, b_r\rangle \subset \mathbb{R}^{n_x}$ where*

$$\begin{aligned}
G_r^c &= \begin{bmatrix} (A_p - B_p[\mathbf{I}_{n_u}\ \mathbf{0}]\overline{P})G_x^c & \mathbf{0} \end{bmatrix} + B_p[\mathbf{I}_{n_u}\ \mathbf{0}]G_*^c,\\
G_r^b &= \begin{bmatrix} (A_p - B_p[\mathbf{I}_{n_u}\ \mathbf{0}]\overline{P})G_x^b & \mathbf{0} \end{bmatrix},\\
c_r &= (A_p - B_p[\mathbf{I}_{n_u}\ \mathbf{0}]\overline{P})c_x + B_p[\mathbf{I}_{n_u}\ \mathbf{0}]c_*,\\
A_r^c &= A_*^c,\ A_r^b = A_*^b,\ b_r = b_*.
\end{aligned} \tag{4.29}$$

Proof. Let $\mathcal{R}_h = \langle G_r^c, G_r^b, c_r, A_r^c, A_r^b, b_r\rangle \subset \mathbb{R}^{n_x}$ denote the hybrid zonotope given by (4.29). For any $\tilde{r} \in \mathcal{R}_h$ there exists some $\xi_r^c \in \mathcal{B}_\infty^{n_{g,r}}$ and $\xi_r^b \in \{-1, 1\}^{n_{b,r}}$ such that $A_*^c\xi_r^c + A_*^b\xi_r^b = b_*$ and $\tilde{r} = G_r^c\xi_r^c + G_r^b\xi_r^b + c_r$. Let $\xi_r^c = (\xi_x^c\ \xi_z^c\ \xi_s^c)$ and $\xi_r^b = (\xi_x^b\ \xi_p^b)$, where $\xi_x^c \in \mathbb{R}^{n_{g,x}}$, $\xi_z^c \in \mathbb{R}^{Nn_u}$, $\xi_s^c \in \mathbb{R}^{4n_h}$, $\xi_x^b \in \{-1, 1\}^{n_{b,x}}$, and $\xi_p^b \in \{-1, 1\}^{n_h}$. Letting $x_0 = G_x^c\xi_x^c + G_x^b\xi_x^b + c_x$ then results in $x_0 \in \mathcal{X}_0$ and $z^*(x_0) = G_*^c\xi_r^c + c_*$ gives $z^*(x_0) \in \mathcal{Z}^*(x_0)$. Expanding $\tilde{r} = G_r^c\xi_r^c + G_r^b\xi_r^b + c_r$ then gives $\tilde{r} = A_px_0 + B_p[\mathbf{I}_{n_u}\ \mathbf{0}](z^*(x_0) - \overline{P}x_0)$ and substituting $z^*(x_0) = \hat{U}^*(x_0) + \overline{P}x_0$ results in $\tilde{r} = A_px_0 + B_pu_0^*(x_0)$. Thus $\tilde{r} \in \mathcal{R}_+$ and $\mathcal{R}_h \subseteq \mathcal{R}_+$.

Conversely, for any $r \in \mathcal{R}_+$ there exists some $x_0 \in \mathcal{X}_0$ and a unique $z^*(x_0) \in \mathcal{Z}^*(x_0)$ such that $u_0^*(x_0) = [\mathbf{I}_{n_u}\ \mathbf{0}](z^*(x_0) - \overline{P}x_0)$ and $r = A_px_0 + B_pu_0^*(x_0)$. For any $z^*(x_0) \in \mathcal{Z}^*(x_0)$ there exists some $\xi_r^c \in \mathcal{B}_\infty^{n_{g,r}}$ and $\xi_r^b \in \{-1, 1\}^{n_{b,r}}$ such that $A_*^c\xi_r^c + A_*^b\xi_r^b = b_*$, $z^*(x_0) = G_*^c\xi_r^c + c_*$,

and $x_0 = \begin{bmatrix} G_x^c & \mathbf{0} \end{bmatrix} \xi_r^c + \begin{bmatrix} G_x^b & \mathbf{0} \end{bmatrix} \xi_r^b + c_x$. Then $r = G_r^c \xi_r^c + G_r^b \xi_r^b + c_r \in \mathcal{R}_h$, $\mathcal{R}_+ \subseteq \mathcal{R}_h$ and $\mathcal{R}_h = \mathcal{R}_+$. □

The set of all optimizers defined by Theorem 4.2.1 contains both the constraints enforcing the KKT conditions of the QP and the parameter set $\mathcal{X}_0$. Thus for any $z^*(x_0) \in \mathcal{Z}^*(x_0)$ there exists some $x_0 \in \mathcal{X}_0$. The requirement that the set of initial conditions is a subset of the set of feasible states, $\mathcal{X}_0 \subseteq \mathcal{X}_{feas}$, guarantees that the converse is also true, i.e. for any $x_0 \in \mathcal{X}_0$ there exists a unique $z^*(x_0) \in \mathcal{Z}^*(x_0)$. Theorem 4.2.2 then maps the feasible factors of $\mathcal{Z}^*(x_0)$ to generate the reachable set as $\mathcal{R}_+ = \{x \in \mathbb{R}^{n_x} \mid x = A_p x_0 + B_p \begin{bmatrix} \mathbf{I}_{n_u} & \mathbf{0} \end{bmatrix} (z^*(x_0) - \overline{P} x_0), x_0 \in \mathcal{X}_0\}$, where the plant (A_p, B_p) is not necessarily the same as the prediction model used in the MPC. Given that hybrid zonotopes are closed under Minkowski sums, the effects of additive, bounded disturbances described by the hybrid zonotope $\mathcal{V} \subset \mathbb{R}^{n_x}$ may be accounted for efficiently as $\mathcal{R}_+ \oplus \mathcal{V}$. The set of states reachable from $\mathcal{X}_0 \subseteq \mathcal{X}_{feas}$ in k time steps may be found through iterative applications of Theorem 4.2.2. If during the iterative analysis $\mathcal{R}_\mathrm{j} \not\subseteq \mathcal{X}_{feas}$ for some $1 \leq \mathrm{j} \leq k$, then recursive feasibility is not maintained by the system for all $\mathcal{X}_0$. In such cases, the states outside $\mathcal{X}_{feas}$ become infeasible and are excluded in the next step of the analysis. The set representation complexity grows as a function of k:

$$n_{g,r}(k) = (N n_u + 4 n_h) k + n_{g,x} \,, \tag{4.30a}$$

$$n_{b,r}(k) = n_h k + n_{b,x} \,, \tag{4.30b}$$

$$n_{c,r}(k) = (N n_u + 3 n_h) k + n_{c,x} \,, \tag{4.30c}$$

where $n_h = N n_{hu} + (N-1) n_{hx} + n_{hn}$ is the number of inequality constraints of (4.27). Note that the same redundancy removal techniques described in Remark 4.2.3 may be applied to the hybrid zonotope $\mathcal{R}_+$ given by (4.29).

4.2.5 Numerical Example

This section presents an illustrative example of representing the set of optimizers and reachable sets of a linear MPC as hybrid zonotopes. For clarity of exposition, the system considered has two states and a single input, though the same approach and analysis

technique may be applied to discrete-time systems with higher dimensions and will exhibit the linear growth in complexity given by (4.30). Comparisons of the explicit solution are made to results generated using the Multi-Parametric Toolbox (MPT) [12]. All optimization problems are solved using Gurobi [69]. Numerical results are generated with MATLAB on a desktop computer using one core of a 3.0 GHz intel i7 processor and 32 GB of RAM.

This example considers the MPC of the discrete-time double integrator

$$x_{k+1} = \begin{bmatrix} 1 & 1 \\ 0 & 1 \end{bmatrix} x_k + \begin{bmatrix} 1 \\ 0.5 \end{bmatrix} u_k \,, \tag{4.31}$$

with state and input constraints given by the H-rep polytopes $\mathcal{X} = [-5, 5]^2$ and $\mathcal{U} = [-1, 1]$. An MPC is designed with weight matrices $Q = I$ and $R = 1$. The terminal weight and state constraint set are chosen to guarantee stability and recursive feasibility of the nominal closed-loop system as $Q_N = P_\infty^{LQR}$ and $\mathcal{X}_N = \mathcal{O}_\infty^{LQR}$, where P_∞^{LQR} and $\mathcal{O}_\infty^{LQR}$ are the cost and maximal invariant set, respectively, of the infinite-horizon LQR problem with weights Q and R [14], and are found using the MPT [12].

Following the process described in Section 4.2.4, define the parameter set $\mathcal{X}_p$ as a hybrid zonotope such that $\mathcal{X} \subseteq \mathcal{X}_p$. In the presented case, the parameter set is given in HCG-rep by $\mathcal{X}_p = \langle G_x^c, \emptyset, c_x \emptyset, \emptyset, \emptyset \rangle$ for $G_x^c = 5I_2$ and $c_x = \mathbf{0}$. The set of admissible control inputs may similarly be represented exactly by the zonotope $\overline{\mathcal{U}} = \{G_u \xi_u + c_u \mid \|\xi_u\|_\infty \leq 1\}$ for $G_u = 1$ and $c_u = 0$. When the constraint sets are arbitrary convex polytopes, $\mathcal{X}_p$ and $\overline{\mathcal{U}}$ may be taken as any over-approximative zonotopes such that $\mathcal{X} \subseteq \mathcal{X}_p$ and $\mathcal{U} \subseteq \overline{\mathcal{U}}$; tight approximations may be found using the methods described in [11]. Under the change of variables (4.26), the set of feasible optimizers of the mp-QP (4.27) is then over-approximated by the zonotope $\overline{\mathcal{Z}} = \{G_z \xi_z + c_z \mid \|\xi_z\|_\infty \leq 1\}$ for

$$\begin{aligned} &G_z = \operatorname{diag}(\Delta) \,,\; c_z = (c_u \;\; \cdots \;\; c_u) + \overline{P} c_x \,, \\ &\Delta = \sum_{\mathrm{i}=1}^{n_{g,u}} \left| \begin{pmatrix} g_u^{(\mathrm{i})} & \cdots & g_u^{(\mathrm{i})} \end{pmatrix} \right| + \sum_{\mathrm{i}=1}^{n_{g,x}} \left| \overline{P} g_x^{(\mathrm{i})} \right| \,, \end{aligned} \tag{4.32}$$

where $G_u = [g_u^{(1)} \ \dots \ g_u^{(n_{g,u})}]$, $G_x = [g_x^{(1)} \ \dots \ g_x^{(n_{g,x})}]$, and $g_u^{(\mathrm{i})}$ for all $\mathrm{i} = 1, \dots, n_{g,u}$ and c_u are repeated N times in their respective column vectors. Once the prediction horizon N is fixed and $\overline{\mathcal{Z}}$ is chosen, the mp-QP (4.28) of the MPC is fully defined over the constrained state space $\mathcal{X} \subset \mathbb{R}^2$.

Representation and Explicit Solution of the MPC Inputs

Applying Theorem 4.2.1, the set of all feasible optimizers is given by the hybrid zonotope $\mathcal{Z}^*(x_p) = \langle G_*^c, G_*^b, c_*, A_*^c, A_*^b, b_* \rangle$ and may be transformed by the change of variables (4.26) to give the set of MPC inputs and feasible initial states over the prediction horizon as

$$\mathcal{X}_{feas} = \langle [G_x^c \ \mathbf{0} \ \mathbf{0}], \mathbf{0}, c_x, A_*^c, A_*^b, b_* \rangle \, , \tag{4.33a}$$

$$\mathcal{U}^*(x_p) = \langle [-\overline{P} G_x^c \ G_z \ \mathbf{0}], \mathbf{0}, c_z - \overline{P} c_x, A_*^c, A_*^b, b_* \rangle. \tag{4.33b}$$

The explicit control law is visualized as a function of the state by the hybrid zonotope $\mathcal{X} \circ \mathcal{U}_0^* = \langle G_{xu}^c, \mathbf{0}, c_{xu}, A_*^c, A_*^b, b_* \rangle \subset \mathbb{R}^{n_x + n_u}$ by concatenating the continuous generators and centers of (4.33a) with the first n_u rows of the continuous generators and centers of (4.33b) as

$$G_{xu}^c = [I_q \ \mathbf{0}] \begin{bmatrix} G_x^c & \mathbf{0} & \mathbf{0} \\ -\overline{P} G_x^c & G_z & \mathbf{0} \end{bmatrix}, c_{xu} = [I_q \ \mathbf{0}] \begin{bmatrix} c_x \\ c_z - \overline{P} c_x \end{bmatrix},$$

where $q = n_x + n_u = 3$. As discussed in Corollary 4.2.1, the hybrid zonotope $\mathcal{X} \circ \mathcal{U}_0^*$ may be decomposed by enumerating the feasible combinations of the binary factors to give the explicit control law as a collection of constrained zonotopes as shown in Fig. 4.5. The set representation complexities of $\mathcal{U}^*(x_p)$ and $\mathcal{X}_{feas}$, after applying the redundancy removal techniques described in Remarks 4.2.2 and 4.2.3, are given in Table 4.6 for varying prediction horizons. The complexity of the representation of the critical regions as minimal H-rep polytopes found using the MPT is provided for comparison.

Reachability Analysis

Now the reachability analysis of the closed-loop plant under the designed MPC with a prediction horizon of $N = 5$ is presented for two scenarios, (1) nominal: plant is equivalent

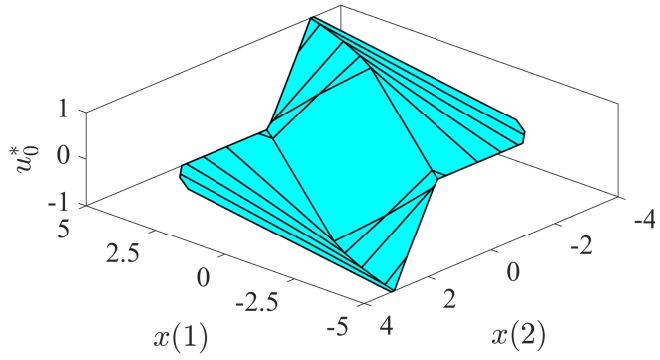

Figure 4.5. Explicit control law $(x\ u_0^*(x)) \in \mathcal{X} \circ \mathcal{U}_0^*$ for a prediction horizon of $N = 5$ as a hybrid zonotope. Decomposition of the hybrid zonotope into its equivalent collection of 25 constrained zonotopes is depicted by solid black lines.

Table 4.6. Set representation complexity of the hybrid zonotopes $\mathcal{U}^*(\mathcal{X}_p)$ and $\mathcal{X}_{feas}$ compared to the total number of n_x-dimensional halfspaces required to represent the critical regions as a collection of H-rep polytopes for varying prediction horizons.

Prediction	Hybrid Zonotope			MPT $\mathcal{CR}_i$	
N	$n_{g,*}$	$n_{c,*}$	$n_{b,*}$	H-rep	Regions
3	37	27	8	74	19
5	53	41	10	104	25
7	73	57	14	124	29
9	97	77	18	144	33
11	105	83	20	150	35
13	107	85	20	150	35

to the prediction model with no disturbances, and (2) perturbed: plant is modeled with a slight perturbation from the nominal prediction model and the closed-loop system is subject to additive disturbances.

Nominal: The states reachable by the plant $(A_p, B_p) = (A, B)$ from the set of all feasible initial conditions $\mathcal{X}_{feas}$ in five discrete updates of the MPC is generated through iterative applications of Theorem 4.2.2 and is depicted in Fig. 4.6. The set representation complexity and computation time for the final set $\mathcal{R}_5$ is given in Table 4.7 with and without redundancy removal. After removing redundant factors and constraints, the set of states reachable by the system in five time steps is given by a hybrid zonotope equivalent to the union of 403

constrained zonotopes using only 195 continuous generators, 38 binary generators, and 155 linear equality constraints.

As expected from the formulation of the state constraints and the definition of $\mathcal{X}_{feas}$, recursive feasibility of the MPC is verified from the first step of the reachability analysis as $\mathcal{R}_1 \subseteq \mathcal{X}_{feas}$. From observation, it is also possible to deduce some insight into the performance of the closed-loop system. Although not strictly enforced by the formulation of the MPC, all trajectories of the nominal closed-loop system lie within the maximal LQR invariant set after five updates of the MPC. Furthermore, it can be observed that initial conditions in the top right and bottom left quadrants have a higher potential to violate state constraints when the closed-loop system encounters disturbances due to the reachable set intersecting the boundary of $\mathcal{X}_{feas}$ for multiple updates.

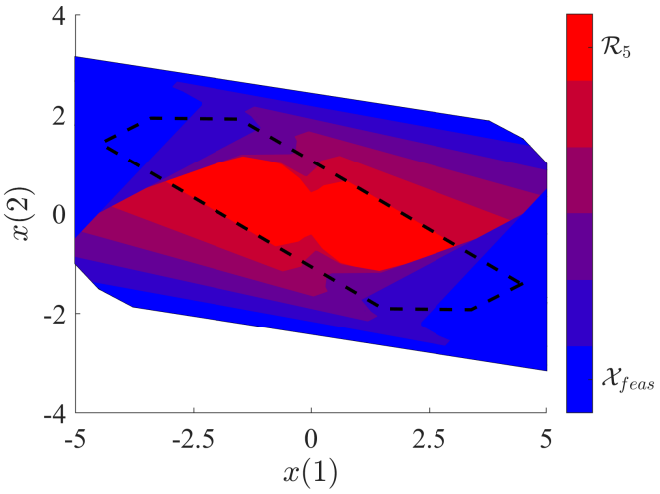

Figure 4.6. Reachable sets of the nominal MPC for five discrete time steps from the set of initial conditions given by $\mathcal{X}_0 = \mathcal{X}_{feas}$. Maximal LQR invariant set depicted by dashed lines.

Perturbed: Now consider the case when the plant dynamics do not match the nominal prediction model (4.31) and the closed-loop system is subject to a bounded disturbance.

From the set of initial conditions $\mathcal{X}_0 = \{x \in \mathbb{R}^2 \mid \|x(1)\|_\infty \leq 5,\, x(2) = 0\}$, it is to be verified that the open-loop unstable plant (A_p, B_p) given by

$$A_p = \begin{bmatrix} 1.1 & 1 \\ 0 & 1 \end{bmatrix}, \; B_p = \begin{bmatrix} 1 \\ 0.5 \end{bmatrix}, \tag{4.34}$$

retains feasibility over ten updates of the nominal MPC while subject to additive disturbances $x_{k+1} = A_p x_k + B_p u_k^* + v_k$, for all v_k belonging to the bounded set

$$\mathcal{V} = \left\{ v \in \mathbb{R}^2 : \|v\|_\infty \leq 0.25 \right\}.$$

Disturbances are accounted for in the iterative applications of Theorem 4.2.2 by performing the Minkowski sum $\mathcal{R}_k = \mathcal{R}_+ \oplus \mathcal{V}$ and introducing an additional two generators at each time step. The resulting reachable set is provided in Fig. 4.7. The complexity and computation time for the final reachable set $\mathcal{R}_{10}$ is given in Table 4.7. After removing redundant factors and constraints, the set of states reachable by the system in ten time steps is given by a hybrid zonotope equivalent to the union of 2315 constrained zonotopes using only 279 continuous generators, 45 binary generators, and 200 linear equality constraints. This exact reachability analysis verifies that the perturbed closed-loop system maintains feasibility over ten discrete time steps, as $\mathcal{R}_\mathrm{i} \subseteq \mathcal{X}_{feas}$ for $\mathrm{i} = 1, \ldots, 10$, although there is no *a priori* guarantee that this will occur.

Table 4.7. Hybrid zonotope set representation complexity for the reachable sets of the closed-loop MPC at k time steps with redundancy removal, $\mathcal{R}_k^r$, and without, $\mathcal{R}_k$.

Case	Set	$n_{g,r}$	$n_{c,r}$	$n_{b,r}$	$\lvert\mathcal{T}\rvert$	Time (sec)
Nominal	$\mathcal{R}_5$	265	213	50	403	0.02
	$\mathcal{R}_5^r$	195	155	38	403	12.20
Perturbed	$\mathcal{R}_{10}$	531	410	100	2315	0.03
	$\mathcal{R}_{10}^r$	279	200	45	2315	50.71

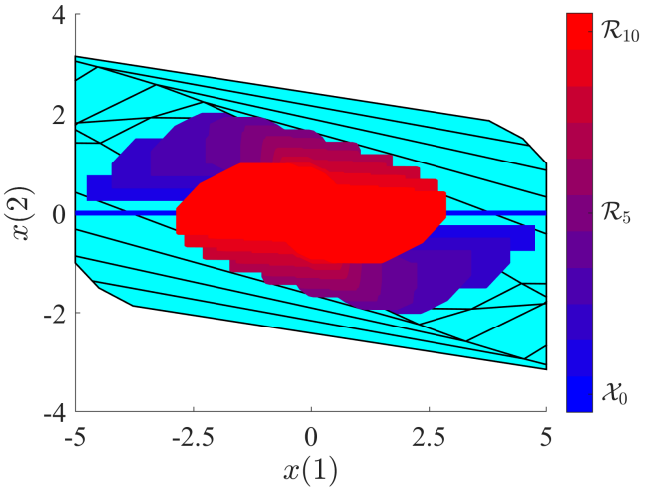

Figure 4.7. Reachable sets of the closed-loop perturbed system (4.34) with additive disturbances for ten discrete time steps. Decomposition of $\mathcal{X}_{feas}$ into critical regions given in cyan.

4.3 Chapter Summary

In this chapter I have derived closed-form solutions for the exact reachable sets of linear hybrid systems modeled as MLD systems and linear systems closed-loop under linear MPC. These identities contain all guard set intersections, changes in dynamics, and reset maps implicitly as properties of the MLD model and multiparametric solution. The resulting reachable set is represented as a single hybrid zonotope equivalent to the union an exponential number of convex sets while exhibiting linear growth in set representation complexity. These methods show how well suited the hybrid zonotope is to the reachability analysis of hybrid systems, in which discrete changes in dynamics can cause branching of sets.

Two MLD systems were used to demonstrate the use of the proposed method for forward reachable sets. The first example in which only one guard crossing occurred was used to provide intuition into the given identity and use of the MLD system framework. The second example showed the scalability of the approach by extending an existing benchmark example to consider state dimensions ranging from three continuous states with one binary state to twelve continuous states with four binary states. In this extended example, methods for the removal of redundant continuous factors, binary factors, and linear equality constraints of

such reachable sets substantially reduced the set representation complexity. These reductions provided substantial improvements in computational efficiency when compared to existing exact methods.

The proposed method for representing the forward reachable sets of systems closed-loop under MPC was applied to an MPC designed for a discrete-time double integrator in two scenarios: the nominal plant from the set of all feasible initial conditions and a perturbed plant with additive disturbances. The perturbed case verified that when beginning from rest, the closed loop system was robust to model mismatch and bounded disturbances with no *a priori* guarantees being made. Beyond safety verification, this method for reachability analysis may be used to evaluate the trade-offs in performance, conservatism, and complexity among various MPC formulations and designs.

5. BACKWARD REACHABLE SETS OF HYBRID SYSTEMS

In this chapter I present a closed-form solution to the exact backwards reachable sets of linear hybrid systems as hybrid zonotopes, as previously published by Jacob A. Siefert, Trevor J. Bird, Justin P. Koeln, Neera Jain, and Herschel C. Pangborn in the *IEEE Control Systems Letters* [85] and is included here with minor modifications. This approach relies on generating a set containing all possible state transitions of a dynamic system over a region of interest named the *state-update set*, a novel contribution of my colleague Jacob A. Siefert. Using the state-update set, both forward and backward reachability analysis may be performed using only projection and intersection set operations. The reachable sets may be made robust to bounded disturbances when the set of possible values are represented by a zonotope through Minkowski sums and differences. The technical contributions of this chapter are as follows: Jacob A. Siefert is responsible for the concept of the state-update set and its use in determining successor and precursor operators; Trevor J. Bird is responsible for deriving the identities for representing the state-update sets as hybrid zonotopes for MLD systems and closed-loop systems under linear MPC, as well as the derivation of the Minkowski differences of hybrid zonotopes; the results presented in the numerical examples were an equal contribution of both Jacob and Trevor. Trevor J. Bird was advised by Professor Neera Jain at Purdue University, as well as Professor Justin P. Koeln (University of Texas Dallas) and Professor Herschel Pangborn (The Pennsylvania State University).

This chapter is organized as follows. In Section 5.1 I provide an alternative definition for reachable sets and extend the Minkowski differences of constrained zonotopes to hybrid zonotopes. In Section 5.2 I define state-update sets and derive identities for the robust successor and precursor sets leveraging the state-update set. In Section 5.3 I show how the state-update sets of MLD systems and linear systems closed-loop under MPC may be constructed as hybrid zonotopes. In Section 5.4 I provide examples of the forward and backward reachable sets of several hybrid systems, including the calculation of the closed-loop maximal positive invariant set for MPC.

5.1 Background

This section describes a different definition for the forward and backward reachable sets of a dynamic system as the output from successor and precursor operators. These operators are defined as explicit functions of the state, input, and disturbance sets, and provide additional flexibility that will be leveraged in the following derivations.

Consider the discrete-time, dynamic system described by the difference equation

$$x_+ = f(x,u) + v\,, \tag{5.1}$$

where $x \in \mathbb{R}^{n_x}$ is the vector of initial states, $u \in \mathbb{R}^{n_u}$ is the vector of controllable inputs to the system, $v \in \mathbb{R}^{n_x}$ is the vector of additive disturbances, and $x_+ \in \mathbb{R}^{n_x}$ is the vector of trajectories after one discrete-time step. The states, inputs, and disturbances of the dynamic system (5.1) are constrained to belong to the sets $\mathcal{X} \subseteq \mathbb{R}^{n_x}$, $\mathcal{U} \subseteq \mathbb{R}^{n_u}$, and $\mathcal{V} \subseteq \mathbb{R}^{n_x}$ respectively. The forward and backward reachable sets when no disturbances are present is first considered, i.e. $\mathcal{V} = \emptyset$.

Assumption 5.1.1. *The function $f(x,u)$ for the discrete-time, dynamic system (5.1) is well-defined such that for a fixed x and u there is a unique x_+ satisfying the dynamics (5.1).*

Definition 5.1.1. [14, Ch. 10] *For the dynamic system (5.1) and a given set of states $\mathcal{R}_k \subseteq \mathcal{X} \subset \mathbb{R}^{n_x}$, the successor set for all admissible inputs belonging to the set $\mathcal{U} \subset \mathbb{R}^{n_u}$ is given by*

$$\texttt{Suc}(\mathcal{R}_k,\mathcal{U}) = \{x_+ \in \mathbb{R}^{n_x} \mid \exists x \in \mathcal{R}_k,\, u \in \mathcal{U},\; s.t.\; x_+ = f(x,u)\}\;. \tag{5.2}$$

Definition 5.1.2. [14, Ch. 10] *For the dynamic system (5.1) and a given set of states $\mathcal{R}_k \subseteq \mathcal{X} \subset \mathbb{R}^{n_x}$, the precursor set for all admissible inputs belonging to the set $\mathcal{U} \subset \mathbb{R}^{n_u}$ is given by*

$$\texttt{Pre}(\mathcal{R}_k,\mathcal{U}) = \{x_- \in \mathbb{R}^{n_x} \mid \exists u \in \mathcal{U},\; s.t.\; f(x_-,u) \in \mathcal{R}_k\}\;. \tag{5.3}$$

Given an initial set of states $\mathcal{R}_k \subseteq \mathcal{X}$, the set $\texttt{Suc}(\mathcal{R}_k,\mathcal{U})$ contains all possible trajectories of the dynamics system (5.1) at time step $k+1$ for some admissible control input $\mathcal{U}$. Conversely, given a set of states $\mathcal{R}_k \subseteq \mathcal{X}$, the set all states at time step $k-1$ that may be driven

to $\mathcal{R}_k$ by an admissible control input $u \in \mathcal{U}$ is given by $\texttt{Pre}(\mathcal{R}_k, \mathcal{U})$. Once the successor and precursor operators have been defined, the k^{th} forward and k^{th} backward reachable sets, R_k and R_{-k}, from an initial set R_0 can be found by k recursions of the operators, respectively. That is $\mathcal{R}_{k+1} = \texttt{Suc}(\mathcal{R}_k, \mathcal{U})$ and $\mathcal{R}_{k-1} = \texttt{Pre}(\mathcal{R}_k, \mathcal{U})$ when $\mathcal{R}_k \subseteq \mathcal{X}$.

Now consider when the disturbance set $\mathcal{V} \subset \mathbb{R}^{n_x}$ is nonempty, and these sets must be robust to all possible disturbances.

Definition 5.1.3. [14, Ch. 10] *For the dynamic system (5.1) and a given set of states $\mathcal{R}_k \subseteq \mathcal{X} \subset \mathbb{R}^{n_x}$, the robust successor set for all admissible control inputs belonging to the set $\mathcal{U} \subset \mathbb{R}^{n_u}$, and disturbances belonging to the set $\mathcal{V} \subset \mathbb{R}^{n_x}$ is given by*

$$\texttt{Suc}(\mathcal{R}_k, \mathcal{U}, \mathcal{V}) = \{x_+ \in \mathbb{R}^{n_x} \mid \exists x \in \mathcal{R}_k,\ u \in \mathcal{U},\ v \in \mathcal{V},\ s.t.\ x_+ = f(x,u) + v\}\ . \tag{5.4}$$

Definition 5.1.4. [14, Ch. 10] *For the dynamic system (5.1) and a given set of states $\mathcal{R}_k \subseteq \mathcal{X} \subset \mathbb{R}^{n_x}$, the robust precursor set for all admissible inputs belonging to the set $\mathcal{U} \subset \mathbb{R}^{n_u}$, and disturbances belonging to the set $\mathcal{V} \subset \mathbb{R}^{n_x}$ is given by*

$$\texttt{Pre}(\mathcal{R}_k, \mathcal{U}, \mathcal{V}) = \{x_- \in \mathbb{R}^{n_x} \mid \exists u \in \mathcal{U},\ s.t.\ f(x_-, u) + v \in \mathcal{R}_k\ \forall\, v \in \mathcal{V}\}\ . \tag{5.5}$$

Now that additive disturbances are considered, the robust successor set is the set of all points that could be driven from an initial state at time k for some *combination* of a controllable input and unknown disturbance. Thus the robust successor set has additional possibilities, i.e. $\texttt{Suc}(\mathcal{R}_k, \mathcal{U}) \subseteq \texttt{Suc}(\mathcal{R}_k, \mathcal{U}, \mathcal{V})$. On the other hand, the robust precursor set is the set of all points that could be driven to $\mathcal{R}_k$ *despite* the possible disturbances. Thus the robust precursor set has fewer possibilities, i.e. $\texttt{Pre}(\mathcal{R}_k, \mathcal{U}, \mathcal{V}) \subseteq \texttt{Pre}(\mathcal{R}_k, \mathcal{U})$. Given that the considered disturbances are additive, the difference between the successor and robust successor sets is that of a Minkowski addition such that

$$\texttt{Suc}(\mathcal{R}_k, \mathcal{U}, \mathcal{V}) = \texttt{Suc}(\mathcal{R}_k, \mathcal{U}) \oplus \mathcal{V}\ . \tag{5.6}$$

Similarly, the difference between the precursor and robust precursor sets is that of a Minkowski difference such that

$$\texttt{Pre}(\mathcal{R}_k, \mathcal{U}, \mathcal{V}) = \texttt{Pre}(\mathcal{R}_k \ominus \mathcal{V}, \mathcal{U}) \,. \tag{5.7}$$

These properties follow directly from the definitions of Minkowski sums and differences, and those of successor and precursor sets (see Section 2.2 as well as detailed discussion on robust successor and precursor sets in [14, Ch. 10]). The Minkowski difference of a hybrid zonotope by a zonotope may be calculated using the following extension of the same operation for zonotopes and constrained zonotopes [20], [34].

Proposition 5.1.1 (Minkowski Difference)**.** *For any hybrid zonotope* $\mathcal{Z}_h = \langle G_z^c, G_z^b, c_z, A_z^c, A_z^b, b_z \rangle \subset \mathbb{R}^n$ *and zonotope* $\mathcal{V} = \langle G_v, c_v \rangle \subset \mathbb{R}^n$*, where* $G_v = \begin{bmatrix} g_v^{(1)} & \dots & g_v^{(n_{g,v})} \end{bmatrix}$*, the Minkowski difference* $\mathcal{Z}_d = \mathcal{Z}_h \ominus \mathcal{V}$ *is a hybrid zonotope computed by the recursion:*

$$\mathcal{Z}_{int}^{(0)} = \mathcal{Z}_h - c_v \,, \tag{5.8a}$$

$$\mathcal{Z}_{int}^{(\mathrm{i})} = \left(\mathcal{Z}_{int}^{(\mathrm{i}-1)} + g_v^{(\mathrm{i})}\right) \cap \left(\mathcal{Z}_{int}^{(\mathrm{i}-1)} - g_v^{(\mathrm{i})}\right) \,, \tag{5.8b}$$

$$\mathcal{Z}_d = \mathcal{Z}_{int}^{(n_{g,v})} \,. \tag{5.8c}$$

Proof. The proof mirrors that for the Minkowski difference of two zonotopes [34, Thm. 1]. The Minkowski difference of an arbitrary set and a zonotope given by the above recursion only requires that the subtrahend is the Minkowski sum of the generators $g_v^{(\mathrm{i})}\ \forall\, \mathrm{i} \in \{1, \dots, n_{g,v}\}$ shifted by the center c_v. The minuend $\mathcal{Z}_h$ is an arbitrary set. It follows that the hybrid zonotope's closure under Minkowski sums and intersections allows the recursion (5.8) to be generated through a finite number of set operations to give the Minkowski difference as the hybrid zonotope $\mathcal{Z}_d$. □

Time complexity of Minkowski differences given by Proposition 5.1.1 is $\mathcal{O}(nn_{g,v})$. Complexity of the resulting set representation, $\mathcal{Z}_d$, is $n_{g,d} = 2^{n_{g,v}} n_{g,z}$, $n_{b,d} = 2^{n_{b,v}} n_{b,z}$, and $n_{c,d} = 2^{n_{c,v}} n_{c,z} + n n_{c,v}$. These can be derived by applying the Minkowski sum and intersection operation results from Section 3.2.

5.2 Reachability via State-Update Sets

This section introduces a new concept named the state-update set that encodes all possible state transitions satisfying the discrete-time dynamics (5.1) in one time step into a single $2n_x$-dimensional set. It is then shown how the state-update set may be used to define the successor and predecessor operators for finding forward and backward reachable sets.

Definition 5.2.1. *Given any discrete-time dynamic system (5.1) with a successor operator over a domain $D(\Phi)$ and set of admissible control inputs $\mathcal{U} \subset \mathbb{R}^{n_u}$, the system's state-update set $\Phi \subseteq \mathbb{R}^{2n_x}$ is given by*

$$\Phi = \left\{ \begin{bmatrix} x_k \\ x_{k+1} \end{bmatrix} \;\middle|\; \begin{array}{c} x_{k+1} \in \texttt{Suc}(\{x_k\}, \mathcal{U}), \\ x_k \in D(\Phi) \end{array} \right\} . \tag{5.9}$$

The domain of the state-update set Φ is denoted by $\mathrm{D}(\Phi) \subseteq \mathcal{X}$, and is typically chosen as some region of interest for analysis. A simple choice is to set $\mathrm{D}(\Phi) = \mathcal{X}$ for a system with state constraints. The range of the state-update set Φ, on the other hand, is the set of all points output by the successor operator over the chosen domain and admissible control inputs, and is denoted by $\mathrm{R}(\Phi)$. Thus given a domain $\mathrm{D}(\Phi) \subseteq \mathcal{X}$ and set $\mathcal{U}$, $\mathrm{R}(\Phi) = \texttt{Suc}(\mathrm{D}(\Phi), \mathcal{U})$. Also note that the domain and range of the state-update set Φ are its projections onto the first n_x and last n_x dimensions, respectively, as

$$\mathrm{D}(\Phi) = \begin{bmatrix} \mathbf{I}_{n_x} & \mathbf{0}_{n_x} \end{bmatrix} \Phi \, , \tag{5.10a}$$

$$\mathrm{R}(\Phi) = \begin{bmatrix} \mathbf{0}_{n_x} & \mathbf{I}_{n_x} \end{bmatrix} \Phi \, . \tag{5.10b}$$

Theorem 5.2.1. *Given a set of states $\mathcal{R}_k \subseteq \mathbb{R}^{n_x}$ and state-update set $\Phi \subseteq \mathbb{R}^{2n_x}$, if $\mathcal{R}_k \subseteq D(\Phi)$ then*

$$\texttt{Suc}(\mathcal{R}_k, \mathcal{U}, \mathcal{V}) = \begin{bmatrix} \mathbf{0}_{n_x} & \mathbf{I}_{n_x} \end{bmatrix} \left(\Phi \cap_{[\mathbf{I}_{n_x} \;\; \mathbf{0}_{n_x}]} \mathcal{R}_k \right) \oplus \mathcal{V} \, . \tag{5.11}$$

Proof. By the definition of generalized intersections (2.1d) and Definition 5.2.1,

$$\Phi \cap_{[\mathbf{I}_{n_x} \ \mathbf{0}_{n_x}]} \mathcal{R}_k \ = \left\{ \begin{bmatrix} x_k \\ x_{k+1} \end{bmatrix} \middle| \begin{array}{c} x_{k+1} \in \texttt{Suc}(\{x_k\}, \mathcal{U}), \\ x_k \in \mathcal{R}_k \cap \mathrm{D}(\Phi) \end{array} \right\}.$$

If $\mathcal{R}_k \subseteq \mathrm{D}(\Phi)$, then $\mathcal{R}_k \cap \mathrm{D}(\Phi) = \mathcal{R}_k$. Thus the right hand side of (5.11) yields

$$\{x_{k+1} \mid x_{k+1} \in \mathrm{Suc}(\{x_k\}, \mathcal{U}),\ x_k \in \mathcal{R}_k\} \oplus \mathcal{V}, \tag{5.12}$$

giving the desired result by Definition 5.1.3. □

The containment condition in Theorem 5.2.1, $\mathcal{R}_k \subseteq \mathrm{D}(\Phi)$, is in general not restrictive as modeled dynamics are often only valid over some region of interest, which the user may specify as $\mathrm{D}(\Phi)$ when constructing the state-update set. If $\mathcal{R}_k \not\subseteq \mathrm{D}(\Phi)$, it can be shown that the right side of (5.11) gives $\texttt{Suc}(\mathcal{R}_k \cap \mathrm{D}(\Phi), \mathcal{U}, \mathcal{V})$ due to the intersection with the domain of the state-update set.

Remark 5.2.1. *The result of Theorem 5.2.1 gives cause for healthy skepticism. That is, if the robust successor operator is already defined, what is the advantage of going through the additional steps to achieve the same result as that of applying the robust successor operator? The advantage is that the state-update set given by Φ is a set of points, and the successor operator only needs to be applied once when finding Φ. Thus the only restrictions imposed by Theorem 5.2.1 is that the set representation used to represent Φ is closed under generalized intersections and may have Minkowski sums applied for the additive disturbance set $\mathcal{V}$. Furthermore, Φ can be manipulated using set operations prior to performing any analysis, which is unique to the proposed approach.*

It is now shown how the robust precursor set may also be defined using the state-update set.

Lemma 5.2.1. *The state-update set (5.9) is equivalently defined in terms of the precursor set as*

$$\Phi = \left\{ \begin{bmatrix} x_{k-1} \\ x_k \end{bmatrix} \;\middle|\; \begin{array}{c} x_{k-1} \in \texttt{Pre}(\{x_k\}, \mathcal{U}), \\ x_{k-1} \in D(\Phi) \end{array} \right\} . \tag{5.13}$$

Proof. Let Φ be given by Definition 5.2.1. For any $\phi \in \Phi \subseteq \mathbb{R}^{2n_x}$, let $(x_{k-1}\ x_k) = \phi$. Then for all x_k there exists some $x_{k-1} \in \mathrm{D}(\Phi)$ such that $x_k \in \texttt{Suc}(\{x_{k-1}\}, \mathcal{U})$, and from Definition 5.1.1 it holds that $x_k = f(x_{k-1}, u)$ for some $u \in \mathcal{U}$. Thus it follows that $x_{k-1} \in \texttt{Pre}(\{x_k\}, \mathcal{U})$. □

Theorem 5.2.2. *Given a set of states $\mathcal{R}_k \subseteq \mathbb{R}^n$ and state-update set Φ, if $\mathcal{R}_k \ominus \mathcal{V} \subseteq R(\Phi)$, then*

$$\texttt{Pre}(\mathcal{R}_k, \mathcal{U}, \mathcal{V}) \cap D(\Phi) = \begin{bmatrix} \mathbf{I}_{n_x} & \mathbf{0}_{n_x} \end{bmatrix} \left(\Phi \cap_{[\mathbf{0}_{n_x}\ \mathbf{I}_{n_x}]} (\mathcal{R}_k \ominus \mathcal{V}) \right) . \tag{5.14}$$

Proof. Let $\mathcal{K} = \mathcal{R}_k \ominus \mathcal{V}$, then for any $x_k \in \mathcal{K}$ it holds that $x_k + v \in \mathcal{R}_k \; \forall \; v \in \mathcal{V}$. By the definition of generalized intersections and Lemma 5.2.1,

$$\Phi \cap_{[\mathbf{0}_{n_x}\ \mathbf{I}_{n_x}]} \mathcal{K} = \left\{ \begin{bmatrix} x_{k-1} \\ x_k \end{bmatrix} \;\middle|\; \begin{array}{l} x_{k-1} \in \texttt{Pre}(\{x_k\}, \mathcal{U}) \, , \\ x_{k-1} \in \mathrm{D}(\Phi) \, , \; x_k \in \mathcal{K} \end{array} \right\} .$$

Thus the right-hand side of (5.14) yields

$$\{ x_{k-1} \mid x_{k-1} \in \texttt{Pre}(\{x_k\}, \mathcal{U}) \cap \mathrm{D}(\Phi) \, , \; x_k + v \in \mathcal{R}_k \; \forall \; v \in \mathcal{V} \} \, , \tag{5.15}$$

giving the desired result by Definition 5.1.4. □

When Φ is generated for a domain $\mathrm{D}(\Phi)$ corresponding to a region of interest for analysis, the condition $\texttt{Pre}(\mathcal{R}_k, \mathcal{U}, \mathcal{V}) \cap \mathrm{D}(\Phi)$ of Theorem 5.2.2 is not restrictive. For the use case of systems with state constraints, when the domain is chosen as $\mathrm{D}(\Phi) = \mathcal{X}$, robust backwards reachable sets and invariant sets can be determined using the proposed precursor operator. In general, suitable choice of $\mathrm{D}(\Phi)$ will result in $\mathrm{Pre}(\mathcal{R}_k, \mathcal{U}, \mathcal{V}) \subseteq \mathrm{D}(\Phi) \implies \mathrm{Pre}(\mathcal{R}_k, \mathcal{U}, \mathcal{V}) \cap \mathrm{D}(\Phi) = \mathrm{Pre}(\mathcal{R}_k, \mathcal{U}, \mathcal{V})$. The condition $\mathcal{R}_k \ominus \mathcal{V} \subseteq \mathrm{R}(\Phi)$ requires that the set to be operated on

is fully contained within the range of the state-update set. If this condition does not hold, i.e. $\mathcal{R}_k \ominus \mathcal{V} \not\subseteq \mathrm{R}(\Phi)$, then information is lost during the intersection with the state-update set. Specifically, there exists some $x_k \in \mathcal{R}_k$ that can be reached, but for which no combination of $x_{k-1} \in \mathrm{D}(\Phi)$, $u \in \mathcal{U}$, and $v \in \mathcal{V}$ can account.

5.3 Reachability using Hybrid Zonotope State-Update Sets

It is now shown how state-update sets can be generated for MLD systems and linear systems under closed-loop MPC using hybrid zonotopes and the forward reachability results from Chapter 4.

Assumption 5.3.1. *Note that the Minkowski difference required in the robust successor set given by Theorem 5.2.2 may only be performed using the identity given in Proposition 5.1.1 when the possible disturbances are represented by a zonotope in G-rep such that*

$$\mathcal{V} = \langle G_v^c, c_v \rangle \subset \mathbb{R}^{n_x} . \tag{5.16}$$

It is assumed that all disturbance sets in this chapter are given by the zonotope (5.16).

Using hybrid zonotopes, the proposed state-update set method has reduced time complexity for forward reachable sets when compared to the proposed methods in Chapter 4. Specifically, the time complexity of the successor set given by (5.11) is $\mathcal{O}(n)$, as the linear mappings $[\mathbf{I}_{n_x}\ \mathbf{0}_{n_x}]$ and $[\mathbf{0}_{n_x}\ \mathbf{I}_{n_x}]$ are projections that amount to matrix concatenation. The time complexity of the precursor set given by (5.14) is $\mathcal{O}(nn_{g,v})$ due to the Minkowski difference. Set complexity growth of the successor set is given by

$$n_{g,\mathtt{Suc}} = n_{g,r} + n_{g,\phi} + n_{g,v} , \tag{5.17a}$$

$$n_{b,\mathtt{Suc}} = n_{b,r} + n_{b,\phi} , \tag{5.17b}$$

$$n_{c,\mathtt{Suc}} = n_{c,r} + n_{c,\phi} + n , \tag{5.17c}$$

and that of the precursor set is given by

$$n_{g,\texttt{Pre}} = 2^{n_{g,v}} n_{g,r} + n_{g,\phi} \,, \tag{5.18a}$$

$$n_{b,\texttt{Pre}} = 2^{n_{g,v}} n_{b,r} + n_{b,\phi} \,, \tag{5.18b}$$

$$n_{c,\texttt{Pre}} = 2^{n_{g,v}} n_{c,r} + 2^{n_{g,v}} n + n_{c,\phi} \,, \tag{5.18c}$$

where $n_{\cdot,r}$ is the set representation complexity of the hybrid zonotope $\mathcal{R}_k$, $n_{\cdot,\phi}$ is the set representation complexity of the state-update set in HCG-rep, and $n_{g,v}$ is the number of generators used to represent the possible disturbances in G-rep. Iterative calculation of successor sets (5.11) results in linear complexity growth dependent on the complexity of Φ and $\mathcal{V}$. Due to the difficulty of computing Minkowski differences, iterative calculations of the precursor sets (5.11) results in exponential complexity growth. If $n_{g,v} = 0$, time complexity of precursor sets (5.14) reduces to $\mathcal{O}(n)$ and iterative applications of the precursor operator give linear complexity growth.

Remark 5.3.1. *Given that the state-update set is defined as a hybrid zonotope, all redundancy removal and order reduction techniques described in Chapter 6 may be used to reduce the the complexity growth of the resulting forward and backward reachable sets. When applied to the state-update set, these order reduction techniques only need to be applied once, not iteratively.*

5.3.1 State-Update Set: MLD Systems

This section shows how the identity for the forward reachable sets of MLD systems by Theorem 4.1.1 may be used to generate a state-update set for the system. The complexity of finding the state-update set is the same as finding the one-step forward reachable set.

Proposition 5.3.1. *Given a well-posed MLD system given by (4.1) and defined over $\mathcal{X} \subset \mathbb{R}^{n_x}$, let*

$$\mathcal{Q} = \begin{bmatrix} \mathbf{0} \\ B_u \\ E_u \end{bmatrix} \mathcal{U} \oplus \begin{bmatrix} \mathbf{0} \\ B_w \\ E_w \end{bmatrix} \mathcal{W} \oplus \begin{bmatrix} \mathbf{0} \\ B_{aff} \\ \mathbf{0} \end{bmatrix}, \tag{5.19}$$

and define $\mathcal{H} = \{s \in \mathbb{R}^{n_e} \mid s \leq E_{aff}\}$. Then a state-update set with $D(\Phi) = \mathcal{X}$ for the MLD system is given by

$$\Phi = [\mathbf{I}_{2n_x} \ \mathbf{0}_{n_e}] \left[\left([\mathbf{I}_{n_x} \ A^T \ E_x^T]^T \mathcal{X} \oplus \mathcal{Q} \right) \cap_{[\mathbf{0}_{2n_x} \ \mathbf{I}_{n_e}]} \mathcal{H} \right]. \tag{5.20}$$

Proof. Let $\hat{\Phi}$ be the hybrid zonotope given by the right-hand side of (5.20) and Φ the state-update set of the MLD system given by Definition 5.2.1 with $\mathrm{D}(\Phi) = \mathcal{X}$. For any $p \in [\mathbf{I}_{n_x} \ A^T \ E_x^T]^T \mathcal{X} \oplus \mathcal{Q}$, there exists some $x \in \mathcal{X}, u \in \mathcal{U}$, and $w \in \mathcal{W}$ such that

$$p = \begin{bmatrix} p_1 \\ p_2 \\ p_3 \end{bmatrix} = \begin{bmatrix} x \\ Ax + B_u u + B_w w + B_{aff} \\ E_x x + E_u u + E_w w \end{bmatrix}.$$

For any $\hat{\phi} \in \hat{\Phi}$, $\hat{\phi} = [\mathbf{I}_{2n_x} \ \mathbf{0}_{n_e}]p$ and $[\mathbf{0}_{2n_x} \ \mathbf{I}_{n_e}]p \in \mathcal{H}$. By Theorem 4.1.1, this implies that $[\mathbf{0}_{n_x} \ \mathbf{I}_{n_x}]\hat{\phi} \in \mathtt{Suc}([\mathbf{I}_{n_x} \ \mathbf{0}_{n_x}]\hat{\phi}, \mathcal{U})$ and therefore $\hat{\phi} \in \Phi$. Given that the MLD is well-defined for all $x \in \mathcal{X}$, it holds that $\mathrm{D}(\hat{\Phi}) = \mathcal{X}$ and therefore $\hat{\Phi} = \Phi$. □

5.3.2 State-Update Set: Linear MPC

This section demonstrates the construction of a hybrid zonotope state-update set for a discrete-time linear time-invariant system under MPC by leveraging Theorem 4.2.2. It is possible to construct an MLD system equivalent to a linear system under closed-loop MPC [14], [81] which can be used to construct a state-update set using the results of Section 5.3.1. Thus the proof of Proposition 5.3.1 holds. Instead, this section provides a direct method with

no MLD conversion to generate the state-update set for the linear system under closed-loop MPC.

Given the linear discrete-time system (4.21) and MPC formulation (4.22), consider the augmented system

$$\hat{A} = \begin{bmatrix} \mathbf{0} & \mathbf{I}_{n_x} \\ \mathbf{0} & A \end{bmatrix}, \ \hat{B} = \begin{bmatrix} \mathbf{0} \\ B \end{bmatrix}, \ \hat{Q} = \begin{bmatrix} \mathbf{0} & \mathbf{0} \\ \mathbf{0} & Q \end{bmatrix}, \hat{Q}_N = \begin{bmatrix} \mathbf{0} & \mathbf{0} \\ \mathbf{0} & Q_N \end{bmatrix},$$

$$\hat{R} = R\,, \ \hat{X} = \mathcal{X} \times \mathcal{X}\,, \ \hat{X}_n = \mathcal{X} \times \mathcal{X}_n\,, \ \hat{\mathcal{U}} = \mathcal{U}\,. \tag{5.21}$$

The augmented system (5.21) stacks a static system with the linear system of interest (A, B). The static states are not penalized and have no effect on the optimal inputs. Leveraging Theorem 4.2.2 to find the one-step forward reachable set of the augmented system (5.21) under closed-loop MPC from the initial set $\hat{\mathcal{X}}_0 = [\mathbf{0}_{n_x} \ \mathbf{I}_{n_x}]^T \mathcal{X}$ yields the state-update set with $\mathrm{D}(\Phi) = \mathcal{X}$.

5.4 Numerical Examples

The following examples calculate forward and backward reachable sets and invariant sets using the methods proposed in Section 5.2 with state-update sets calculated as in Section 5.3. MLD representations of the considered hybrid systems are obtained using HYSDEL 3.0 [75]. Results are generated with MATLAB on a desktop computer with a 3.0 GHz Intel i7 processor and 16 GB of RAM.

5.4.1 Piece-Wise Affine System with Two Equilibrium Points

This example extends the PWA system with two equilibrium points considered in Section 4.1.4 by introducing a control input and additive disturbance as

$$x[k+1] = \begin{cases} A_1 x[k] + B_1 + u[k] + w[k]\,, & \text{if } x_1[k] \leq 0\,, \\ A_2 x[k] + B_2 + u[k] + w[k]\,, & \text{otherwise}\,, \end{cases}$$

$$A_1 = \begin{bmatrix} 0.75 & 0.25 \\ -0.25 & 0.75 \end{bmatrix}, \; B_1 = \begin{bmatrix} -0.25 \\ -0.25 \end{bmatrix}, \; A_2 = A_1^T, \; B_2 = \begin{bmatrix} 0.25 \\ -0.25 \end{bmatrix}.$$

The inputs and disturbances are constrained to belong to scaled unit hypercubes such that $u[k] \in \mathcal{U} = s_u \mathcal{B}_\infty^2$ and $w[k] \in \mathcal{W} = s_w \mathcal{B}_\infty^2$. Forward $(\mathcal{R}_4, \mathcal{R}_5, \mathcal{R}_6)$ and backward $(\mathcal{R}_0, \mathcal{R}_1, \mathcal{R}_2)$ reachable sets are calculated from

$$\mathcal{R}_3 = \left\langle \begin{bmatrix} 0.15 & 0.05 \\ -0.05 & 0.15 \end{bmatrix}, \begin{bmatrix} -0.0520 \\ 0.8465 \end{bmatrix} \right\rangle,$$

and shown in Figure 5.1 for three cases of input and disturbance sets defined in Table 5.1. This example system and choice of $\mathcal{R}_3$ are chosen to facilitate comparison with forward reachability results from Section 4.1.4. The state-update set for Case 1 and Case 2 where no inputs are applied is calculated and found to have complexity $n_{g,\phi} = 16$, $n_{b,\phi} = 1$, $n_{c,\phi} = 10$. The state-update set for Case 3 has 2 additional continuous generators associated with the input resulting in $n_{g,\phi} = 18$. Computation times and reachable set complexities are reported in Table 5.1.

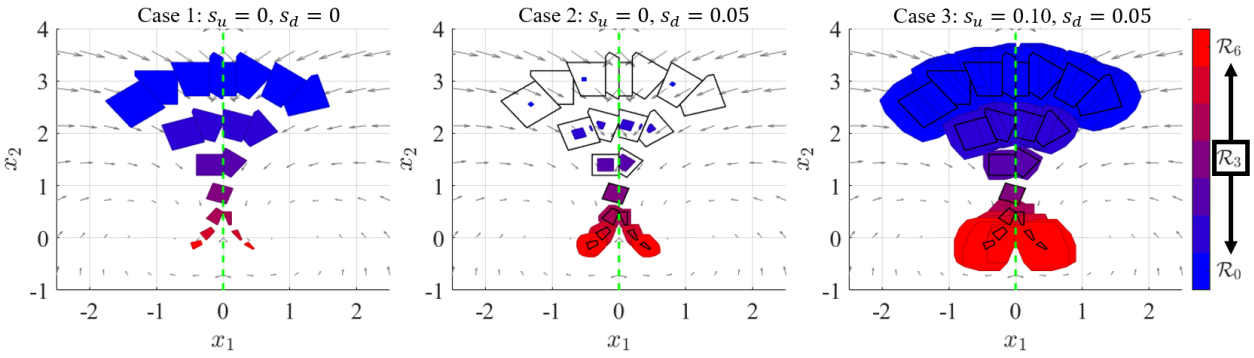

Figure 5.1. Forward $(\mathcal{R}_4, \mathcal{R}_5, \mathcal{R}_6)$ and backward $(\mathcal{R}_0, \mathcal{R}_1, \mathcal{R}_2)$ reachable sets from $\mathcal{R}_3$ for three cases of input and disturbance sets. Sets from the Case 1 subplot are also shown in wire frame in the Case 2 and 3 subplots for comparison.

In Figure 5.1, forward reachable sets are shown to split along the guard, while backward reachable sets branch when their precursors set span both sides of the guard. Comparison of Case 1 and Case 2 demonstrates that backward reachable sets are smaller when required

Table 5.1. Forward and backward reachable set complexities and computation times for the two-equilibrium system.

Case	Direction/Set	$n_{g,r}$	$n_{b,r}$	$n_{c,r}$	Time [ms]
1) $s_u = 0$, $s_w = 0$	Forward: $\mathcal{R}_6$	50	3	36	0.13
	Backward: $\mathcal{R}_0$	50	3	36	0.12
2) $s_u = 0$, $s_w = 0.05$	Forward: $\mathcal{R}_6$	56	3	36	0.23
	Backward: $\mathcal{R}_0$	464	21	378	2.92
3) $s_u = 0.10$, $s_w = 0.05$	Forward: $\mathcal{R}_6$	62	3	36	0.24
	Backward: $\mathcal{R}_0$	506	21	378	3.12

to be robust to a disturbance, while forward reachable sets become larger. Comparison of Case 2 and Case 3 demonstrates that adding control authority causes forward and backward reachable sets to become larger.

In Case 1, backward and forward reachable sets are calculated with similar computation times and have identical complexity growth when there is no disturbance. The addition of a disturbance in Case 2, and both a disturbance and an input in Case 3, has a small effect on computation times and complexity growth of forward reachable sets. However, because the robust precursor set relies on a Minkowski difference when a disturbance is present, the computation time and complexity growth of the backward reachable sets increase significantly. These results are consistent with the complexity equations in Section 5.3 and motivate future work on approximation methods to reduce reachable set complexity through developing methods for inner-approximations. Similar to how hybrid zonotopes are able to leverage over-approximation methods developed for zonotopes (see Chapter 6), hybrid zonotopes may be able to leverage approximation methods developed for the inner-approximations of zonotopes and constrained zonotopes [20], [35].

Using the methods from Section 4.1 for *exact* redundancy removal, 5 continuous generators and 3 constraints are removed from the state-update set. The 6-step backward reachable sets from $\mathcal{R}_3$ for Case 2 using the nominal ($\mathcal{R}_{-3}$) and reduced ($\mathcal{R}_{-3}^{red}$) state-update sets are shown in Table 5.2. Computation time of the reduced set includes 0.5 seconds to reduce the state-update set prior to iteration over precursor sets. This enables a 62% reduction in total

computation time, 22% reduction in number of continuous generators, and 6% reduction in number of constraints.

Table 5.2. Backward reachability with nominal (row 1) vs. reduced (row 2) state-update set for the two-equilibrium system.

Case 2	Direction/Set	$n_{g,r}$	$n_{b,r}$	$n_{c,r}$	Time [s]
$s_u = 0\ , s_w = 0.05$	Backward: $\mathcal{R}_{-3}$	30032	1365	24570	50
	Backward: $\mathcal{R}_{-3}^{red}$	23207	1365	23207	19

5.4.2 Thermostat-Controlled Heated Rooms

To demonstrate scalability, backward reachability is performed for the benchmark room heating example with 6 rooms and 2 heaters, given by Case$(6, 2)$ in Section 4.1.4 assuming a constant outdoor temperature of $u = 0$. The state-update set has complexity $n_{g,\phi} = 24$, $n_{b,\phi} = 8$, $n_{c,\phi} = 18$. Backward reachable sets are found beginning at $\mathcal{R}_{50}$ from the forward reachability analysis performed in Section 4.1.4, which has complexity $n_{g,50} = 68$, $n_{b,50} = 13$, $n_{c,50} = 62$. The 50-step backward reachable set $\mathcal{R}_0$ is calculated in 0.34 seconds with complexity $n_{g,0} = 1268$, $n_{b,0} = 413$, $n_{c,r0} = 1362$.

An alternative to the proposed approach is to calculate the reachable set as a collection of convex sets, as done for forward reachability in [86] and backward reachability in [32]. This exhibits worst-case exponential growth in set complexity over time, while the proposed approach has linear complexity growth. At every time step, *each* convex set in the collection is propagated backward under the dynamics of *each* mode, and sets corresponding to inactive modes are eliminated. For comparison to the proposed approach, $\mathcal{R}_0$ is calculated using [32, Section IV] and implemented using constrained zonotopes [18]. This results in a collection of 1125 constrained zonotopes with 147,637 total generators and 28,387 total constraints and takes 202 seconds to compute. This is nearly 600 times longer than the proposed approach due to the large number of convex sets to be propagated and eliminated.

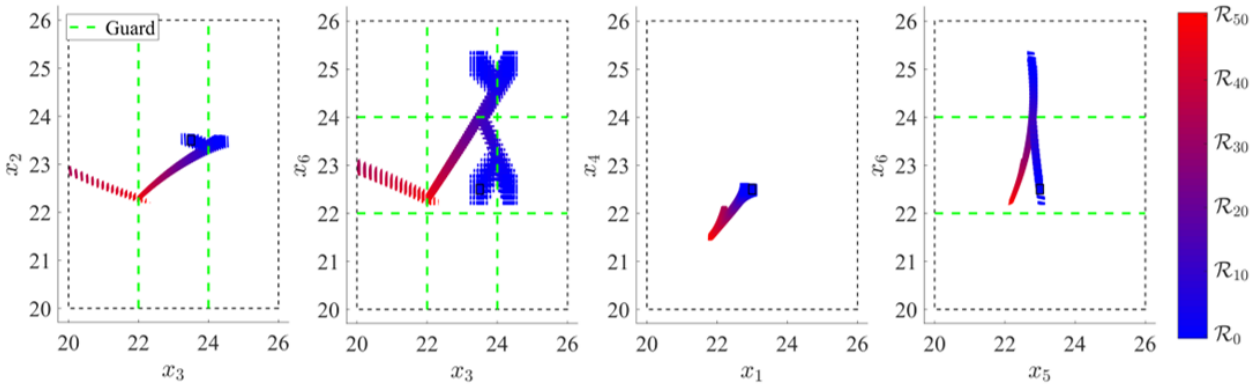

Figure 5.2. Projections of backward reachable sets of the room heating example. Backward reachable sets are calculated from $\mathcal{R}_{50}$ for 50 steps. Guards determining heater logic (green dashed lines) and the region over which the MLD is defined (black dashed lines) are also depicted. The initial set used to find $\mathcal{R}_{50}$ is depicted by solid black box.

5.4.3 Model Predictive Control

The maximal positive invariant set $\mathcal{O}_\infty^{MPC}$ of a closed-loop system under MPC consists of all initial conditions that generate recursively feasible trajectories. This example shows how the proposed methods enable computation of a less conservative $\mathcal{O}_\infty^{MPC}$ as compared to conventional methods.

Consider the double integrator from [14, Example 12.1],

$$x[k+1] = \begin{bmatrix} 1 & 1 \\ 0 & 1 \end{bmatrix} x[k] + \begin{bmatrix} 0 \\ 1 \end{bmatrix} u[k] \,,$$

under MPC (4.22) with $P = Q = \mathbf{I}$, $R = 10$, and $N = 3$. Input and state trajectories are constrained by $u[k] \in \mathcal{U} = \frac{1}{2}\mathcal{B}_\infty^1$, $x[k] \in \mathcal{X} = 5\mathcal{B}_\infty^2$, $\forall k \in [1, N-1]$. Two cases of terminal state constraints are considered.

Case 1: For this case, we set $\mathcal{X}_N = \mathcal{X}$. Algorithm 10.1 of [14] provides a general method for calculating $\mathcal{O}_\infty$ for autonomous dynamics using precursor and intersection calculations, but its application to hybrid systems was previously limited due to the lack of a scalable precursor set identity. However, this algorithm can be applied using hybrid zonotopes and the precursor set identity in Theorem 5.2.2 to calculate $\mathcal{O}_\infty^{MPC}$, as plotted in Figure 5.3a.

Also plotted is $\mathcal{X}_{feas}$, the set of states for which the optimization program has a feasible solution but are not necessarily recursively feasible trajectories.

Case 2: Absent efficient methods to compute $\mathcal{O}_\infty^{MPC}$ under the PWA control laws, conventional approaches ensure recursive feasibility by artificially constraining $\mathcal{X}_N$ to a positively invariant set associated with a simpler control law. This results in $\mathcal{O}_\infty^{MPC} = \mathcal{X}_{feas}$ [14, Chapter 12.3.1]. A common choice is $\mathcal{X}_N = \mathcal{O}_\infty^{LQR}$, where $\mathcal{O}_\infty^{LQR}$ is the maximal linear quadratic regulator (LQR) invariant set [14, Definition 11.1]. This set and the resulting $\mathcal{X}_{feas}$ are shown in Figure 5.3b.

Comparison of cases 1 and 2 in Figure 5.3 demonstrates that introducing the terminal constraint $\mathcal{X}_N = \mathcal{O}_\infty^{LQR}$ results in a smaller maximal region of recursive feasibility than when $\mathcal{X}_N = \mathcal{X}$. Thus the proposed methods enable reduced conservatism in the control design by allowing $\mathcal{O}_\infty^{MPC}$ to be computed for a less restrictive terminal constraint. The terminal constraint in case 2 may also negatively affect performance [14, Remark 12.2].

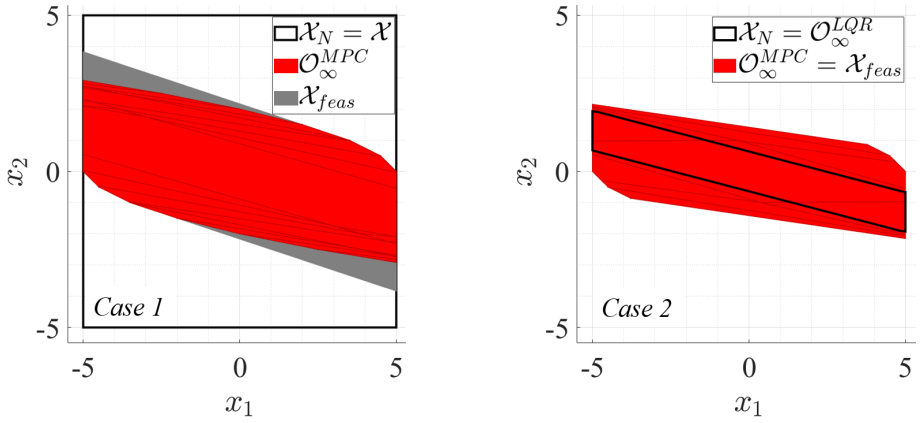

Figure 5.3. 5.3a The maximal positive invariant set under MPC $\mathcal{O}_\infty^{MPC}$ is calculated using the scalable precursor set identity presented in this paper. 5.3b Conventional methods use an artificial terminal constraint to obtain $\mathcal{O}_\infty^{MPC}$, however this makes the set smaller.

5.5 Chapter Summary

In this chapter I have presented a closed-form solution for the exact backward reachable sets of linear hybrid systems as hybrid zonotopes. This approached leveraged a new

construct named the *state-update set* that encodes all possible state transitions over one discrete time step within a single set. Using the state-update set, identities were proven for both the robust forward and robust backward reachable sets of general well-posed discrete-time dynamic systems. When the considered system is modeled as an MLD or a linear system in closed-loop under MPC, it was shown how the state-update sets may be generated as hybrid zonotopes by leveraging the results in Chapter 4. The reachable sets are then propagated with *linear* growth in the number of zonotope factors when performing forward reachability or backward reachability with no disturbances, and exponential growth when performing backward reachability with disturbances due to the complexity growth associated with Minkowski differences. These methods show that finding the one step forward reachable set of a system over a region of interest can be used to generate forward reachable, backward reachable, and invariant sets. Numerical results demonstrate forward and backward reachability of MLD systems and computation of a maximal positive invariant set for a PWA control law of MPC.

6. COMPLEXITY REDUCTION OF HYBRID ZONOTOPES

Many of the set operations I have proposed in this dissertation increase the complexity of the set representation. Although having reduced memory and computational complexity when compared to the *exact* methods existing in the literature, use of the hybrid zonotope while maintaining exactness is inherently limited to a finite number of operations. To address this challenge, in this chapter I present methods for reducing the complexity of hybrid zonotopes by extending procedures developed for constrained zonotopes as well as through general mathematical programming. The proposed methods provide an approach for conservatively reducing the complexity of the set representation such that additional operations may be continually applied while remaining computationally tractable. The technical contributions of this chapter are as follows: Trevor J. Bird is responsible for all derivations of the proposed order reduction techniques, error metrics, and numerical examples; Jacob A. Siefert is responsible for the volume estimation method by sampling random points. Trevor J. Bird was advised by Professor Neera Jain at Purdue University, as well as Professor Justin P. Koeln (University of Texas Dallas) and Professor Herschel Pangborn (The Pennsylvania State University).

This chapter is organized as follows. First I provide methods for removing redundancy from the hybrid zonotope set representation to reduce complexity of future operations without altering the set in Section 6.1. In Section 6.2 I develop algorithms for reducing the number of continuous generators, binary generators, and equality constraints of the hybrid zonotope to provide over-approximations. In Section 6.3 I derive error metrics for evaluating the effectiveness of the proposed over-approximations. Finally in Section 6.4 I provide numerical examples demonstrating the usefulness of the proposed techniques and apply them to the reachability analysis of hybrid systems.

6.1 Redundancy Removal

In this section I provide methods for identifying and removing redundancy in the equality constraints, continuous generators, and binary generators of hybrid zonotopes. These methods are advantageous as they can be used to avoid unnecessary growth in the set rep-

resentation complexity without altering the set. In Section 6.1.1 I show how redundant equality constraints may be identified and removed from the set representation. In Section 6.1.2 I show how redundancy in the continuous generators may be identified and removed while also reducing the number of equality constraints. Finally in Section 6.1.3 I show how redundant binary factors may be identified and removed from the hybrid zonotope.

6.1.1 Redundant Equality Constraints

Given any hybrid zonotope $\mathcal{Z}_h = \langle G^c, G^b, c, A^c, A^b, b \rangle \subset \mathbb{R}^n$, the equality constraints are given by the linear system of n_c equations $A^c\xi^c + A^b\xi^b = b$. It is possible that some rows of this system of equations are redundant. This redundancy may arise in reachable sets of hybrid systems, using the identities discussed in Chapters 4 and 5, when guard set intersections do not occur and other constraints and variables have been removed through various redundancy removal and order reduction techniques. Iterative applications of the forward, and backward, reachable set operators may therefore result in redundant equality constraints.

Some redundant equality constraints may be present in the form of linearly dependent rows. This redundancy can be determined by evaluating the linear dependence of each of the rows using rank revealing LU decomposition [87]. To do this, the constraint matrices are concatenated such that

$$\hat{A} = \begin{bmatrix} A^c & A^b & b \end{bmatrix} \in \mathbb{R}^{n_c \times (n_g + n_b + 1)} . \tag{6.1}$$

Performing QR decomposition on (6.1) results in $\hat{A}P = QR$, where $P \in \mathbb{R}^{(n_g+n_b+1)\times(n_g+n_b+1)}$ is a permutation matrix, $Q \in \mathbb{R}^{n_c \times n_c}$ is an orthogonal matrix, and $R \in \mathbb{R}^{n_c \times (n_g+n_b+1)}$ is an upper triangular matrix [88]. Linearly dependent rows may then be detected by the rows of R that have elements less than a prescribed zero tolerance ϵ, i.e. $R_{\mathrm{j},\cdot} \leq \epsilon$ implies that row j of the permuted matrix $\hat{A}P$ is linearly dependent. Given that their information is already contained in another row of the matrix, these linearly dependent rows may then be removed without altering the set.

6.1.2 Redundant Continuous Generators

In all zonotopes, constrained zonotopes, and hybrid zonotopes, the continuous factors are constrained to belong to the unit hypercube, $\mathcal{B}_\infty^{n_g} = \{x \in \mathbb{R}^{n_g} \mid \|x\|_\infty \leq 1\}$. Within the MILP formulation of the hybrid zonotope (3.44), this is equivalent to enforcing the constraint that the continuous factors lie within the interval of $[-1, 1]$ such that $-1 \leq \xi^c_{\mathrm{j}} \leq 1$ for all $\mathrm{j} \in \{1, \dots, n_g\}$. For the case of zonotopes, these bounds are absolute and the vertices of the represented polytope are obtained when some combination of the factors lie on the vertices or center of the unit hypercube, i.e. for any zonotope $\mathcal{Z} = \langle G^c, c \rangle \subset \mathbb{R}^n$ with an equivalent V-rep $\mathcal{Z} = \{\sum_{\mathrm{i}=1}^{n_v} \alpha_{\mathrm{i}} v_{\mathrm{i}} \,|\, \alpha_{\mathrm{i}} \geq 0,\ \sum_{\mathrm{i}=1}^{n_v} \alpha_{\mathrm{i}} = 1\}$, $G^c\xi^c + c = v_{\mathrm{i}}$ implies that $\xi^c_{\mathrm{j}} \in \{-1, 0, 1\}$ for all $\mathrm{j} \in \{1, \dots, n_g\}$ [65]. Once linear equality constraints are introduced into the set definition, such as for constrained and hybrid zonotopes, the infinity norm constraints on certain continuous factors may be unnecessary.

Similar to the approach used for rescaling the continuous generators of constrained zonotopes [18, Sec. 4.1], the implicit bounds on the continuous factors of a hybrid zonotope may be found by solving the $2n_g$ MILPs given by

$$\xi^c_{L,\mathrm{i}} = \min \left\{ \xi^c_{\mathrm{i}} \;\middle|\; A^c\xi^c + A^b\xi^b = b\,,\ \|\xi^c_{\mathrm{j}\neq\mathrm{i}}\|_\infty \leq 1\,,\ \xi^b \in \{-1, 1\}^{n_b} \right\}, \tag{6.2a}$$

$$\xi^c_{U,\mathrm{i}} = \max \left\{ \xi^c_{\mathrm{i}} \;\middle|\; A^c\xi^c + A^b\xi^b = b\,,\ \|\xi^c_{\mathrm{j}\neq\mathrm{i}}\|_\infty \leq 1\,,\ \xi^b \in \{-1, 1\}^{n_b} \right\}, \tag{6.2b}$$

where $\xi^c_{L,\mathrm{i}}$ is the lower bound and $\xi^c_{U,\mathrm{i}}$ the upper bound of the i^{th} continuous generator when its infinity norm constraint is relaxed. If the interval resulting from (6.2) satisfies $[\xi^c_{L,\mathrm{i}}, \xi^c_{U,\mathrm{i}}] \subseteq [-1, 1]$, then the linear inequality constraints $-1 \leq \xi^c_{\mathrm{i}} \leq 1$ are redundant [20]. This redundancy occurs because the value of the continuous factor is already constrained to a tighter interval through the combination of the other equality, infinity norm, and integrality constraints of the hybrid zonotope. Once an infinity norm constraint has been identified as redundant, the variable is considered free and may be substituted out of the set representation using a single equality constraint. Doing so, the information of the continuous factor is maintained while reducing the number of continuous factors and equality constraints by one. This result follows closely from reduction methods of constrained zonotopes [18], [20]

which are a special case of redundancy removal techniques used in presolve methods of linear programs [89].

Proposition 6.1.1. *For any* $\mathcal{Z}_h = \langle G^c, G^b, c, A^c, A^b, b \rangle \subset \mathbb{R}^n$ *with implicit bounds on the* i^{th} *continuous generator given by* (6.2) *satisfying* $[\xi^c_{L,\mathrm{i}}, \xi^c_{U,\mathrm{i}}] \subseteq [-1, 1]$, $\mathcal{Z}_h$ *may be exactly represented with* $n_g - 1$ *continuous generators and* $n_c - 1$ *constraints by the hybrid zonotope*

$$\mathcal{Z}^r_h = \left\langle G^c - \Lambda_G A^c, G^b - \Lambda_G A^b, c + \Lambda_G b, A^c - \Lambda_A A^c, A^b - \Lambda_A A^b, b - \Lambda_A b \right\rangle , \tag{6.3}$$

where $\Lambda_G = G^c E_{\mathrm{i},k} (A^c_{k,\mathrm{i}})^{-1} \in \mathbb{R}^{n \times n_c}$, $\Lambda_A = A^c E_{\mathrm{i},k} (A^c_{k,\mathrm{i}})^{-1} \in \mathbb{R}^{n_c \times n_c}$, $E_{\mathrm{i},k} \in \mathbb{R}^{n_g \times n_c}$ *is a matrix with zero entries except for a one in the* (i, k) *position, and* $k \in \{1, \dots, n_c\}$ *such that* $A^c_{k,\mathrm{i}} \neq 0$.

Proof. Following the procedures of [20, Sec. 4], for any $z \in \mathcal{Z}_h$ there exists some $\xi^c \in \mathcal{B}^{n_g}_\infty$ and $\xi^b \in \{-1, 1\}^{n_b}$ such that $z = G^c \xi^c + G^b \xi^b + c$ and $A^c \xi^c + A^b \xi^b = b$. Choose some $k \in \{1, \dots, n_g\}$ such that $A^c_{k,\mathrm{i}} \neq 0$ and solve the k^{th} equality constraint such that $\xi^c_{\mathrm{i}} = (b_k - \sum_{\mathrm{j} \neq \mathrm{i}} A^c_{k,\mathrm{j}} \xi^c_{\mathrm{j}} - A^b_{k,\cdot} \xi^b)(A^c_{k,\mathrm{i}})^{-1}$. Substituting this expression for ξ^c_{i} in the remaining equations results in

$$z = (G^c - \Lambda_G A^c)\xi^c + (G^b - \Lambda_G A^b)\xi^b + (c + \Lambda_G b) , \tag{6.4a}$$

$$(A^c - \Lambda_A A^c)\xi^c + (A^b - \Lambda_A A^b)\xi^b = b - \Lambda_A b , \tag{6.4b}$$

where $\Lambda_G = G^c E_{\mathrm{i},k} (A^c_{k,\mathrm{i}})^{-1} \in \mathbb{R}^{n \times n_c}$, $\Lambda_A = A^c E_{\mathrm{i},k} (A^c_{k,\mathrm{i}})^{-1} \in \mathbb{R}^{n_c \times n_c}$, and $E_{\mathrm{i},k} \in \mathbb{R}^{n_g \times n_c}$ is a matrix with zero entries except for a one in the (i, k) position. Making this substitution results in the i^{th} column of the continuous generator matrix and k^{th} row of equality constraints being equal to zero. While the information of the i^{th} generator is still imposed in the hybrid zonotope $\mathcal{Z}^r_h$, the ability to enforce its infinity norm constraint is lost. However, given that the implicit bounds on the continuous factor satisfies $\xi^c_{\mathrm{i}} \in [\xi^c_{L,\mathrm{i}}, \xi^c_{U,\mathrm{i}}] \subseteq [-1, 1]$ when the infinity norm constraint is relaxed, the constraint is redundant. Removing the k^{th} zero row of the equality constraints and i^{th} zero column of the continuous generator and constraint matrices results in a hybrid zonotope $\mathcal{Z}^r_h = \mathcal{Z}_h$ with $n_g - 1$ continuous generators and $n_c - 1$ equality constraints. □

Remark 6.1.1. *Proposition 6.1.1 provides a method of removing redundancy while reducing the number of continuous factors and equality constraints by one without altering the set of points represented by the hybrid zonotope. Performing this reduction requires that* $n_c \neq 0$ *and that there exists some* $A^c_{k,\mathrm{i}} \neq 0$*. This will always be the case. If* $A^c_{\cdot,\mathrm{i}} = 0$ *then the* i^{th} *factor is not present in the constraints and will thus have implicit bounds of* $[\xi^c_{L,\mathrm{i}}, \xi^c_{U,\mathrm{i}}] = [-\infty, \infty]$*. For this case, solving the MILPs (6.2) to determine the implicit bounds is unnecessary.*

6.1.3 Redundant Binary Generators

Given a hybrid zonotope with $n_b > \log_2(|\mathcal{T}|)$, where $|\mathcal{T}|$ is the number of feasible leaves of the hybrid zonotope's binary tree (see Sec. 3.3), it is possible that the set may be represented with a reduced number of binary factors. One case where the number of binary factors may be reduced is when their values in the integer feasible set $\mathcal{T}$ are not linearly independent. In this case, some of the binary factors may be equivalently represented as a linear combination of the other factors. Another possibility is when all feasible values of a binary factor are the same. In this case, the binary factor can be removed after shifting the hybrid zonotope's center and the right hand side of the linear equality constraints by a constant.

Once $\mathcal{T}$ is known, linearly dependent binary factors may be detected and removed as follows. First, let $T \in \mathbb{R}^{n_b \times |\mathcal{T}|}$ be a matrix with each column an element of $\mathcal{T}$, thus $T(\mathrm{i},\mathrm{j}) = \pm 1 \; \forall \, \mathrm{i},\mathrm{j}$. Letting $n_\phi = \mathrm{rank}(T)$, if $n_\phi < n_b$ then there exists a linear mapping

$$M_1 T(\Phi, \cdot) = T \,, \tag{6.5}$$

where $\Phi \in \mathbb{N}_+^{n_\phi}$ are the indices of the linearly independent rows of T. Thus the hybrid zonotope $\mathcal{Z}_h = \langle G^c, G^b, c, A^c, A^b, b \rangle$ is equivalent to $\mathcal{Z}_h^r = \langle G^c, G^b M_1, c, A^c, A^b M_1, b \rangle$ where $\mathcal{Z}_h^r$ has $n_b^r = n_\phi < n_b$ binary factors. The integer feasible set of $\mathcal{Z}_h^r$ is then given by

$$\mathcal{T}^r = \bigcup_{\mathrm{i}=1}^{|\mathcal{T}|} T(\Phi, \mathrm{i}) \,. \tag{6.6}$$

If all feasible values of a binary factor are the same, it can be removed as follows. Let $T(\Phi)$ be sorted such that the constant linearly independent row occurs first, i.e. $T(\Phi(1), \cdot) = 1$ or -1, and let

$$M_2 = M_1 \begin{bmatrix} \mathbf{0}_{1 \times n_\phi - 1} \\ I_{n_\phi - 1} \end{bmatrix} , \; m_2 = M_1 \begin{bmatrix} T(\Phi(1), 1) \\ \mathbf{0}_{n_\phi - 1 \times 1} \end{bmatrix} . \tag{6.7}$$

Then $\mathcal{Z}_h = \langle G^c, G^b, c, A^c, A^b, b \rangle$ is equivalent to $\mathcal{Z}_h^r = \langle G^c, G^b M_2, c + G^b m_2, A^c, A^b M_2, b - A^b m_2 \rangle$ where $\mathcal{Z}_h^r$ has $n_b^r = n_\phi - 1 < n_b$ binary factors. The integer feasible set of $\mathcal{Z}_h^r$ is then given by

$$\mathcal{T}^r = \bigcup_{\mathrm{i}=1}^{|\mathcal{T}|} T(\Phi_2, \mathrm{i}) \, , \tag{6.8}$$

where $\Phi_2 = \Phi(\mathrm{j})$ for $\mathrm{j} = 2, \ldots, n_\phi$.

The linearly independent columns of the matrix T may be found through QR decomposition, and the matrix M_1 may be found using the Moore–Penrose inverse. The total time complexity of these operations scales as $\mathcal{O}(n_b |\mathcal{T}|^2)$. Although the number of binary factors, and equivalently the number of layers in the binary tree, are reduced, the nonempty leaves of the binary tree are not changed [67]. Thus detecting and removing redundancy in the binary factors through the described approach reduces the complexity of the hybrid zonotope set representation without altering the set.

Remark 6.1.2. *The proposed method of removing redundant binary variables is an application of aggregating implied free variables within MILPs. The method described here is rigorous and exact; however, approximations may be used as done during the presolve stage of commercial MILP solvers [63].*

6.2 Over Approximations

Methods for generating over-approximations of hybrid zonotopes while reducing the number of continuous generators, binary generators, and constraints are now presented. Using these methods allows for set operations to be performed continually while providing conservative results. In Section 6.2.1 I show how the continuous generators may be rescaled to reduce potential error introduced in the following over-approximation methods. In Section

6.2.2 I show how one continuous generator and equality constraint may be removed. In Section 6.2.3 I show how order reduction techniques developed for zonotopes may be applied to reduce the number of continuous generators in hybrid zonotopes. Finally in Section 6.2.4 I show how binary generators may be relaxed to continuous generators, which may then be removed using the previously presented methods.

6.2.1 Rescaling Continuous Generators

This section shows how the bounds on the continuous factors of hybrid zonotopes may be tightened to reduce potential error introduced in the following over-approximation techniques. This tightening leverages the possibility that the combination of equality, infinity norm, and integrality constraints of the hybrid zonotope implicitly constrain the continuous factors to lie within the unit hypercube. In Section 6.1.2, the implicit bounds calculated using (6.2) satisfied $[\xi^c_{L,\mathrm{i}}, \xi^c_{U,\mathrm{i}}] \subseteq [-1, 1]$ and were therefore redundant. However, it is possible that the implicit interval does not satisfy $[\xi^c_{L,\mathrm{i}}, \xi^c_{U,\mathrm{i}}] \subseteq [-1, 1]$, but that one bound could be tightened without altering the set, e.g. when $\xi^c_{L,\mathrm{i}} \leq -1$ and $\xi^c_{U,\mathrm{i}} \leq 1$, the infinity norm constraint on the i^{th} continuous factor could be replaced with $\xi^c_{\mathrm{i}} \in [-1, \xi^c_{U,\mathrm{i}}]$. Following the procedure for rescaling the factors of constrained zonotopes [18, Sec. 4.1], the continuous factors of the hybrid zonotope may be rescaled to embed the tightened constraints of $\xi^c \in [\max(\xi^c_{L,\mathrm{i}}, -1), \min(\xi^c_{U,\mathrm{i}}, 1)] \subseteq [-1, 1]$ for all $\mathrm{i} = 1, \ldots, n_g$ as follows.

Proposition 6.2.1. *For any $\mathcal{Z}_h = \langle G^c, G^b, c, A^c, A^b, b \rangle \subset \mathbb{R}^n$ with ξ^c_L and ξ^c_U given by (6.2), $\mathcal{Z}_h$ may be equivalently represented by*

$$\mathcal{Z}_h = \langle G^c \, diag(\xi^c_r), G^b, c + G^c \xi^c_m, A^c \, diag(\xi^c_r), A^b, b - A^c \xi^c_m \rangle \,, \tag{6.9}$$

where

$$\xi^c_{r,\mathrm{i}} = \frac{\min(\xi^c_{U,\mathrm{i}}, 1) - \max(\xi^c_{L,\mathrm{i}}, -1)}{2} \,, \; \xi^c_{m,\mathrm{i}} = \frac{\min(\xi^c_{U,\mathrm{i}}, 1) + \max(\xi^c_{L,\mathrm{i}}, -1)}{2} \,, \tag{6.10}$$

for all $\mathrm{i} = 1, \ldots, n_g$.

Proof. Following the procedure of [18, Sec. 4.1], let

$$\mathcal{X} = \langle G^c \text{diag}(\xi_r^c), G^b, c + G^c \xi_m^c, A^c \text{diag}(\xi_r^c), A^b, b - A^c \xi_m^c \rangle \subseteq \mathbb{R}^n \,, \tag{6.11}$$

denote the hybrid zonotope given by the right hand side of (6.9). For any $x \in \mathcal{X}$ there exists some $\xi_x^c \in \mathcal{B}_\infty^{n_g}$ and $\xi_x^b \in \{-1, 1\}^{n_b}$ such that $A^c \text{diag}(\xi_r^c)\xi_x^c + A^b \xi_x^b = b - A^c \xi_m^c$, and $x = G^c \text{diag}(\xi_r^c)\xi^c + G^b \xi^b + c + G^c \xi_m^c$. For any $z \in \mathcal{Z}_h$ there exists some $\xi_z^c \in \mathcal{B}_\infty^{n_g}$ and $\xi_z^b \in \{-1, 1\}^{n_b}$ such that $A^c \xi_z^c + A^b \xi_z^b = b$, $z = G^c \xi_z^c + G^b \xi_z^b + c$, and $\xi_{z,\mathrm{i}}^c \in [\max(\xi_{L,\mathrm{i}}^c, -1), \min(\xi_{U,\mathrm{i}}^c, 1)]$ for all $\mathrm{i} = 1, \ldots, n_g$. Let $\gamma = \text{diag}(\xi_r^c)\xi_x^c + \xi_m^c$. Then $\gamma_\mathrm{i} \in [\max(\xi_{L,\mathrm{i}}^c, -1), \min(\xi_{U,\mathrm{i}}^c, 1)]$ for all $\mathrm{i} = 1, \ldots, n_g$. Furthermore, $x = G^c \gamma + G^b \xi^b + c$ and $A^c \gamma + A^b \xi_x^b = b$. Thus $x \in \mathcal{Z}_h$ and $\mathcal{X} \subseteq \mathcal{Z}_h$. Conversely, given that $\xi_{z,\mathrm{i}}^c \in [\max(\xi_{L,\mathrm{i}}^c, -1), \min(\xi_{U,\mathrm{i}}^c, 1)]$, letting $\xi_{z,\mathrm{i}}^c = \text{diag}(\xi_r^c)\xi_x^c + \xi_m^c$ implies that $\xi_x^c \in \mathcal{B}_\infty^{n_g}$. Thus $z = G^c(\text{diag}(\xi_r^c)\xi_x^c + \xi_m^c) + G^b \xi_z^b + c$ and $A^c(\text{diag}(\xi_r^c)\xi_x^c + \xi_m^c) + A^b \xi^b = b$. Therefore $z \in \mathcal{X}$, $\mathcal{Z}_h \subseteq \mathcal{X}$ and $\mathcal{X} = \mathcal{Z}_h$. □

The procedure for rescaling the continuous generators of a hybrid zonotope is desribed in Algorithm 2 and requires solving $2n_g$ MILPs to determine the tightest bounds on the continuous factors induced by the other constraints.

Algorithm 2 Rescale the continuous generators to tighten the bounds on the infinity norm constraints.

Input: $\mathcal{Z}_h = \langle G^c, G^b, c, A^c, A^b, b \rangle \subset \mathbb{R}^n$
Output: $\tilde{\mathcal{Z}}_h = \mathcal{Z}_h$ such that $[\max(\xi_{L,\mathrm{i}}^c, -1), \min(\xi_{U,\mathrm{i}}^c, 1)] = [-1, 1] \; \forall \, \mathrm{i} \in \{1, \ldots, n_g\}$

1: **procedure** RESCALE($\mathcal{Z}_h$)
2: **for** $\mathrm{i} = 1, \ldots, \tilde{n}_g$ **do**
3: $\xi_{L,\mathrm{i}}^c \leftarrow \min \left\{ \xi_\mathrm{i}^c \;\middle|\; A^c \xi^c + A^b \xi^b = b \,,\; \|\xi_{\mathrm{j} \neq \mathrm{i}}^c\|_\infty \leq 1 \,,\; \xi^b \in \{-1, 1\}^{n_b} \right\}$
4: $\xi_{U,\mathrm{i}}^c \leftarrow \max \left\{ \xi_\mathrm{i}^c \;\middle|\; A^c \xi^c + A^b \xi^b = b \,,\; \|\xi_{\mathrm{j} \neq \mathrm{i}}^c\|_\infty \leq 1 \,,\; \xi^b \in \{-1, 1\}^{n_b} \right\}$
5: **end for**
6: $\tilde{\mathcal{Z}}_h \leftarrow$ rescaled by Proposition 6.2.1 for ξ_L^c and ξ_U^c
7: **end procedure**

Remark 6.2.1. *Tightening the bounds on continuous variables is a common procedure in MILP presolve methods [63]. This approach is advantageous as it also tightens the linear relaxation of the problem when integrality constraints are relaxed, i.e. in branch and bound algorithms [53]. The method shown here differs from these approaches as it directly embeds*

the tightened bounds within the generator and constraint matrices while maintaining the infinity norm constraints, $\xi^c \in \mathcal{B}_\infty^{n_g}$, of the hybrid zonotope set definition. While the bounds on the continuous factors are found exactly in (6.2), over-approximation methods exist which rely on linear relaxations as described in [63].

6.2.2 Constraint Reduction

This section shows how over-approximations of hybrid zonotopes may be generated while reducing the number of continuous generators and equality constraints by one. This procedure follows closely from that of removing redundant continuous generators as described in Section 6.1.2; however, it removes continuous generators that do not have redundant infinity norm constraints. Thus when the i^{th} continuous generator is substituted out of the set representation, the continuous generators information in the generator and constraint matrices is maintained, but the ability to enforce the constraints of $\xi_\mathrm{i}^c \in [-1, 1]$ is lost. Similar to the procedure in [18, Sec. 4.2] for constraint reduction of constrained zonotopes, the constraints of the hybrid zonotope may also be conservatively removed.

Proposition 6.2.2. *For any $\mathcal{Z}_h = \langle G^c, G^b, c, A^c, A^b, b\rangle \subset \mathbb{R}^n$, the set $\tilde{\mathcal{Z}}_h$ with $\tilde{n}_g = n_g - 1$ and $\tilde{n}_c = n_c - 1$ satisfies $\mathcal{Z}_h \subseteq \tilde{\mathcal{Z}}_h$ for*

$$\tilde{\mathcal{Z}}_h = \left\langle G^c - \Lambda_G A^c, G^b - \Lambda_G A^b, c + \Lambda_G b, A^c - \Lambda_A A^c, A^b - \Lambda_A A^b, b - \Lambda_A b \right\rangle , \tag{6.12}$$

where $\Lambda_G = G^c E_{\mathrm{i},k}(A^c_{k,\mathrm{i}})^{-1} \in \mathbb{R}^{n\times n_c}$, $\Lambda_A = A^c E_{\mathrm{i},k}(A^c_{k,\mathrm{i}})^{-1} \in \mathbb{R}^{n_c\times n_c}$, $E_{\mathrm{i},k} \in \mathbb{R}^{n_g\times n_c}$ is a matrix with zero entries except for a one in the (i, k) position, and $k \in \{1, \dots, n_c\}$ such that $A^c_{k,\mathrm{i}} \neq 0$.

Proof. Following the procedures of [18, Sec. 4.2], for any $z \in \mathcal{Z}_h$ there exists some $\xi^c \in \mathcal{B}_\infty^{n_g}$ and $\xi^b \in \{-1, 1\}^{n_b}$ such that $z = G^c\xi^c + G^b\xi^b + c$ and $A^c\xi^c + A^b\xi^b = b$. Thus it holds that $z = G^c\xi^c + G^b\xi^b + c + \Lambda_G(b - A^c\xi^c + A^b\xi^b)$ and $A^c\xi^c + A^b\xi^b + \Lambda_A(b - A^c\xi^c + A^b\xi^b) = b$ because $b - A^c\xi^c + A^b\xi^b = \mathbf{0}$. Therefore $z \in \tilde{\mathcal{Z}}_h$ and $\mathcal{Z}_h \subseteq \tilde{\mathcal{Z}}_h$. This result is independent of the choice of Λ_G and Λ_A. The specific choice of $\Lambda_G = G^c E_{\mathrm{i},k}(A^c_{k,\mathrm{i}})^{-1} \in \mathbb{R}^{n\times n_c}$ and $\Lambda_A = A^c E_{\mathrm{i},k}(A^c_{k,\mathrm{i}})^{-1} \in \mathbb{R}^{n_c\times n_c}$ results in the i^{th} continuous generator and k^{th} row of equality

constraints being equal to zero by substituting the k^{th} equality constraint solved for the i^{th} continuous generator into the other equations. Removing the zero row and column results in $\mathcal{Z}_h \subseteq \tilde{\mathcal{Z}}_h$ with $\tilde{n}_g = n_g - 1$ continuous generators and $\tilde{n}_c = n_c - 1$ equality constraints. $\square$

Proposition 6.2.2 provides a method of reducing the number of equality constraints and continuous generators by relaxing the infinity norm constraint on one of the continuous factors. Thus the set representation is less strict and introduces additional points that satisfy the HCG-rep. The given choice of Λ_G and Λ_A requires that $\exists\, k \in \{1, \dots, n_c\}$ such that $A^c_{k,\mathrm{i}} \neq 0$. Note that since the purpose is to reduce the number of constraints, this condition is always true. The goal is then to relax the infinity norm constraint that will introduce the fewest additional points to provide the tightest over-approximation. The level of conservatism of the over-approximation may be evaluated using the error metrics discussed in Section 6.3 for each of the continuous generators. Once the continuous generator has been chosen, any row $k \in \{1, \dots, n_c\}$ such that $A^c_{k,\mathrm{i}} \neq 0$ may be used in the substitution. However, numerical experiments have shown that choosing the row with the largest element has the best numerical stability. The specific strategy is summarized in Algorithm 3. Note that the potential error introduced can be reduced by first rescaling the continuous generators using the procedure described by Algorithm 2, which only needs to be applied once. The procedure in Algorithm 3 may then be applied to a hybrid zonotope until $n_c = 0$, resulting in the representation of the union of a collection of zonotopes that over-approximate the original set.

Example 6.2.1. *This example considers a randomly generated hybrid zonotope $\mathcal{Z}_h \subset \mathbb{R}^2$ with $n_g = 8$ continuous generators, $n_b = 2$ binary generators, and $n_c = 3$ equality constraints. Algorithm 3 is applied iteratively using a volume ratio error metric as defined in Section 6.3. The resulting over-approximating hybrid zonotopes $\tilde{\mathcal{Z}}^{\mathrm{i}}_h$ with* i *constraints removed are depicted in Figure 6.1. The final hybrid zonotope $\tilde{\mathcal{Z}}^3_h$ has $\tilde{n}_c = 0$ constraints and is equivalent to* 4 *shifted zonotopes each having $\tilde{n}_g = 5$ continuous generators.*

Algorithm 3 Reduce the number of continuous generators and constraints.

Input: $\mathcal{Z}_h \subset \mathbb{R}^n$, $n_c^r \in \{0, \ldots, n_c - 1\}$
Output: $\tilde{\mathcal{Z}}_h \supseteq \mathcal{Z}_h$ with $\tilde{n}_c = n_c^r$ and $\tilde{n}_g = n_g - n_c + n_c^r$

procedure REDUCECONSTRAINTS($\mathcal{Z}_h$,n_c^r)
  $\tilde{\mathcal{Z}}_h \leftarrow \mathcal{Z}_h$
  while $\tilde{n}_c > n_c^r$ **do**
    for $\mathrm{i} = 1, \ldots, \tilde{n}_g$ s.t. $\exists\, k \in \{1, \ldots, \tilde{n}_c\}$ and $\tilde{A}^c_{k,\mathrm{i}} \neq 0$ **do**
      $\hat{\mathcal{Z}}_h \leftarrow$ Proposition 6.2.2 for $\tilde{\mathcal{Z}}_h$ and (i, k)
      $E_\mathrm{i} \leftarrow$ ERRORMETRIC($\hat{\mathcal{Z}}_h, \tilde{\mathcal{Z}}_h$)
    end for
    $\mathrm{i} \leftarrow$ index such that $E_\mathrm{i} = \min(E)$
    $\tilde{\mathcal{Z}}_h \leftarrow$ Proposition 6.2.2 for $\tilde{\mathcal{Z}}_h$ and (i, k) such that $A^c_{k,\mathrm{i}} = \max(A^c_{\cdot,\mathrm{i}})$
  end while
end procedure

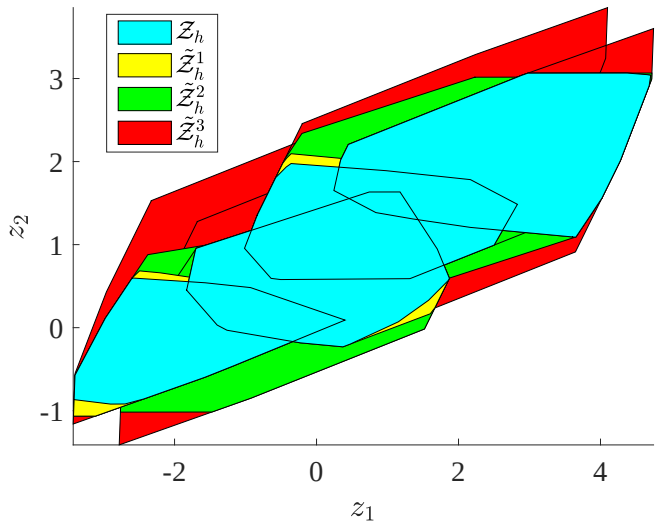

Figure 6.1. Example of iteratively removing one continuous generator and constraint from the hybrid zonotope $\mathcal{Z}_h$ using Algorithm 3 to generate the over-approximations $\tilde{\mathcal{Z}}_h^\mathrm{i}$, where i is the number of constraints removed.

6.2.3 Continuous Generator Reduction

In Section 6.2.2 it is shown how one continuous generator and equality constraint pair may be removed to generate an over-approximation. However, this requires that the continuous generator appears in the constraints. This section shows how the number of continuous generators may be reduced by applying order reduction techniques developed for zonotopes.

To do so, it is first necessary to extend the notion of the lifted zonotope form of constrained zonotopes [18] to the hybrid zonotope.

Proposition 6.2.3. *Any hybrid zonotope* $\mathcal{Z}_h = \langle G^c, G^b, c, A^c, A^b, b \rangle \subset \mathbb{R}^n$ *may be lifted to an* $n_+ = n + n_c$ *dimensional hybrid zonotope given by*

$$\mathcal{Z}_h^+ = \left\langle \begin{bmatrix} G^c \\ A^c \end{bmatrix}, \begin{bmatrix} G^b \\ A^b \end{bmatrix}, \begin{bmatrix} c \\ -b \end{bmatrix}, \emptyset, \emptyset, \emptyset \right\rangle , \tag{6.13}$$

such that $z \in \mathcal{Z}_h$ *if and only if* $(z \ \mathbf{0}) \in \mathcal{Z}_h^+$.

Proof. For any $z \in \mathcal{Z}_h$ there exists some $\xi^c \in \mathcal{B}_\infty^{n_g}$ and $\xi^b \in \{-1, 1\}^{n_b}$ such that $z = G^c\xi^c + G^b\xi^b + c$ and $A^c\xi^c + A^b\xi^b - b = \mathbf{0}$. Thus it follows that

$$\begin{bmatrix} z \\ \mathbf{0} \end{bmatrix} = \begin{bmatrix} G^c \\ A^c \end{bmatrix} \xi^c + \begin{bmatrix} G^b \\ A^b \end{bmatrix} \xi^b + \begin{bmatrix} c \\ -b \end{bmatrix} . \tag{6.14}$$

Therefore $(z \ \mathbf{0}) \in \mathcal{Z}_h^+$. Conversely, for any $z^+ \in \mathcal{Z}_h^+$ there exists some $\xi^c \in \mathcal{B}_\infty^{n_g}$ and $\xi^b \in \{-1, 1\}^{n_b}$ such that

$$z^+ = \begin{bmatrix} G^c \\ A^c \end{bmatrix} \xi^c + \begin{bmatrix} G^b \\ A^b \end{bmatrix} \xi^b + \begin{bmatrix} c \\ -b \end{bmatrix} . \tag{6.15}$$

Choosing any ξ^c and ξ^b satisfying $A^c\xi^c + A^b\xi^b = b$ results in $[\mathbf{I}_{n_g} \ \mathbf{0}_{n_c}]z^+ \in \mathcal{Z}_h$. If no such point exists, then $\mathcal{Z}_h = \emptyset$. □

The process of converting between the lifted and original representation of a hybrid zonotope is depicted in Figure 6.2. Lifting the hybrid zonotope to an $n_+ = n + n_c$ hybrid zonotope without constraints using Proposition 6.2.3 is advantageous as it allows for the decoupling of the continuous and binary factors. Given any hybrid zonotope $\mathcal{Z}_h$, define $\mathcal{Z}_h^+$ by Proposition 6.2.3. Then it follows that

$$\mathcal{Z}_h^+ = \mathcal{Z}_h^{c,+} \oplus \mathcal{Z}_h^{b,+} , \tag{6.16}$$

where

$$\mathcal{Z}_h^{c,+} = \left\langle \begin{bmatrix} G^c \\ A^c \end{bmatrix}, \emptyset, \begin{bmatrix} c \\ -b \end{bmatrix}, \emptyset, \emptyset, \emptyset \right\rangle \tag{6.17}$$

is a lifted constrained zonotope with order $o^+ = \frac{n_g}{n+n_c}$ and

$$\mathcal{Z}_h^{b,+} = \left\langle \emptyset, \begin{bmatrix} G^b \\ A^b \end{bmatrix}, \begin{bmatrix} \mathbf{0} \\ \mathbf{0} \end{bmatrix}, \emptyset, \emptyset, \emptyset \right\rangle , \tag{6.18}$$

is a hybrid zonotope containing only discrete points. Given that $\mathcal{Z}_h^{c,+}$ is a lifted constrained zonotope, it can be reduced using any order reduction method developed for zonotopes such that $\mathcal{Z}_h^{c,+} \subseteq \tilde{\mathcal{Z}}_h^{c,+}$ [18]. Applying (6.16) with the reduced, lifted constrained zonotope then results in

$$\mathcal{Z}_h^{+} \subseteq \tilde{\mathcal{Z}}_h^{+} = \tilde{\mathcal{Z}}_h^{c,+} \oplus \mathcal{Z}_h^{b,+} , \tag{6.19}$$

where

$$\tilde{\mathcal{Z}}_h^{+} = \left\langle \begin{bmatrix} \tilde{G}^c \\ \tilde{A}^c \end{bmatrix}, \begin{bmatrix} G^b \\ A^b \end{bmatrix}, \begin{bmatrix} c \\ -b \end{bmatrix}, \emptyset, \emptyset, \emptyset \right\rangle . \tag{6.20}$$

It then holds from Proposition 6.2.3 that the desired result of $\mathcal{Z}_h \subseteq \tilde{\mathcal{Z}}_h$ is achieved for

$$\tilde{\tilde{\mathcal{Z}}}_h = \langle \tilde{G}^c, G^b, c, \tilde{A}^c, A^b, b \rangle . \tag{6.21}$$

The lifted constrained zonotope (6.17) may reduced until $o^+ = 1$, thus the number of continuous generators of the reduced hybrid zonotope is limited by $\tilde{n}_g \geq n + n_c$. To further reduce the complexity, reduction of the number of equality constraints as described in Section 6.2.2 is required.

Many order reduction methods exist for zonotopes and may all be applied to hybrid zonotopes using this lifted strategy. The methods with the most wide spread use are described and compared in [19] and [90]. From numerical experiments, the zonotope order reduction method developed for lifted constrained zonotopes in [18] and [90] has resulted in the tightest over-approximations. The proposed method of lifting and reducing is advantageous as

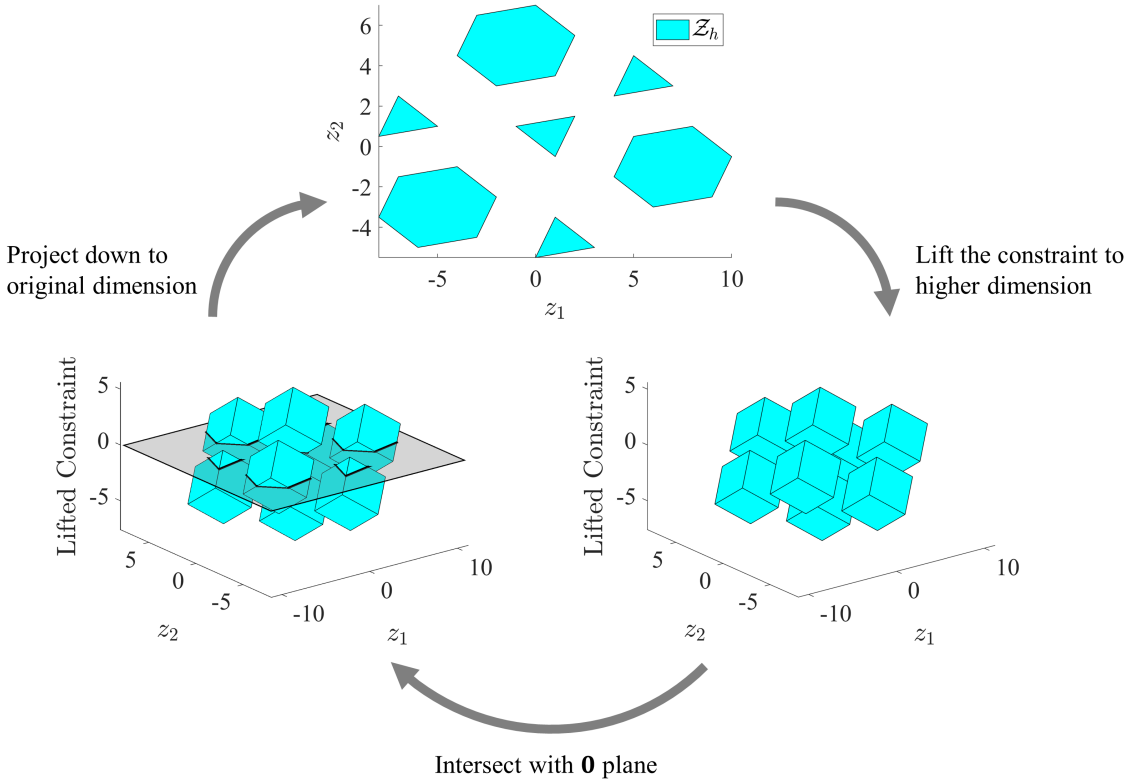

Figure 6.2. Visual depiction of the process of converting between the original and lifted representation of the example two-dimensional hybrid zonotope (3.6) with a single equality constraint. Lifting the single constraint using Proposition 6.2.3 results in a three-dimensional hybrid zonotope. This lifted representation may be converted back to the original HCG-rep by intersecting with the zero plane in the lifted constraint dimension and projecting back down to the original dimensions of the hybrid zonotope.

zonotope order reduction techniques are performed algebraically and do not require solving any optimization problems.

Example 6.2.2. *This example considers a randomly generated hybrid zonotope* $\mathcal{Z}_h \subset \mathbb{R}^2$ *with* $n_g = 8$ *continuous generators,* $n_b = 2$ *binary generators, and* $n_c = 3$ *equality constraints. The number of continuous generators are reduced using the lifted hybrid zonotope approach to find a hybrid zonotope* $\tilde{\mathcal{Z}}_h^{\mathrm{i}}$ *given by* (6.21) *with* i *generators removed. The zonotope order reduction method described in [18] and [90] is used to reduce the lifted hybrid zonotope. The resulting over-approximating hybrid zonotopes are depicted in Figure 6.3. The final hybrid*

zonotope $\tilde{\mathcal{Z}}_h^3$ *has* $\tilde{n}_g = 5$ *continuous generators and* $\tilde{n}_c = 3$ *constraints and can no longer be reduced using this approach.*

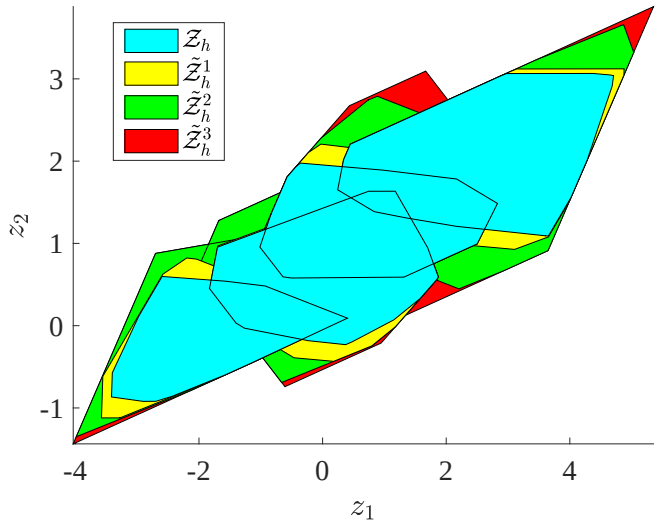

Figure 6.3. Example of iteratively removing one continuous generator from the hybrid zonotope $\mathcal{Z}_h$ using Proposition 6.2.3 and zonotope order reduction technique [90] to generate the over-approximations $\tilde{\mathcal{Z}}_h^{\mathrm{i}}$, where i is the number of continuous generators removed.

6.2.4 Binary Generator Reduction

Iterative applications of set operations on hybrid zonotopes may increase the number of binary generators present in the set. As this number increases, the number of possible nonempty convex subsets of the decomposed set given by Theorem 3.1.1 increases exponentially, as shown by the set's binary tree as discussed in Section 3.3. This number of nonempty convex subsets may also increase the computational complexity of the MILP used to analyze the resulting set through Propositions 3.2.8 and 3.2.9, Definition 3.2.1, and Theorem 3.2.1. To provide a more computationally efficient set representation, it is therefore imperative to reduce the number of binary variables within the HCG-rep.

In Lemma 3.1.1 it was shown that the constrained zonotope $\mathcal{Z}_c = \langle [G^c \, G^b], c, [A^c \, A^b], b \rangle \subset \mathbb{R}^n$ satisfies $\mathcal{Z}_h \subseteq \mathcal{Z}_c$. In the integer programming literature, this constrained zonotope is referred to as the linear relaxation of the hybrid zonotope's MILP formulation given by

(3.44). This linear relaxation is solved at the root node of the binary tree to provide an upper bound on the possible optimal values of a MILP, and provides the first bound in branch and bound algorithms [53]. This section shows how the number of binary generators may be reduced by relaxing the integrality constraints of $\xi_{\mathrm{i}}^b \in \{-1, 1\}$ to $\xi_{\mathrm{i}}^b \in [-1, 1]$ for only some $\mathrm{i} \in \{1, \ldots, n_b\}$; that is, only select binary generators are relaxed to be continuous.

Proposition 6.2.4. *For any hybrid zonotope* $\mathcal{Z}_h = \langle G^c, G^b, c, A^c, A^b, b \rangle \subset \mathbb{R}^n$ *with* n_g *continuous generators and* n_b *binary generators, define the hybrid zonotope* $\tilde{\mathcal{Z}}_h = \langle \tilde{G}^c, \tilde{G}^b, c, \tilde{A}^c, \tilde{A}^b, b \rangle$ *with* $n_g + 1$ *continuous generators and* $n_b - 1$ *binary generators where*

$$\tilde{G}^c = \begin{bmatrix} G^c & g^{(b,\mathrm{i})} \end{bmatrix}, \; \tilde{A}^c = \begin{bmatrix} A^c & a^{(b,\mathrm{i})} \end{bmatrix}, \tag{6.22}$$

$$\tilde{G}^b = \begin{bmatrix} g^{(b,1)} & \cdots & g^{(b,\mathrm{i}-1)} & g^{(b,\mathrm{i}+1)} & \cdots & g^{(b,n_b)} \end{bmatrix}, \tag{6.23}$$

$$\tilde{A}^b = \begin{bmatrix} a^{(b,1)} & \cdots & a^{(b,\mathrm{i}-1)} & a^{(b,\mathrm{i}+1)} & \cdots & a^{(b,n_b)} \end{bmatrix}. \tag{6.24}$$

Then it holds that $\mathcal{Z}_h \subseteq \tilde{\mathcal{Z}}_h$.

Proof. The proof follows a generalization of Lemma 3.1.1. For any $z \in \mathcal{Z}_h$ there exists some $\xi^c \in \mathcal{B}_\infty^{n_g}$ and $\xi^b \in \{-1, 1\}^{n_b}$ such that $A^c\xi^c + A^b\xi^b = b$ and $z = G^c\xi^c + G^b\xi^b + c$. Let $\gamma = \begin{pmatrix} \xi^c & \xi^{(b,\mathrm{i})} \end{pmatrix}$ and $\alpha = \begin{pmatrix} \xi^{(b,1)} & \cdots & \xi^{(b,\mathrm{i}-1)} & \xi^{(b,\mathrm{i}+1)} & \cdots & \xi^{(b,n_b)} \end{pmatrix}$, thus $\gamma \in \mathcal{B}_\infty^{n_g+1}$ and $\alpha \in \{-1, 1\}^{n_b-1}$. Then $z = [G^c \; g^{(b,\mathrm{i})}]\gamma + [g^{(b,1)} \; \cdots \; g^{(b,\mathrm{i}-1)} \; g^{(b,\mathrm{i}+1)} \; \cdots \; g^{(b,n_b)}]\alpha + c$ and $z \in \tilde{\mathcal{Z}}_h$. Therefore $\mathcal{Z}_h \subseteq \tilde{\mathcal{Z}}_h$. □

Proposition 6.2.4 provides a method of reducing the number of binary generators by relaxing them to be continuous. Given that the constraints of the reduced HCG-rep are less strict, that is $\{-1, 1\} \subset [-1, 1]$, this approach provides an over-approximation. Making this reduction will also reduce the total number of possible nonempty leaves in the set's binary tree, thus reducing the computational burden of decomposing the set into a collection of convex sets for analysis and visualization. While any binary generator may be relaxed by shifting it into the continuous generator matrix, the goal is to choose the binary factors that will result in the tightest over-approximation. To do this, each binary generator is iteratively relaxed and the resulting conservatism is evaluated using one of the error metrics discussed

in Section 6.3. This procedure is described by Algorithm 4. Once the binary generator to be relaxed has been chosen, Proposition 6.2.4 is applied. The new continuous generator may then be removed using the methods described in Sections 6.2.2 and 6.2.3 to continue to reduce the complexity of the hybrid zonotope while maintaining an over-approximation.

Algorithm 4 Reduce the number of binary generators by relaxing them to be continuous.

Input: $\mathcal{Z}_h \subset \mathbb{R}^n$, $n_b^r \in \{0, \ldots, n_b - 1\}$
Output: $\tilde{\mathcal{Z}}_h \supseteq \mathcal{Z}_h$ with $\tilde{n}_b = n_b^r$ and $\tilde{n}_g = n_g + n_b^r$

1: **procedure** REDUCEBINARY($\mathcal{Z}_h$,n_b^r)
2: $\quad\tilde{\mathcal{Z}}_h \leftarrow \mathcal{Z}_h$
3: $\quad$**while** $\tilde{n}_b > n_b^r$ **do**
4: $\quad\quad$**for** i $= 1, \ldots, \tilde{n}_b$ **do**
5: $\quad\quad\quad\hat{\mathcal{Z}}_h \leftarrow$ Proposition 6.2.4 for $\tilde{\mathcal{Z}}_h$ and i
6: $\quad\quad\quad E_\text{i} \leftarrow$ ERRORMETRIC($\hat{\mathcal{Z}}_h, \tilde{\mathcal{Z}}_h$)
7: $\quad\quad$**end for**
8: $\quad\quad$i $\leftarrow$ index such that $E_\text{i} = \min(E)$
9: $\quad\quad\tilde{\mathcal{Z}}_h \leftarrow$ Proposition 6.2.4 for $\tilde{\mathcal{Z}}_h$ and i
10: $\quad$**end while**
11: **end procedure**

Remark 6.2.2. *Rather than reducing the number of binary variables to a desired value of $n_b^r < n_b$, it is possible to reduce the binary variables until a desired limit on the number of nonempty convex subsets of the hybrid zonotope given by Theorem 3.1.1 is achieved. This modification to Algorithm 4 requires iteratively exploring the reduced hybrid zonotope's binary tree after line 9 using Algorithm 1. This approach is advantageous when the goal is to visualize the reachable set of the hybrid zonotope, where this possible exponential growth in the decomposition is the limiting factor.*

Example 6.2.3. *This example considers a randomly generated hybrid zonotope $\mathcal{Z}_h \subset \mathbb{R}^2$ with $n_g = 8$ continuous generators, $n_b = 2$ binary generators, and $n_c = 3$ equality constraints. The number of binary generators is reduced using Algorithm 4 to generate the over-approximating hybrid zonotope $\tilde{\mathcal{Z}}_h^\text{i}$ with* i *binary generators removed. The over- approximations are depicted in Figure 6.4. The final hybrid zonotope $\tilde{\mathcal{Z}}_h^2$ has $\tilde{n}_b = 0$ binary generators and is equivalent to a constrained zonotope with $\tilde{n}_g = 10$ continuous generators and $\tilde{n}_c = 3$ constraints.*

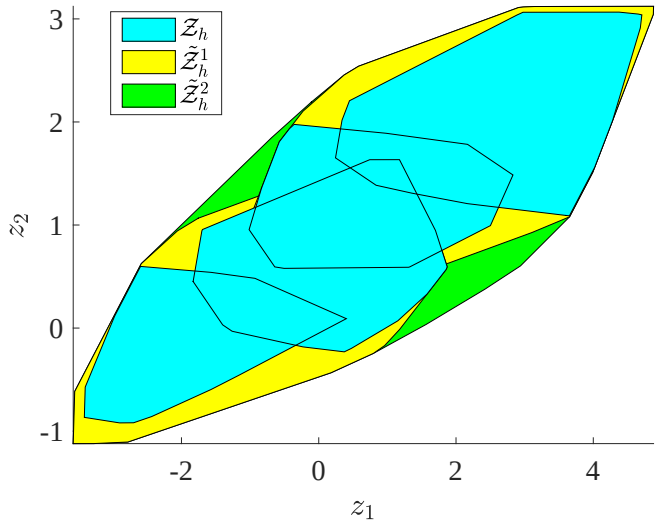

Figure 6.4. Example of iteratively relaxing one binary generator from the hybrid zonotope $\mathcal{Z}_h$ through Algorithm 4 to generate the over-approximations $\tilde{\mathcal{Z}}_h^{\mathrm{i}}$, where i is the number of binary generators removed.

6.2.5 Combined Algorithm

An algorithm combining the redundancy removal and order reduction techniques for reducing the complexity of hybrid zonotopes is now proposed. Specifically, given any hybrid zonotope $\mathcal{Z}_h \subset \mathbb{R}^n$ with n_g continuous generators, n_b binary generators, and n_c constraints, the algorithm reduces the hybrid zonotope, in an over-approximative way, to one with n_g^r continuous generators, n_b^r binary generators, and n_c^r constraints, where $n_\cdot^r$ are user specified values. This approach is given by Algorithm 5.

Algorithm 5 first finds the binary tree of the hybrid zonotope through Algorithm 1. Using the binary tree, redundancy is removed from the binary generators, continuous generators, and equality constraints as described in Section 6.1. The hybrid zonotope is then rescaled as discussed in Section 6.2.1 to reduce potential error introduced in the over-approximations. Following rescaling, the number of continuous generators is reduced using zonotope order

Algorithm 5 Reduce the hybrid zonotope and return over-approximation.

Input: $\mathcal{Z}_h \subset \mathbb{R}^n$, $n_c^r \in \{0, \ldots, n_c\}$, $n_g^r \in \{n + n_c^r, \ldots, n_g\}$, $n_b^r \in \{0, \ldots, n_b\}$
Output: $\tilde{\mathcal{Z}}_h \supseteq \mathcal{Z}_h$ with $\tilde{n}_b = n_b^r$ and $\tilde{n}_g = n_g^r$

1: $\mathcal{T} \leftarrow$ binary tree of $\mathcal{Z}_h$ using Algorithm 1
2: $\tilde{\mathcal{Z}}_h \leftarrow$ remove redundancy from $\mathcal{Z}_h$
3: $\tilde{\mathcal{Z}}_h \leftarrow \textsc{rescale}(\tilde{\mathcal{Z}}_h)$
4: $\tilde{\mathcal{Z}}_h \leftarrow$ lift then reduce continuous generators until $o^+ = (n_g^r + n_c - n_c^r)/(n + \tilde{n}_c)$ or $o^+ = 1$
5: $\tilde{\mathcal{Z}}_h \leftarrow \textsc{reduceBinary}(\tilde{\mathcal{Z}}_h, n_b^r)$
6: $\tilde{\mathcal{Z}}_h \leftarrow \textsc{reduceConstraints}(\tilde{\mathcal{Z}}_h, n_c^r)$
7: **if** $\tilde{n}_g > n_g^r$ **then**
8: $\quad \tilde{\mathcal{Z}}_h \leftarrow$ lift then reduce continuous generators until $o^+ = n_g^r/(n + \tilde{n}_c)$ or $o^+ = 1$
9: **end if**

reduction methods on the lifted hybrid zonotope as described in Section 6.2.3. The target order for the lifted hybrid zonotope is set to

$$o^+ = (n_g^r + n_c - n_c^r)/(n + \tilde{n}_c)\,, \tag{6.25}$$

to reduce the number of continuous generators to $n_g^r + n_c - n_c^r$ and to account for the additional continuous generators that will be removed while reducing the number of equality of constraints. If $n_g^r + n_c - n_c^r < 1$, then the target order is set to $o^+ = 1$. The algorithm then reduces the number of binary variables as discussed in Section 6.2.4 by relaxing some of them to be continuous. The number of constraints is reduced using the method described in Section 6.2.2. If the number of continuous generators is still above the desired number n_g^r, then the algorithm performs another iteration of lifting then reducing the hybrid zonotope. This is necessary because it is possible that the lifted order could only be reduced to $o^+ = 1$ in line 4 because there were too many constraints. It is possible to reduce the number of constraints first to avoid this issue; however, it is advantageous to reduce as many continuous generators as possible prior to performing constraint reduction since the number of error metrics evaluated in this step is equal to the number of continuous generators.

To avoid unacceptably large growth in the hybrid zonotope, it is possible to intersect the reduced set with the interval hull of the unreduced set through Proposition 3.2.10 after applying Algorithm 5. This is advantageous as it guarantees that the resulting over-approximating

set will be at least as good as the original set's interval hull. This step requires solving $2n$ MILPs and introduces an additional n continuous generators and n constraints to the over-approximating hybrid zonotope $\tilde{\mathcal{Z}}_h \leftarrow \tilde{\mathcal{Z}}_h \cap \mathcal{B}(\mathcal{Z}_h)$. These additional generators and constraints can be accounted for in the reduction of the hybrid zonotope when choosing n_g^r and n_c^r. If the intersection with the interval hull is redundant, this redundancy will be detected and removed at the next iteration of the analysis.

6.3 Error Metrics

In this section I derive and compare methods for evaluating the differences in hybrid zonotopes. These methods provide error metrics used for finding tight over-approximations in the algorithms described in Section 6.2, as well as providing metrics for drawing comparisons. The provided error metrics include approximations of the radius of the set as well as the volume of hybrid zonotopes. In Section 6.3.1 I show how the radius of the hybrid zonotope may be approximated to measure the set's growth outward from it's geometric center. In Section 6.3.2 I show how the volume of the hybrid zonotope may be approximated to measure the change in the set's nonconvexity.

First it is important to note two challenges that arise in comparing hybrid zonotopes.

1. Depending on what the hybrid zonotope represents, each of the dimensions may have different units. When using metrics such as radius and volume, it is important to specify the possible range of values each of the dimensions may take. The hybrid zonotope may then be scaled prior to applying the following methods as

$$\hat{\mathcal{Z}}_h = \text{diag}(w)\mathcal{Z}_h \,, \tag{6.26}$$

   where $w \in \mathbb{R}^n$ is a vector of weights used to normalize the different dimensions and $\text{diag}(w) \in \mathbb{R}^{n \times n}$ is a diagonal matrix with entries $\text{diag}(w)_{\text{i,i}} = w_{\text{i}}$. It is assumed that all hybrid zonotopes have been properly scaled prior to applying error metrics.

2. It is also possible for a hybrid zonotope to have dimensions that are fully discrete. In this case, describing the volume of such a set is meaningless. To avoid this issue and still

provide insight on the other dimensions, hybrid zonotopes with a mix of continuous, hybrid, and fully discrete dimensions are projected onto the continuous and hybrid parts. A discrete dimension i may be found using an ordinary sorting algorithm to find the rows of the generator matrices such that $\nexists\, G^c_{\mathrm{i},\cdot} \neq 0$; if no continuous generators exist, then the dimension is a constant or a collection of discrete points. The hybrid zonotope may then be projected onto the dimensions containing continuous parts as $S\mathcal{Z}_h$, where $S \in \mathbb{R}^{m \times n_z}$ is a staircase matrix having a single one in each of the m rows located in the ith column corresponding to the index of each dimension of $\mathcal{Z}_h$ that is continuous or hybrid.

6.3.1 Radius Ratio

The first metric considered to evaluate the difference of two hybrid zonotopes is the sets' n-dimensional radii. Given any two hybrid zonotopes $\mathcal{Z}_{h,1}$ and $\mathcal{Z}_{h,2}$, their radius ratio is defined as

$$\Theta_R = \frac{R(\mathcal{Z}_{h,1})}{R(\mathcal{Z}_{h,2})}\,, \tag{6.27}$$

where $R(\mathcal{Z}_h)$ is the radius of $\mathcal{Z}_h$. The radius of a set is defined as the radius of the tightest n-dimensional ball that encloses the set. This can be expressed as the solution to the optimization problem

$$\min_{r,\hat{c}} \left\{ r \mid \|z - \hat{c}\|_2 \leq r \;\forall\, z \in \mathcal{Z}_h \right\}\,, \tag{6.28}$$

where r is the radius of the enclosing ball and $\hat{c}$ its center. Thus when r and $\hat{c}$ are the solution to (6.28), $\mathcal{Z}_h \subset \{x \in \mathbb{R}^n \mid x + c \leq r + \epsilon\}$ only if $\epsilon \geq 0$. This optimization problem can be equivalently expressed as the bilevel program

$$\min_{\hat{c}} \max_{z \in \mathcal{Z}_h} \|z - \hat{c}\|_2\,. \tag{6.29}$$

Even when the set to be enclosed by the ball is convex, this optimization problem is non-convex and difficult to solve [91]. This issue is further exacerbated by the fact that the containment condition of the hybrid zonotope $z \in \mathcal{Z}_h$ (see Proposition 3.2.8) appearing in both optimization problems requires mixed-integer constraints. Finding the radius of

the set thus requires solving a nonconvex mixed-integer bilevel program, which poses many computational challenges and is a major area of research [92],[93].

Instead of solving the complex optimization problems posed by (6.28) and (6.29), the radius of a hybrid zonotope is approximated by the radius of the set's interval hull using various norms. The interval hull of a hybrid zonotope $\mathcal{B}(\mathcal{Z}_h) = [\rho_L, \rho_U]$ given by (3.52) is the tightest axis oriented box that encloses the set. The vector of lengths of the box is given by $\rho_U - \rho_L$. The radius of the hybrid zonotope is then approximated as

$$R_p(\mathcal{Z}_h) = \|\rho_U - \rho_L\|_p \,, \tag{6.30}$$

where p is the chosen norm. Note that the true radius of the set is guaranteed to be below that obtained by evaluating (6.30) for $p = 2$ as the resulting ball fully encloses the interval hull of the set, while no guarantees can be made for norms $p > 2$. The approximated radii of the hybrid zonotope (3.6) from Example 3.1.1 for $p = 2$ and $p = \infty$ are depicted in Figure 6.5. While the radius ratio gives a way to compare the relative sizes of two hybrid zonotopes, it gives no insight into the differences of the sets' nonconvexity.

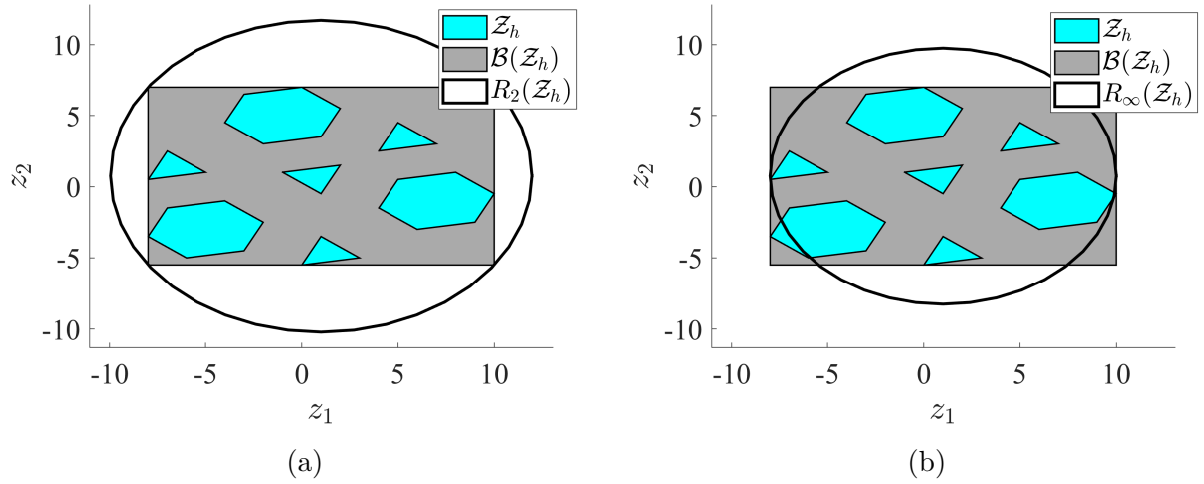

Figure 6.5. Example of approximating the radius of hybrid zonotopes based on the length of the set's interval hull. 6.5a Radius of the hybrid zonotope approximated using $p = 2$ norm. 6.5b Radius of the hybrid zonotope approximated using $p = \infty$ norm. Note that only using $p \leq 2$ norm is guaranteed to give an over-approximation of the hybrid zonotope's true radius.

6.3.2 Volume Ratio

Given any two hybrid zonotopes $\mathcal{Z}_{h,1} \subset \mathbb{R}^n$ and $\mathcal{Z}_{h,2} \subset \mathbb{R}^n$, their volume ratio is defined as

$$\Theta_V = \left(\frac{v(\mathcal{Z}_{h,1})}{v(\mathcal{Z}_{h,2})} \right)^{\frac{1}{n}} , \tag{6.31}$$

where $v(\mathcal{Z}_h)$ is the volume of $\mathcal{Z}_h$. Determining the volume of sets is a difficult task. Even finding the volumes of simple zonotopes is computationally expensive and requires calculating the determinants of all combinations of sub-matrices of the generator matrix [94]. Due to the limitations arising from the combinatorial nature of calculating the exact volume, approximation methods using random sampling are often employed for complex zonotopes (see [95], [96] and the references within). The volume of arbitrary convex sets may be approximated using random walk algorithms that scale with the set dimension as $\mathcal{O}(n^5)$ [97], [98]. Exact methods for finding volumes of nonconvex sets in general do not exist, and algorithms using sub-pavings are often employed to provide guaranteed bounds [99]; however, these algorithms grow exponentially with respect to the dimension of the set. In Theorem 3.1.1 it was shown that the hybrid zonotope may be decomposed into a collection of convex subsets, and it follows that the volume of each subset could be estimated using any of the existing convex approaches. However, it is possible that these convex sets overlap and therefore the volume estimation using this approach would only provide a, possibly very large, over-approximation. Furthermore there is a potentially exponential number of convex subsets that would need to be evaluated.

Instead, this section presents two methods for approximating the volume of a hybrid zonotope, both of which require sampling N points, or hyperboxes, from the interval hull and evaluating if $p_{\mathrm{i}} \in \mathcal{Z}_h$, or $\mathcal{B}_{\mathrm{i}} \cap \mathcal{Z}_h = \emptyset$, by Proposition 3.2.8. Given the interval hull of a hybrid zonotope $\mathcal{B}(\mathcal{Z}_h) = [\rho_L, \rho_U]$ by (3.52), the n-dimensional volume of the interval hull is calculated as

$$v(\mathcal{B}(\mathcal{Z}_h)) = v([\rho_L, \rho_U]) = \prod_{\mathrm{i}=1}^{n} (\rho_U(\mathrm{i}) - \rho_L(\mathrm{i})) , \tag{6.32}$$

where $\rho_U(\mathrm{i}) - \rho_L(\mathrm{i})$ is the length of the interval hull in the i^{th} direction. The volume of the hybrid zonotope is upper bounded by that of the interval hull; however, this value gives no

insight beyond that obtained by the set's radius. To provide a better approximation of the hybrid zonotope's volume, regions from within the interval hull are tested within a series of trials. Given a total of N trials sampled from the interval hull $\mathcal{B}(\mathcal{Z}_h)$ and X of which are successful, the volume of $\mathcal{Z}_h$ may then be estimated as

$$\hat{v}(\mathcal{Z}_h) = \frac{X}{N} v\left(\mathcal{B}(\mathcal{Z}_h)\right) . \tag{6.33}$$

The trials used to determine $\hat{v}$ are found in two ways, one that uses a collection of hyperboxes that cover the set and another that samples random points from a uniform distribution over the interval hull.

Collection of hyperboxes

Given any hybrid zonotope $\mathcal{Z}_h \subset \mathbb{R}^n$, it is possible to partition the set's intervall hull into a collection of N smaller, disjoint hyperboxes $\mathcal{B}_\mathrm{i} \subset \mathbb{R}^n$ such that $\mathcal{B}(\mathcal{Z}_h) = \bigcup_{\mathrm{i}=1}^{N} \mathcal{B}_\mathrm{i}$ and $\mathcal{B}_\mathrm{i}^\circ \cap \mathcal{B}_\mathrm{j}^\circ = \emptyset$ for $\mathrm{i} \neq \mathrm{j}$. Given that each hyperbox is defined as an n-dimensional interval $\mathcal{B}_\mathrm{i} = [\rho_{L,\mathrm{i}}, \rho_{U,\mathrm{i}}]$, its volume is trivially calculated as the product of the length of each dimension by (6.32). Furthermore, each of the hyperboxes may be represented as a zonotope in G-rep simply as

$$\mathcal{B}_\mathrm{i} = \left\langle \mathrm{diag}\left(\frac{\rho_{U,\mathrm{i}} - \rho_{L,\mathrm{i}}}{2}\right), \frac{\rho_{U,\mathrm{i}} + \rho_{L,\mathrm{i}}}{2} \right\rangle , \tag{6.34}$$

such that the intersection of the hyperbox and the hybrid zonotope, $\mathcal{Z}_h \cap \mathcal{B}_\mathrm{i}$, is given by Proposition 3.2.3. Whether or not this intersected region is empty may be determined by evaluating the feasibility of a MILP by Proposition 3.2.8. Let $\mathcal{B}_\cup = \{\mathcal{B}_1, \ldots, \mathcal{B}_N\}$ be a collection of disjoint hyperboxes such that $\mathcal{Z}_h \subseteq \bigcup_{\mathrm{i}=1}^{N} \mathcal{B}_\mathrm{i}$ and let $\mathcal{I} = \{\mathrm{i} \in \{1, \ldots, N\} \mid \mathcal{Z}_h \cap \mathcal{B}_\mathrm{i} \neq \emptyset\}$ be the set of indices of all hyperboxes that intersect the hybrid zonotope. Then it follows that $\mathcal{Z}_h \subseteq \bigcup_{\mathrm{i}\in\mathcal{I}} \mathcal{B}_\mathrm{i}$ and therefore,

$$v(\mathcal{Z}_h) \leq \sum_{\mathrm{i}\in\mathcal{I}} v(\mathcal{B}_\mathrm{i}) . \tag{6.35}$$

Thus given any disjoint covering of $\mathcal{Z}_h$ by a collection of hyperboxes, it is possible to determine an upper bound on the set's volume.

A naive method for determining a partition of hyperboxes that covers the hybrid zonotope is to grid the interval hull for some given tolerance on the lengths, $\rho_{U,\mathrm{i}} - \rho_{L,\mathrm{i}} = \epsilon$. Given that the interval hull of the hybrid zonotope is known, this tolerance can be decided based on either the desired precision of the resulting volume estimate or the tolerable number of optimization calls. Unfortunately, this approach scales exponentially with respect to the dimension of the set. For example, partitioning each dimension of the interval hull into N uniform lengths results in a total of n^N hyperboxes that must be evaluated.

Another approach for finding a covering of $\mathcal{Z}_h$ by hyperboxes is to employ a bisection algorithm, where the interval hull is iteratively cut into smaller non-overlapping hyperboxes until a prescribed precision is achieved [99]. This method is known as sub-paving and is often used to approximate the inversion of sets by nonlinear functions [100], nonlinear set-based state estimators [101], and parameter estimation [102].

Inspired by these methods, Algorithm 6 aims to find the tightest covering of $\mathcal{Z}_h$ with the fewest optimization calls. The conventional bisection algorithms [99] begin with a single box giving some specified region of interest. Instead, Algorithm 6 samples the interval hull and initializes the covering with its bisection in all n dimensions. Doing so, lines (3-6) of Algorithm 6 creates an initial covering with 2^n even bisections covering the interval hull. Lines (7-19) iteratively identify the hyperbox from the covering with the greatest edge length, bisect along that dimension, then tightens the interval that was bisected for the two newly introduced hyperboxes. Given a hyperbox $\mathcal{B}_M = [\rho_L, \rho_U]$ with maximum edge length in the i^{th} dimension, line 10 splits $\mathcal{B}_M$ into two equally sized hyperboxes

$$\mathcal{B}_L = \begin{bmatrix} \rho_L(1) & , & \rho_U(1) \\ \vdots & , & \vdots \\ \rho_L(\mathrm{i}) & , & \frac{\rho_U(\mathrm{i})+\rho_L(\mathrm{i})}{2} \\ \vdots & , & \vdots \\ \rho_L(n) & , & \rho_U(n) \end{bmatrix}, \mathcal{B}_R = \begin{bmatrix} \rho_L(1) & , & \rho_U(1) \\ \vdots & , & \vdots \\ \frac{\rho_U(\mathrm{i})+\rho_L(\mathrm{i})}{2} & , & \rho_U(\mathrm{i}) \\ \vdots & , & \vdots \\ \rho_L(n) & , & \rho_U(n) \end{bmatrix}. \tag{6.36}$$

The i^{th} intervals of the bisected boxes are tightened over the domains of $\mathcal{Z}_h \cap \mathcal{B}_L$ and $\mathcal{Z}_h \cap \mathcal{B}_R$, respectively, on lines (11-18) by solving the four MILPs

$$\tilde{\rho}_{L,L}(\mathrm{i}) = \min \left\{ \mathrm{e_i}(G^c\xi^c + G^b\xi^b + c) \;\middle|\; \begin{array}{c} A^c\xi^c + A^b\xi^b = b\,, \\ \|\xi^c\|_\infty \leq 1\,,\ \xi^b \in \{-1,1\}^{n_b}\,, \\ G^c\xi^c + G^b\xi^b + c \in \mathcal{B}_L \end{array} \right\}, \tag{6.37a}$$

$$\tilde{\rho}_{U,L}(\mathrm{i}) = \max \left\{ \mathrm{e_i}(G^c\xi^c + G^b\xi^b + c) \;\middle|\; \begin{array}{c} A^c\xi^c + A^b\xi^b = b\,, \\ \|\xi^c\|_\infty \leq 1\,,\ \xi^b \in \{-1,1\}^{n_b}\,, \\ G^c\xi^c + G^b\xi^b + c \in \mathcal{B}_L \end{array} \right\}, \tag{6.37b}$$

$$\tilde{\rho}_{L,R}(\mathrm{i}) = \min \left\{ \mathrm{e_i}(G^c\xi^c + G^b\xi^b + c) \;\middle|\; \begin{array}{c} A^c\xi^c + A^b\xi^b = b\,, \\ \|\xi^c\|_\infty \leq 1\,,\ \xi^b \in \{-1,1\}^{n_b}\,, \\ G^c\xi^c + G^b\xi^b + c \in \mathcal{B}_R \end{array} \right\}, \tag{6.37c}$$

$$\tilde{\rho}_{U,R}(\mathrm{i}) = \max \left\{ \mathrm{e_i}(G^c\xi^c + G^b\xi^b + c) \;\middle|\; \begin{array}{c} A^c\xi^c + A^b\xi^b = b\,, \\ \|\xi^c\|_\infty \leq 1\,,\ \xi^b \in \{-1,1\}^{n_b}\,, \\ G^c\xi^c + G^b\xi^b + c \in \mathcal{B}_R \end{array} \right\}, \tag{6.37d}$$

where $\mathrm{e_i}$ is the standard i^{th} unit vector. The new hyperboxes introduced to the list $\mathcal{B}_\cup$ are then given by

$$\tilde{\mathcal{B}}_L = \begin{bmatrix} \rho_L(1) & , & \rho_U(1) \\ \vdots & , & \vdots \\ \tilde{\rho}_{L,L}(\mathrm{i}) & , & \tilde{\rho}_{U,L}(\mathrm{i}) \\ \vdots & , & \vdots \\ \rho_L(n) & , & \rho_U(n) \end{bmatrix}, \; \tilde{\mathcal{B}}_R = \begin{bmatrix} \rho_L(1) & , & \rho_U(1) \\ \vdots & , & \vdots \\ \tilde{\rho}_{L,R}(\mathrm{i}) & , & \tilde{\rho}_{U,R}(\mathrm{i}) \\ \vdots & , & \vdots \\ \rho_L(n) & , & \rho_U(n) \end{bmatrix}. \tag{6.38}$$

The tightened hyperboxes are then stored in the list $\mathcal{B}_\cup$, which remains disjoint because of the constraint that $G^c\xi^c + G^b\xi^b + c \in \mathcal{B}_L$ in (6.37a) and (6.37b) and $G^c\xi^c + G^b\xi^b + c \in \mathcal{B}_R$ in (6.37c) and (6.37d). If during an iteration the intersection $\mathcal{Z}_h \cap \mathcal{B}_L$ or $\mathcal{Z}_h \cap \mathcal{B}_R$ is empty, the hyperbox is discarded from the list since it does not contribute to the volume. Once the

covering of hyperboxes $\mathcal{B}_\cup$ is returned by the algorithm, the volume of the hybrid zonotope is over-approximated by (6.35).

Algorithm 6 Bisection algorithm for covering of $\mathcal{Z}_h$ by collection of disjoint hyperboxes $\mathcal{B}_\mathrm{i}$.

Input: $\mathcal{Z}_h \subset \mathbb{R}^n$, $\epsilon \in \mathbb{R}$

Output: $\mathcal{B}_\cup = \{\mathcal{B}_1, \ldots, \mathcal{B}_N\}$ s.t. $\mathcal{Z}_h \subseteq \bigcup_\mathrm{i}^N \mathcal{B}_\mathrm{i}$, $\mathcal{B}_\mathrm{i}^\circ \cap \mathcal{B}_\mathrm{j}^\circ = \emptyset$ for all $\mathrm{i} \neq \mathrm{j}$, and $v(\mathcal{B}_\mathrm{i}) \leq \epsilon^n$

$\mathcal{B}(\mathcal{Z}_h) \leftarrow$ interval hull of $\mathcal{Z}_h$
Initialize list of hyperboxes $\mathcal{B}_\cup \leftarrow \{\mathcal{B}(\mathcal{Z}_h)\}$
for $\mathrm{i} = 1, \ldots, n$ **do**
    Bisect all hyperboxes in $\mathcal{B}_\cup$ in i^{th} dimension
    Replace list $\mathcal{B}_\cup$ with bisected boxes
end for
while Max edge length of all hyperboxes in $\mathcal{B}_\cup$ is $\geq \epsilon$ **do**
    Remove hyperbox with max edge length $\mathcal{B}_M$ from list $\mathcal{B}_\cup$
    $\mathrm{i} \leftarrow$ dimension of max edge length of $\mathcal{B}_M$
    Bisect $\mathcal{B}_M$ in i^{th} dimension such that $\mathcal{B}_M = \mathcal{B}_L \cup \mathcal{B}_R$
    if $\mathcal{Z}_h \cap \mathcal{B}_L \neq \emptyset$ **then**
        $\tilde{\mathcal{B}}_L \leftarrow$ bounds on i^{th} interval tightened such that $\mathcal{Z}_h \cap \mathcal{B}_L \subseteq \tilde{\mathcal{B}}_L$
        Store $\tilde{\mathcal{B}}_L$ in $\mathcal{B}_\cup$
    end if
    if $\mathcal{Z}_h \cap \mathcal{B}_R \neq \emptyset$ **then**
        $\tilde{\mathcal{B}}_R \leftarrow$ bounds on i^{th} interval tightened such that $\mathcal{Z}_h \cap \mathcal{B}_R \subseteq \tilde{\mathcal{B}}_R$
        Store $\tilde{\mathcal{B}}_R$ in $\mathcal{B}_\cup$
    end if
end while

Uniform sampling

Algorithm 6 may provide tighter bounds on the volume of a hybrid zonotope with fewer optimization calls than the naive approach of uniformly partitioning the interval hull into uniform hyperboxes. However, the method still scales exponentially with respect to the dimension of the set, as each direction needs to be iteratively split and tightened until the specified precision is met. This section proposes an alternative sampling method to provide estimates on the volume for higher dimensional sets with a fixed number of calls to the optimization program. However, only statistical guarantees can be made on the resulting estimate.

Given any hybrid zonotope $\mathcal{Z}_h \subset \mathbb{R}^n$, first find the interval hull $\mathcal{B}(\mathcal{Z}_h)$. Let p be a collection of $N \in \mathbb{Z}$ points randomly sampled from a uniform distribution over the interval hull such that $p_\mathrm{i} \in \mathcal{B}(\mathcal{Z}_h) \forall \mathrm{i} \in \{1, \ldots, N\}$. Whether each of these random points belong to the hybrid zonotope may be determined by evaluating the feasibility of a MILP by Proposition 3.2.8. Let $X \in \mathbb{Z}$ be the number of random points found to satisfy $p_\mathrm{i} \in \mathcal{Z}_h$ of the N total trials. Then the volume of the hybrid zonotope may be approximated as

$$\hat{v}(\mathcal{Z}_h) = \frac{X}{N} v(\mathcal{B}(\mathcal{Z}_h)) \,, \tag{6.39}$$

where $v(\mathcal{B}(\mathcal{Z}_h))$ is the volume of the interval hull calculated by (6.33).

Each point randomly sampled from the interval hull has two possibilities, $p_\mathrm{i} \in \mathcal{Z}_h$ or $p_\mathrm{i} \notin \mathcal{Z}_h$. The proposed method of sampling, and testing, a uniform distribution of N points is therefore a series of Bernoulli trials. The value to be estimated is the ratio of points that belong to the hybrid zonotope compared to those that belong to the interval hull, i.e. the probability that $p_\mathrm{i} \in \mathcal{B}(\mathcal{Z}_h) \implies p_\mathrm{i} \in \mathcal{Z}_h$. As the number of sampled points grows large, $N \to \infty$, the estimate given by (6.39) converges to the true volume, $\hat{v}(\mathcal{Z}_h) \to v(\mathcal{Z}_h)$. The probability that a point will belong to the hybrid zonotope is thus given by a binomial distribution. For a specified confidence $\alpha \in [0, 1]$, the confidence intervals can be determined based on the binomial distribution of the sampled data [103]. While not providing a guaranteed estimate, this approach provides bounds on the estimated volume within a confidence interval of

$$\hat{v}_L \leq v \leq \hat{v}_U \,, \tag{6.40}$$

in a more computationally tractable way.

Comparison of volume estimations

This section compares the three volume estimation techniques. Each method is coded as

$V1_N$: volume is over-approximated by partitioning the set's interval hull into N uniform hyperboxes,

$V2_N$: volume is over-approximated by Algorithm 6 with $N/2$ total bisections,

$V3_N$: volume is estimated by sampling N random points from the set's interval hull.

To draw a comparison between these three approaches, methods $V1_N$ and $V2_N$ are formulated based on the number of calls to the MILP solver rather than a user specified tolerance on edge length of the covering hyperboxes. Thus all three methods have the same number of MILPs evaluated and comparable computational effort. Note that methods $V1_N$ and $V2_N$ guarantee an over-approximation of the volume while $V3_N$ is only able to provide an estimated range of volumes based on a user defined confidence interval $\alpha \in [0, 1]$. The confidence is chosen as $\alpha = 0.05$ corresponding to a 95% confidence interval.

Consider the hybrid zonotope (3.6) from Example 3.1.1. Decomposing the hybrid zonotope into its convex subsets $\mathcal{Z}_h = \bigcup_{\xi_\mathrm{i}^b \in \mathcal{T}} \mathcal{Z}_{c,\mathrm{i}}$ by Theorem 3.1.1 results in seven disjoint constrained zonotopes. The volume of the hybrid zonotope is then given by the sum of the volumes of the constrained zonotopes. This property of the considered set is advantageous as the volume of each constrained zonotope can be found exactly using the Multi-Parametric Toolbox (MPT) [12]. First, the constrained zonotope $\mathcal{Z}_{c,\mathrm{i}}$ is converted to an H-rep polytope by defining $\mathcal{B}_\infty(A^c, b - A^b\xi_\mathrm{i}^b)$ as a polyhedron and performing one linear mapping and Minkowski sum as

$$\mathcal{P}_\mathrm{i} = G^c\mathcal{B}_\infty(A^c, b - A^b\xi_\mathrm{i}^b) \oplus (c + G^b\xi_\mathrm{i}^b)\,. \tag{6.41}$$

Thus by Definition 2.9, $\mathcal{Z}_{c,\mathrm{i}} = \mathcal{P}_\mathrm{i}$. The MPT volume routine is then used to find the exact volume of each convex subset. The volume of the hybrid zonotope is then given by their sum as

$$v(\mathcal{Z}_h) = \sum_{\mathrm{i}=1}^{|\mathcal{T}|} v(\mathcal{P}_\mathrm{i})\,. \tag{6.42}$$

Note that the computational complexity of linear mappings and volume computations of polyhedron restricts this approach to hybrid zonotopes in low dimensions with relatively few continuous factors, as discussed in Section 2.3.1. The estimated volumes for a varying number of calls to the MILP solver, denoted by N, is given in Figure 6.6. The resulting coverings of $\mathcal{Z}_h$ and random points sampled are depicted in Figure 6.7 for $N = 100$ and in Figure 6.8 for $N = 400$.

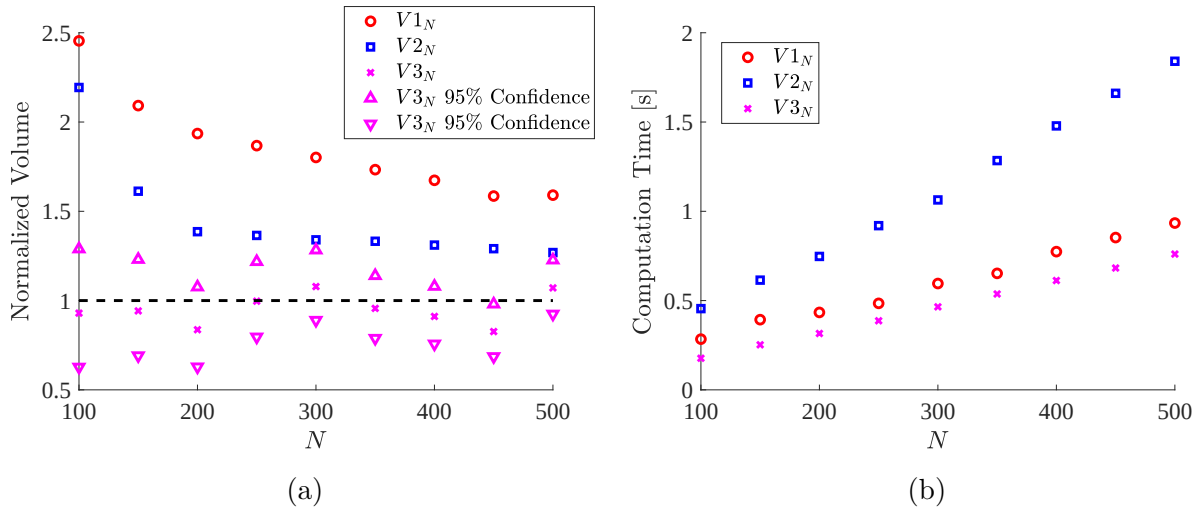

Figure 6.6. Comparison of the proposed volume estimation techniques for varying number of calls to the MILP solver for the 2-dimensional example hybrid zonotope (3.6). 6.6a Comparison of the estimated volumes using the proposed methods. Volumes are normalized with respect to the exact volume calculated using MPT. 6.6b Computation time required to estimate the set volume using the proposed methods.

This same comparison was performed on 100 randomly generated two dimensional hybrid zonotopes. The hybrid zonotopes were generated with $n_g = 15$ continuous generators, $n_b = 5$ binary generators, and $n_c = 5$ constraints. The specific matrices were generated following the procedure for generating random zonotopes [90]. Specifically, the elements of G^c, G^b, c, A^c, A^b, and b are sampled from a uniform distribution on $[-1, 1]$ then scaled by a random value $\alpha \in [0, 60]$. The baseline volume for comparison was found using routines in the MPT. Given that the convex subsets of the hybrid zonotopes were not guaranteed to be disjoint, a numerically expensive algorithm was used to separate the collection into non-overlapping polyhedron. This approach was found to be intractable for hybrid zonotopes with additional continuous and binary generators and in higher than two dimensions. The resulting volume estimations averaged over the 100 sets is provided in Figure 6.9.

The results from these numerical experiments confirm that methods $V1_N$ and $V2_N$ are able to over-approximate the true volume of the hybrid zonotope. Method $V2_N$ provides a tighter over-approximation at the cost of additional computation time. This additional computation time is due to Algorithm 6 performing optimization over the MILP rather

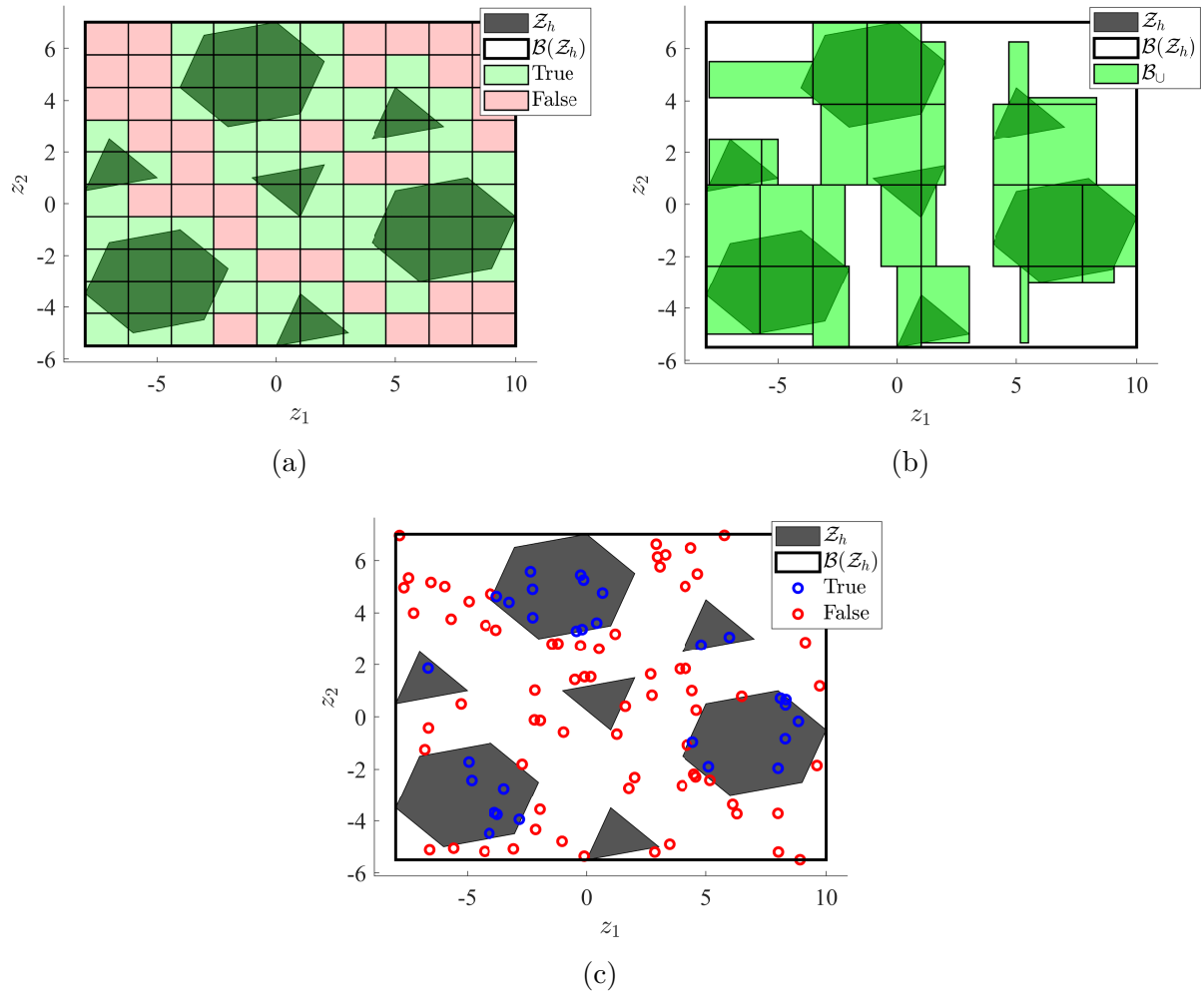

Figure 6.7. Comparison of three volume estimation techniques for $N = 100$ calls to the MILP solver for example with $v(\mathcal{Z}_h) = 60.5$. 6.7a Depiction of method $V1_{100}$ partitioning the interval hull into 100 uniform boxes. Resulting in an over-approximated volume estimate of $\hat{v}(\mathcal{Z}_h) = 148.5$. 6.7b Covering $\mathcal{B}_\cup$ of $\mathcal{Z}_h$ after performing $N/2 = 50$ bisections of Algorithm 6. Resulting in an over-approximated volume estimate of $\hat{v}(\mathcal{Z}_h) = 132.70$. 6.7c Depiction of $N = 100$ randomly sampled points from the interval hull. Resulting in an over-approximated volume estimate of $\hat{v}(\mathcal{Z}_h) = 65.25$ with 95% confidence interval of $45.80 \leq v \leq 87.58$.

than checking feasibility, which is a more computationally demanding process. Method $V3_N$ sampling N random points on average provided the most accurate estimation of the hybrid zonotopes volume. As the number of points sampled was increased, the confidence interval tightened near the same rate as methods $V1_N$ and $V2_N$.

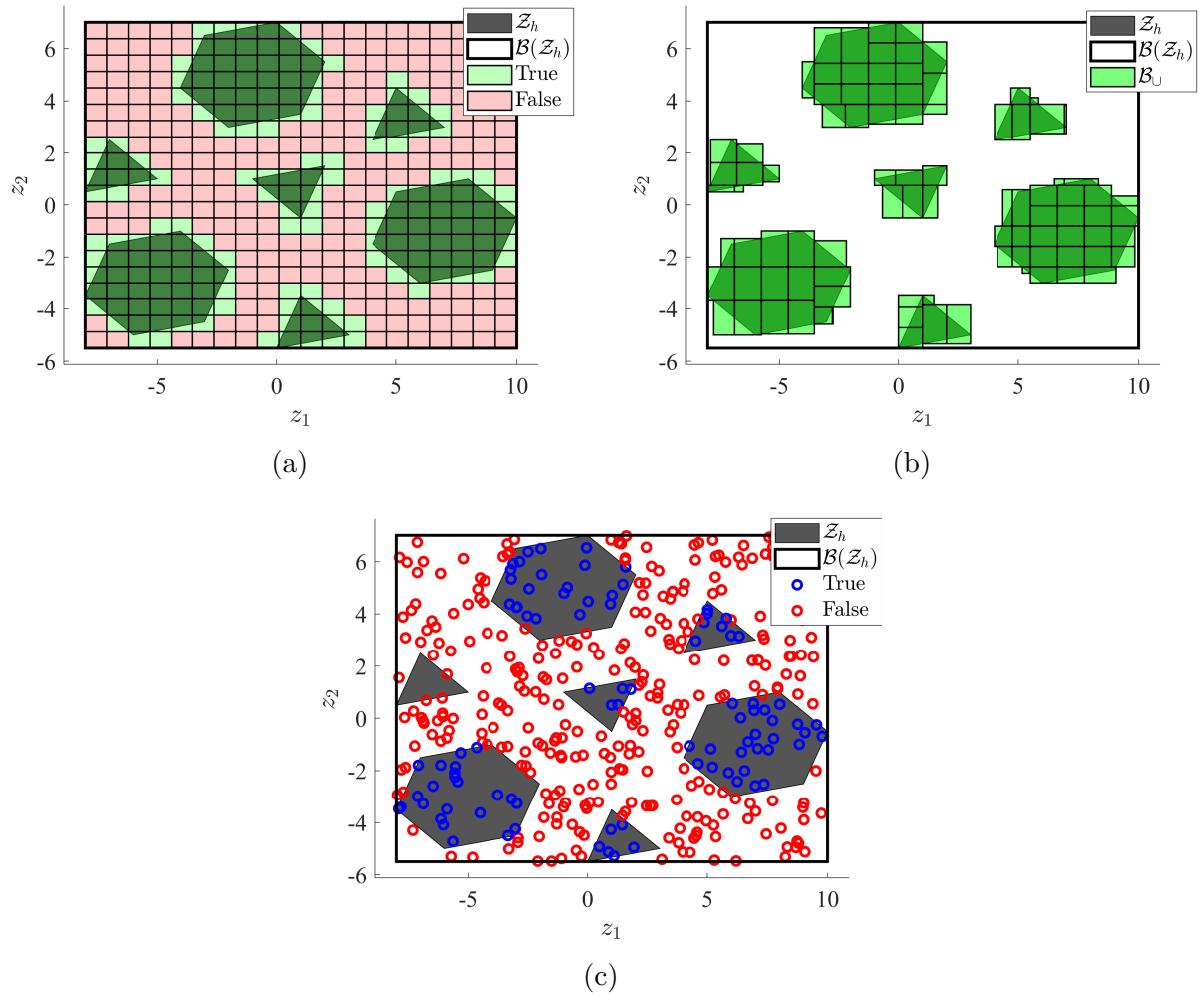

Figure 6.8. Comparison of three volume estimation techniques for $N = 400$ calls to the MILP solver for example with $v(\mathcal{Z}_h) = 60.5$. 6.8a Depiction of method $V1_{400}$ partitioning the interval hull into 400 uniform boxes. Resulting in an over-approximated volume estimate of $\hat{v}(\mathcal{Z}_h) = 101.25$. 6.8b Covering $\mathcal{B}_\cup$ of $\mathcal{Z}_h$ after performing $N/2 = 200$ bisections of Algorithm 6. Resulting in an over-approximated volume estimate of $\hat{v}(\mathcal{Z}_h) = 79.56$. 6.8c Depiction of $N = 400$ randomly sampled points from the interval hull. Resulting in a volume estimate of $\hat{v}(\mathcal{Z}_h) = 51.75$ with 95% confidence interval of $42.67 \leq v \leq 61.74$.

6.3.3 Heuristics

The previous sections provide estimates on the radial size and volume of the hybrid zonotope. While both of these approaches give insight into the physical characteristics of any given set, it is possible to leverage error metrics that are useful in the proposed

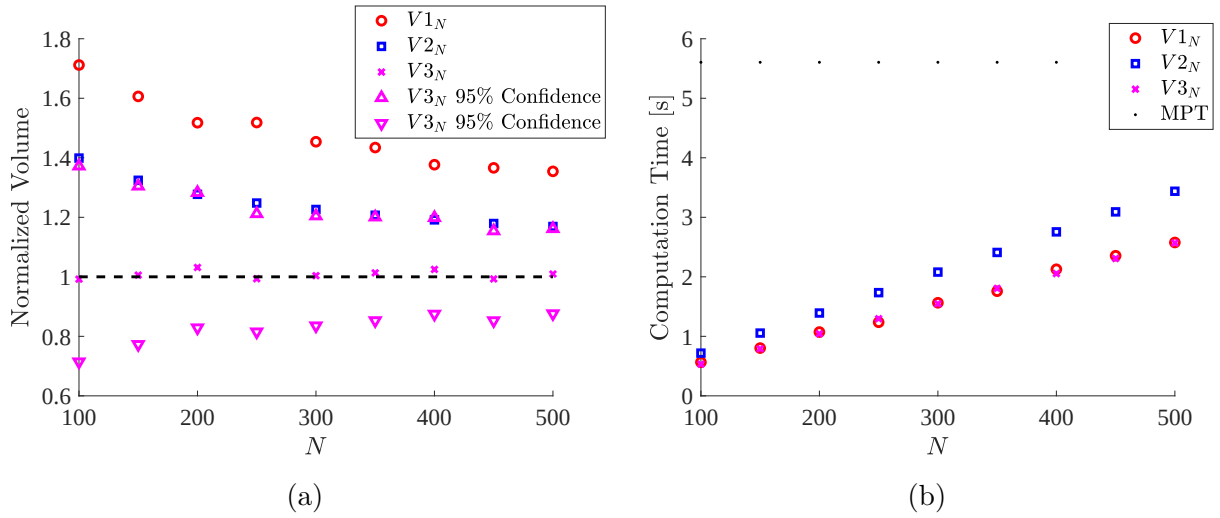

Figure 6.9. Comparison of the proposed volume estimation techniques for varying number of calls to the MILP solver averaged over 100 randomly generated 2-dimensional hybrid zonotopes. 6.6a Comparison of the estimated volumes using the proposed methods. Volumes are normalized with respect to the exact volume calculated using MPT. 6.6b Computation time required to estimate the set volume using the proposed methods.

over-approximation techniques that are not rooted in these fundamental measures. This section provides heuristics that aim to give a ranking of the candidate over-approximations in Algorithms 3 and 4 by building off the radius and volume ratios developed in the previous sections. Specifically, three heuristics are proposed: one that sums the radii of all the hybrid zonotope's convex subsets, one that uses the radius of the hybrid zonotope to determine which candidates should be further explored using one of the other methods, and one that combines the information from both the radius and the volume of the set.

Sum of radii: First, given any hybrid zonotope $\mathcal{Z}_h \subset \mathbb{R}^n$, let $\bigcup_{\xi_i^b \in \mathcal{T}} \mathcal{Z}_{c,i}$ be its collection of decomposed constrained zonotopes by Theorem 3.1.1. An error metric is then defined as the sum of all the radii of the $|\mathcal{T}|$ constrained zonotopes as

$$\overline{R}_p(\mathcal{Z}_h) = \sum_{\xi_i^b \in \mathcal{T}} R_p(\mathcal{Z}_{c,i}) \,, \tag{6.43}$$

where $R_p(\mathcal{Z}_{c,i})$ is the i^{th} constrained zonotope's radius defined by (6.30). This error metric is valuable when comparing the order reduction of two sets because it: (1) penalizes the growth

in each of the convex subsets, and (2) penalizes an increase in the number of nonempty convex subsets. While two candidate over-approximating hybrid zonotopes using the methods given in Algorithms 3 and 4 may have the same volume, it is beneficial to choose the one that has the fewest convex subsets, both in decomposition for visualization as well as when evaluating the set by solving MILPs. From numerical experiments, this heuristic has shown great success in determining over-approximations with small growth in error. While providing a useful metric, calculating (6.43) requires solving $2n|\mathcal{T}|$ linear programs, which can be computationally expensive as $\mathcal{T}$ grows, possibly exponentially, large. However, as discussed in Remark 6.2.2, $\mathcal{T}$ may be bounded by reducing the number of binary generators during iterative set operations. It is also possible to only apply this expensive metric to the candidate sets that have the least growth in radius of the hybrid zonotope as described next.

Radius ranking: Another possibility is to use the radius ratio to select which of the potential approximations should be further evaluated using one of the more computationally expensive metrics. Note that of the provided methods, the radius ratio is the least computationally expensive. Given a collection of N candidate hybrid zonotopes, let $\mathcal{I}_R \subset \{1, \dots, N_R\}$ be the indices of the N_r hybrid zonotopes with the smallest radius by (6.30). Then the more computationally expensive error metric may only be evaluated for the $\mathrm{i} \in \mathcal{I}_R$ hybrid zonotopes as

$$\overline{E}_R = \{E_\mathrm{i}\}_{\mathrm{i}\in\mathcal{I}_R} \,, \tag{6.44}$$

where E_i is calculated using one of the more computationally expensive error metrics.

Multiple metrics: The final approach described is to combine multiple error metrics. For example, similar to the use of multiple objective functions in optimization problems [104], it is possible to combine multiple error metrics as

$$\tilde{E} = \sum_{\mathrm{i}=1}^{N} \alpha_\mathrm{i} E_\mathrm{i} \,, \tag{6.45}$$

where $\alpha_\mathrm{i} \in \mathbb{R}$ such that $\alpha_\mathrm{i} \geq 0$, and E_i is any of the defined error metrics. While this combined error metric no longer gives a value representing the set's physical characteristics, it gives the engineer performing the analysis a method for reducing complexity by using

multiple criteria. For example, estimating the volume of a high dimensional hybrid zonotope by sampling few points may give poor estimates; however, this rough estimate of the volume ratio may be useful when combined with the set's radius ratio.

6.4 Numerical Examples

In this section I provide multiple numerical examples to evaluate the effectiveness of the proposed order reduction techniques. In Section 6.4.1 the order reduction techniques are applied to randomly generated hybrid zonotopes to compare the difference in the resulting over-approximations and required computation times of the different error metrics. Then the heated room hybrid system explored in the previous examples is reduced to display the effectiveness of the order reduction techniques to reachable sets in Section 6.4.2. Finally, in Section 6.4.3 it is shown how order reduction may be applied iteratively to extend the considered time horizon in forward reachability analysis and is applied to the closed-loop MPC system.

6.4.1 Random Hybrid Zonotopes

This example evaluates the proposed methods for generating over-approximations of randomly generated hybrid zonotopes with varying dimensions and sizes. These methods are applied to each random hybrid zonotope using Algorithm 5 employing each of the error metrics described in Section 6.3. The matrices defining these random hybrid zonotopes are generated following the procedure for producing random zonotopes in [90]. Specifically, the elements of G^c, G^b, c, A^c, A^b, and b are sampled from a uniform distribution on $[-1, 1]$ then scaled by a random value $\alpha \in [0, 60]$. The binary generators are then multiplied by 20 to avoid producing random sets with few nonconvex features. The respective volume error metrics used in Algorithms 3 and 4 are all determined by evaluating $N = 100n$ MILPs, where n is the dimension of the random hybrid zonotope. The accuracy of the proposed methods are evaluated by comparing the ratio of the reduced set's volume with that of the unreduced set by (6.31). Volumes are estimated for these comparisons using the sampling

method described in Section 6.3.2 by solving $1000n$ MILPs. The error metrics used are coded as

R: radius of the set by (6.30) with $p = 2$ norm,

RS: sum of the radii of all convex subsets by (6.30) with $p = 2$ norm,

RS_s: sum of the radii of all convex subsets calculated for the $n_\cdot^r/2$ candidate hybrid zonotopes with the best radii by (6.30) with $p = 2$ norm,

VS: volume estimated by sampling $100n$ random points from the set's interval hull by (6.39),

VS_u: volume estimated as the upper bound on the 95% confidence interval by sampling $100n$ random points from the set's interval hull by (6.40),

VB: volume over-approximated by Algorithm 6 with $100n/2$ total bisections.

The volume ratios and computation times for the proposed methods are first evaluated for hybrid zonotopes in two dimensions. Specifically, 20 random hybrid zonotopes are generated with $n = 2$, $n_g = 50$ continuous generators, $n_b = 10$ binary generators, and $n_c = 15$ constraints. Algorithm 5 is applied to generate over-approximating hybrid zonotopes with complexity $n_g^r = 40$, $n_b^r = 8$, and $n_c^r = 12$. An example of one of the randomly generated hybrid zonotopes and it's over-approximation is depicted in Figure 6.10. The resulting normalized volume ratios and computations times for computing the over-approximating hybrid zonotopes are provided in Figure 6.11. In this set of trials, using the sampling method, VS, with a total of $100n = 200$ randomly sampled points resulted in the worst over-approximation. Using the upper bound on the 95% confidence interval on the sampled approximation, VS_u, performed slightly better. On the other hand, the method that performed the best was computing the sum of the radii of all the hybrid zonotope's convex subsets, RS. However, the computational effort of this approach is a direct consequence of the number of the hybrid zonotope's nonempty leaves, which in this experiment, was the result of randomly generated constraints. This variation in effort is reflected in the computation time of RS having the widest range in the box plot. The high computational complexity

of RS is reduced in method RS_s by first evaluating the growth in the radius of the candidate hybrid zonotopes, then summing the radii of all convex subsets for only the best half, which had similar results in the increase in volume ratio caused by the over-approximation. Of the volume estimation methods, method VB using the bisection approach to cover the hybrid zonotope by hyperboxes as described in Algorithm 6 performed the best. However, this approach had the greatest computation time when performing a total of $100n/2 = 100$ bisections.

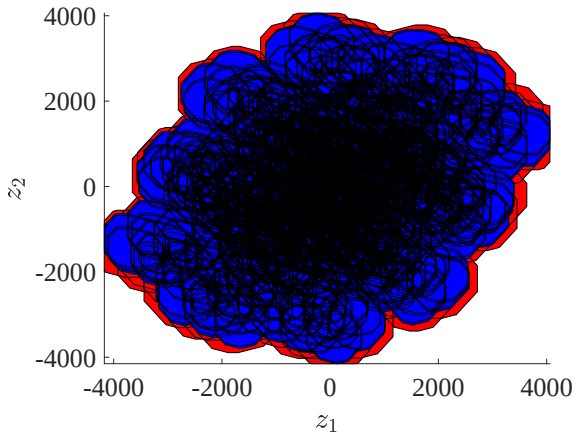

Figure 6.10. Example of a randomly generated two-dimensional hybrid zonotope and it's over-approximation.

The same analysis is applied to random hybrid zonotopes in four dimensions, and the results are provided in Figure 6.12. Specifically, 20 random hybrid zonotopes are generated with $n = 4$, $n_g = 70$ continuous generators, $n_b = 15$ binary generators, and $n_c = 20$ constraints. Algorithm 5 is applied to generate over-approximating hybrid zonotopes with complexity $n_g^r = 56$, $n_b^r = 12$, and $n_c^r = 16$. In this case, the randomly generated hybrid zonotopes with $n_b = 15$ had potentially $|\mathcal{T}| \geq 32 \times 10^3$ nonempty leaves, resulting in variations of summing over the radii of the convex subsets, methods RS and RS_s, becoming too computationally expensive, and are therefore excluded from the analysis. Similar to the results when reducing two dimensional hybrid zonotopes, in this case the error metric VB using the bisection approach to cover the hybrid zonotope by hyperboxes as described in Algorithm 6 performed the best. However, the computation time to perform all $100n/2 = 200$

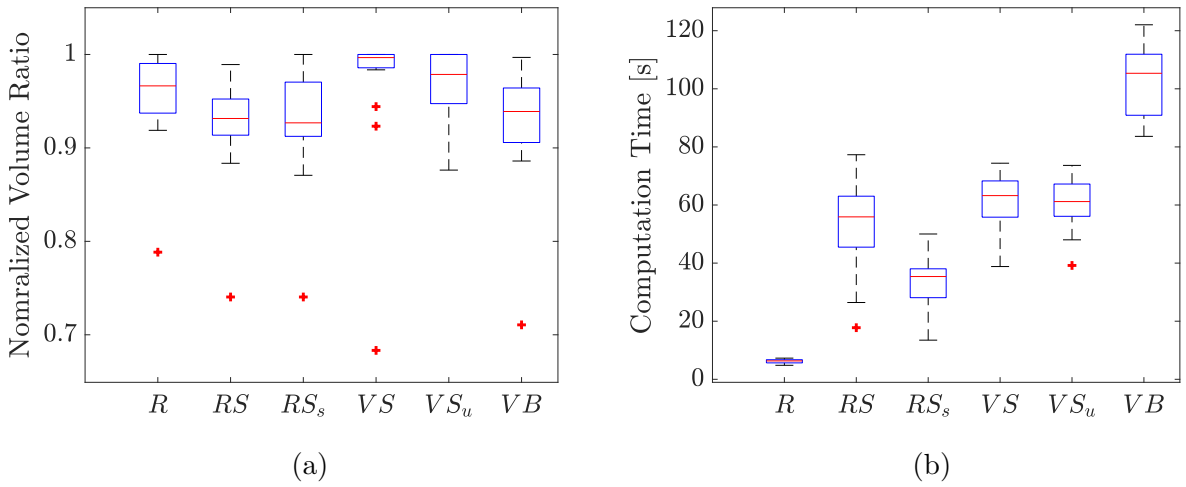

Figure 6.11. Comparison of the using the different error metrics in the order reduction method given by Algorithm 5 for 20 randomly generated hybrid zonotopes. The hybrid zonotopes are reduced from ones with $n_g = 50$, $n_b = 10$, and $n_c = 15$ to have complexity $n_g^r = 40$, $n_b^r = 8$, and $n_c^r = 12$. 6.11a Comparison of the resulting volume ratios. 6.11b Comparison of the time required to perform each of the reductions.

bisections required more than twice the computation time of the other methods. Surprisingly, in this experiment using the radius metric R outperformed sampling the volume VS with $100n = 400$ randomly sampled points in both the volume ratio and computation time.

6.4.2 Thermostat-Controlled Heated Rooms

This example demonstrates the use of the proposed order reduction techniques on the forward reachable sets of the hybrid system modeling the temperature dynamics of six adjacent rooms with two thermostat-controlled heaters, as previously examined in Section 4.1.4. The goal of this example is to demonstrate that the complex reachable sets can be represented more compactly as hybrid zonotopes for use in further analysis.

In Section 4.1.4 it was shown that the reachable set for Case$(6, 2)$ at time step $k = 100$ could be represented compactly by removing redundant binary factors and linear inequality constraints of the MLD system. Using these two redundancy removal methods resulted in the reachable set $\mathcal{R}_{100}$ represented by $n_{g,100} = 283$ continuous generators, $n_{b,100} = 29$

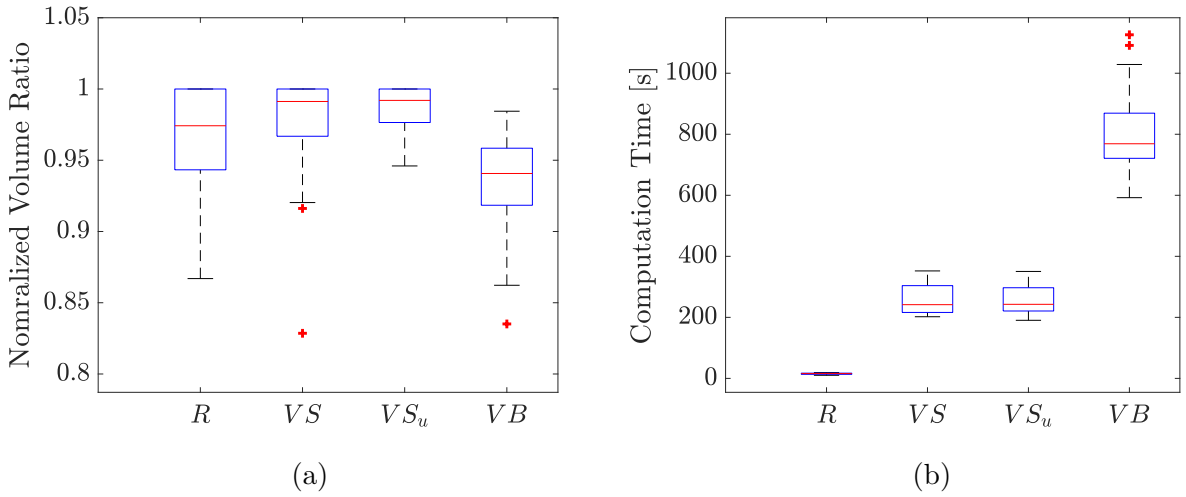

Figure 6.12. Comparison of the using the different error metrics in the order reduction method given by Algorithm 5 for 20 randomly generated hybrid zonotopes. The hybrid zonotopes are reduced from ones with $n_g = 50$, $n_b = 10$, and $n_c = 15$ to have complexity $n_g^r = 40$, $n_b^r = 8$, and $n_c^r = 12$. 6.11a Comparison of the resulting volume ratios. 6.11b Comparison of the time required to perform each of the reductions.

binary generators, and $n_{c,100} = 177$ constraints and was found in 10.4 seconds (see Tables 4.2 and 4.3). Applying the additional redundancy removal techniques described in Section 6.1, the reachable set $\mathcal{R}_{100}^r$ has only $n_{g,100}^r = 137$ continuous generators, $n_{b,100}^r = 29$ binary generators, and $n_{c,100}^r = 31$ constraints to represent the same union of 657 convex polytopes. The hybrid zonotope is then rescaled using Algorithm 2. Identifying and removing this additional redundancy and rescaling the hybrid zonotope took an additional 18.54 seconds. It is now shown how each of the order reduction techniques for finding over-approximations effect the reachable set $\mathcal{R}_{100}$ individually.

Lift then reduce continuous generators: the hybrid zonotope $\mathcal{R}_{100}^r$ with redundancy removed is now reduced to the over-approximating hybrid zonotope $\tilde{\mathcal{R}}_{100}^r$ with a reduced $\tilde{n}_{g,100}^r = 100$ continuous generators, and the same $\tilde{n}_{b,100}^r = 29$ binary generators and $\tilde{n}_{c,100}^r = 31$ equality constraints from the previous step, using the lift then reduce strategy described in Section 6.2.3. This is performed using the zonotope order reduction method developed for constrained zonotopes in [18] and [90]. Removing 37 continuous generators using this

method took 0.04 seconds. The over-approximating hybrid zonotope is depicted in Figure 6.13.

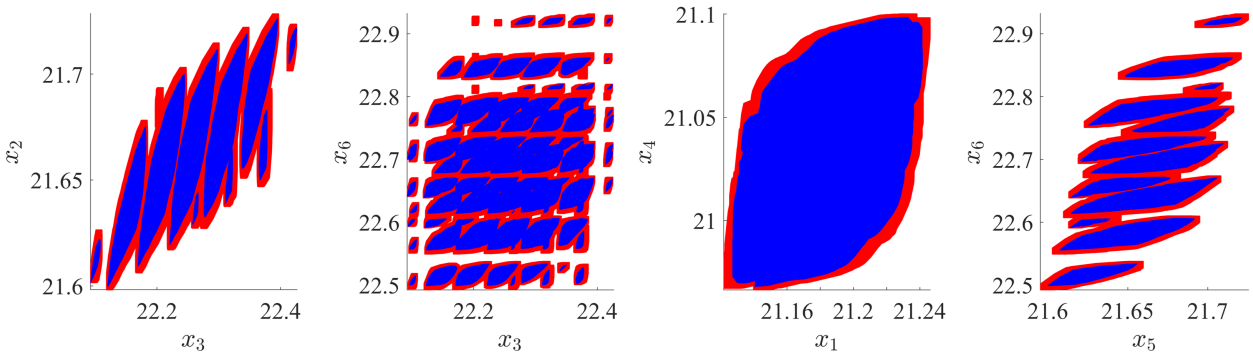

Figure 6.13. Projections of the over-approximated reachable set $\tilde{\mathcal{R}}^r_{100}$ with continuous generators reduced from $n^r_{g,100} = 137$ to $\tilde{n}^r_{g,100} = 100$ using the lift then reduce strategy. Exact reachable set $\mathcal{R}^r_{100}$ is shown in blue and it's over-approximation $\tilde{\mathcal{R}}^r_{100}$ in red.

Relax binary factors: the hybrid zonotope $\mathcal{R}^r_{100}$ with redundancy removed is now reduced to the over-approximating hybrid zonotope $\tilde{\mathcal{R}}^r_{100}$ with a reduced $\tilde{n}^r_{b,100} = 20$ binary generators, an increased $\tilde{n}^r_{g,100} = 146$ continuous generators, and the same $\tilde{n}^r_{c,100} = 31$ equality constraints using Algorithm 4. The over-approximating hybrid zonotope has a reduced $|\mathcal{T}| = 123$ convex subsets. The reduction method is performed using the error metric summing over the $n^r_b/2$ best candidate over-approximations (see RS_s in Section 6.4.1). Removing these 9 binary generators using this error metric took 427.96 seconds. The resulting hybrid zonotope is depicted in Figure 6.14.

Remove equality constraints: the hybrid zonotope $\mathcal{R}^r_{100}$ with redundancy removed is now reduced to the over-approximating hybrid zonotope $\tilde{\mathcal{R}}^r_{100}$ with a reduced $\tilde{n}^r_{c,100} = 25$ equality constraints and $\tilde{n}^r_{g,100} = 131$ continuous generators, and the same $\tilde{n}^r_{b,100} = 29$ binary generators using Algorithm 3. The reduction method is performed using the volume ratio estimated by randomly sampling 600 points from the interval hull (see VS from Section 6.4.1). Removing these 6 equality constraints using this error metric took 625.59 seconds. The resulting hybrid zonotope is depicted in Figure 6.15.

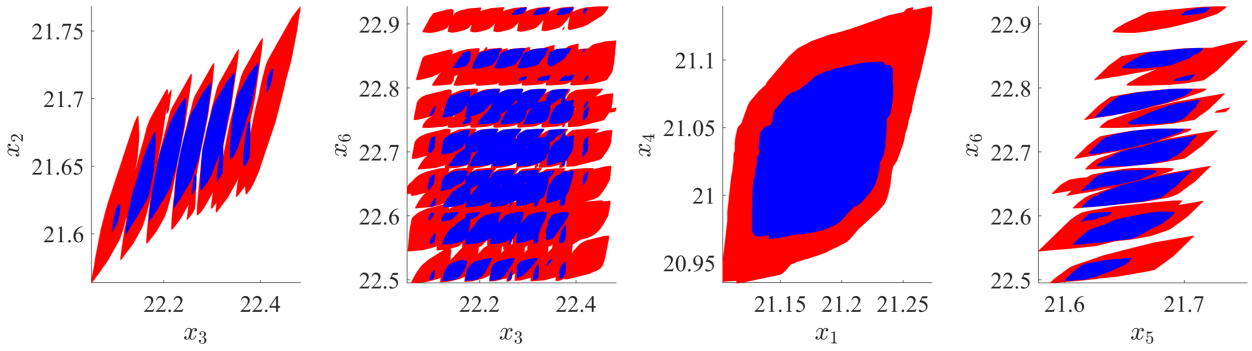

Figure 6.14. Projections of the over-approximated reachable set $\tilde{\mathcal{R}}^r_{100}$ with binary generators reduced to from $n^r_{b,100} = 29$ to $\tilde{n}^r_{b,100} = 20$ using Algorithm 4. Exact reachable set $\mathcal{R}^r_{100}$ is shown in blue and it's over-approximation $\tilde{\mathcal{R}}^r_{100}$ in red.

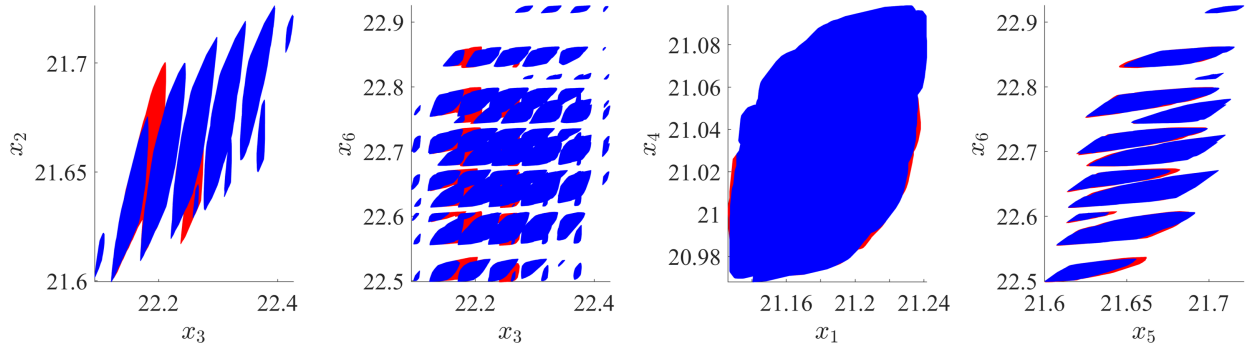

Figure 6.15. Projections of the over-approximated reachable set $\tilde{\mathcal{R}}^r_{100}$ with equality constraints reduced to from $n^r_{c,100} = 31$ to $\tilde{n}^r_{c,100} = 25$ using Algorithm 3. Exact reachable set $\mathcal{R}^r_{100}$ is shown in blue and it's over-approximation $\tilde{\mathcal{R}}^r_{100}$ in red.

Reducing the reachable set: All three of the previously describe steps are now performed on the same hybrid zonotope in series. First, the number of continuous generators are reduced to $\tilde{n}^r_g = 100$, then binary generators are relaxed until $\tilde{n}^r_b = 20$, finally the equality constraints are removed until $\tilde{n}^r_c = 25$, using the individually described methods. The total process took 1152 seconds. The resulting hybrid zonotope has $\tilde{n}^r_g = 87$ continuous generators, $\tilde{n}^r_b = 20$ binary generators, and $\tilde{n}^r_c = 25$ constraints and is depicted in Figure 6.16.

Reducing the complexity of the hybrid zonotope in all three of these process results in a hybrid zonotope with a volume ratio of $\Theta_V = 1.70$ compared to the exact reachable set. The large computation time is primarily due to the evaluation of the error metrics for each of the candidate over-approximations, resulting in many MILPs needing to be evaluated. Nonetheless, this approach provides a nonconvex outer-approximation of the true reachable set, and allows for the analysis to be continued with a fixed computational effort by iteratively applying the proposed reduction techniques.

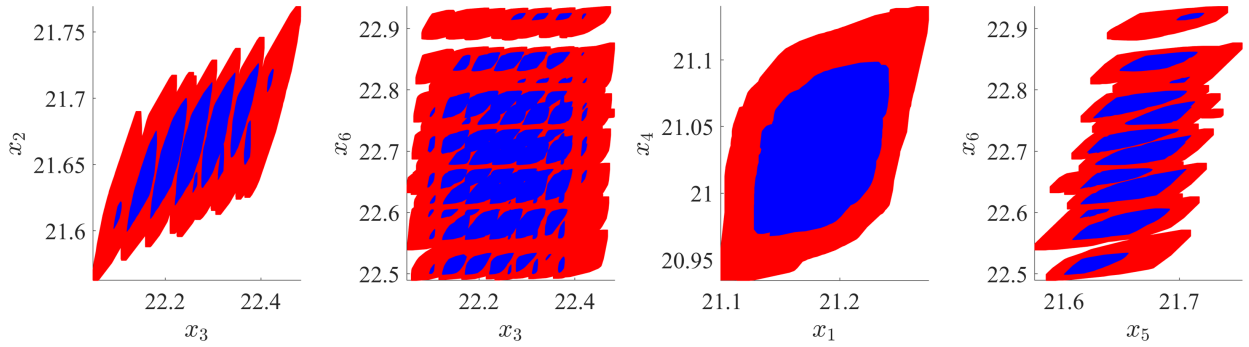

Figure 6.16. Projections of the over-approximated reachable set $\tilde{\mathcal{R}}^r_{100}$ with $\tilde{n}^r_g = 87$, $\tilde{n}^r_b = 20$ binary generators, and $\tilde{n}^r_c = 25$ equality constraints. Exact reachable set $\mathcal{R}^r_{100}$ is shown in blue and it's over-approximation $\tilde{\mathcal{R}}^r_{100}$ in red.

6.4.3 Model Predictive Control

This example shows how the proposed order reduction techniques combined in Algorithm 5 may be used iteratively in the forward reachability analysis of hybrid systems and applies them to the double integrator under closed-loop MPC, as previously examined in Section 4.2.5. Specifically, the perturbed case considering model mismatch and when the closed-loop system is subjected to bounded, additive disturbances is reevaluated. The goal of this example is to demonstrate how order reduction allows the time horizon to be extended to any specified amount while maintaining a reduced computational complexity to provide conservative results.

The dynamics are propagated for twenty discrete time steps using the successor operator given by Theorem 5.11 leveraging state-update sets while performing order reduction using

Algorithm 5 at every third time step. The set-points used for the desired complexity of the over-approximative reachable sets are

$$\tilde{n}_g \leq 150\,, \tag{6.46a}$$

$$\tilde{n}_b \leq 15 \ \wedge \ |\tilde{\mathcal{T}}| \leq 100\,, \tag{6.46b}$$

$$\tilde{n}_c \leq 100\,, \tag{6.46c}$$

where the number of binary factors are reduced until they are less than 15 and the number of convex subsets of the hybrid zonotope's binary tree is less than 100. Each step of the order reduction described by Algorithm 5 is only performed if the resulting volume ratio of the input and reduced set given by (6.31) remains below $\Theta_v \leq 1.1$. That is, if at any point the algorithm detects that the introduced error is too large, the procedure is exited and the next step in the order reduction algorithm is attempted. All error metrics are evaluated using the over-approximated volume estimated from the disjoint covering produced by the bisection algorithm with 250 total cuts, as described in Section 6.3.2. Additionally, the resulting reduced hybrid zonotope is intersected with the original set's interval hull to guarantee that the over-approximation is at least as good as the convex enclosure.

The first step in the reachability analysis is to generate the state-update set using the method described in Section 5.3.2. The resulting hybrid zonotope $\Phi \subset \mathbb{R}^4$ has $n_{g,\phi} = 55$ continuous generators, $n_{b,\phi} = 10$ binary generators, and $n_{c,\phi} = 43$ constraints and requires only 0.001 seconds to determine. Finding the representation of the MPC's explicit control law as a hybrid zonotope required to generate the state-update set as described in Section 4.2.3 took 2.11 seconds. The complexity of the resulting state-update set may be minimized by applying the redundancy removal techniques described in Section 6.1 and results in a reduced hybrid zonotope $\Phi^r \subset \mathbb{R}^4$ with $n^r_{g,\phi} = 34$ continuous generators, $n^r_{b,\phi} = 10$ binary generators, and $n^r_{c,\phi} = 22$ constraints, requiring an additional 1.83 seconds of computation time. Performing this redundancy removal upfront substantially reduces the complexity that will be introduced through iterative applications of the successor operator defined by Theorem 5.2.1, and took an additional computation time of 3.94 seconds. Once the state-

update set has been found, the dynamics are propagated forward in time for twenty discrete time steps while performing order reduction at every third iteration.

The reachability analysis beings at the initial set $\mathcal{X}_0 = \{x \in \mathbb{R}^2 \mid \|x_1\|_\infty \leq 5, x_2 = 0\}$ and the resulting over-approximating reachable sets are depicted in Figure 6.17. The result of this reachability analysis with an extended time horizon shows that the forward reachable set converges, and that the system is safe for all time. This inferred invariance follows from the fact that $\mathcal{R}_{20} \subset \bigcup_0^{20} \mathcal{R}_\text{i}$. This property can be verified visually from Figure 6.17, which was easily plotted because of the reduction in the number of nonempty convex subsets achieved by the proposed order reduction techniques.

The computation time of only using redundancy removal was 435 seconds to find the exact reachable set, while using order reduction in addition to redundancy removal took $4,457$ seconds. While the computation time required by the order reduction increases by ten times that of using redundancy removal alone, this additional time was spent almost entirely in computing the error metrics, which were chosen to be rigorous by employing the bisection algorithm with 250 cuts. Improvements in the computation time could be achieved by employing one of the other error metrics described in Section 6.3, for example the radius ratio, at the cost of potentially introducing additional error in the over-approximations.

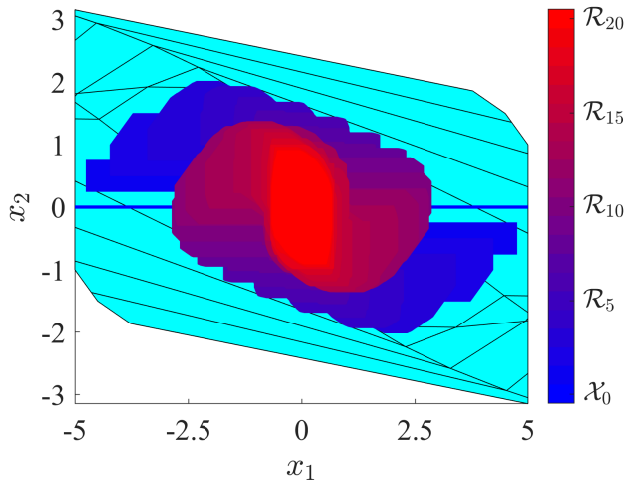

Figure 6.17. Depiction of the over-approximative forward reachable sets of the perturbed closed-loop system under model predictive control for twenty time steps. The reachable set converging proves the system is safe for all time.

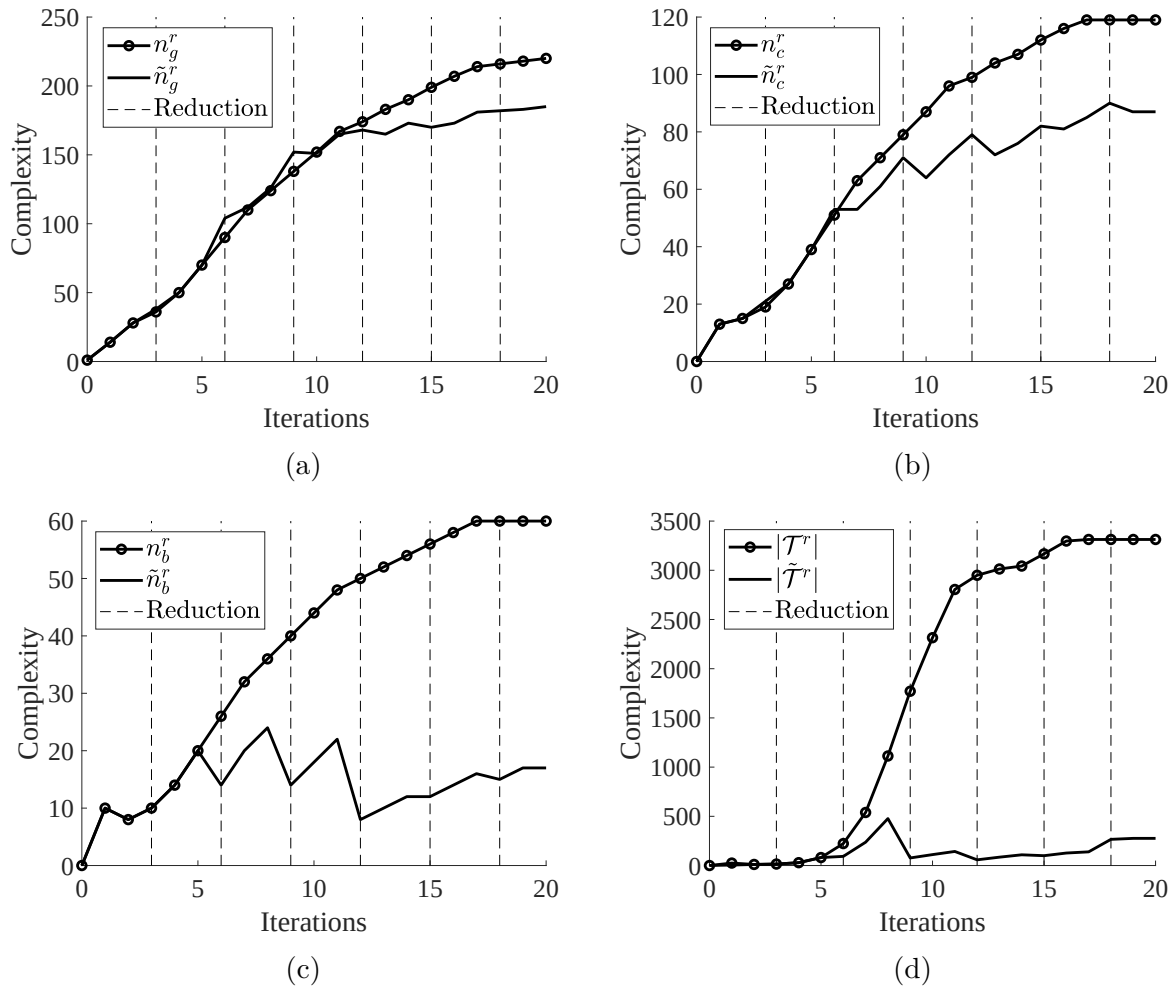

Figure 6.18. Comparison of the representation complexity of the over-approximative reachable sets with the exact sets found using only redundancy removal for the perturbed closed-loop system under model predictive control. Iterations where order reduction was performed are denoted by vertical dashed lines. 6.18a Comparison of the number of continuous generators. 6.18b Comparison of the number of equality constraints. 6.18c Comparison of the number of binary generators. 6.18d Comparison of the number of nonempty leaves in the set's binary tree.

A comparison of the representation complexity of the exact reachable sets found using only redundancy removal and that of the over-approximating hybrid zonotopes are given in Figure 6.18. The number of continuous generators of the over-approximation is reduced to a value of $\tilde{n}_{g,20}^r = 195$ which is a modest reduction when compared to the number of non-redundant continuous generators of $n_{g,20}^r = 220$. Note that in this case, reducing the number

of continuous generators to below the target value of 150 resulted in too much additional error, and was not achieved at each iteration. The number of reduced equality constraints was $\tilde{n}^r_{c,20} = 85$ which is a considerable reduction below that of using redundancy removal alone of $n^r_{c,20} = 119$ and remains below the target value of 100. The binary generators on the other-hand are aggressively reduced from $n^r_{b,20} = 60$ to $\tilde{n}^r_{b,20} = 12$, resulting in a substantial reduction in the number of nonempty convex subsets from $|\mathcal{T}^r_{20}| = 3313$ to $|\tilde{\mathcal{T}}^r_{20}| = 103$. Also note that these binary factors were relaxed to be continuous, which can be seen in the increase in continuous factors at the iterations where order reduction is performed. However, this relaxation of the binary factors often resulted in additional redundancy that was detected and removed at the next iteration. The effectiveness of the proposed approach can be seen by the estimated volume ratio between the exact reachable sets and the over-approximations as shown in Figure 6.19. Note that the accumulated error due to iterative over-approximations decays quickly due to the controller successfully driving the set of system trajectories toward the origin. The resulting over-approximations at iterations $k = 6, 9, 12, 15$ are depicted in Figure 6.20. In these figures, it can be seen that the over-approximations maintain the nonconvexity of the set and provide better approximations than could be achieved by a convex enclosure.

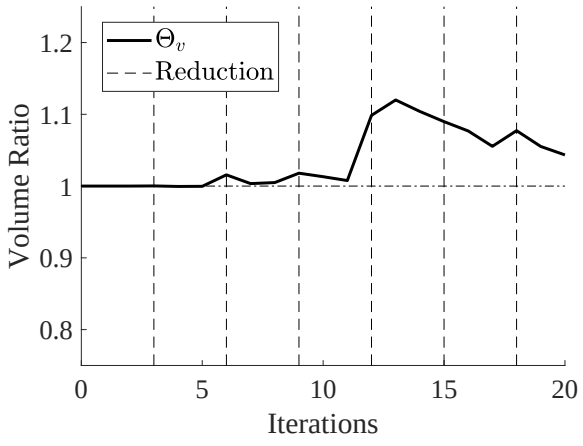

Figure 6.19. Estimated volume ratio between the exact reachable sets of the perturbed closed-loop MPC system and the over-approximated reachable sets. Iterations where order reduction is performed are denoted by vertical dashed lines.

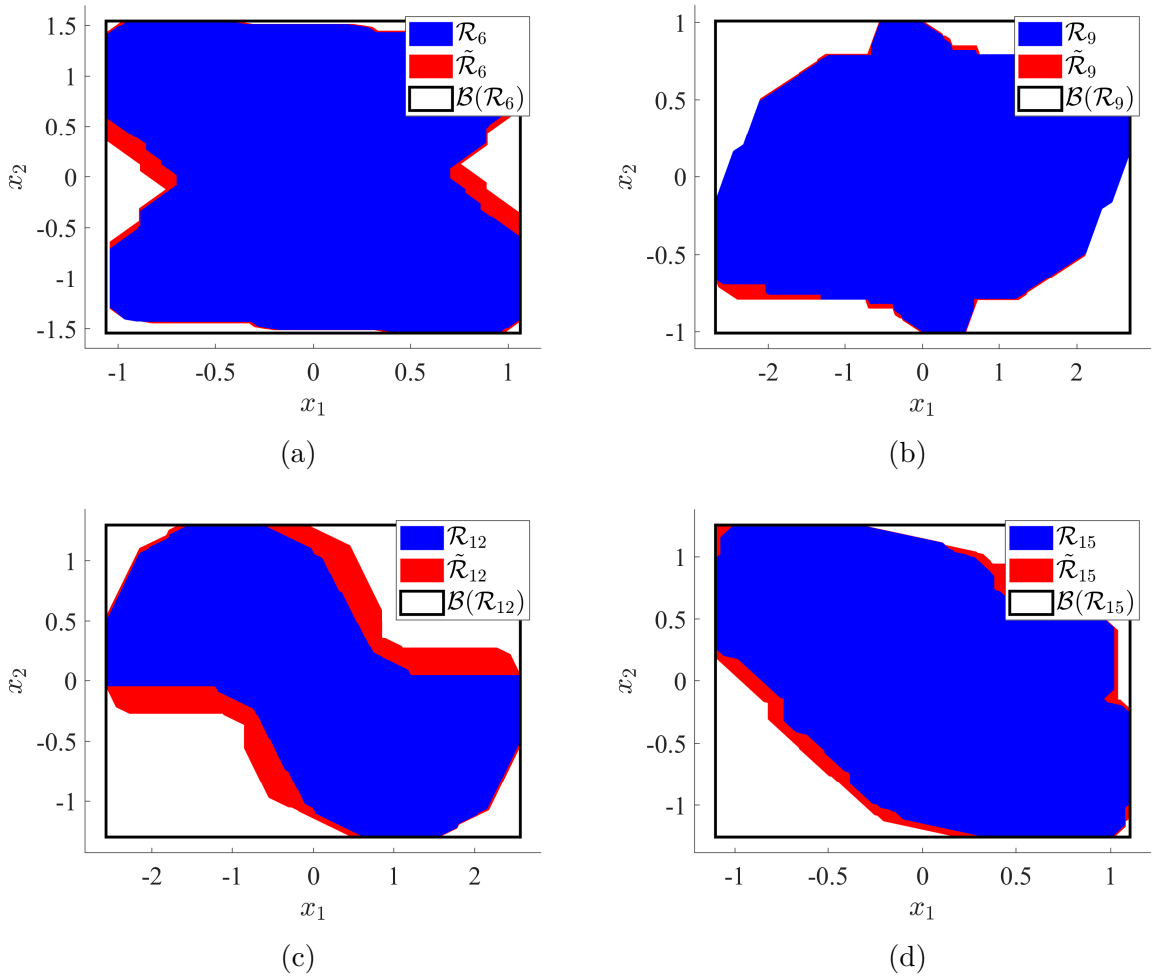

Figure 6.20. Depiction of the over-approximations at iterations $k = 6, 9, 12, 15$ produced by the order reduction techniques for the perturbed closed-loop MPC system. The sets input to Algorithm 5 are shown in blue and the resulting over-approximations shown in red. 6.20a Result of order reduction at time step $k = 6$. 6.20b Result of order reduction at time step $k = 9$. 6.20c Result of order reduction at time step $k = 12$. 6.20d Result of order reduction at time step $k = 15$.

6.5 Chapter Summary

In this chapter I have presented methods for reducing the complexity of hybrid zonotopes. I have shown how redundancy in every aspect of the hybrid zonotope set definition, including continuous generators, binary generators, and equality constraints, may be detected and removed. I developed order reduction techniques to further reduce the complexity of hybrid

zonotopes to generate nonconvex over-approximations. These order reduction techniques extend methods developed for zonotopes, constrained zonotopes, and mixed-integer programs. I then developed error metrics to evaluate the differences between multiple hybrid zonotopes. The presented error metrics include approximation of the set's physical characteristics, such as radius and volume, as well as heuristics that are useful in determining tight over-approximations. Using the proposed methods for order reduction and redundancy removal give the user a way to tune the trade-off in computational complexity and accuracy. Applying the proposed methods within iterative set operations on hybrid zonotopes, analysis may be performed indefinitely to provide conservative results of complex nonconvex problems. Numerical examples show the effectiveness of the proposed methods as well as evaluate the benefits of the different error metrics.

7. Conclusions

7.1 Summary of Research Contributions

The reachability analysis of hybrid systems is inherently complex. As intersections with guard sets occur and uncertain discrete inputs are applied, the number of nonconvex features grows exponentially. The state of the art often reduces the problem to a collection of convex sets, resulting in conservative algorithms with case-specific trade-offs in accuracy and computational effort. In this dissertation, I derived a new mixed-integer set representation named the *hybrid zonotope* that is able to represent nonconvex sets with an exponential number of features using a linear number of continuous and discrete variables. I have shown how the hybrid zonotope is equivalent to the union of 2^N constrained zonotopes (convex polytopes) through the addition of N binary zonotope factors, and is thus able to compactly represent nonconvex and disconnected sets.

I have derived identities for, and proven closure under, linear mappings, Minkowski sums, generalized intersections, halfspace intersections, Cartesian products, unions, and complements of hybrid zonotopes. To improve computational performance, I have derived redundancy removal techniques that reduce the complexity of hybrid zonotopes without altering the set. When further computational benefits are necessary, I have derived overapproximation techniques that allow more complex analysis to be performed to generate conservative results, while maintaining the nonconvexity of the set. Thus providing a nonconvex set representation applicable to a broad class of set-theoretic controls problems.

Beyond the derivation of set operations, I have shown how linear mixed-integer constraints may be embedded within the hybrid zonotope set representation. Using this approach, I have shown how the exact forward reachable sets of hybrid systems, including mixed logical dynamical systems and closed-loop MPC, may be found algebraically with linear growth in representation complexity. In addition, I have shown how optimality conditions may be embedded within the hybrid zonotope, resulting in the explicit solution of general multiparametric quadratic programs represented by a single hybrid zonotope. This representation of the optimal set may then be decomposed into a collection of constrained zonotopes to give the quadratic program's explicit solution.

Building upon these results for forward reachability, I have presented a closed-form solution for the exact backward reachable sets of linear hybrid systems as hybrid zonotopes by leveraging a new construct named the *state-update set* that encodes all possible state transitions of a dynamic system over one discrete time step within a single set. I have shown how the state-update sets of mixed logical dynamical systems and closed-loop MPC may be represented as hybrid zonotopes by calculating the system's one step forward reachable set under augmented dynamics. Thereafter I have shown how state-update sets may be used to find both the forward and backward reachable sets, and how they may be made robust to bounded disturbances. I have shown through multiple examples the scalability of these approaches and how they can be used to provide robust certificates of a system's safety and reduce the conservatism of previous methods in the literature.

7.2 Future Research Directions

The research presented in this dissertation has focused on developing the fundamental tools for the use of hybrid zonotopes in set-theoretic methods. Using these fundamental tools, it is now possible to extend many of the existing algorithms that rely on convex approximations of nonconvex sets to be performed exactly. This approach to exact analysis could be used to not only improve the accuracy of the results, but give a way to expose the level of conservatism induced by the traditional convex approximations.

The operations presented in this dissertation were exact and rigorous, and often employ many calls to commercial mixed-integer linear programming solvers. There is potential to improve the computation time of these methods by replacing the calls to commercial solvers with heuristics developed for mixed-integer programs to provide conservative bounds. These heuristics may be customized to leverage the hybrid zonotope's structured form and have potential for substantial improvement in the computation time and scalability of the proposed methods.

Providing a more scalable approach for the exact backwards reachable sets of hybrid system's provides a promising approach for finding positive invariant sets to be used in optimal control policies. While this dissertation has provided an example of how this may be

done and improves upon previous results for linear MPC, the convergence of the algorithm was determined by observation. While set containment can be verified using the provided propositions, the approach has potentially exponential growth in complexity when the superset is nonconvex. Furthermore, when the invariant set is found, it may be too complex for use as a constraint in online optimal control algorithms. Derivation of conditions for the containment of convex sets within hybrid zonotopes may extend the proposed methods to provide less conservative invariant sets when compared to traditional results, and that may be easily implemented online.

The results for reachable sets of hybrid systems in this dissertation were limited to those with linear differential equations. A potentially impactful result would be to extend these results to system's with nonlinear differential equations by leveraging existing over-approximation methods in the literature. Applying linear model predictive control to nonlinear systems is common in practice, and providing over-approximations of the reachable sets of such closed-loop nonlinear systems could provide robust a posteriori certificates of safety. This could be achieved using the same set of optimal inputs derived in this dissertation represented by a hybrid zonotope combined with an over-approximation method for the propagation of the nonlinear dynamics.

Finally, the representation of general multiparametric quadratic programs as hybrid zonotopes provides a way to compactly represent these complex solutions. Previous results in the literature are often limited by the possible exponential growth in the number of critical regions. There is potential for the results in this dissertation to curve this exponential growth and extend explicit control policies to more complex systems. Methods of efficiently using the hybrid zonotope's binary tree to find these solutions could provide a new approach with improved scalability.

REFERENCES

[1] F. Blanchini and S. Miani, *Set-Theoretic Methods in Control*, Second. Cham: Springer International Publishing, 2015, ISBN: 978-3-319-17933-9.

[2] B. Chachuat, B. Houska, R. Paulen, N. Peri'c, J. Rajyaguru, and M. E. Villanueva, "Set-Theoretic Approaches in Analysis, Estimation and Control of Nonlinear Systems," *IFAC-PapersOnLine*, vol. 48, no. 8, pp. 981–995, Jan. 2015, ISSN: 2405-8963. DOI: 10.1016/j.ifacol.2015.09.097.

[3] E. Asarin, T. Dang, G. Frehse, A. Girard, C. Le Guernic, and O. Maler, "Recent progress in continuous and hybrid reachability analysis," in *2006 IEEE Conference on Computer Aided Control System Design, 2006 IEEE International Conference on Control Applications, 2006 IEEE International Symposium on Intelligent Control*, Oct. 2006, pp. 1582–1587. DOI: 10.1109/CACSD-CCA-ISIC.2006.4776877.

[4] J. K. Scott, R. Findeisen, R. D. Braatz, and D. M. Raimondo, "Design of active inputs for set-based fault diagnosis," in *2013 American Control Conference*, Jun. 2013, pp. 3561–3566. DOI: 10.1109/ACC.2013.6580382.

[5] D. Ioan, I. Prodan, F. Stoican, S. Olaru, and S. Niculescu, "Complexity Bounds for Obstacle Avoidance within a Zonotopic Framework," in *2019 American Control Conference (ACC)*, Jul. 2019, pp. 335–340. DOI: 10.23919/ACC.2019.8814976.

[6] S. Rakovic, P. Grieder, M. Kvasnica, D. Mayne, and M. Morari, "Computation of invariant sets for piecewise affine discrete time systems subject to bounded disturbances," in *2004 43rd IEEE Conference on Decision and Control (CDC) (IEEE Cat. No.04CH37601)*, vol. 2, Dec. 2004, 1418–1423 Vol.2. DOI: 10.1109/CDC.2004.1430242.

[7] M. Althoff, O. Stursberg, and M. Buss, "Reachability analysis of nonlinear systems with uncertain parameters using conservative linearization," in *2008 47th IEEE Conference on Decision and Control*, Dec. 2008, pp. 4042–4048. DOI: 10.1109/CDC.2008.4738704.

[8] G. Frehse, C. Le Guernic, A. Donzé, *et al.*, "SpaceEx: Scalable Verification of Hybrid Systems," in *Computer Aided Verification*, G. Gopalakrishnan and S. Qadeer, Eds., Berlin, Heidelberg: Springer, 2011, pp. 379–395, ISBN: 978-3-642-22110-1. DOI:
.

[9] G. Frehse, R. Kateja, and C. Le Guernic, "Flowpipe approximation and clustering in space-time," in *Proceedings of the 16th international conference on Hybrid systems: computation and control*, New York, NY, USA: Association for Computing Machinery, Apr. 2013, pp. 203–212, ISBN: 978-1-4503-1567-8. DOI: 10.1145/2461328.2461361.

[10] M. Althoff, G. Frehse, and A. Girard, "Set Propagation Techniques for Reachability Analysis," *Annual Review of Control, Robotics, and Autonomous Systems*, vol. 4, no. 1, 2021. DOI: 10.1146/annurev-control-071420-081941.

[11] M. Althoff, O. Stursberg, and M. Buss, "Computing reachable sets of hybrid systems using a combination of zonotopes and polytopes," *Nonlinear Analysis: Hybrid Systems*, vol. 4, no. 2, pp. 233–249, May 2010, ISSN: 1751-570X. DOI: 10.1016/j.nahs.2009.03.009.

[12] M. Herceg, M. Kvasnica, C. N. Jones, and M. Morari, "Multi-Parametric Toolbox 3.0," in *2013 European Control Conference (ECC)*, Jul. 2013, pp. 502–510. DOI: 10.23919/ECC.2013.6669862.

[13] I. Prodan, F. Stoican, S. Olaru, and S.-I. Niculescu, *Mixed-Integer Representations in Control Design: Mathematical Foundations and Applications*. Springer International Publishing, 2016, ISBN: 978-3-319-26993-1. DOI: 10.1007/978-3-319-26995-5.

[14] F. Borrelli, A. Bemporad, and M. Morari, *Predictive Control for Linear and Hybrid Systems*, Jun. 2017. DOI: 10.1017/9781139061759.

[15] W. Hagemann, "Efficient Geometric Operations on Convex Polyhedra, with an Application to Reachability Analysis of Hybrid Systems," *Mathematics in Computer Science*, vol. 9, no. 3, pp. 283–325, Oct. 2015, ISSN: 1661-8289. DOI: 10.1007/s11786-015-0238-9.

[16] E. Boros, K. Elbassioni, V. Gurvich, and H. R. Tiwary, "The negative cycles polyhedron and hardness of checking some polyhedral properties," *Annals of Operations Research*, vol. 188, no. 1, pp. 63–76, Aug. 2011, ISSN: 1572-9338. DOI: 10.1007/s10479-010-0690-5.

[17] P. McMullen, "On zonotopes," *Transactions of the American Mathematical Society*, vol. 159, pp. 91–109, 1971, ISSN: 0002-9947, 1088-6850. DOI: 10.1090/S0002-9947-1971-0279689-2.

[18] J. K. Scott, D. M. Raimondo, G. R. Marseglia, and R. D. Braatz, "Constrained zonotopes: A new tool for set-based estimation and fault detection," *Automatica*, vol. 69, pp. 126–136, Jul. 2016, ISSN: 0005-1098. DOI: 10.1016/j.automatica.2016.02.036.

[19] A. Kopetzki, B. Schürmann, and M. Althoff, "Methods for order reduction of zonotopes," in *2017 IEEE 56th Annual Conference on Decision and Control (CDC)*, Dec. 2017, pp. 5626–5633. DOI: 10.1109/CDC.2017.8264508.

[20] V. Raghuraman and J. P. Koeln, "Set operations and order reductions for constrained zonotopes," *Automatica*, vol. 139, p. 110 204, May 1, 2022, ISSN: 0005-1098. DOI: 10.1016/j.automatica.2022.110204.

[21] J. Koeln, V. Raghuraman, and B. Hencey, "Vertical hierarchical MPC for constrained linear systems," *Automatica*, vol. 113, p. 108 817, Mar. 2020, ISSN: 0005-1098. DOI: 10.1016/j.automatica.2020.108817.

[22] B. S. Rego, D. M. Raimondo, and G. V. Raffo, "Set-based state estimation of nonlinear systems using constrained zonotopes and interval arithmetic*," in *2018 European Control Conference (ECC)*, Jun. 2018, pp. 1584–1589. DOI: 10.23919/ECC.2018.8550353.

[23] B. S. Rego, G. V. Raffo, J. K. Scott, and D. M. Raimondo, "Guaranteed methods based on constrained zonotopes for set-valued state estimation of nonlinear discrete-time systems," *Automatica*, vol. 111, p. 108 614, Jan. 2020, ISSN: 0005-1098. DOI: 10.1016/j.automatica.2019.108614.

[24] V. Raghuraman, V. Renganathan, T. H. Summers, and J. P. Koeln, "Hierarchical MPC with coordinating terminal costs," in *2020 American Control Conference (ACC)*, Jul. 2020, pp. 4126–4133. DOI: 10.23919/ACC45564.2020.9147685.

[25] R. Alur, C. Courcoubetis, N. Halbwachs, *et al.*, "The algorithmic analysis of hybrid systems," *Theoretical Computer Science*, vol. 138, no. 1, pp. 3–34, Feb. 1995, ISSN: 0304-3975. DOI: 10.1016/0304-3975(94)00202-T.

[26] A. Bemporad, F. D. Torrisi, and M. Morari, "Optimization-Based Verification and Stability Characterization of Piecewise Affine and Hybrid Systems," in *Hybrid Systems: Computation and Control*, N. Lynch and B. H. Krogh, Eds., Berlin, Heidelberg: Springer, 2000, pp. 45–58, ISBN: 978-3-540-46430-3. DOI: .

[27] V. D. Blondel and J. N. Tsitsiklis, "Complexity of stability and controllability of elementary hybrid systems," *Automatica*, vol. 35, no. 3, pp. 479–489, Mar. 1999, ISSN: 0005-1098. DOI: 10.1016/S0005-1098(98)00175-7.

[28] D. Liberzon, *Switching in Systems and Control*. Birkhäuser Basel, 2003, ISBN: 978-0-8176-4297-6.

[29] L. Doyen, G. Frehse, G. J. Pappas, and A. Platzer, "Verification of Hybrid Systems," in *Handbook of Model Checking*, E. M. Clarke, T. A. Henzinger, H. Veith, and R. Bloem, Eds., Cham: Springer International Publishing, 2018, pp. 1047–1110, ISBN: 978-3-319-10575-8. DOI: .

[30] M. Chen and C. J. Tomlin, "Hamilton–Jacobi Reachability: Some Recent Theoretical Advances and Applications in Unmanned Airspace Management," *Annual Review of Control, Robotics, and Autonomous Systems*, vol. 1, no. 1, pp. 333–358, 2018. DOI: 10.1146/annurev-control-060117-104941.

[31] M. Althoff and B. H. Krogh, "Avoiding geometric intersection operations in reachability analysis of hybrid systems," in *Proceedings of the 15th ACM international conference on Hybrid Systems: Computation and Control*, New York, NY, USA: Association for Computing Machinery, Apr. 2012, pp. 45–54, ISBN: 978-1-4503-1220-2. DOI: 10.1145/2185632.2185643.

[32] S. V. Rakovic, M. Baric, and M. Morari, "Max-min control problems for constrained discrete time systems," in *2008 47th IEEE Conference on Decision and Control*, Dec. 2008, pp. 333–338. DOI: 10.1109/CDC.2008.4739218.

[33] G. Palmieri, M. Barić, L. Glielmo, and F. Borrelli, "Robust vehicle lateral stabilisation via set-based methods for uncertain piecewise affine systems," *Vehicle System Dynamics*, vol. 50, no. 6, pp. 861–882, Jun. 1, 2012, ISSN: 0042-3114. DOI: 10.1080/00423114.2012.666353.

[34] M. Althoff, "On Computing the Minkowski Difference of Zonotopes," *arXiv:1512.02794 [cs]*, Nov. 2016.

[35] L. Yang and N. Ozay, "Scalable zonotopic under-approximation of backward reachable sets for uncertain linear systems," *IEEE Control Systems Letters*, vol. 6, pp. 1555–1560, 2022, ISSN: 2475-1456. DOI: 10.1109/LCSYS.2021.3123228.

[36] X. Chen, E. Ábrahám, and S. Sankaranarayanan, "Taylor Model Flowpipe Construction for Non-linear Hybrid Systems," in *2012 IEEE 33rd Real-Time Systems Symposium*, Dec. 2012, pp. 183–192. DOI: 10.1109/RTSS.2012.70.

[37] M. Althoff, "Reachability analysis of nonlinear systems using conservative polynomialization and non-convex sets," in *Proceedings of the 16th international conference on Hybrid systems: computation and control*, Philadelphia, Pennsylvania, USA: Association for Computing Machinery, Apr. 2013, pp. 173–182, ISBN: 978-1-4503-1567-8. DOI: 10.1145/2461328.2461358.

[38] N. Kochdumper and M. Althoff, "Constrained Polynomial Zonotopes," *arXiv:2005.08849 [math]*, May 2020.

[39] I. Mitchell, A. Bayen, and C. Tomlin, "A time-dependent Hamilton-Jacobi formulation of reachable sets for continuous dynamic games," *IEEE Transactions on Automatic Control*, vol. 50, no. 7, pp. 947–957, Jul. 2005, ISSN: 1558-2523. DOI: 10.1109/TAC.2005.851439.

[40] M. Chen, S. L. Herbert, M. S. Vashishtha, S. Bansal, and C. J. Tomlin, "Decomposition of reachable sets and tubes for a class of nonlinear systems," *IEEE Transactions on Automatic Control*, vol. 63, no. 11, pp. 3675–3688, Nov. 2018, ISSN: 1558-2523. DOI: 10.1109/TAC.2018.2797194.

[41] J. Holaza, B. Takács, M. Kvasnica, and S. Di Cairano, "Safety verification of implicitly defined MPC feedback laws," in *2015 European Control Conference (ECC)*, Jul. 2015, pp. 2547–2552. DOI: 10.1109/ECC.2015.7330921.

[42] M. Kvasnica, P. Bakaráč, and M. Klaučo, "Complexity reduction in explicit MPC: A reachability approach," *Systems & Control Letters*, vol. 124, pp. 19–26, Feb. 2019, ISSN: 0167-6911. DOI: 10.1016/j.sysconle.2018.12.002.

[43] C. Le Guernic and A. Girard, "Reachability analysis of hybrid systems using support functions," in *Computer Aided Verification*, A. Bouajjani and O. Maler, Eds., Berlin, Heidelberg: Springer, 2009, pp. 540–554, ISBN: 978-3-642-02658-4. DOI: .

[44] C. Fan, B. Qi, S. Mitra, M. Viswanathan, and P. S. Duggirala, "Automatic reachability analysis for nonlinear hybrid models with c2e2," in *Computer Aided Verification*, S. Chaudhuri and A. Farzan, Eds., Cham: Springer International Publishing, 2016, pp. 531–538, ISBN: 978-3-319-41528-4. DOI: .

[45] X. Chen, E. Ábrahám, and S. Sankaranarayanan, "Flow*: An analyzer for non-linear hybrid systems," in *International Conference on Computer Aided Verification*, Springer, 2013, pp. 258–263.

[46] M. Althoff, "An Introduction to CORA 2015," in *EPiC Series in Computing*, vol. 34, EasyChair, Dec. 2015, pp. 120–151. DOI: 10.29007/zbkv.

[47] S. Schupp, E. Ábrahám, I. B. Makhlouf, and S. Kowalewski, "H y p ro: A c++ library of state set representations for hybrid systems reachability analysis," in *NASA Formal Methods Symposium*, Springer, 2017, pp. 288–294.

[48] S. Bogomolov, M. Forets, G. Frehse, K. Potomkin, and C. Schilling, "JuliaReach: A toolbox for set-based reachability," in *Proceedings of the 22nd ACM International Conference on Hybrid Systems: Computation and Control*, New York, NY, USA: Association for Computing Machinery, Apr. 16, 2019, pp. 39–44, ISBN: 978-1-4503-6282-5. DOI: 10.1145/3302504.3311804.

[49] E. Asarin, O. Bournez, T. Dang, and O. Maler, "Approximate Reachability Analysis of Piecewise-Linear Dynamical Systems," in *Hybrid Systems: Computation and Control*, N. Lynch and B. H. Krogh, Eds., Springer Berlin Heidelberg, 2000, pp. 20–31, ISBN: 978-3-540-46430-3.

[50] F. Blanchini and S. Miani, "Control of parameter-varying systems," in *Set-Theoretic Methods in Control*, F. Blanchini and S. Miani, Eds., Cham: Springer International Publishing, 2015, pp. 289–335, ISBN: 978-3-319-17933-9. DOI: .

[51] C. C. Pinter, *A book of set theory*. Courier Corporation, 2014.

[52] S. Bogomolov, M. Forets, G. Frehse, F. Viry, A. Podelski, and C. Schilling, "Reach set approximation through decomposition with low-dimensional sets and high-dimensional matrices," in *Proceedings of the 21st International Conference on Hybrid Systems: Computation and Control (part of CPS Week)*, New York, NY, USA: Association for Computing Machinery, Apr. 11, 2018, pp. 41–50, ISBN: 978-1-4503-5642-8. DOI: 10.1145/3178126.3178128.

[53] A. Lodi, "Mixed Integer Programming Computation," in *50 Years of Integer Programming 1958-2008: From the Early Years to the State-of-the-Art*, M. Jünger, T. M. Liebling, D. Naddef, *et al.*, Eds., Berlin, Heidelberg: Springer, 2010, pp. 619–645, ISBN: 978-3-540-68279-0. DOI: .

[54] F. Stoican, I. Prodan, and S. Olaru, "Hyperplane arrangements in mixed-integer programming techniques. Collision avoidance application with zonotopic sets," in *2013 European Control Conference (ECC)*, Jul. 2013, pp. 3155–3160. DOI: 10.23919/ECC.2013.6669645.

[55] P. Gritzmann and B. Sturmfels, "Minkowski Addition of Polytopes: Computational Complexity and Applications to Gröbner Bases," *SIAM Journal on Discrete Mathematics*, vol. 6, no. 2, pp. 246–269, May 1993, ISSN: 0895-4801. DOI: 10.1137/0406019.

[56] M. Althoff and J. M. Dolan, "Online Verification of Automated Road Vehicles Using Reachability Analysis," *IEEE Transactions on Robotics*, vol. 30, no. 4, pp. 903–918, Aug. 2014, ISSN: 1941-0468. DOI: 10.1109/TRO.2014.2312453.

[57] T. J. Bird, H. C. Pangborn, N. Jain, and J. P. Koeln, *Hybrid zonotopes: A new set representation for reachability analysis of mixed logical dynamical systems*, May 31, 2022. DOI: 10.48550/arXiv.2106.14831. arXiv: 2106.14831[cs,eess].

[58] T. J. Bird and N. Jain, "Unions and complements of hybrid zonotopes," *IEEE Control Systems Letters*, pp. 1–1, 2021, ISSN: 2475-1456. DOI: 10.1109/LCSYS.2021.3133126.

[59] C. Le Guernic and A. Girard, "Reachability analysis of linear systems using support functions," *Nonlinear Analysis: Hybrid Systems*, vol. 4, no. 2, pp. 250–262, May 1, 2010, ISSN: 1751-570X. DOI: 10.1016/j.nahs.2009.03.002.

[60] A. Kulmburg and M. Althoff, "On the co-NP-completeness of the zonotope containment problem," *European Journal of Control*, Jun. 2021, ISSN: 0947-3580. DOI: 10.1016/j.ejcon.2021.06.028.

[61] J. K. Scott, R. Findeisen, R. D. Braatz, and D. M. Raimondo, "Input design for guaranteed fault diagnosis using zonotopes," *Automatica*, vol. 50, no. 6, pp. 1580–1589, Jun. 2014, ISSN: 0005-1098. DOI: 10.1016/j.automatica.2014.03.016.

[62] S. Sadraddini and R. Tedrake, "Linear Encodings for Polytope Containment Problems," in *2019 IEEE 58th Conference on Decision and Control (CDC)*, Dec. 2019, pp. 4367–4372. DOI: 10.1109/CDC40024.2019.9029363.

[63] T. Achterberg, R. E. Bixby, Z. Gu, E. Rothberg, and D. Weninger, "Presolve reductions in mixed integer programming," *INFORMS Journal on Computing*, vol. 32, no. 2, pp. 473–506, Apr. 1, 2020, ISSN: 1091-9856. DOI: 10.1287/ijoc.2018.0857.

[64] F. Blanchini and S. Miani, "Convex sets and their representation," in *Set-Theoretic Methods in Control*, F. Blanchini and S. Miani, Eds., Cham: Springer International Publishing, 2015, pp. 93–119, ISBN: 978-3-319-17933-9. DOI: .

[65] A. Girard and C. L. Guernic, "Efficient reachability analysis for linear systems using support functions," *IFAC Proceedings Volumes*, vol. 41, no. 2, pp. 8966–8971, Jan. 1, 2008, ISSN: 1474-6670. DOI: 10.3182/20080706-5-KR-1001.01514.

[66] L. A. Wolsey, *Integer and Combinatorial Optimization*. Hoboken: Wiley, 2014, ISBN: 978-0-471-35943-2.

[67] D. E. Knuth, *The Art of Computer Programming*. Pearson Education, 1997, ISBN: 978-0-201-89685-5.

[68] J. Lofberg, "YALMIP : A toolbox for modeling and optimization in MATLAB," in *2004 IEEE International Conference on Robotics and Automation (IEEE Cat. No.04CH37508)*, Sep. 2004, pp. 284–289. DOI: 10.1109/CACSD.2004.1393890.

[69] L. Gurobi Optimization, *Gurobi Optimizer Reference Manual*, 2021.

[70] I. Prodan, F. Stoican, S. Olaru, and S.-I. Niculescu, "Enhancements on the hyperplanes arrangements in mixed-integer programming techniques," *Journal of Optimization Theory and Applications*, vol. 154, no. 2, pp. 549–572, 2012.

[71] F. Stoican, I. Prodan, and E. I. Grøtli, "Exact and overapproximated guarantees for corner cutting avoidance in a multiobstacle environment," *International Journal of Robust and Nonlinear Control*, vol. 28, no. 15, pp. 4528–4548, 2018, ISSN: 1099-1239. DOI: 10.1002/rnc.4248.

[72] T. J. Bird, N. Jain, H. C. Pangborn, and J. P. Koeln, "Set-based reachability and the explicit solution of linear MPC using hybrid zonotopes," in *2022 American Control Conference (ACC)*, 2022.

[73] A. Bemporad and M. Morari, "Control of systems integrating logic, dynamics, and constraints," *Automatica*, vol. 35, no. 3, pp. 407–427, Mar. 1999, ISSN: 0005-1098. DOI: 10.1016/S0005-1098(98)00178-2.

[74] W. P. M. H. Heemels, B. De Schutter, and A. Bemporad, "Equivalence of hybrid dynamical models," *Automatica*, vol. 37, no. 7, pp. 1085–1091, Jul. 2001, ISSN: 0005-1098. DOI: 10.1016/S0005-1098(01)00059-0.

[75] F. D. Torrisi and A. Bemporad, "HYSDEL-a tool for generating computational hybrid models for analysis and synthesis problems," *IEEE Transactions on Control Systems Technology*, vol. 12, no. 2, pp. 235–249, Mar. 2004, ISSN: 1558-0865. DOI: 10.1109/TCST.2004.824309.

[76] A. Bemporad and M. Morari, "Verification of Hybrid Systems via Mathematical Programming," in *Hybrid Systems: Computation and Control*, F. W. Vaandrager and J. H. van Schuppen, Eds., Berlin, Heidelberg: Springer, 1999, pp. 31–45, ISBN: 978-3-540-48983-2. DOI: .

[77] D. Q. Mayne, "Model predictive control: Recent developments and future promise," *Automatica*, vol. 50, no. 12, pp. 2967–2986, Dec. 2014, ISSN: 0005-1098. DOI: 10.1016/j.automatica.2014.10.128.

[78] D. Q. Mayne, M. M. Seron, and S. V. Raković, "Robust model predictive control of constrained linear systems with bounded disturbances," *Automatica*, vol. 41, no. 2, pp. 219–224, Feb. 2005, ISSN: 0005-1098. DOI: 10.1016/j.automatica.2004.08.019.

[79] S. Yu, M. Reble, H. Chen, and F. Allgöwer, "Inherent robustness properties of quasi-infinite horizon nonlinear model predictive control," *Automatica*, vol. 50, no. 9, pp. 2269–2280, Sep. 2014, ISSN: 0005-1098. DOI: 10.1016/j.automatica.2014.07.014.

[80] S. Di Cairano, D. Yanakiev, A. Bemporad, I. V. Kolmanovsky, and D. Hrovat, "Model Predictive Idle Speed Control: Design, Analysis, and Experimental Evaluation," *IEEE Transactions on Control Systems Technology*, vol. 20, no. 1, pp. 84–97, Jan. 2012, ISSN: 1558-0865. DOI: 10.1109/TCST.2011.2112361.

[81] A. Bemporad, W. Heemels, and B. De Schutter, "On hybrid systems and closed-loop MPC systems," *IEEE Transactions on Automatic Control*, vol. 47, no. 5, pp. 863–869, May 2002, ISSN: 1558-2523. DOI: 10.1109/TAC.2002.1000287.

[82] A. Bemporad, M. Morari, V. Dua, and E. N. Pistikopoulos, "The explicit linear quadratic regulator for constrained systems," *Automatica*, vol. 38, no. 1, pp. 3–20, Jan. 2002, ISSN: 0005-1098. DOI: 10.1016/S0005-1098(01)00174-1.

[83] J. Fortuny-Amat and B. McCarl, "A Representation and Economic Interpretation of a Two-Level Programming Problem," *Journal of the Operational Research Society*, vol. 32, no. 9, pp. 783–792, Sep. 1981, ISSN: 1476-9360. DOI: 10.1057/jors.1981.156.

[84] A. Gupta, S. Bhartiya, and P. S. V. Nataraj, "A novel approach to multiparametric quadratic programming," *Automatica*, vol. 47, no. 9, pp. 2112–2117, Sep. 2011, ISSN: 0005-1098. DOI: 10.1016/j.automatica.2011.06.019.

[85] J. A. Siefert, T. J. Bird, J. P. Koeln, N. Jain, and H. C. Pangborn, "Robust successor and precursor sets of hybrid systems using hybrid zonotopes," *IEEE Control Systems Letters*, vol. 7, pp. 355–360, 2023, ISSN: 2475-1456. DOI: 10.1109/LCSYS.2022.3188477.

[86] A. Bemporad, *Modeling, control, and reachability analysis of discrete-time hybrid systems*, University of Sienna, 2003.

[87] L. Miranian and M. Gu, "Strong rank revealing LU factorizations," *Linear Algebra and its Applications*, vol. 367, pp. 1–16, Jul. 1, 2003, ISSN: 0024-3795. DOI: 10.1016/S0024-3795(02)00572-4.

[88] T. A. Davis, "Algorithm 915, SuiteSparseQR: Multifrontal multithreaded rank-revealing sparse QR factorization," *ACM Transactions on Mathematical Software*, vol. 38, no. 1, 8:1–8:22, Dec. 7, 2011, ISSN: 0098-3500. DOI: 10.1145/2049662.2049670.

[89] E. D. Andersen and K. D. Andersen, "Presolving in linear programming," *Mathematical Programming*, vol. 71, no. 2, pp. 221–245, Dec. 1, 1995, ISSN: 1436-4646. DOI: 10.1007/BF01586000.

[90] X. Yang and J. K. Scott, "A comparison of zonotope order reduction techniques," *Automatica*, vol. 95, pp. 378–384, Sep. 2018, ISSN: 0005-1098. DOI: 10.1016/j.automatica.2018.06.006.

[91] Y. C. Eldar, A. Beck, and M. Teboulle, "Bounded error estimation: A chebyshev center approach," in *2007 2nd IEEE International Workshop on Computational Advances in Multi-Sensor Adaptive Processing*, Dec. 2007, pp. 205–208. DOI: 10.1109/CAMSAP.2007.4498001.

[92] M. Fischetti, I. Ljubić, M. Monaci, and M. Sinnl, "A new general-purpose algorithm for mixed-integer bilevel linear programs," *Operations Research*, vol. 65, no. 6, pp. 1615–1637, Dec. 2017, ISSN: 0030-364X. DOI: 10.1287/opre.2017.1650.

[93] Z. H. Gümüş and C. A. Floudas, "Global optimization of mixed-integer bilevel programming problems," *Computational Management Science*, vol. 2, no. 3, pp. 181–212, Jul. 1, 2005, ISSN: 1619-6988. DOI: 10.1007/s10287-005-0025-1.

[94] E. Gover and N. Krikorian, "Determinants and the volumes of parallelotopes and zonotopes," *Linear Algebra and its Applications*, vol. 433, no. 1, pp. 28–40, Jul. 15, 2010, ISSN: 0024-3795. DOI: 10.1016/j.laa.2010.01.031.

[95] L. J. Guibas, A. Nguyen, and L. Zhang, "Zonotopes as bounding volumes," in *Proceedings of the fourteenth annual ACM-SIAM symposium on Discrete algorithms*, Baltimore, Maryland: Society for Industrial and Applied Mathematics, Jan. 2003, pp. 803–812, ISBN: 978-0-89871-538-5.

[96] A. Chalkis, I. Z. Emiris, and V. Fisikopoulos, "Practical volume estimation of zonotopes by a new annealing schedule for cooling convex bodies," in *Mathematical Software – ICMS 2020*, A. M. Bigatti, J. Carette, J. H. Davenport, M. Joswig, and T. de Wolff, Eds., Cham: Springer International Publishing, 2020, pp. 212–221, ISBN: 978-3-030-52200-1. DOI: .

[97] M. Simonovits, "How to compute the volume in high dimension?" *Mathematical Programming*, vol. 97, no. 1, pp. 337–374, Jul. 1, 2003, ISSN: 1436-4646. DOI: 10.1007/s10107-003-0447-x.

[98] R. Kannan, L. Lovász, and M. Simonovits, "Random walks and an o*(n5) volume algorithm for convex bodies," *Random Structures & Algorithms*, vol. 11, no. 1, pp. 1–50, 1997, ISSN: 1098-2418. DOI: 10.1002/(SICI)1098-2418(199708)11:1⟨1::AID-RSA1⟩3.0.CO;2-X.

[99] L. Jaulin, M. Kieffer, O. Didrit, and É. Walter, "Interval analysis," in *Applied Interval Analysis: With Examples in Parameter and State Estimation, Robust Control and Robotics*, L. Jaulin, M. Kieffer, O. Didrit, and É. Walter, Eds., London: Springer, 2001, pp. 11–43, ISBN: 978-1-4471-0249-6. DOI: .

[100] L. Jaulin and E. Walter, "Set inversion via interval analysis for nonlinear bounded-error estimation," *Automatica*, vol. 29, no. 4, pp. 1053–1064, Jul. 1, 1993, ISSN: 0005-1098. DOI: 10.1016/0005-1098(93)90106-4.

[101] M. Kieffer and E. Walter, "Guaranteed nonlinear state estimator for cooperative systems," *Numerical Algorithms*, vol. 37, no. 1, pp. 187–198, Dec. 1, 2004, ISSN: 1572-9265. DOI: 10.1023/B:NUMA.0000049466.96588.a6.

[102] L. Jaulin and E. Walter, "Guaranteed nonlinear parameter estimation from bounded-error data via interval analysis," *Mathematics and Computers in Simulation*, vol. 35, no. 2, pp. 123–137, Apr. 1, 1993, ISSN: 0378-4754. DOI: 10.1016/0378-4754(93)90008-I.

[103] L. Brown and X. Li, "Confidence intervals for two sample binomial distribution," *Journal of Statistical Planning and Inference*, vol. 130, no. 1, pp. 359–375, Mar. 1, 2005, ISSN: 0378-3758. DOI: 10.1016/j.jspi.2003.09.039.

[104] *Multicriteria Optimization*. Berlin/Heidelberg: Springer-Verlag, 2005, ISBN: 978-3-540-21398-7. DOI: 10.1007/3-540-27659-9.

PUBLICATIONS

Journal Articles

- **Trevor J. Bird**, Jacob A. Siefert, Justin P. Koeln, Herschel C. Pangborn, and Neera Jain, "Complexity Reduction of Hybrid Zonotopes," 2022 (In Preparation)
- Jacob A. Siefert, **Trevor J. Bird**, Neera Jain, Justin P. Koeln, and Herschel C. Pangborn, "Nonlinear State-Update Sets for Reachability Analysis, State Estimation, and Parameter Identification," 2022. (In Preparation)
- **Trevor J. Bird**, Herschel C. Pangborn, Neera Jain, and Justin P. Koeln, "Hybrid Zonotopes: A New Set Representation for Reachability Analysis of Mixed Logical Dynamical Systems," Automatica, 2022. (Provisionally Accepted)
- Jacob A. Siefert, **Trevor J. Bird**, Justin P. Koeln, Neera Jain, and Herschel C. Pangborn, "Robust Successor and Predecessor Sets of Hybrid Systems using Hybrid Zonotopes," The IEEE Control Systems Letters, 2022.
- **Trevor J. Bird** and Neera Jain, "Unions and Complements of Hybrid Zonotopes," The IEEE Control Systems Letters, 2021.
- **Trevor J. Bird** and Neera Jain, "Dynamic Modeling and Validation of a Micro-combined Heat and Power System with Integrated Thermal Energy Storage," Applied Energy, 2020.
- Austin Nash, Brian Fu, **Trevor J. Bird**, Neera Jain, and Timothy Fisher, "Control-Oriented Modeling of Integrated Flash Boiling for Rapid Transient Heat Dissipation," Journal of Thermophysics and Heat Transfer, 2019.

Conference Articles

- **Trevor J. Bird**, Jacob A. Siefert, Herschel C. Pangborn, Neera Jain, and Justin P. Koeln, "The Hybrid Zonotope Toolbox: A Mixed-Integer Toolbox For Nonconvex Set-Theoretic Methods," 2023. (In Preparation)

- **Trevor J. Bird**, Neera Jain, Herschel C. Pangborn, and Justin P. Koeln, "Set-Based Reachability and the Explicit Solution of Linear MPC using Hybrid Zonotopes," Proceedings of the American Controls Conference, 2022.
  ⋆ ACC Best Student Paper Award

- **Trevor J. Bird**, Catherine Weaver, and Neera Jain. "Switched Linear Model of a Stratified Hot Water Tank for Control of micro-CHP Systems," Proceedings of the ASME Dynamic Systems and Control Conference, 2019.
  ⋆ ASME Energy Systems Technical Committee Best Paper Award

Invited Talks

- **Trevor J. Bird** and Neera Jain, "Unions and Complements of Hybrid Zonotopes," Proceedings of the 2022 American Controls Conference, Atlanta, GA, June 2022.

- **Trevor J. Bird**, "Hybrid Zonotopes: A Mixed-Integer Set Representation for the Analysis of Hybrid Systems," University of Texas at Dallas Controls Seminar, Richardson, TX, March 2022.